Université de Montréal

Rôle de la protéine-associée aux microtubules MAP2 dans l'acquisition et le maintien du phénotype neuronal

Par
Carole Abi Farah

Département de physiologie
Faculté de Médecine

Thèse présentée à la Faculté des études supérieures
en vue de l'obtention du grade de Ph.D.
en Sciences Neurologiques

Avril, 2004

Université de Montréal
Faculté des études supérieures

Cette thèse de doctorat intitulée :

Rôle de la protéine-associée aux microtubules MAP2 dans l'acquisition et le maintien du phénotype neuronal

présentée par :

Carole Abi Farah

a été évaluée par un jury composé des personnes suivantes :

Dr Vincent Castellucci
président-rapporteur

Dr Nicole Leclerc
directeur de recherche

Dr Adriana Di Polo
membre du jury

Dr Andréa Leblanc
examinateur externe

Dr Louis-Éric Trudeau
représentant du doyen de la FES

RÉSUMÉ

Les neurones, unités fonctionnelles du système nerveux, possèdent une morphologie polaire extrêmement complexe qui détermine leur fonction. Ces cellules acquièrent leur polarité en émettant deux types de prolongements cytoplasmiques : les dendrites et l'axone. Ces deux compartiments se distinguent par des critères morphologiques, moléculaires ainsi que par leur composition en organelles. Au niveau morphologique, les dendrites sont multiples, relativement courts et ont un diamètre qui diminue par rapport à la distance du corps cellulaire alors que l'axone est unique, relativement long et a un diamètre uniforme le long de la majorité de sa trajectoire. De plus, l'espacement entre les microtubules est plus élevé dans les dendrites que dans l'axone. Au niveau moléculaire, la distinction la plus importante est la présence de protéines associées aux microtubules différentes dans les dendrites et l'axone, soit la MAP2 dans le premier compartiment et tau dans le deuxième. Au niveau de la distribution des organelles, le réticulum endoplasmique rugueux est retrouvé dans les dendrites et non dans l'axone. Les évènements moléculaires précis qui conduisent à l'acquisition et au maintien de la polarité neuronale sont encore peu connus. D'ailleurs, cette polarité est sévèrement perturbée, voire perdue, dans les maladies neurodégénératives telles que la sclérose latérale amyotrophique et la maladie d'Alzheimer. Afin de mieux comprendre au niveau moléculaire les mécanismes qui conduisent à l'élaboration et au maintien de la polarité neuronale, nous nous sommes penchés sur la protéine associée aux microtubules dendritique, la MAP2 puisque : 1) cette protéine compte parmi les protéines les plus abondantes dans les dendrites du système nerveux central mammifère adulte, 2) l'inhibition de l'expression de la MAP2 dans des cultures primaires de neurones bloque la différentiation neuronale et 3) un changement dans le niveau d'expression et/ou l'état de phosphorylation de la MAP2 dans le cerveau adulte a été corrélé au remodelage dendritique. Dans le cadre de la présente étude, nous avons étudié en premier lieu le rôle des domaines fonctionnels de la MAP2 dans la capacité de la protéine à induire la formation de prolongements cytoplasmiques dans les cellules Sf9. Nos résultats démontrent que la formation de

prolongements dans ce système cellulaire est induite par le domaine de liaison aux microtubules de la MAP2 et est régulée par son domaine de projection. De plus, la longueur du domaine de projection ainsi que sa conformation, semblent contrôler l'espacement entre les microtubules. En deuxième lieu, nous avons étudié les altérations du niveau protéique et de la distribution membranaire des protéines associées aux microtubules MAP2, tau et MAP1A dans un modèle animal qui récapitule le tableau neuropathologique de la maladie neurodégénérative, la sclérose latérale amyotrophique. Nos résultats démontrent une diminution significative du niveau protéique de la MAP2, tau et de la MAP1A cinq mois avant l'apparition des symptômes cliniques chez des souris transgéniques qui expriment une forme mutante de la superoxide dismutase 1 (SOD1). De plus, une altération de la distribution membranaire de la MAP2 corrèle avec la neurodégénérescence chez ces souris. En dernier lieu, nous avons vérifié si la MAP2 contribue à la polarisation des organelles au cours du développement neuronal. Nous avons démontré par fractionnement cellulaire et par microscopie électronique dans un essai de reconstitution *in vitro* ainsi que dans les cellules Sf9 surexprimant la MAP2c, que la MAP2 interagit avec le réticulum endoplasmique rugueux et pourrait donc contribuer à la ségrégation de celui-ci dans les dendrites au cours de la différenciation neuronale.

Mots-clés *:* Neurone, polarité neuronale, dendrites, microtubules, MAP2, domaine de projection, réticulum endoplasmique rugueux, sclérose latérale amyotrophique, tau, MAP1A.

SUMMARY

Neurons are the functional signalling units of the nervous system. The morphology of these highly complex polarized cells defines their function. Neurons become polar by elaborating two types of cytoplasmic processes: dendrites and an axon. These two compartments can be distinguished at the morphological level: the dendrites are multiple, relatively short and have a tapering diameter whereas the axon is unique, can extend many centimetres from the cell body and is uniform in diameter along most of its length. The spacing between microtubules is also higher in dendrites than in the axon. Furthermore, these two compartments are distinct at the molecular level: the microtubule-associated protein MAP2 is found in the dendritic compartment and tau in the axonal one. Moreover, dendrites and the axon differ in their content with membranous organelles: the rough endoplasmic reticulum is found in the somato-dendritic compartment but not in the axonal one. The precise molecular events that contribute to the elaboration and the maintenance of the neuronal phenotype are still largely unknown. On the other hand, neuronal polarity was reported to be lost in neurodegenerative diseases such as amyotrophic lateral sclerosis and Alzheimer's disease. To better understand the molecular mechanisms that lead to the establishment and the maintenance of neuronal polarity, we studied the dendritic microtubule-associated protein MAP2. This protein is one of the most abundant cytoskeletal proteins in the dendrites of the adult mammalian central nervous system. Furthermore, no neurite outgrowth is observed when the expression of MAP2 is inhibited in primary neuronal cultures. Moreover, changes in the protein level and/or phosphorylation state of MAP2 were reported to accompany dendritic remodeling in adult rat brain. In the present project, we first studied the effect of the functional domains of MAP2 on the process formation activity of this protein in Sf9 cells. Our results show that the formation of processes in Sf9 cells is induced by the microtubule-binding domain of MAP2 and is regulated by its projection domain. Furthermore, the length of the projection domain of MAP2 as well as its conformation, seem to regulate the spacing between microtubules. Second, we studied alterations of the protein level and distribution of the microtubule-

associated proteins MAP2, tau and MAP1A in a mouse model of the neurodegenerative disease, amyotrophic lateral sclerosis. Our results show a significant decrease of the protein levels of MAP2, tau and MAP1A, five months before onset of clinical symptoms in mutant superoxide dismutase 1 (SOD1) mice. Furthermore, we report an altered distribution of MAP2 in these mice that correlates with neurodegeneration. Third, we verified whether MAP2 contributes to the polarization of membranous organelles during neuronal differentiation. We showed using subcellular fractionation and electron microscopy in an in vitro reconstitution assay and in Sf9 cells overexpressing MAP2c that MAP2 is associated with the rough endoplasmic reticulum and thus, may contribute to its segregation in the dendritic compartment during the establishment of neuronal polarity.

Keywords *:* Neuron, neuronal polarity, dendrites, microtubules, MAP2, projection domain, rough endoplasmic reticulum, amyotrophic lateral sclerosis, tau, MAP1A.

TABLE DES MATIÈRES

LISTE DES TABLEAUX

LISTE DES FIGURES

INTRODUCTION

PREMIER ARTICLE

DEUXIÈME ARTICLE

TROISIÈME ARTICLE

DISCUSSION

QUATRIÈME ARTICLE

LISTE DES ABBRÉVIATIONS

a.a.....amino acids

ABP.....Actin-binding protein

Actine-F.....Actin Filamenteuse

Actine-G.....Actine Globulaire

ALS.....Amyotrophic lateral sclerosis

ATP.....Adenosine triphosphate

CAMKII.....Calcium-calmodulin-dependent kinase II

CD.....Cytochalasin D

Cdk5.....cyclin-dependent kinase 5

CLASP.....CLIP-associated protein

CLIMP.....Cytoskeleton-linking membrane protein

CLIP.....Cytosolic linker protein

CNS.....Central nervous system

DLB.....Dendritic lamellar bodies

ERK.....Extracellular signal regulated kinase

ERM.....Ezrin-radixin-moesin

GTP.....Guanosine triphosphate

HRP.....Horseradish peroxidase

JAK3.....Janus kinase 3

LTP.....Long-term potentiation

MAP.....Microtubule-associated protein

MARK.....Microtubule-affinity regulating kinase

NF.....Neurofilament

NMDA.....N-methyl-D-aspartate

PEM.....Pipes-EGTA-$MgCl_2$

PKC.....Protein kinase C

PMSF.....Phenyl methyl sulfonyl fluoride

PP.....Protein phosphatase

M.O.I.....Multiplicity of infection

Mt.....Microtubule-binding domain

PI.....Phosphoinositide

PKA.....Protein kinase A

Prob.....Projection domain of MAP2b

Proc.....Projection domain of MAP2c

RER.....Rough endoplasmic reticulum

SDS.....Sodium Dodecyl Sulfate

Sf.....Spodoptera frugiperda

SM.....Smooth membranes

SOD1.....Superoxide dismutase 1

VDAC.....Voltage dependent anion channel

REMERCIEMENTS

Mes remerciements s'adressent aux personnes suivantes :

- Ma directrice de recherche le Dr. Nicole Leclerc pour m'avoir donné la chance de faire mes études doctorales dans son laboratoire, m'avoir fait confiance, m'avoir préparée à une carrière de recherche, et pour les fous rires aussi, un grand merci !
- Le Dr. Jacques Paiement pour son enthousiasme éternel, sa patience et ses encouragements.
- Le responsable du comité du programme en sciences neurologiques, Dr. John Kalaska, qui m'a supporté tout le long de mes études de PhD surtout lorsque j'ai changé de laboratoire de recherche.
- Ma petite famille actuelle du laboratoire, Dalinda Liazoghli, Sébastien Perreault, Mylène Desjardins, Marilyse Piché et ceux qui sont déjà partis du laboratoire, Chantal Labelle, Alain Guimont, Sylvie Cornibert, Dave Bélanger et Mélanie Dufour. Ces années n'auraient pas aussi agréables sans votre présence.
- Les membres du département de pathologie et biologie cellulaire que j'ai cotoyés durant toutes ces années, en particulier les membres du laboratoire du Dr. Guy Doucet, Dr. Lisa McKerracher, Dr. Adriana Di Polo et Dr. Jacques Paiement.
- Mon « parrain » le Dr. Vincent Castellucci et ma « marraine » le Dr. Adriana Di Polo pour leurs conseils précieux le long de mes études doctorales.
- Mon mari Sydney pour ses encouragements, sa patience et son amour.
- Mes parents Georges et Jeanne-D'Arc: sans votre support depuis le début de mes études, je n'en serais pas là dans ma carrière aujourd'hui.
- Tous mes amis et membres de famille qui étaient toujours là dans les hauts et les bas pendant ces cinq dernières années en particulier Rosa, Calloune, Charbel et Nisrine, un très grand merci !

Je tiens aussi à remercier le Groupe de Recherche sur le Système Nerveux Central (GRSNC), la Faculté des études supérieures de l'Université de Montréal ainsi que le Fonds pour la Formation de Chercheurs et l'Aide à la Recherche (FCAR) pour leur soutien financier.

1 INTRODUCTION

'Following their dominance as the highly visible indicators of neuronal diversity during the early phase of anatomical analysis, when the Golgi stain reigned supreme, dendrites seemed almost to vanish from the landscape of neuroscience during the middle decades of the last century. This was the period when prevailing ideas about brain circuits had them reduced to 'neural networks' in which the cell body 'nodes' were connected to one another by axonal 'wires'. This imbalance began to be redressed by the work of Wilfrid Rall using compartmental models of dendritic integration, and the key roles of dendrites as integrators of neuronal signals and sites of synaptic plasticity have now been recognized and are being rapidly explored....the fallow period, when many neuroscientists regarded dendrites as irrelevant to neuronal function, is well and truly over'.

Matus, A. and Shepherd, G.M. (2000)
The Millenium of the Dendrite? Neuron 27, 431-434.

1.1 LE NEURONE

1.1.1 Historique

Les cellules nerveuses furent décrites pour la première fois vers la fin des années 1800 par Camillo Golgi et Santiago Rámon Y Cajal. Golgi a réussi à colorer les neurones révélant ainsi leur structure sous microscope. Il a pu déterminer que les neurones avaient des corps cellulaires et deux types majeurs de projections ou de prolongements: les dendrites qui se ramifient à une extrémité et l'axone tout seul à l'autre extrémité. Par la suite, Rámon Y Cajal utilisa la technique de Golgi pour marquer les cellules individuelles démontrant ainsi que le cerveau était formé d'un réseau de

cellules distinctes. Rámon Y Cajal fut le premier à établir la 'doctrine du neurone', émettant le principe que les neurones individuels sont les unités de signalisation élémentaires du système nerveux. Dans les années 1920, l'embryologiste américain Ross Harrison a démontré que les deux types majeurs de projections neuronales, soit les dendrites et l'axone, émanent du corps cellulaire et que ceci est possible même lorsqu'un neurone est isolé des autres neurones en culture. Dans les années suivantes, la pharmacologie a eu un impact sur notre compréhension du système nerveux en établissant un lien entre les médicaments administrés et la base chimique de communication entre les neurones. Par la suite, l'émergence de la psychologie du comportement a vite fait de nous convaincre du lien direct qui existe entre la fonction neuronale et le comportement d'une personne. Aujourd'hui, on ne peut être plus convaincu de ce qu'Hippocrates avait stipulé au cinquième siècle (avant J.-C.): 'l'homme doit savoir que c'est du cerveau et uniquement du cerveau que proviennent nos plaisirs, nos joies, nos rires et nos plaisanteries ainsi que nos souffrances, nos peines, nos douleurs et nos pleurs…'.

L'importance d'une communication appropriée entre les neurones, en bref d'une fonction neuronale normale, n'est plus à démontrer. Or, la fonction d'un neurone est déterminée par sa morphologie. Celle-ci est plutôt stable à l'âge adulte. Cependant, un changement de la structure neuronale a déjà été rapporté dans certaines régions du cerveau mature. Ce phénomène, communément appelé plasticité neuronale, a été corrélé à l'apprentissage et à la mémoire. Par contre, la morphologie neuronale est aussi sévèrement perturbée dans des conditions pathologiques tel que le retard mental et dans les premiers stades de la maladie d'Alzheimer et la sclérose latérale amyotrophique.

Dans ce contexte, il devient impératif de comprendre les mécanismes exacts qui conduisent à l'élaboration de la structure neuronale au cours du développement et au maintien de cette structure à l'âge adulte afin de permettre une communication appropriée entre les neurones. Dans la présente thèse, nous nous sommes concentrés en particulier sur les dendrites, étant à l'ère où les chercheurs ressentent le besoin de mieux comprendre le fonctionnement de ce compartiment qui avait été négligé pendant trop longtemps en faveur du compartiment axonal.

Étant donné que le cytosquelette est le déterminant intrinsèque majeur de la morphologie neuronale (Letourneau, 1982), nous introduirons celui-ci dans la section suivante.

1.1.2 Le cytosquelette neuronal

Le cytosquelette est composé de trois principales structures filamenteuses: les microtubules, les neurofilaments et les microfilaments d'actine (Hirokawa, 1991). Les microtubules sont des polymères tubulaires de 24 nm de diamètre composés de 13 protofilaments. Chaque protofilament est formé par des dimères de α- et β-tubuline (Hirokawa, 1991). Les microtubules sont considérés polaires puiqu'ils possèdent une extrémité à élongation rapide (l'extrémité plus) et une autre à élongation lente (l'extrémité moins). Ils sont hautement dynamiques et peuvent subir des transitions soudaines entre élongation et rétraction pendant la division cellulaire. Ce phénomène est appelé « instabilité dynamique » (Horio and Hotani, 1986; Mitchison and Kirschner, 1988; Janson *et al.*, 2003). Dans les neurones (cellules post-mitotiques), les microtubules

sont moins dynamiques que dans les cellules mitotiques (Hirokawa, 1994). Ceci est surtout du à la présence de protéines associées aux microtubules structurelles tel que la MAP1A, la MAP2 et tau. Ces protéines stabilisent les microtubules en diminuant leur instabilité dynamique (Drechsel *et al.*, 1992; Takemura *et al.*, 1992; Weisshaar *et al.*, 1992). Récemment, plusieurs nouvelles MAPs structurelles qui stabilisent les microtubules furent identifiées tel que la dystonine, la LIS1 et la doublecortine (Yang *et al.*, 1999; Gleeson, 2000; Lin *et al.*, 2000; Taylor *et al.*, 2000). D'un autre côté, il est important de noter qu'il existe une autre catégorie de MAPs structurelles qui sont connues pour déstabiliser les microtubules. Ces protéines peuvent, soit séquestrer la tubuline soluble (ex. Stathmine, SCG10), inhiber la nucléation des microtubules (ex. MINUS) ou les couper (ex. Katanine) (McNally and Vale, 1993; Belmont *et al.*, 1996; Belmont and Mitchison, 1996; Fanara *et al.*, 1999). Les microtubules ainsi que les protéines qui leur sont associées jouent un rôle crucial dans la formation des prolongements neuronaux et l'établissement de la polarité neuronale au cours du développement (Mitchison and Kirschner, 1988; Allan *et al.*, 1991; Tanaka and Sabry, 1995; Waterman-Storer and Salmon, 1999). Ils sont également importants pour le maintien de la structure et la fonction neuronale à l'âge adulte (Mitchison and Kirschner, 1988; Allan *et al.*, 1991; Tanaka and Sabry, 1995; Waterman-Storer and Salmon, 1999).

Les filaments intermédiaires neuronaux ou les neurofilaments (NF) sont composés de trois sous-unités protéiques, la NF-L (60 kDa), la NF-M (100 kDa) et la NF-H (115 kDa), qui co-polymérisent pour former des filaments de 10nm de diamètre (Shaw, 1991). Deux autres protéines peuvent faire partie des filaments intermédiaires neuronaux. Ce sont la α-internexine et la périphérine. Les neurofilaments semblent être

importants pour le maintien du calibre axonal (Al-Chalabi and Miller, 2003). De plus, une étude récente par Chan et collègues a démontré la présence d'une population de neurofilaments hautement dynamiques dans le cône de croissance axonal. Cette population semble être impliquée dans le remodelage local du cytosquelette pendant l'élongation de l'axone (Chan *et al.*, 2003).

Les microfilaments d'actine (actine-F) sont des polymères polaires de 8nm de diamètre formés de monomères d'actine globulaire (actine-G) ainsi que de protéines de liaison à l'actine (ABPs). Les ABPs sont connues pour moduler la structure et la fonction de l'actine. Selon une revue récente par Dos Remedios et collègues (dos Remedios *et al.*, 2003), les ABPs peuvent être classifiées en sept groupes: 1) les protéines de liaison à l'actine monomérique qui séquestrent l'actine globulaire (actine-G) et l'empêchent de polymériser (ex. thymosine β4, DNase I), 2) les protéines qui dépolymérisent les microfilaments induisant la conversion de l'actine filamenteuse (actine-F) en actine-G (ex. CapZ and cofiline), 3) les protéines qui se lient à l'extrémité du microfilament empêchant ainsi l'échange de monomères aux extrémités pointue (ex. tropomoduline) et barbelée (ex. CapZ), 4) Les protéines de section des microfilaments qui diminuent la longueur moyenne de ceux-ci en se liant sur les côtés et les coupant en deux morceaux (ex. gelsoline), 5) Les protéines qui lient les microfilaments d'actine l'un à l'autre; ces protéines doivent contenir au moins deux domaines de liaison à l'actine ou bien avoir la capacité de dimériser pour faciliter la formation de faisceaux parallèles, à angle ou de réseaux tri-dimensionnels d'actine filamenteuse (ex. Arp2/3), 6) Les protéines stabilisatrices qui se lient sut les côtés des microfilaments d'actine et inhibent leur dépolymérisation (ex. tropomyosine) et 7) Les protéines motrices qui voyagent le

long de l'actine filamenteuse (ex. la famille myosine). Ces dernières maintiennent la structure et la fonction des microfilaments (dos Remedios *et al.*, 2003). Les microfilaments jouent un rôle important entre autres dans la division cellulaire et la motilité du cône de croissance pendant l'établissement de la polarité neuronale au cours du développement (Tanaka and Sabry, 1995; Waterman-Storer and Salmon, 1999). Dans le neurone mature, l'induction du phénomène de potentiation synaptique à long terme (LTP) est associée à une réorganisation du cytosquelette d'actine présent dans les épines dendritiques (Krucker *et al.*, 2000; Fukazawa *et al.*, 2003). De plus, l'inhibition de la polymérisation de l'actine dans ce système altère le maintien de la LTP (Fukazawa *et al.*, 2003).

1.1.3 Cytosquelette et polarité neuronale

La différenciation neuronale suit des étapes spécifiques *in vitro* (Dotti *et al.*, 1988). En premier lieu, le neurone développe une lamellipode qui se fragmente pour former des prolongements cytoplasmiques appelés neurites mineures. En deuxième lieu, une de ces neurites s'allonge plus rapidement que les autres et devient l'axone. La différenciation des autres neurites mineures en dendrites s'ensuit. En dernier lieu, les contacts synaptiques se forment (Dotti *et al.*, 1988).

On parle de polarité neuronale puisque les dendrites et l'axone représentent deux compartiments distincts à plusieurs niveaux. Premièrement, les dendrites et l'axone ont des fonctions différentes: les dendrites reçoivent le signal électrique et le relaient vers le corps cellulaire alors que l'axone propage le signal à partir du corps cellulaire vers les autres neurones. Deuxièmement, les dendrites et l'axone diffèrent au niveau

morphologique: les dendrites sont multiples, relativement courts et ont un diamètre qui décroît par rapport à la distance du corps cellulaire alors que l'axone est unique, relativement long et a un diamètre uniforme le long de la majorité de sa trajectoire (Bartlett and Banker, 1984b, a; Dotti *et al.*, 1988; Hillman, 1988). Troisièmement, le réticulum endoplasmique rugueux (RER) est retrouvé dans le compartiment somato-dendritique et non dans l'axone et le nombre de ribosomes libres est plus élevé dans les dendrites que dans l'axone (Bartlett and Banker, 1984b, a; Peters *et al.*, 1991). Quatrièmement, au niveau du cytosquelette, le nombre de microtubules est plus élevé dans les dendrites que dans l'axone alors que l'inverse est observé pour les neurofilaments (Bartlett and Banker, 1984b, a; Hirokawa, 1991). De plus, les microtubules dendritiques ont une orientation mixte alors que les microtubules axonaux ont une orientation uniforme avec l'extrémité plus qui pointe vers la partie distale de l'axone (Baas *et al.*, 1988; Burton, 1988). Au niveau biochimique, la distinction la plus importante est la présence de protéines associées aux microtubules structurelles différentes (MAPs) dans les dendrites et l'axone, soit la MAP2 dans le premier compartiment et tau, dans le deuxième (Caceres *et al.*, 1984; Hirokawa, 1991; Ludin and Matus, 1993). Ces MAPs sont connues pour promouvoir l'assemblement des microtubules et leur stabilisation dans le cytoplasme (Tucker, 1990; Hirokawa, 1994; Mandelkow and Mandelkow, 1995; Sanchez *et al.*, 2000a). Cependant, la présence de MAPs différentes dans les dendrites et l'axone suggère que le rôle de ces protéines ne se limite pas à la stabilisation des microtubules.

Dans la présente thèse, nous nous sommes concentrés sur la protéine associée aux microtubules dendritique MAP2 pour les raisons suivantes: 1) MAP2 compte parmi

les protéines du cytosquelette les plus abondantes dans les dendrites du système nerveux central mammifère adulte (Wiche, 1989), 2) MAP2 est cruciale pour la différenciation neuronale puisque l'inhibition de son expression dans des cultures primaires de neurones à l'aide d'oligonucléotides antisens inhibe la formation de neurites mineurs (Dinsmore and Solomon, 1991; Caceres *et al.*, 1992; Sharma *et al.*, 1994), 3) Nos travaux ainsi que ceux de plusieurs autres groupes ont démontré que la surexpression de la MAP2 dans des cellules non-neuronales induit la formation de prolongements cytoplasmiques similaires aux dendrites (Edson *et al.*, 1993; Leclerc *et al.*, 1993; Langkopf *et al.*, 1995; Leclerc *et al.*, 1996; Kalcheva *et al.*, 1998; Boucher *et al.*, 1999; Belanger *et al.*, 2002) et 4) MAP2 semble être importante pour le maintien de la morphologie neuronale à l'âge adulte puisque sa suppression et sa dégradation ont été corrélés à la perte des dendrites et au remodelage de ceux-ci (Sharma *et al.*, 1994; Faddis *et al.*, 1997; Sanchez *et al.*, 2000a).

1.2 LA PROTÉINE ASSOCIÉE AUX MICROTUBULES MAP2

1.2.1 Structure primaire

La protéine associée aux microtubules MAP2 fut découverte pour la première fois co-purifiant avec les microtubules cytoplasmiques préparés à partir du cerveau (Ray *et al.*, 1979; Travis *et al.*, 1980; Bloom *et al.*, 1985). La structure primaire de la MAP2 comprend deux domaines fonctionnels majeurs: le domaine de liaison aux microtubules et le domaine de projection. Le domaine de liaison aux microtubules qui est hautement basique, est situé à l'extrémité C-terminale de la protéine (Lewis *et al.*, 1988; Lewis *et al.*, 1989). Ce domaine contient 3 à 4 séquences répétées imparfaites de 18 a.a. chaque,

séparées par des séquences de 13-14 a.a. Ces séquences répétées se lient à la tubuline et diminuent la concentration critique de tubuline nécessaire pour polymériser en microtubules (Murphy and Borisy, 1975; Sloboda *et al.*, 1975; Lewis *et al.*, 1988; Lewis *et al.*, 1989). Le domaine de projection de la MAP2, qui est hautement acidique, est situé à l'extrémité N-terminale de la protéine. Ce domaine projette à la surface des microtubules et est surtout connu pour déterminer l'espacement entre les microtubules (Kim *et al.*, 1979; Chen *et al.*, 1992). Entre le domaine de liaison aux microtubules et le domaine de projection, on retrouve une région riche en prolines. En interagissant avec les séquences répétées du domaine de liaison aux microtubules, la région riche en prolines régule la capacité de la MAP2 à se lier aux microtubules et à les assembler (Sanchez *et al.*, 1996; Felgner *et al.*, 1997; Goode *et al.*, 1997).

1.2.2 Épissage alternatif

Plusieurs isoformes de la MAP2 sont générées par épissage alternatif au cours du développement à partir d'un seul gène situé sur le chromosome 2 (Neve *et al.*, 1986; Shafit-Zagardo and Kalcheva, 1998). Il existe au moins quatre isoformes de la MAP2 qui peuvent être divisées en deux groupes: 1) les MAP2 de haut poids moléculaires (HMW MAP2): MAP2a (280 kDa) et MAP2b (270 kDa) et 2) les MAP2 de faible poids moléculaire (LMW MAP2): MAP2c (70 kDa) et MAP2d (75 kDa) (Figure 1). La différence majeure entre les HMW MAP2 et les LMW MAP2 est l'insertion d'une séquence de 1372 a.a. dans le domaine de projection des HMW MAP2 (Lewis *et al.*, 1988; Kindler *et al.*, 1990). MAP2a diffère de MAP2b par la présence d'une séquence additionnelle de 82 a.a. dans son domaine de projection (Chung *et al.*, 1996). MAP2d

contient 4 séquences répétées dans son domaine de liaison aux microtubules alors que MAP2c en a 3 (Ferhat *et al.*, 1994). L'expression de MAP2a, MAP2b et MAP2c est spécifique aux neurones alors que MAP2d peut aussi être retrouvée dans les cellules gliales (Doll *et al.*, 1993b; Ferhat *et al.*, 1994).

L'expression des isoformes de la MAP2 est régulée temporellement au cours du développement (Tableau 1). L'expression de MAP2b précède celle de MAP2a. MAP2a apparaît autour du jour postnatal 10 et est surtout proéminente dans le cerveau des rats âgés (Tucker, 1990; Chung *et al.*, 1996). Le niveau d'expression de MAP2c est élevé pendant le développement neuronal. Par la suite, MAP2c disparaît mais demeure exprimée dans le cerveau mature dans la rétine et le bulbe olfactif où la neurogénèse persiste tout le long de la vie adulte (Tucker and Matus, 1988; Viereck *et al.*, 1989; Tucker, 1990). MAP2d est détectée autour du jour postnatal 5 (Doll *et al.*, 1993b; Ferhat *et al.*, 1994). On retrouve les HMW MAP2 dans le corps cellulaire et les dendrites du système nerveux central mammifère alors que les LMW MAP2 sont retrouvées dans tous les compartiments neuronaux (Caceres *et al.*, 1984; Caceres *et al.*, 1986; Tucker and Matus, 1988; Meichsner *et al.*, 1993; Albala *et al.*, 1995; Chung *et al.*, 1996).

1.2.3 MAP2 : un régulateur de la dynamique des microtubules

Plusieurs études ont démontré que MAP2 module le comportement dynamique des microtubules *in vitro* et *in vivo*. MAP2 se lie aux microtubules le long des protofilaments individuels formant probablement des ponts entre les interfaces de tubuline (Al-Bassam *et al.*, 2002). Lorsque la MAP2 est liée aux microtubules *in vitro*, elle diminue le taux de rétraction rapide des microtubules et augmente le taux

d'élongation (Hirokawa, 1991). *In vivo*, nos travaux ainsi que ceux d'autres groupes ont démontré que l'expression de MAP2 dans des cellules non-neuronales induit la formation de faisceaux rigides de microtubules (Weisshaar *et al.*, 1992; Leclerc *et al.*, 1993; Matus, 1994). Les séquences répétées de 18 a.a. du domaine de liaison aux microtubules, en particulier la troisième séquence, ainsi que les régions qui les entourent, semblent être importants pour la formation de faisceaux de microtubules (Takemura *et al.*, 1995; Ludin *et al.*, 1996). La formation de faisceaux de microtubules pourrait être: 1) une conséquence de la liaison des microtubules entre eux du à la dimérisation de MAP2 ou 2) un effet non-spécifique de la MAP2 qui augmente la rigidité des microtubules (Sanchez *et al.*, 2000a).

1.2.4 MAP2 : une protéine de liaison à l'actine et aux neurofilaments

Plusieurs études ont démontré que la MAP2 est une ABP qui peut lier les microfilaments d'actine l'un à l'autre et causer la formation de faisceaux parallèles ou à angle *in vitro* et que ces activités dépendent de l'état de phosphorylation de la MAP2 (Sattilaro *et al.*, 1981; Selden and Pollard, 1983; Sattilaro, 1986; Selden and Pollard, 1986; Yamauchi and Fujisawa, 1988; Cunningham *et al.*, 1997).

Afin de causer la formation de faisceaux d'actine-F, une protéine doit posséder deux sites de liaison à l'actine ou bien doit avoir la capacité de former des dimères (Puius *et al.*, 1998). Dans le cas de la MAP2, un seul site de liaison à l'actine a déjà été identifié. Ce site correspond à la deuxième séquence répétée de 18 a.a. située dans le domaine de liaison aux microtubules de la MAP2 (Sattilaro, 1986; Correas *et al.*, 1990). Cependant, nous ne pouvons écarter la possibilité de la présence d'un deuxième site de

liaison à l'actine qui serait localisé dans le domaine de projection de la MAP2. En accord avec cette hypothèse, le domaine de projection de la MAP2 peut causer la formation de faisceaux parallèles d'actine-F *in vitro* (Leclerc, N. et Jamney, P., communication personnelle). De plus, les domaines de projection de la MAP2b et de la MAP2c co-localisent avec l'actine périphérique dans les cellules Sf9 (Belanger *et al.*, 2002). Donc, MAP2 pourrait contenir deux sites de liaison à l'actine-F, un qui serait situé dans son domaine de liaison aux microtubules et l'autre dans son domaine de projection, permettant ainsi la liaison d'un microfilament d'actine à un autre. D'un autre côté, MAP2 a une tendance prononcée à former des dimères antiparallèles (Wille *et al.*, 1992c; Wille *et al.*, 1992b). Donc, en dimérisant, MAP2 pourrait également causer la formation de faisceaux d'actine-F.

In vivo, MAP2 est capable de réorganiser les microfilaments d'actine dans les cellules Sf9 (Boucher *et al.*, 1999; Belanger *et al.*, 2002). De plus, MAP2c induit la formation de lamelles riches en actine dans une lignée cellulaire de mélanome qui est déficiente en ABP-280, une protéine stabilisatrice de l'actine-F (Cunningham *et al.*, 1997). En outre, la phosphorylation de la MAP2c au niveau de trois résidus Sérine, un dans chaque séquence répétée de 18 a.a., augmente l'association de la MAP2c avec le réseau cortical d'actine-F (Ozer and Halpain, 2000).

La MAP2 n'interagit pas seulement avec les microtubules et les microfilaments d'actine. En effet, MAP2 peut aussi interagir avec la sous-unité 70kDa des neurofilaments et peut lier les neurofilaments aux microtubules *in vitro* (Leterrier *et al.*, 1982; Heimann *et al.*, 1985; Hirokawa *et al.*, 1988). *In vivo*, MAP2 fait partie des ponts

qui lient les neurofilaments aux microtubules dans les dendrites des motoneurones de la moêlle épinière de rat (Hirokawa *et al.*, 1988).

En établissant un lien entre les microtubules, les microfilaments et les neurofilaments, MAP2 pourrait agir comme un intégrateur du cytosquelette neuronal. Récemment, une famille de protéines appelées 'plakines' a été identifiée qui peut lier les composantes du cytosquelette l'une à l'autre ainsi qu'aux jonctions adhésives associées à la membrane (Ruhrberg *et al.*, 1997; Green *et al.*, 1999; Karakesisoglou *et al.*, 2000; Leung *et al.*, 2001; van den Heuvel *et al.*, 2002). Les mutations dans les gènes de la famille des plakines conduisent à des défectuosités de l'intégrité tissulaire et de la fonction au niveau de la peau, du muscle et du système nerveux chez l'humain et la souris. Chez la Drosophile, ces mutations conduisent à la perte de l'adhésion entre le muscle et les cellules épidermales et à des défectuosités au niveau de la croissance neuronale (Borradori *et al.*, 1998; Mahoney *et al.*, 1998; Green *et al.*, 1999; Leung *et al.*, 1999a; Karakesisoglou *et al.*, 2000; Olivry *et al.*, 2000; Fujiwara *et al.*, 2001; Leung *et al.*, 2001; Lee and Kolodziej, 2002). De plus, plusieurs études ont confirmé l'importance des protéines de liaison du cytosquelette de type 'plakine' sur l'organisation et la fonction du cytosquelette (Andra *et al.*, 1998; Dalpe *et al.*, 1998; Dalpe *et al.*, 1999; Yang *et al.*, 1999). Que MAP2 soit capable de connecter les trois composantes cytosquelettiques suggère que cette protéine joue non seulement un rôle structurel dans le maintien de l'architecture du cytosquelette mais aussi un rôle fonctionnel dans la stabilisation et la déstabilisation des réseaux auxquels elle se lie. En accord avec ceci, MAP2 se promène entre les microfilaments et les microtubules pendant la croissance axonale dans des cultures primaires de neurones d'hippocampe de rat (Kwei *et al.*,

1998). De plus, les changements morphologiques induits par le ganglioside GM1 dans les cellules de neuroblastome Neuro-2a sont accompagnés par une réorganisation de l'association de MAP2 avec les microtubules et les microfilaments (Wang *et al.*, 1996a; Wang *et al.*, 1998; Kozireski-Chuback *et al.*, 1999; Colella *et al.*, 2000).

1.2.5 Interaction de MAP2 avec des protéines de signalisation

Mise à part son interaction avec les trois composantes du cytosquelette, MAP2 peut également interagir avec des protéines de signalisation. Par exemple, MAP2 peut interagir avec la sous-unité régulatrice RII de la protéine kinase AMP-cyclique dépendante (PKA). De plus, MAP2 peut ancrer la PKA au niveau de compartiments spécifiques dans la cellule (Rubino *et al.*, 1989; Davare *et al.*, 1999). Chez les souris mutantes nulles pour la MAP2, il y a une réduction du nombre total de PKA dans les dendrites et le taux d'induction du CREB phosphorylé est réduit suite à la stimulation par la forskoline (Harada *et al.*, 2002). D'un autre côté, MAP2b peut se lier directement à la sous-unité α-1 des canaux calciques de classe C - type L dans les neurones (Davare *et al.*, 1999). En interagissant simultanément avec la sous-unité régulatrice de la PKA et avec les canaux calciques de classe C - type L, MAP2b pourrait réguler la fonction neuronale en permettant la phosphorylation des canaux calciques enrichis aux sites postsynaptiques (Davare *et al.*, 1999). MAP2 peut également interagir avec les domaines SH3 des protéines c-Src et Grb2 *in vitro* (Lim and Halpain, 2000). Src et Grb2 interagissent surtout avec la MAP2c lorsque celle-ci n'est pas liée aux microtubules (Lim and Halpain, 2000). En outre, la séquence de 1372 a.a. de la MAP2b contient un

site de liaison pour la calmoduline, qui est connue pour inhiber la liaison de la MAP2b à l'actine (Kotani *et al.*, 1985; Kindler *et al.*, 1990). MAP2b contient également deux sites de liaison au phosphatidylinositol (PI): un site de liaison de faible affinité situé à l'extrémité C-terminale et un site de liaison de haute affinité situé dans la séquence additionelle de 1372 a.a. dans le domaine de projection de la protéine (Surridge and Burns, 1994; Burns and Surridge, 1995). L'association du PI avec la MAP2c inhibe l'interaction de celle-ci avec la tubuline et donc, module la dynamique des microtubules (Yamauchi and Purich, 1987). De plus, le PI inhibe l'interaction de MAP2 avec l'actine (Yamauchi and Purich, 1993). Finalement, une étude récente a rapporté que MAP2 interagit fortement avec les sous-unités 2A/B des récepteurs N-méthyl-D-aspartate (NMDA) (Buddle *et al.*, 2003).

1.2.6 Interaction de MAP2 avec la mitochondrie

Plusieurs groupes ont rapporté que la MAP2 pouvait interagir avec la mitochondrie (Jancsik *et al.*, 1989; Linden *et al.*, 1989a; Jung *et al.*, 1993). Le mouvement ainsi que la structure de la mitochondrie sont régulés par l'interaction de celle-ci avec le cytosquelette en particulier avec les microtubules (Linden *et al.*, 1989b). L'interaction entre MAP2 et la surface externe de la mitochondrie de cerveau de rat a été démontrée *in vitro* et *in situ* (Jancsik *et al.*, 1989; Linden *et al.*, 1989a; Jung *et al.*, 1993). Lorsque la MAP2 se lie à la mitochondrie, elle induit un changement physique dans les propriétés de la membrane externe de celle-ci, ce qui conduit à une association plus ferme de la protéine mitochondriale 'Porine' avec la membrane (Linden *et al.*,

1989a; Linden *et al.*, 1989b). Bien que les deux domaines fonctionnels de la MAP2 puissent se lier à la mitochondrie, il semblerait que l'association se fait surtout par le domaine de liaison aux microtubules (Jancsik *et al.*, 1989).

1.2.7 La Phosphorylation: un mécanisme de régulation de la fonction de MAP2

La phosphorylation est la modification post-traductionelle la plus importante que MAP2 subit. MAP2 est le substrat de plusieurs kinases et phosphatases et peut contenir jusqu'à 46 moles de phosphate par mole de protéine *in vivo* (Tsuyama *et al.*, 1987; Sanchez *et al.*, 2000a). Dans la figure 2, nous présentons les sites de phosphorylation précis qui ont été identifiés jusqu'à présent dans la MAP2. Dans cette section, je ferai un aperçu des principales kinases et phosphatases et leur effet sur la fonction de MAP2.

MAP2 est riche en résidus Sérine/Thréonine et donc, est un bon substrat pour les kinases Ser/Thr. Par exemple, la PKA phosphoryle la MAP2 *in vitro* sur au moins 11 différentes sérines situées dans le domaine de liaison aux microtubules et le domaine de projection de MAP2 (Goldenring *et al.*, 1985; Yamamoto *et al.*, 1985; Goldenring and DeLorenzo, 1986). La phosphorylation de MAP2 par la PKA: 1) inhibe ses activités de liaison et de nucléation des microtubules *in vivo* et *in vitro*, 2) inhibe sa capacité à induire la formation de faisceaux d'actine *in vitro* et augmente l'association de MAP2c avec l'actine périphérique *in vivo* lorsque celle-ci est phosphorylée au niveau de trois résidus Sérine, un dans chaque séquence répétée de 18 a.a. (figure 2) et 3) protège la MAP2 contre la dégradation par les calpaines (Burns *et al.*, 1984; Yamamoto *et al.*, 1985; Yamauchi and Fujisawa, 1988; Johnson and Foley, 1993; Alexa *et al.*, 1996; Itoh

et al., 1997; Ozer and Halpain, 2000). La protéine kinase calcium-calmoduline dépendante II (CAMKII) peut aussi phosphoryler la MAP2 *in vitro* sur au moins 18 sites situés dans le domaine de liaison aux microtubules et le domaine de projection de la MAP2 (Yamauchi and Fujisawa, 1982; Hernandez *et al.*, 1987a; Walaas and Nairn, 1989). La phosphorylation de MAP2 par la CAMKII: 1) inhibe sa capacité à promouvoir l'assemblement des microtubules *in vitro* et 2) inhibe sa capacité à induire la formation de faisceaux d'actine *in vitro* (Yamamoto *et al.*, 1983; Yamamoto *et al.*, 1985; Yamauchi and Fujisawa, 1988). Finalement, la protéine kinase C (PKC) peut aussi phosphoryler MAP2 sur au moins 15 différents sites *in vitro*, dont la plupart sont situés dans le domaine de projection de la protéine (Akiyama *et al.*, 1986; Hernandez *et al.*, 1987a; Tsuyama *et al.*, 1987; Walaas and Nairn, 1989; Ainsztein and Purich, 1994). La phosphorylation de MAP2 par la PKC: 1) inhibe sa capacité à induire la polymérisation de la tubuline, 2) lorsque trois résidus sérine sont phosphorylés dans le domaine de liaison aux microtubules, l'association de MAP2 avec les microtubules est complètement abolie (figure 2), 3) inhibe sa capacité à se lier aux microfilaments et 4) protège la MAP2 contre la dégradation par les calpaines (Akiyama *et al.*, 1986; Hoshi *et al.*, 1988; Ainsztein and Purich, 1994; Alexa *et al.*, 1996).

Les kinases 'proline-directed' (PDK) constituent une autre catégorie d'enzymes qui peuvent phosphoryler MAP2 dans les régions riches en prolines de la protéine. Les résidus proline peuvent exister en deux conformations: cis et trans. La phosphorylation d'une protéine au niveau de résidus proline peut donc causer des changements importants de sa conformation ce qui peut également affecter sa fonction. Les kinases régulées par les signaux extracellulaires (ERKs) appartiennent à la famille des PDKs et

peuvent phosphoryler MAP2 *in vitro* (Cobb *et al.*, 1991; Avruch, 1998). La plupart des sites de phosphorylation sont situés dans le domaine de projection de MAP2 (Fellous *et al.*, 1994). La phosphorylation de MAP2 par les ERKs inhibe sa capacité à induire la polymérisation de la tubuline (Hoshi *et al.*, 1992). La GSK3β est une autre PDK qui peut phosphoryler MAP2 au niveau du résidu Ser^{136} et de deux résidus thréonines, Thr^{1620} et Thr^{1623}, qui sont situés dans la région riche en prolines (figure 2) (Berling *et al.*, 1994; Sanchez *et al.*, 1996). La phosphorylation de MAP2 par la GSK3β inhibe ses capacités à se lier aux microtubules et à les organiser en faisceaux *in vivo* (Sanchez *et al.*, 2000b).

Plusieurs autres kinases peuvent aussi phosphoryler MAP2. Par exemple, les kinases associées à Rho phosphorylent MAP2 sur le résidu Ser^{1796} *in vitro* et les kinases régulatrices de l'affinité aux microtubules (MARKs) phosphorylent MAP2 dans son domaine de liaison aux microtubules (Drewes *et al.*, 1997; Drewes *et al.*, 1998; Amano *et al.*, 2003). La phosphorylation de MAP2 par les MARKs la détache des microtubules (Drewes *et al.*, 1997; Drewes *et al.*, 1998).

MAP2 est également le substrat de plusieurs phosphatases. Les principales protéines phosphatases (PP) exprimées dans le cerveau sont: PP1, PP2A, PP2B et PP2C (Cohen, 1989; Cohen and Cohen, 1989; Cohen *et al.*, 1989; Pei *et al.*, 1994). MAP2 peut être déphosphorylée *in vitro* par les PP1, PP2A et PP2B (Goto *et al.*, 1985; Patterson and Flavin, 1986; Sanchez *et al.*, 1996). *In vivo*, l'inhibition de l'activité de la PP2A par l'acide okadaique inhibe la capacité de MAP2 à se lier aux microtubules (Gong *et al.*,

2000a). En dernier lieu, une étude récente par Amano et collègues a démontré que MAP2 est un substrat pour les myosines phosphatases (Amano *et al.*, 2003).

Une modification de l'état de phosphorylation de MAP2 en réponse à des signaux externes pourrait être à la base des changements morphologiques qui ont lieu au cours de la différenciation neuronale et du remodelage dendritique qui a lieu à l'âge adulte. En accord avec cette hypothèse, une augmentation de l'état de phosphorylation de MAP2 de haut poids moléculaire corrèle avec l'arborisation dendritique dans des cultures primaires de neurones de l'hippocampe (Diez-Guerra and Avila, 1995). De plus, une augmentation de l'état de phosphorylation de MAP2 résulte en un nombre élevé de branchements neuritiques et une diminution de son état de phosphorylation en un faible nombre de branchements neuritiques (Audesirk *et al.*, 1997). À l'âge adulte, un changement de l'état de phosphorylation de MAP2 de haut poids moléculaire accompagne les changements d'efficacité synaptique qu'on soupçonne être sous-jacents au remodelage morphologique (Diaz-Nido *et al.*, 1993; Quinlan and Halpain, 1996b, a).

Mais comment est-ce qu'un changement de l'état de phosphorylation de MAP2 peut-il se traduire en changements morphologiques au niveau du neurone? Étant donné qu'une modification de l'état de phosphorylation de MAP2 affecte son association avec les microtubules et les microfilaments d'actine, l'hypothèse la plus plausible est que MAP2 pourrait agir surtout sur la dynamique des microtubules et sur l'organisation des microfilaments d'actine. Cependant, le fait que la MAP2 puisse aussi interagir avec les neurofilaments, avec des compartiments membranaires et avec des protéines de signalisation laisse soupçonner un changement de son interaction avec ces composantes-là également lorsque la structure neuronale est modifiée.

Dans cette thèse, nous avons tenté de comprendre de quelle manière MAP2 participe-t-elle à l'établissement de la polarité neuronale au cours du développement et au maintien de cette structure à l'âge adulte. En premier lieu, nous avons tenté de mieux définir le rôle du domaine de projection de MAP2. Dans le passé, certaines études avaient suggéré un rôle structurel pour ce domaine dans la régulation de l'espacement entre les microtubules. Nos résultats confirment ce rôle et démontrent que ce domaine régule la capacité de MAP2 à induire la formation de prolongements cytoplasmiques. En deuxième lieu, nous avons étudié les altérations du niveau d'expression protéique et de la distribution membranaire de la MAP2 chez des souris mutantes SOD1. Ces souris récapitulent le tableau neuropathologique de la sclérose latérale amyotrophique, une maladie neurodégénérative dans laquelle on assiste à une perte de la structure et de la fonction neuronale. Nos résultats démontrent que le niveau d'expression de la MAP2 diminue cinq mois avant l'apparition des symptômes cliniques chez les souris mutantes SOD1 et que la distribution membranaire de MAP2 est non seulement altérée mais corrèle avec la neurodégénérescence chez ces souris. En dernier lieu, nous avons démontré que MAP2 interagit avec le réticulum endoplasmique rugueux et peut même effectuer un lien entre celui-ci et les microtubules. Nos résultats suggèrent donc que la MAP2 pourrait contribuer à la polarisation des composantes membranaires au cours de la différenciation neuronale et au maitien de leurs structures à l'âge adulte.

Tableau 1. Changement du niveau protéique des MAP2 de haut poids moléculaire (HMW MAP2), soit la MAP2a et la MAP2b et de celles de faible poids moléculaire (LMW MAP2) dans le cerveau de rat à différents âges. La technique d'immunobuvardage fut utilisée. Les chiffres représentent l'intensité relative des bandes protéiques mesurée à l'aide d'un densitomètre de réflectance (*adapté de Riederer and Matus (1985)*)

	P0	P5	P10	P15	P20	ad*
MAP2a	X	X	X	0.57	0.89	0.67
MAP2b	1	0.98	1.11	1.07	1.11	0.88
LMW MAP2	0.84	0.71	0.63	0.58	0.15	0.07

P = âge postnatal, * ad = adulte

Figure 1. Plusieurs isoformes de la MAP2 sont générées par épissage alternatif au cours du développement neuronal. Ces isoformes peuvent être regroupées en deux catégories: 1) Les MAP2 de haut poids moléculaire (HMW MAP2), soit la MAP2a et la MAP2b et 2) Les MAP2 de faible poids moléculaire (LMW MAP2), soit la MAP2c et la MAP2d.

MAP2 de faible poids moléculaire (LMW MAP2)

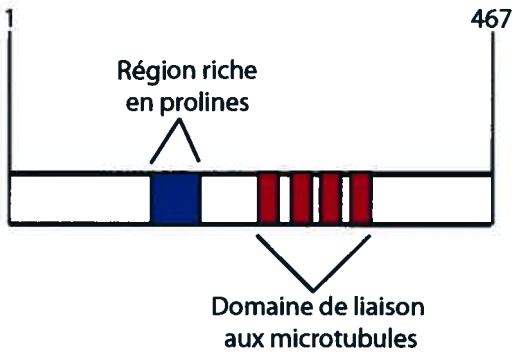

MAP2 de haut poids moléculaire (HMW MAP2)

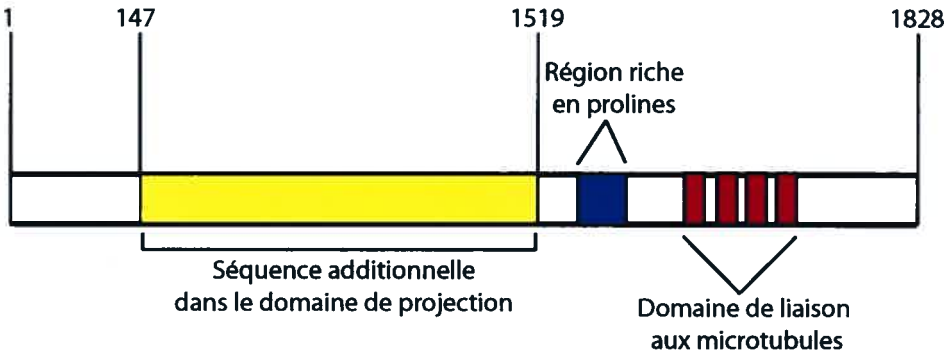

Figure 2. Les sites de phosphorylation précis qui ont été identifiés jusqu'à présent au niveau de la MAP2 sont indiqués en caractère gras (*adaptée de Sanchez et al., 2000a)*. Les cercles représentent les résidus qui sont phosphorylés par la PKC et les rectangles, ceux qui sont phosphorylés par la PKA.

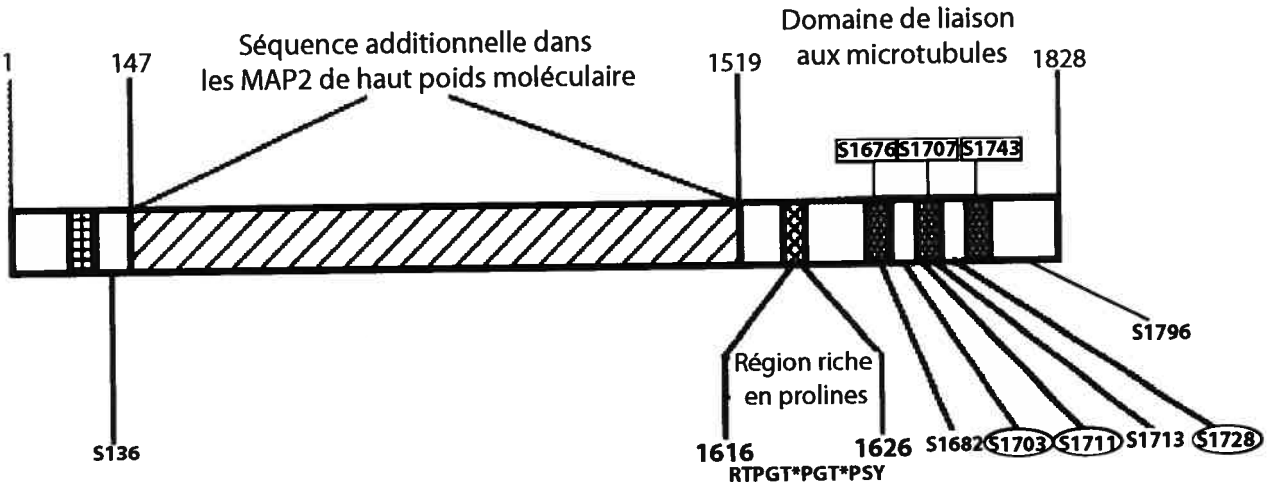
1
147
Séquence additionnelle dans
les MAP2 de haut poids moléculaire
1519
Domaine de liaison
aux microtubules
1828
S1676
S1707
S1743
S1796
Région riche
en prolines
S136
1616
RTPGT*PGT*PSY
1626
S1682
S1703
S1711
S1713
S1728

2 PREMIER ARTICLE

"Bélanger, D., Abi Farah, C., Nguyen, M.D., Lauzon, M., Cornibert, S., et Leclerc, N. (2002) The projection domain of MAP2b regulates microtubule protrusion and process formation in Sf9 cells. *Journal of Cell Science* **115**: 1523-1539."

The projection domain of MAP2b regulates microtubule protrusion and process formation in Sf9 cells

Dave Bélanger*, Carole Abi Farah *, Minh Dang Nguyen¶, Michel Lauzon, Sylvie Cornibert and Nicole Leclerc

Département de pathologie et biologie cellulaire, Université de Montréal, Montréal, Québec, Canada, H3T 1J8; ¶ Montreal General Hospital Research Institute in Neuroscience, McGill University, Montréal, Canada, H3G 1A4

* D.B. and C.A.F. have equally contributed to the experimental work in this study

Running title: MAP2b-induced microtubule protrusion

Corresponding author:
Dr Nicole Leclerc
Département de pathologie et biologie cellulaire
Université de Montréal
C.P.6128, Succ. Centre-ville
Montréal, Québec
Canada H3C 3J7
Phone: (514)-343-5657
Fax: (514)-343-5755
[redacted]

ACKNOWLEDGEMENTS

We thank Dr. Virginia Lee (University of Pennsylvania, USA) for providing the antibody 46.1. We acknowledge the excellent technical help of Gaston Lambert and Antonio Allegia. We also thank Michel Lamoureux, Alexandre Cusson and Yves Lepage for their help in the statistical analysis. We are grateful to Annie Vallée for her technical help. This work was supported by Medical Research Council of Canada grant (MT-13245), by National Sciences and Engineering Research Council of Canada grant (NSERC) and by FCAR grant to N.L. NL is Scholar of the FRSQ. C. Abi Farah has a studentship from CRSN and M.D. Nguyen has a studentship from MRC.

2.1 ABSTRACT

The expression of microtubule-associated protein-2 (MAP2), developmentally regulated by alternative splicing, coincides with neurite outgrowth. MAP2 proteins contain a microtubule-binding domain (C-terminal) that promotes microtubule assembly and a poorly characterized domain, the projection domain (N-terminal), extending at the surface of microtubules. MAP2b differs from MAP2c by an additional sequence of 1372 amino acids in the projection domain. In this study, we examined the role of the projection domain in the protrusion of microtubules from cell surface leading to process formation in Sf9 cells. In this system, MAP2b has a lower capacity to induce process formation than MAP2c. To investigate the role of the projection domain in this event, we expressed truncated forms of MAP2b and MAP2c that have partial or complete deletion of their projection domain in Sf9 cells. Our results indicate that process formation is induced by the microtubule-binding domain of these MAP2 proteins and is regulated by their projection domain. Furthermore, the microtubule binding activity of MAP2b and MAP2c truncated forms as well as the structural properties of the microtubule bundles induced by them do not seem to be the only determinants that control the protrusion of microtubules from cell surface in Sf9 cells. Our data rather suggests that microtubule protrusion and process formation would be regulated by intramolecular interactions between the projection domain and its microtubule- binding domain in MAP2b.

2.2 INTRODUCTION

Neurons undergo important morphological remodeling during their differentiation and adaptative events in adult brain. Differentiating neurons become polar by elaborating two types of neuritic compartments: dendrites and axon. The cytoskeletal proteins act as intrinsic determinants in the acquisition of the shape of a neuron during its differentiation. As such, the microtubule-associated proteins are involved in the elaboration of the neuritic compartments. In particular, the suppression of the microtubule-associated protein-2 (MAP2) expression in primary neuronal culture inhibits the formation of neurites (Caceres *et al.*, 1992). Moreover, the inhibition of MAP2 expression in ECP19 cells which undergo neuronal differentiation in the presence of retinoic acid inhibits the development of neurites as well as the withdrawal of these cells from the cell cycle (Dinsmore and Solomon, 1991). In adult neurons, MAP2 is enriched in dendrites (Ludin and Matus, 1993) and seems to exert a stabilizing effect on the dendritic morphology since its suppression or degradation was correlated with dendritic loss or remodeling (Sharma *et al.*, 1994; Faddis *et al.*, 1997). Futhermore, changes of MAP2 phosphorylation were observed during neuronal plasticity (Halpain and Greengard, 1990; Quinlan and Halpain, 1996b).

Diverse MAP2 isoforms generated by alternative splicing contribute to neuronal differentiation (Tucker, 1990). In the COOH-terminus, these isoforms present a microtubule-binding domain similar to that found in MAP4 and in the low molecular weight MAP, tau (Lewis *et al.*, 1988; Lewis *et al.*, 1989). It contains 3 to 4 imperfect repeats of 18 amino acids (a.a.) responsible for the binding to microtubules. The NH_2-

terminus is called the projection domain since it projects at the surface of microtubules. There exists at least four isoforms of MAP2: MAP2a, MAP2b, MAP2c and MAP2d. MAP2a and MAP2b, the high molecular weight isoforms, are the predominant isoforms found in the neurons of the adult CNS (Chung *et al.*, 1996). They are only expressed in dendrites. MAP2b is expressed before MAP2a during neuronal differentiation (Tucker, 1990). Recently, new variants of the high molecular weight MAP2 have been identified that contain additional sequences in the amino- and carboxyl-terminus (Couchie *et al.*, 1996; Forleo *et al.*, 1996; Kalcheva *et al.*, 1997). MAP2c and MAP2d, the low molecular weight isoforms of MAP2 differ by the fact that MAP2d contains 4 repeats in the carboxyl-terminus for the binding to microtubules whereas MAP2c has three repeats (Ferhat *et al.*, 1994b). MAP2c is found in growing dendrites and, in certain populations of neurons, also in growing axons (Tucker, 1990). Interestingly, it remains expressed in neurons that have the capacity to regenerate in the adult CNS (Tucker, 1990).

MAP2b and MAP2c are the two best characterized isoforms of MAP2. MAP2c is a 467 amino acid (a.a.) protein whereas MAP2b is a 1828 a.a. protein that contains an additional sequence of 1372 a.a. in the amino-terminus whose function is unknown (Neve *et al.*, 1986; Papandrikopoulou *et al.*, 1989). This additional sequence shifts the apparent molecular weight of MAP2b from 70 KDa to 280 KDa. The most studied functions of these isoforms are their ability to promote microtubule assembly and to stabilize microtubules (Ludin and Matus, 1993). They also induce microtubule bundling but the spacing between microtubules is less in MAP2c-induced microtubules than in MAP2b-induced microtubules (Chen *et al.*, 1992; Leclerc *et al.*, 1996). Thus, it has been

concluded that the length of the projection domain of MAP2 is one primary determinant of the spacing between microtubules.

When overexpressed in cultured non-neuronal cells, MAP2b and MAP2c induce microtubule protrusion from cell surface thus causing the formation of cytoplasmic processes (Edson *et al.*, 1993; Leclerc *et al.*, 1993; Langkopf *et al.*, 1995; Leclerc *et al.*, 1996; Boucher *et al.*, 1999). In some systems, depolymerisation of the actin cortical network is required to allow microtubule protrusion from cell surface (Edson *et al.*, 1993). In other systems such as Sf9 cells, spontaneous protrusion of microtubules and process formation occurs upon overexpressing MAP2b or MAP2c (Leclerc *et al.*, 1993; Leclerc *et al.*, 1996). In this study, we used the baculoviral expression system in Sf9 cells to characterize the role of the projection domain of MAP2 in the protrusion of microtubules from the cell surface leading to process formation in these cells. In Sf9 cells, MAP2c has a higher capacity than MAP2b to induce process formation(Leclerc *et al.*, 1993; Leclerc *et al.*, 1996). Thus, it appears that the additional sequence of 1372 a.a. contained in the projection domain of MAP2b influences the protrusion of microtubules from the cell surface in these cells. In the present study, we generated truncated forms of MAP2b and MAP2c that had partial or complete deletion of the projection domain. Our results indicate that the formation of processes is induced by the microtubule-binding domain and is regulated by the projection domain of these MAP2 proteins. Furthermore, our results indicate that the structural properties of the microtubule bundles induced by MAP2c and MAP2b truncated forms are not the sole factors contributing to microtubule protrusion from Sf9 cells. The regulatory effects of the projection domain on

microtubule protrusion would involve intramolecular interactions between this domain and the microtubule-binding domain.

2.3 MATERIALS AND METHODS

2.3.1 Baculoviral recombinants

All MAP2 constructs contain a 6xHis tag at the NH_2-terminus. The engineering of MAP2-His fusion protein was performed in three steps. First, the full-length MAP2b cDNA cloned in the baculovirus expression vector pVL1392 was digested with BamHI and cloned into the sites BamHI and BglII of the vector pBacPAK His2 (Clontech, Palo Alta, CA, USA) (MAP2b-Bac PAK His2). Second, the non-coding sequence of MAP2b was deleted to engineer the His fusion protein. This was done by adding by PCR a BamHI site in 5' of the coding sequence of MAP2b. All PCR products were generated by using the Pfu enzyme (Stratagene, La Jolla, CA, USA) and were cloned into the blunt end vector Pstblue (Novagen). The PCR product, cloned in the Pstblue vector, containing the BamHI site, was digested with BamHI and XhoI and cloned into the pBacPAK His2 vector (PCR1-BacPAK His2). Third, the PCR1-Bac PAK His2 was digested with NcoI (this site is comprised in the MAP2b sequence amplified by PCR) and inserted in the MAP2b-pBacPak His2 that was also digested with NcoI.

Five MAP2b constructs having a deletion of nucleotides 656 to 1921 (MAP2b-1), 1921 to 3320 (MAP2b-2), 3329 to 4772 (MAP2b-3), 1 to 4772 (Mt) and 4772 to 5881 (Prob) were produced. To delete the nucleotides 656 to 1921 (MAP2b-1), a ScaI site was inserted in 3' of nucleotide 656 by PCR. A PCR product containing the MAP2b sequence from nucleotide 378 to 656-ScaI (PCR-C1) was cloned into the blunt end

Pstblue vector. The insertion of PCR-C1 into the MAP2b-BacPAK His2 vector was done in three steps. First, the sequence from 1 to 5471 of MAP2b-His sequence was subcloned into the BamHI and XhoI sites of the Bluescript vector ($MAP2b_{1\text{-}5471\text{-}BS}$). The nucleotides from 378 to 1921 of the MAP2b sequence were deleted by digestion of $MAP2b_{1\text{-}5471\text{-}BS}$ with KasI and ScaI. Second, the PCR-C1 cloned into the Pstblue vector was digested with KasI and ScaI and subcloned into the sites KasI and ScaI of the $MAP2b_{1\text{-}5471\text{-}BS}$ vector (C1-MAP2b1-5471-BS). Third, the sequence of MAP2b containing the deletion from 656 to 1921 was cut from the $MAP2b_{1\text{-}5471\text{-}BS}$ by digestion with BamHI and XhoI and re-inserted in the MAP2b-BacPAK His2 vector.

To delete the nucleotides 1921 to 3329 (MAP2b-2), a Xba1 site was inserted in 3' of nucleotide 1921 by PCR. A PCR product containing the MAP2b sequence from nucleotides 378 to 1921-Xba1 (PCR-C2) was cloned into the vector Pstblue. The insertion of PCR-C2 into MAP2b-BacPAK His2 vector was done in three steps. First the nucleotides 1 to 3121 of MAP2b-His sequence were subcloned into the Bluescript vector ($MAP2b_{1\text{-}3121\text{-}BS}$). Second, the PCR-C2 cloned into the PSTblue vector was digested with Kas1 and Xba1 and subcloned into the corresponding sites of $MAP2b_{1\text{-}3121\text{-}BS}$ (C2-$MAP2b_{1\text{-}3121\text{-}BS}$). Third, the sequence of MAP2b containing the deletion from 1921 to 3329 was cut from the C2-$MAP2b_{1\text{-}3121\text{-}BS}$ by digestion with BamHI and XbaI and re-inserted in the MAP2b-BacPAK His2 vector.

To delete the nucleotides 3329 to 4472 (MAP2b-3), a XbaI site was inserted in 3' of nucleotide 4472 by PCR. A PCR product containing the MAP2b sequence from nucleotides 3329 to 4472-XbaI (PCR-C3) was cloned into the blunt end Pstblue vector.

The insertion of PCR-C3 into MAP2b-BacPAK His2 vector was done in three steps. First, the nucleotides 3329 to 5513 of MAP2b-His sequence was subcloned into the Pstblue vector (MAP2b-$_{3329\text{-}5513\text{-}Pb}$) at the SphI and XbaI sites. Second, the PCR-C3 cloned into the Pstblue vector was digested with SmaI and XbaI and subcloned into the corresponding sites of MAP2b-3329-5513-Pb (C3- MAP2b-$_{3329\text{-}5513\text{-}Pb}$). Third, the sequence of MAP2b containing the deletion from 3329 to 4772 was cut from the C3-MAP2b-$_{3329\text{-}5513\text{-}Pb}$ by digestion with XbaI and SphI and re-inserted in the MAP2b-BacPAK His2 vector.

A truncated form of MAP2b corresponding to the microtubule-binding domain (Mt) was generated by deleting the nucleotides 1 to 4772. To do so, a BamHI site was inserted at the 4765 nucleotide by PCR. MAP2b-pBacPAK His2 was digested with BamHI and SphI. The deleted sequence was replaced by the PCR product digested with the same restriction enzymes.

A truncated form of MAP2b corresponding to the projection domain of MAP2b (Prob) was produced by deleting the nucleotides 4772 to 5881. First, a NotI site was inserted at the 4772 nucleotide of the MAP2b sequence by PCR. MAP2b-pBacPAK His2 was digested with NotI and XbaI. The deleted sequence was replaced by the PCR product digested with the same restriction enzymes.

We also engineered a truncated form that corresponds to the projection domain of MAP2c (Proc) (nucleotides 1 to 444). To do so, the MAP2c sequence was inserted into the pBacPAK vector. MAP2c was removed from the pCMV vector by digestion with NotI and inserted into the pBacPAK His2 at the NotI site. The start codon of

MAP2c and the 5' untranslated region was removed. To do so, a BamHI was inserted at the start codon of MAP2c by directed mutagenesis. MAP2c-pBacPAK was digested with BamHI and PstI. The deleted part was replaced by the PCR product digested with the same restriction enzymes. To generate a truncated form of MAP2c corresponding to its projection domain, a NotI site was inserted by directed mutagenesis at the nucleotide 444 of the MAP2c sequence. MAP2c-pBacPAK His2 was digested with NotI and NcoI. The deleted sequence was replaced by the PCR product digested with the same restriction enzymes.

The transfer vector containing the different mutated forms of MAP2b and MAP2c were co-transfected with the *Bsu36I*-digested BacPAK6 viral DNA onto the Spodoptera frugigerpa (Sf9) cells using bacfectin (Clontech, Palo Alta, CA, USA).

2.3.2 Cell culture

The Sf9 cells were obtained from the American Type Culture Collection (ATCC # CRL 1711; Rockville, MD). Sf9 cells were grown in Grace's medium (Gibco BRL, Burlington, Ontario, Canada) supplemented with 10% fetal bovine serum (Immunocorp, Montreal, Quebec, Canada) as a monolayer at 27°C. For infection, cells were plated on glass coverslips at a density of $1X10^6$ cells/ 60 mm dish. Cells were infected for 24 or 72 hours with viral stock at various multiplicities of infection (m.o.i.).

2.3.3 Immunofluorescence

For immunochemistry, the cells were fixed in 4% paraformaldehyde in phosphate-buffered saline (PBS) for 20 min. Then the cells were permeabilized with

0.2% Triton X-100 in PBS for 5 min. The expression of the truncated forms of MAP2b and MAP2c except MT was revealed by using a monoclonal antibody directed against MAP2 (clone HM2, dilution 1:200) purchased from Sigma (Mississauga, Ontario, Canada). The Mt mutant was revealed by the monoclonal antibody 46.1 directed against the microtubule-binding domain of MAP2 (kindly provided by Dr. V. Lee, University of Pennsylvania, USA). To visualize the microtubule reorganization, a monoclonal antibody directed against α-tubulin (Sigma, dilution 1:500) was used. The actin reorganization was visualized with Rhodamin-phalloidin (Molecular Probe inc. Eugene, Oregon, USA), at a dilution of 1:200. We used the following secondary antibodies (Jackson Immunoresearch Laboratories Inc., Bio/Cam, Mississauga, Ontario, Canada): the anti-mouse Fab fragment conjugated to rhodamine (dilution 1:500) and a donkey anti-mouse conjugated to FITC (dilution 1:500). All these antibodies were diluted in PBS plus 5% BSA. Incubation was carried out at room temperature for 1h. After three washes in PBS, the coverslips were mounted in moviol and visualized by fluorescence microscopy.

2.3.4 Preparation of microtubules

Microtubules were purified from Sf9 cells as previously described by Vallee ('86) with slight modifications (Vallee and Collins, 1986). Briefly, cells were collected by centrifugation at 1000 rpm for 3 min. The cells were then suspended in the PEM buffer (0.1 M Pipes-NaOH, pH 6.6, 1 mM EGTA and 1 mM $MgSO_4$) to which a cocktail of protease inhibitors has been added right before use. Sf9 cells are then homogenized using a Dounce homogenizer and centrifuged for 30 min at 18,000 rpm at 2°C. The

supernatant is recovered and centrifuged at 45,000 rpm for 90 min at 2°C. The supernatant is collected again. Taxol is added to 20 μm and GTP to 1mM. The solution is warmed to 37°C for 5 min. It is then chilled on ice for 15 min before being transferred to a centrifuge tube. Ice cold sucrose underlayer solution (to which taxol, 20 μm and GTP 1mM were added just prior to use) is introduced at the bottom of the tube with a Pasteur pipette, and the sample is centrifuged at 2°C at 18,000 rpm for 30 min. The microtubule pellet is then resuspended in ice cold PEM buffer (containing taxol and GTP) and centrifuged again in the cold.

2.3.5 Extraction of the cytoskeleton

At 48 hours post-infection, Sf9 cells were washed in PBS and then suspended in the extraction buffer (Pipes, 80 mM, pH 6.8, 0.05% IGEPAL, 1mM $MgCl_2$, 5mM EGTA) to which protease inhibitors were added prior to use. Extraction was allowed to proceed for 2 min. Cells are then centrifuged at 1200 rpm for 2 min. The pellet is resuspended in Pipes, 80 mM, pH 6.8, 1mM $MgCl_2$, 5mM EGTA. Cells are then lysed using PBS buffer containing 1% IGEPAL and 0.1% SDS. For drug treatment, colchicine, 10 μm was added to the cultures 2 hrs prior to extraction. For cold treatment, cultures were incubated in an ice-bath for 30 min before the extraction is performed.

2.3.6 Immunoblotting and dot blotting

The expression of the truncated forms of MAP2 in the Sf9 cells was confirmed by western blot. To do so, the transfected cells were centrifugated at 1000 rpm for 3min.

The pellets were resuspended into PBS containing protease inhibitors (5μg/ml of antipain, aprotinin and leupeptin, 1 mMEDTA, 100μg/ml PMSF and 7 mM DFP). An equal volume of sample buffer was added to the cell suspension and then it was boiled for 5 min. The protein were separated on a 7.5% polyacrylamide gel and transferred on nitrocellulose membrane. The antibodies used to visualized the proteins were HM2 (Sigma) 46.1(kindly provided by Dr. V. Lee, University of Pennsylvania) or an anti-His antibody (Santa Cruz, Santa Cruz, CA, USA). The secondary antibodies were conjugated to HRP (Jackson Immunoresearch Laboratories Inc., Bio/Cam, Mississauga, Ontario, Canada) and revealed by chemiluminescence (Roche, Laval, Québec, Canada). For dot blotting, 30μg of total protein extract prepared from infected cells were applied to a nitrocellulose membrane using a dot blot Manifold apparatus. The membrane was air dried for 30 minutes and was incubated in the primary antibody against MAP2 for 60 min at room temperature. The membrane was then washed and incubated in the secondary antibody conjugated to HRP (Jackson Immunoresearch Laboratories Inc., Bio/Cam, Mississauga, Ontario, Canada) and revealed by chemiluminescence (Roche, Laval, Québec, Canada). To quantify the protein level, the autoradiographic dots were scanned and the digitized data were quantified using the program ImageQuant (Molecular dynamics).

2.3.7 Co-immunoprecipitation

The cells were washed twice in PBS. Then, they were lysed in RIPA buffer (50mM Tris, 150mM NaCl, 0.02% sodium azide, 1% Nonidet P-40, 0.5% sodium dexycholate and 0.1% SDS) containing protease inhibitors for 30 minutes at 4°C. The

cell lysates were centrifuged for 10 minutes at 12 000g at 4°C. The primary antibodies directed against MAP2, AP18 (1:100) or AP20 (1:400), were added to the cell lysates and incubated for 1 hour at 4°C on a rocking platform. Then, 50 µl of protein A-agarose was added to the cell lysates and incubated overnight at 4°C on a rocking platform. The complexes were collected by centrifugation for 20 seconds at 12 000g at 4°C. The supernatant was carefully removed and the beads were resuspended in 1 ml of RIPA and incubated for 20 minutes at 4°C on a rocking platform. This step was repeated four times. Finally, the beads were resuspended in 40µl of loading buffer and boiled for 5 minutes. The protein A-agarose was removed by centrifugation at 12 000g for 20 s at room temperature. The sample were analyzed by SDS-PAGE.

2.3.8 Electron microscopy

For transmission electron microscopy, Sf9 cells were grown on glass coverslips at a density of 2.0 x 10^6 cells / 60 mm dish. Cells were infected for 48 or 72 hours with viral stock at a multiplicity of infection (m.o.i.) of 5. The cultures were fixed in a solution containing 2% glutaraldehyde and 2 mg/ml tannic acid for 15 min, rinsed in a solution of 5% sucrose in 0.1 M cacodylate, postfixed for 10 min with 1% osmium tetroxide, dehydrated with increasing concentrations of ethanol, and embedded using EPON resin (Cedarlane laboratories, Hornby, Ontario, Canada). After curing the resin, cells were sectioned parallel to the long axis of the processes. The spacing between microtubules was measured using either the NIH Image 1.62 program or the Pro

AnalySIS program. Measurements were made in the proximal region of the processes. We performed 50 random measurements per process.

2.3.9 Quantitative morphological analysis

The morphological analysis was performed by two observers. Three sets of experiments were analyzed. The morphological phenotypes observed with the different truncated forms of MAP2 were highly reproductible from one set of experiments to another. To evaluate the number of processes per cell, 150 cells were measured for each truncated form of MAP2 in each set of experiment. To analyze the process length, 50 cells were used for each truncated form of MAP2 in each set of experiment.

2.3.10 Statistical analysis

The distribution of the percentage of cells with one, two or >more than two processes was analyzed for each truncated form and full-length MAP2c and MAP2b in three sets of experiments. To analyze the reproducibility of the data from one set of experiment to another, a chi-square test followed by the Fisher's Exact test was performed. Since the distribution was not statistically different from one experiment to another, the three experiments were combined for the statistical analysis. The differences among truncated and full-length MAP2c and MAP2b in the distribution of the number of processes par cell was analyzed by a chi-square test followed by the Fisher's Exact test. The length of process was analyzed by one-way ANOVA followed by the Sheffe test. For electron microscopy analysis, the statistical significance of the spacing between

microtubules was determined using one-way ANOVA followed by Fisher's PLSD test. Statistical significance was accepted if $p < 0.05$.

2.4 RESULTS

2.4.1 The projection domain of MAP2b regulates negatively the capacity of the microtubule-binding domain to induce process formation in Sf9 cells

Our previous work showed that the expression of MAP2b and MAP2c results in the formation of cytoplasmic processes in Sf9 cells. These processes seem to be induced by the protrusion of microtubule bundles from these cells. MAP2b having a significant lower tendency than MAP2c to induce cell processes indicates that the MAP2b-induced microtubule bundles are less capable than those of MAP2c to protrude at the cell surface. Since MAP2b and MAP2c differ by their projection domain, the above observations suggest that this domain regulates the MAP2-induced protrusion of microtubule bundles. To examine this possibility, we have produced recombinant baculovirus that contain either the projection domain of MAP2b (Prob), the projection domain of MAP2c (Proc) or the microtubule-binding domain (Mt) that is common to MAP2b and MAP2c (Figure 1A). The expression of these truncated forms was analyzed by immunoblotting in Sf9 cells. Each mutant was found to migrate at its expected molecular weight and was immunoreactive to antibodies directed against MAP2 isoforms (Figure 1B). We first examined the ability of each of these constructs to induce process formation in Sf9 cells. As expected, the expression of the truncated form that corresponds to the projection domain of MAP2b (Prob) did not induce process

formation. Similar results were obtained with the truncated form corresponding to MAP2c projection domain (Proc). In contrast, Mt promoted formation of cell processes.

The pattern of process formation of Mt in Sf9 cells was analyzed according to two parameters: number of cells with processes and number of processes per cell. At 24 and 72 h post-infection, to evaluate the percentage of cells having processes, the cells were fixed and stained with the antibody anti-MAP2, HM2 that recognizes MAP2b and MAP2c and the antibody 46.1 directed against an epitope located in Mt (Kosik *et al.*, 1988). Then, the percentage of cells positive to HM2 or 46.1 and having cell processes was determined. 44% of the Mt-expressing cells presented processes compared to 7% and 80% of MAP2b- and MAP2c-expressing cells respectively (Figure 1A). This indicates that the projection domain of MAP2b negatively regulates the capacity of the microtubule-binding domain to induce process formation whereas the projection domain of MAP2c appears to increase its capacity to initiate process formation. Then, for the cells expressing Mt and presenting processes, the number of processes per cell was examined and compared to that of MAP2b and MAP2c. As reported before, MAP2b induced the formation of one process whereas MAP2c had the tendency to induce the formation of multiple processes (Figures 2 and 3). Interestingly, in the cells expressing Mt, the number of processes per cell was significantly different from that of MAP2c-and MAP2b-expressing cells. Indeed, 39% of Mt-expressing cells had multiple processes compared to 57% and 9% of MAP2c- and MAP2b-expressing cells (Figure 3). However, Mt-expressing cells (37%) had a slighty higher tendency than MAP2c-expressing cells (30%) to develop one process but an important lower one than MAP2b-expressing cells (74%). Thus, the projection domain of MAP2c seems to contribute to the production of

multiple processes by Sf9 cells whereas that of MAP2b impairs it. To eliminate the possibility that a difference in Mt pattern of process formation compared to that of full-length MAP2b and MAP2c was imputable to different level of protein expression, their protein level was analyzed by dot blotting. The antibody, 46.1, which recognized an epitope located in the C-terminus of MAP2, was used to compare the protein level of MAP2b, MAP2c and Mt (Kosik *et al.*, 1988). At 72 h post-infection, the expression of Mt was similar to that of MAP2c and MAP2b (Table 1). This indicates that the molar expression of Mt was ~2 times higher than that of MAP2c and ~7 times higher than that of MAP2b at this time of infection. While the molar expression of Mt was higher than that of MAP2c, it induced a lower percentage of cells with processes and a lower number of processes per cell than MAP2c. Thus, the protein level does not influence the pattern of process formation of MAP2 proteins in Sf9 cells as reported before (Leclerc *et al.*, 1996).

2.4.2 Regions of Prob that regulate the process formation by the microtubule-binding domain

To identify which region(s) of the 1372 a.a. domain are involved in regulating the process formation by Mt, we subdivided this sequence into three portions of equal size corresponding to the region adjacent to the N-terminus common to MAP2c and MAP2b (MAP2b-1), to the median region (MAP2b-2) and to the region adjacent to the microtubule-binding domain (MAP2b-3) (Figure 1A). MAP2b-1 is deleted of the amino acids 147a.a. to 569a.a., 147 a.a. is the amino acid located at the splicing site of MAP2c. MAP2b-2 has a deletion from 569 a.a to 1035 a.a.. This deleted sequence includes a

phylogenic conserved sequence in MAP2b projection domain extending from 650 to 940 (Kindler *et al.*, 1990). MAP2b-3 is deleted from the 1035 to 1519 a.a., 1519 corresponding to the splicing site of MAP2c. These truncated forms were expressed in Sf9 cells. Their expression was analyzed by western blotting and each truncated form migrated at the expected apparent molecular weight on SDS-PAGE (Figure 1B). Their protein level was evaluated by dot blotting (Table 1). At 24 and 72h post-infection, MAP2b-3 presented the highest protein level. The protein level of MAP2b-1 was similar to that of MAP2b whereas that of MAP2b-2 was slightly lower than that of MAP2b at 72 h post-infection.

We performed a quantitative morphological analysis as described above to verify whether these truncated forms of MAP2b induced different patterns of process formation in Sf9 cells. As noted for MAP2b, they had the tendency to induce one process per cell (Figures 2, 3). The percentage of cells with processes induced by MAP2b-3 (21%) was significantly higher than that of MAP2b- (7%), MAP2b-1 (12%) and MAP2b-2 (11%) expressing cells (Figure 1A). The percentage of cells with processes induced by MAP2b-1 and MAP2b-2 was not significantly different from that of MAP2b. Then, for the cells expressing MAP2b-1, MAP2b-2 and MAP2b-3 and that presented processes, the number of processes per cell was examined. The number of processes per cell induced by MAP2b-1, MAP2b-2 and MAP2b-3 was reminiscent to that of MAP2b. Indeed, ~74% of the MAP2b-expressing cells had one process compared to 75%, 69% and 71% of the MAP2b-1-, MAP2b-2- and MAP2b-3-expressing cells respectively. Futhermore, their percentage of cells having two or more than two processes was also similar to that of MAP2b. Thus, in the present expression system, it seems that the

deletion of the amino acids 1035 to 1519 deleted in MAP2b-3 had the most important positive effect on the formation of processes by MAP2b in Sf9 cells. This could be related to the fact that MAP2b-3 presented the highest protein level at 72h post-infection. Indeed, there is an increase of the number of cells with processes in parallel to the increase of MAP2 protein expression in Sf9 cells. However, the protein level of MAP2 proteins does not seem to be the sole determinant involved in the production of processes by these cells. For instance, at 24h post-infection, MAP2b-3 protein level was 10 times lower than that of MAP2b at 72h post-infection but the percentage of cells presenting processes (~10%) was identical to that of MAP2b at 72h post-infection (Table 1). This suggests that MAP2b-3 has a higher capacity than MAP2b, MAP2b-1 and MAP2b-2 to initiate process formation. Similarly, Mt and MAP2c protein level does not seem to influence their capacity to induce process formation. At 24h post-infection, Mt and MAP2c had a similar percentage of cells with processes (~20%) despite the fact that the molar expression of Mt is higher than that of MAP2c (Table 1). On the other hand, at 48h post-infection, 44% of Mt-expressing cells had processes compared to 80% of MAP2c. These results indicate that Mt is less efficient than MAP2c to induce process outgrowth in parallel to the increase of its protein level.

2.4.3 Process length induced by MAP2 truncated forms

The process length was analyzed for each truncated form of MAP2b and MAP2c (Figure 4). We first compare the process length of cell bearing one process. MAP2c-expressing cells presented the longest process (72.7$\pm$2.2µm) followed by MAP2b-3 (62.4$\pm$2.5µm), MAP2b-1 (52.4$\pm$1.9µm), Mt (47.9$\pm$2.0µm), MAP2b-2 (41.9$\pm$1.6µm) and

MAP2b (35.8±1.4μm). These differences of process length were statistically significant except for Mt and MAP2b-1. Thus, a partial deletion in the 1372 a.a. domain had a positive effect on process length whereas a deletion of Proc had a negative one. However, the process length of MAP2b-1, MAP2b-2 and MAP2b-3 seems to correlate with their level of protein expression as presented in Table 1. Indeed, MAP2b-2 has the lowest protein expression and the shortest processes whereas MAP2b-3 has the highest protein expression and the longest processes. However, the level of protein expression does not seem to be the only parameter that determines process length since MAP2b-2 that has lower expression of MAP2b has slightly longer processes than MAP2b. Moreover, the process length induced by Mt whose level of expression is a lot higher than that of MAP2b-1 and MAP2b-2 is similar or slightly longer than the process length of these MAP2b constructs. From the above observations, it appears that the additional domain of 1372 a.a. in the projection domain of MAP2b is not only involved in determining the number of processes per cell but also exerts an effect on process length.

Finally, we examined the process length of cells bearing multiple processes. Since MAP2c and Mt induced the highest percentage of cells with multiple processes, the process length was only analyzed for these two constructs. The process length of MAP2c- and Mt-expressing cells bearing multiple processes was 31.5±1.4μm and 29.6±1.4μm respectively. These length were not statistically different but were significantly shorter than the process length of MAP2c- and Mt-expressing cells having one process.

2.4.4 Distribution of the microtubules and actin microfilaments in Sf9 cells expressing MAP2c and MAP2b truncated forms

According to our previous work in Sf9 cells, microtubule formation is required to get process outgrowth in Sf9 cells. Thus, we examined the distribution of microtubules in cells expressing the full-length and the truncated forms of MAP2b and MAP2c. As shown previously, in MAP2c-expressing cells having multiple processes, thin microtubule bundles radiate tangentially from the cell surface to form processes (Boucher *et al.*, 1999). In MAP2b-expressing cells developing one process, a thick bundle of microtubules originating in the cell body extends into the process. In MAP2b-expressing cells without processes, microtubules are organized in a thick bundle that forms a ring under the plasma membrane (Figure 5).

We analyzed the distribution of microtubules in cells expressing the different truncated forms of MAP2b and MAP2c using confocal microscopy (Figure 5). In cells expressing Mt and having one process, several thin bundles of microtubules are found in the cell body that form a thick bundle at the hillock region of the process and extends into the process. In cells having multiple processes, the distribution of the microtubules is reminiscent of that found in MAP2c-expressing cells presenting multiple processes. In MAP2b-1, MAP2b-2 and MAP2b-3-expressing cells, a thick bundle of microtubules was found in the cell body that extended in a process at one pole of the cell body as previously described for MAP2b (Leclerc *et al.*, 1996). In cells expressing either of these MAP2b truncated forms that did not have processes, microtubules formed a ring under the plasma membrane as reported for full-length MAP2b (Boucher *et al.*, 1999). From these observations, it appears that the projection domain is not necessary to induce

microtubule bundling since the construct Mt promoted microtubule bundling. However, the 1372 a.a. domain in MAP2b projection domain seems to favor the formation of a thick bundle of microtubules rather than the formation of multiple thin bundles. Furthermore, the packing density of microtubules does not seem to influence their capacity to protrude from cell surface. For instance, Mt can induce the formation of one thick bundle of microtubules (see figure 5) or of multiple thin bundles. The thick bundles seem to have a similar capacity to protrude from cell surface than the thin ones. Indeed, an equal number of Mt-expressing cells develop multiple processes (37%) and one process (39%).

In cells expressing Prob, there was no formation of microtubules (Figure 9). Interestingly, Prob expression was concentrated in the cell periphery. In these cells, F-actin formed a ring under the plasma membrane and seemed to co-localize with Prob (Figure 6). Proc expression had also the tendency to be concentrated in the cell periphery and to co-localize with F-actin (Figure 6). F-actin nuclear staining was often noted in cells infected with any truncated form of MAP2b and MAP2c as noted in wild-type baculovirus infection (Charlton and Volkman, 1991). Finally, in Sf9 cells expressing either full-length or truncated forms of MAP2b and MAP2c and presenting processes, F-actin was found in the cell body and in the processes (Figure 5).

2.4.5 Bundling of microtubules in Sf9 cells expressing MAP2c and MAP2b truncated forms

As revealed by light microscopy, MAP2c and Mt have a higher tendency to induce multiple thin microtubule bundles than MAP2b, MAP2b-1, MAP2b-2 and

MAP2b-3. This suggests that the 1372 a.a. domain favors the formation of a unique thick bundle of microtubules. To better understand its role in microtubule bundling, we examined the effect of partial or complete deletion of this domain on the spacing between microtubules along the processes in Sf9 cells. This was examined in cells expressing either MAP2b-1, MAP2b-2, MAP2b-3 and Mt as well as full length MAP2b and MAP2c 72 hrs following the infection. Longitudinal sections were used (figure 7). We measured wall to wall spacing between neighboring microtubules at 50 randomly selected locations in the proximal region of the process. The results are shown in table 2. Because of the very low capacity of MAP2b to induce process formation in Sf9 cells, measurements were made in the cell bodies of the round infected cells expressing MAP2b. In these cells, microtubules form a ring under the plasma membrane (figure 7). To confirm that the spacing between microtubules is not different between the cell body of the round infected cells and the processes, we performed measurements in the cell bodies of the round cells expressing MAP2b-2 or MAP2b-3. The microtubules are also organized as bundles under the plasma membrane in these cells (figure 7). There was no statistically significant difference between the cell bodies and the processes for MAP2b-2 and MAP2b-3 expressing cells. Thus, the measurements in these two compartments were combined for those constructs (table 2). However, differences were observed in the case of MAP2c expressing cells where the average spacing between microtubules was 13.05 ± 0.23 nm in the cell bodies compared to 16.40 ± 0.51 nm in the processes.

The average spacing between microtubules in MAP2b and MAP2c induced bundles was 53 ± 1.90 and 16.40 ± 0.51 nm respectively. These values confirm previous findings (Chen *et al.*, 1992; Leclerc *et al.*, 1996). As for MAP2b-1, MAP2b-2 and

MAP2b-3, the average spacing between microtubules is 33.40 ± 1.11, 39.70 ± 1.10 and 41.00 ±1.00 nm respectively. Thus, the spacing between microtubules is significantly different between MAP2b-1 and MAP2b-2 and between MAP2b-1 and MAP2b-3. These results indicate that equal size deletions in the 1372 aa domain of MAP2b give different microtubule spacing. Moreover, MAP2b-1, which deleted sequence was slightly shorter than that of MAP2b-2 and MAP2b-3, gave a narrower microtubule spacing than these constructs. This suggests that the length of the projection domain of MAP2, although important, is not the sole determinant of the spacing between microtubules. As for Mt induced processes, the microtubules were so tightly packed that it was impossible to make measurements (figure 7).

To verify whether the expression level of the protein affects the spacing between microtubules, measurements were made 48 hrs following the infection and no differences were observed (data not shown).

The above observations suggest that the structural properties of microtubule bundling are not the sole parameters that regulate microtubule protrusion from Sf9 cells. Indeed, MAP2b-1, which gives rise to a narrower spacing than MAP2b, MAP2b-2 and MAP2b-3, does not present higher microtubule protrusion than these proteins. Furthermore, MAP2b-3 induces a microtubule spacing similar to that of MAP2b-2 but has a higher capacity to promote microtubule protrusion than MAP2b-2.

2.4.6 Microtubule binding properties of MAP2c and MAP2b truncated forms

The microtubule binding affinity of MAP2b and MAP2c truncated forms was evaluated by quantifying the amount of each truncated form in a preparation of

microtubules by dot-blot. The microtubules were prepared according to the protocol developed by Vallee ('86). As illustrated in Figure 8, similar amounts of tubulin were found in the microtubule preparations from Sf9 cells expressing either the truncated forms of MAP2 or full-length MAP2b and MAP2c. The amount of MAP2b, MAP2c and MAP2 truncated forms in the microtubule preparation is presented as a percentage of the total amount of protein in $4X10^6$ Sf9 cells. All the deletion in the 1372 a.a. domain had a positive effect on the microtubule binding affinity of MAP2b (Figure 8). 5% of MAP2b was found in the microtubule preparation whereas 9%, 50% and 40% of MAP2b-1, MAP2b-2 and MAP2b-3 was bound to microtubules respectively. Interestingly, MAP2b-2 which has the lowest protein level presented the highest microtubule binding affinity. Moreover, the microtubule binding affinity does not seem to influence the capacity of microtubules to protrude from Sf9 cells since MAP2b-2 induced a lower percentage of cells with microtubule protrusion than MAP2b-3. Moreover, MAP2c and Mt which showed a significantly higher percentage of cells with microtubule protrusion than MAP2b-2 and MAP2b-3, presented an equal or lower percentage of protein bound to microtubules than these MAP2b truncated forms. Indeed, 34% and 39% of MAP2c and Mt was bound to microtubules compared to 50% and 40% for MAP2b-2 and MAP2b-3.

The amount of polymerized tubulin induced by the expression of MAP2c and MAP2b truncated forms was also evaluated by extracting the cytoskeleton 48 hrs following the infection as described in methods. Similar amounts of tubulin were found in the extracted cytoskeletal pellets indicating that differences in the binding affinities of MAP2c and MAP2b truncated forms to microtubules did not affect the amount of polymerized tubulin. Thus, the amount of polymerized tubulin is not a limiting factor in

microtubule protrusion from cell surface in Sf9 cells. For instance, MAP2b-3, which has a higher protrusion activity than MAP2b, MAP2b-1 and MAP2b-2, induces a similar amount of polymerized tubulin than these proteins. Furthermore, we examined the effect of cold treatment (30 min) on the stability of the polymerized microtubules in the cells expressing MAP2c and MAP2b truncated forms. The amounts of tubulin remaining in the extracted cytoskeletal pellet following cold treatment compared to control levels are the following: MAP2b, 30%, MAP2c, 30%, MAP2b-1, 35%, MAP2b-2, 28%, MAP2b-3, 25% and Mt, 26%. These results indicate that cold treatment destabilized the microtubule polymers induced by MAP2c and MAP2b truncated forms as well as by full length MAP2b and MAP2c to the same extent. Finally, we examined the effect of treatment with the microtubule depolymerizing agent colchicine (2 hrs) on the stability of the microtubule polymers induced by MAP2c and MAP2b truncated forms. The amounts of tubulin remaining in the extracted cytoskeletal pellet following treatment with colchicine compared to control levels are the following: MAP2b, 34%, MAP2c, 12%, MAP2b-1, 17%, MAP2b-2, 33%, MAP2b-3, 28% and Mt, 25%. Thus, treatment with colchicine destabilized the microtubule polymers induced by MAP2c and MAP2b truncated forms as well as by full length MAP2c and MAP2b to different extents. After 2 hrs of treatment with colchicine, the amount of polymerized tubulin in the extracted cytoskeletal pellet was higher for MAP2b than for MAP2c indicating that MAP2b might confer more resistance to drug treatment. Furthermore, partial deletion in the 1372 aa domain of MAP2b seems to render microtubule polymers less resistant to drug treatment. This is particularly evident for MAP2b-1. Therefore, the 1372 aa domain might play a role in conferring drug resistance to polymerized microtubules. Moreover,

MAP2c seems to induce the formation of microtubule polymers more sensitive to colchicine treatment than Mt. This indicates that the projection domain of MAP2c confers drug sensitivity to polymerized microtubules. Thus, the microtubule resistance to colchicine seems to be mainly induced by Mt but Proc decreases it whereas the 1372 aa domain enhances it.

As reported above for the structural properties of microtubules, one can conclude from the present observations that the microtubule binding affinity and the polymerizing activity of MAP2c and MAP2b truncated forms are not the only factors that control microtubule protrusion and process formation in Sf9 cells.

2.4.7 Interactions between the projection domain and the microtubule-binding domain in Sf9 cells

To explore the mechanism by which Prob regulates microtubule protrusion and process formation in Sf9 cells, we first verified whether Prob has to be attached to Mt to impair the protrusion of microtubule bundles. Thus, Sf9 cells were co-infected with Prob and Mt recombinant baculovirus. A quantitative morphological analysis was performed as described in the previous section. To identify the cells that co-expressed Prob and Mt, the cells were double stained with a polyclonal anti-MAP2 antibody (kindly provided by Dr. Richard Vallee, University of Massachusetts Medical School, Worcester, Massachusetts, USA) that recognizes an epitope contained in the projection domain of MAP2b and the antibody 46.1 that recognizes an epitope found in Mt as described above. For the quantitative morphological analysis, only the cells presenting a high protein level of Prob and Mt were selected (Figure 9). The percentage of Prob/Mt co-

infected cells presenting processes was significantly lower (30%) than that of Mt-infected cells (44%) (Figure 10). Moreover, the number of processes per cell was significantly lower in Prob/Mt-expressing cells than in Mt-expressing cells (Figure 10). In Mt-infected cells, 37% and 39% of the cells had one and multiple processes respectively compared to 51% and 28% of co-infected cells. From this set of experiments, it appears that Prob does not have to be attached to Mt to impair its capacity to induce process formation in Sf9 cells. Interestingly, co-expression of Proc with Mt did not result in the pattern of process formation of full-length MAP2c but rather gave rise to a pattern resembling that of Mt. 38% of the cells co-expressing Proc and Mt had processes compared to 44% of Mt-expressing cells (Figure 10).

The co-infection experiments demonstrated that the projection domain of MAP2b impairs process formation activity of Mt. This could be done by intramolecular interactions between these two domains which would result in masking functional domain(s) involved in process formation. Another possibility is that Prob could compete with Mt for a common element that when bound to Mt, allows microtubule protrusion and process formation and when bound to Prob, blocks them. However, previous studies on MAP2 structure have suggested that MAP2b could adopt different conformations including the formation of hairpin structures (Wille *et al.*, 1992c; Wille *et al.*, 1992b). This indicates that Prob and Mt would interact to give rise to such conformation. Moreover, these electron microscopic studies demonstrated that MAP2b can form anti-parallel dimers reinforcing the possibility that Prob and Mt can interact. To verify this possibility, we performed a co-immunoprecipitation experiment (Figure 11). We used the anti-MAP2 antibody, AP20, that recognizes an epitope located in the additional

sequence of 1372 a.a. in MAP2b projection domain, or the antibody HM2 to immunoprecipitate Prob. The membrane was revealed with AP20 or HM2 to show that Prob was immunoprecipitated. Then, the same membrane was probed with the antibody, 46.1 that recognizes the microtubule-binding domain of MAP2 isoforms to reveal the presence of Mt. As shown in Figure 11, a band corresponding to the apparent molecular weight of Mt co-immunoprecipitated with Prob (lanes 2 and 3). A similar band having a higher intensity was found when Mt was immunoprecipitated with the antibody 46.1 in cells only expressing Mt (lane 4). On the other hand, this band was not detected when Prob was immunoprecipitated from cells only expressing Prob (lanes 6 and 7). These results indicate that Prob interacts with Mt in Sf9 cells. We also verified whether Proc interacts with Mt in Sf9 cells. In the present conditions, no interaction was detected between Proc and Mt.

From the present study, one can conclude that the additional domain of 1372 a.a. in Prob increases the spacing between microtubules and favors the formation of a single thick bundle of microtubules. Most notably, it also regulates the capacity of this microtubule bundle to protrude from cells. This could be through its interaction with Mt.

2.5 DISCUSSION

Even though the expression of MAP2b and MAP2c has been correlated with the differentiation of neurites (Ludin and Matus, 1993; Mandell and Banker, 1996), their respective roles remain elusive. These MAP2 isoforms share a common microtubule-binding domain but in the projection domain, MAP2b has an additional sequence of 1372 a.a. (Papandrikopoulou *et al.*, 1989). In the present study, we showed that a partial

or complete deletion of the projection domain of MAP2b has a strong positive effect on process formation whereas a deletion of the projection domain of MAP2c impairs process formation in Sf9 cells. Indeed, 44% of the cells expressing the microtubule-binding domain common to MAP2c and MAP2b developed processes compared to 7% and 80% of MAP2b- and MAP2c-expressing cells respectively. Moreover, the 1372 a.a. domain decreases the binding affinity of MAP2b to microtubules. This domain also is involved in determining the spacing between microtubules. Most importantly, regions of this domain seem to contribute differently to microtubule spacing. Indeed, our results show that the spacing between microtubules is diminished but is not proportional to the length of the deleted region in the 1372 a.a. domain. Other than determining the structural properties of microtubule bundles, the 1372 a.a. domain also seems to regulate the capacity of these bundles to protrude from Sf9 cells. Our data indicate that this regulatory effect could be mediated by intramolecular interactions between the projection domain and the microtubule-binding domain in MAP2b.

2.5.1 The microtubule-binding domain and the adjacent proline-rich region of MAP2 proteins contain the domains involved in microtubule protrusion and process formation in Sf9 cells

Our present results show that the expression of the construct Mt, which contains the microtubule-binding domain and the adjacent proline-rich region, promotes microtubule bundling, microtubule protrusion and process formation in Sf9 cells. Indeed, it was previously shown that the proline-rich region and the microtubule-binding domain were sufficient to induce microtubule bundling in non-neuronal cells (Umeyama

et al., 1993; Ferralli *et al.*, 1994). The microtubule-binding domain contains the three repeated sequences of 18 a.a. responsible for microtubule assembly that share sequence homology with MAP4 and tau (Lewis *et al.*, 1988). Futhermore, MAP2, MAP4 and tau also present sequence homology in the proline-rich region adjacent to the microtubule-binding domain (Chapin and Bulinski, 1991; West *et al.*, 1991; Ferralli *et al.*, 1994). The homology is found in the 25-30 a.a. adjacent to the first repeat. Two residues, Lys^{215} and Arg^{221}, are highly conserved. These amino acids are known to enhance the microtubule binding activity of the microtubule-binding domain of tau (Goode *et al.*, 1997). The sequence homology indicates that this function is conserved between MAP2, MAP4 and tau. Futhermore, previous studies demonstrated that the proline-rich region adjacent to the microtubule-binding domain in tau interacts with the src-family of non-receptor tyrosine kinases such as fyn through the SH3 domains of these kinases (Lee *et al.*, 1998). Interestingly, the binding of tau to fyn alters cell morphology which is associated with a reorganization of the microtubules. A similar binding sequence to SH3 domains is found in MAP2 isoforms from 286 a.a. to 294 a.a.. However, this region does not seem to be involved in the binding of the SH3 domains of Src and Grb2 to MAP2c (Lim and Halpain, 2000). This interaction is rather mediated by the region from 300 a.a. to 400 a.a. located in the microtubule-binding domain. Moreover, Src and Grb2 interact preferentially with non-microtubule-associated MAP2c (Lim and Halpain, 2000). Nonetheless, these data indicate that, as noted for tau, the proline-rich region in MAP2 proteins could influence the microtubule bundling and protrusion from cells by its binding to signaling proteins.

2.5.2 Effects of the additional domain of 1372 a.a in the projection domain of MAP2b on microtubule protrusion and process formation in Sf9 cells

Here, we show that a partial or complete deletion of the 1372 a.a. domain has a strong positive effect on microtubule protrusion and process formation in Sf9 cells. However, Proc, the projection domain of MAP2c seems to enhance these events since MAP2c presents the highest percentage of cells with processes. This enhancing effect of Proc on MAP2c ability to induce process formation was also reported in human hepatoma cell line PLC (Ferralli *et al.*, 1994). Previous studies have suggested that the capacity of MAP2c constructs to support process formation was related to their strength of binding to microtubules(Ferralli *et al.*, 1994). However, in Sf9 cells, this correlation does not seem to exist. Indeed, Mt has a slightly higher binding affinity than MAP2c but presents a lower capacity to induce process formation in Sf9 cells. This difference might be explained by the fact that in previous studies, cortical actin had to be depolymerized by cytochalasin D to induce process formation whereas in Sf9 cells, process formation occurs spontaneously (Leclerc *et al.*, 1993; Ferralli *et al.*, 1994; Leclerc *et al.*, 1996). Therefore, in Sf9 cells, microtubule protrusion and process formation might require additional cellular elements that influence MAP2 protein activity. Moreover, Proc seems to decrease microubule stability as revealed by the lower percentage of microtubules resistant to colchicine treatment in MAP2c-expressing cells compared to Mt-expressing cells. Our results correlate with previous studies which showed that MAP2c does not confer to microtubules resistance to colchicine (Olmsted *et al.*, 1989; Caceres *et al.*, 1992; Takemura *et al.*, 1995). However, some studies reported that MAP2c can induce

drug resistance to microtubules (Takemura *et al.*, 1992; Ferhat *et al.*, 1996). These studies used immunocytochemistry to evaluate the amount of polymerized tubulin whereas in our study, we used a biochemical approach. Furthermore, a different cellular system was used in these studies. These experimental differences might explain the discrepancy between the results. In neurons, the suppression of MAP2 protein expression blocks the induction of labile or tyrosinated microtubules but does not affect the population of stable or acetylated microtubules resistant to colchicine (Caceres *et al.*, 1992). Moreover, it was shown that in the presence of MAP2c, microtubules display dynamic instability (Kaech *et al.*, 1996). The high capacity of MAP2c to induce microtubule protrusion and process formation might be due to the induction of labile microtubules which are mainly located in the growth region in neurons.

Our present results indicate that the additional domain of 1372 a.a. in MAP2b projection domain decreases the positive effects of Proc on process formation in Sf9 cells. This could be explained by the fact that it significantly decreases the microtubule binding affinity of MAP2b. However, MAP2b-2 and MAP2b-3 which have a higher or similar binding affinity to microtubules than MAP2c, present a lower percentage of cells with processes than MAP2c. Thus, the microtubule binding activity does not seem to be sole factor involved in process formation by MAP2b in Sf9 cells. Interestingly, the 1372 a.a. domain seems to favor the formation of a unique thick bundle of microtubules resulting in the formation of a unique process whereas MAP2c induces the formation of mutliple thin bundles that give rise to the formation of multiple processes. The induction of multiple thin bundles of microtubules was reported in other non-neuronal cell lines (Ferhat *et al.*, 1996). In cells expressing full-length or MAP2b truncated forms that do

not have processes, the thick bundle of microtubules forms a ring under the plasma membrane. Since microtubules have to penetrate in the actin network to protrude from cell surface, the thickness of the microtubule bundles might be a limiting factor (Tanaka and Sabry, 1995). However, this does not seem to be the case in Sf9 cells since MAP2b-3 which induces a thick bundle of microtubules has a three times higher capacity than MAP2b to induce process formation. Futhermore, the 1372 a.a. domain seems to enhance the resistance of microtubules to colchicine, resistance which is mainly induced by Mt expression. This could contribute to lower microtubule dynamics and thereby their capacity to protrude from cells. The distinct organization of microtubule bundles by MAP2c and MAP2b might reflect their distinct role in the elaboration of the dendritic arborization. MAP2c, which leads to the formation of thin and labile microtubule bundles that could easily penetrate the actin network of the growth cone, would be involved in the initial stage of dendritic outgrowth (Tanaka and Sabry, 1995). On the other hand, MAP2b would be involved in the production of thicker bundles to increase the diameter of dendrites and to stabilize microtubules to consolidate the newly formed dendritic branches (Hillman, 1988).

2.5.3 Mechanisms regulating the effects of the additional domain of 1372 a.a in the projection domain of MAP2b on microtubule protrusion in Sf9 cells

Microtubule protrusion and process formation induced by MAP2 proteins depend on actin cytoskeleton as previously shown (Edson *et al.*, 1993; Boucher *et al.*, 1999). Thus, the distinct effect of MAP2b and MAP2c on microtubule protrusion might be related to their distinct effect on actin cytoskeleton. Indeed, MAP2b and MAP2c

organize differentially F-actin in vitro. MAP2c is able to induce the formation of an isotropic gel of F-actin whereas MAP2b induces the formation of F-actin bundles (Cunningham *et al.*, 1997). To bundle or cross-link F-actin, a protein has to contain two actin binding domains or to have the capacity to dimerize (Puius *et al.*, 1998). In either case, the 1372 a.a. domain by allowing different conformational states to MAP2b might modify the structural relation between the actin-binding domains and thereby the organization of F-actin by MAP2b. An actin-binding domain was identified in one of the repeat of the microtubule-binding domain (Correas *et al.*, 1990). Futhermore, as revealed in the present study, Proc and Prob co-localize with F-actin in Sf9 cells indicating that a binding site to F-actin could be located in the region common to MAP2c and MAP2b. This needs to be confirmed by in vitro studies. Finally, since simultaneous changes in microtubule and actin organization are observed in process outgrowth, the 1372 a.a. domain might compromise the molecular link between these cytoskeletal elements and thereby impair process formation (Tanaka and Sabry, 1995). The 1372 a.a. domain also influences the length of the processes since a partial deletion in this domain increases process length in Sf9 cells. This could occur through its effect on actin organization. Indeed, depolymerization of F-actin by cytochalasin increased importantly the rate of process ougrowth in Sf9 cells (Knowles *et al.*, 1994). Thus, the organization of F-actin induced by these MAP2b truncated forms could favor a higher rate of process elongation.

The effect of the domain of 1372 a.a. on process formation can be also mediated through its binding to signaling proteins. This domain contains a binding site for calmodulin which is known to decrease the actin binding activity of MAP2b (Kotani *et*

al., 1985; Kindler *et al.*, 1990). This calmodulin binding domain was deleted in MAP2b-3, the MAP2b truncated form that gave rise to the highest number of cells with processes. Moreover, the domain of 1372 a.a. also contains a high affinity phosphatidylinositol-binding site (Surridge and Burns, 1994; Burns and Surridge, 1995). A recent study demonstrated that MAP2c process outgrowth activity can be inhibited by the co-expression of a subtype of metabotropic glutamate receptors, mGluR1, in Sf9 cells (Huang and Hampson, 2000). mGluR1 stimulates phosphoinositide (PI) hydrolysis (Pickering *et al.*, 1993). Treatment of the cells with a phospholipase C inhibitor reversed the inhibitory effect of mGluR1 suggesting that the PI pathway was involved in the suppression of MAP2c-mediated process formation in Sf9 cells (Huang and Hampson, 2000). It was proposed that binding of PI to MAP2c reduced its binding to tubulin and consequently microtubule assembly (Yamauchi and Purich, 1987). In Sf9 cells, MAP2b promotes microtubule assembly (Leclerc *et al.*, 1996). Therefore, if binding of PI to MAP2b is responsible for its low capacity to induce process formation, it regulates a function of MAP2b other than that of microtubule assembly. PI is also known to decrease the binding of MAP2 to actin (Yamauchi and Purich, 1993). Since MAP2b contains a high affinity PI-binding site, its actin-binding activity might be lower than that of MAP2c.

By co-immunoprecipitation, we showed that intermolecular interactions occur between Prob and Mt in Sf9 cells. Previous studies highlighted the possibility of such interactions by demonstrating that MAP2b is able to form antiparallel dimers that are nearly in complete overlap (Wille *et al.*, 1992c). However, another study reported that autonomous dimerization of MAP2c did not occur in human hepatoma cell line PLC or

Hela cells (Burgin *et al.*, 1994). It was reported that the ERM protein, ezrin, forms oligomers and that the formation of oligomers depends on its state of phosphorylation (Gautreau *et al.*, 2000). Similarly, the interaction between MAP2 proteins might depend on their state of phosphorylation which could vary from one cell type to another. Our present data indicate that, in Sf9 cells, interactions seem to exist between the projection domain and the microtubule-binding domain of MAP2b suggesting that MAP2 proteins could form antiparallel dimers in Sf9 cells. Moreover, these interactions might be responsible for the negative effect that Prob exerts on process formation by Mt. The inhibitory effect of Prob is most likely mediated by the additional domain of 1372 a.a. since we could not co-immunoprecipitate Proc and Mt in Sf9 cells. However, this does not exclude the possibility that Proc interacts with Mt. Indeed, the effect of Prob on process outgrowth could occur through its interaction with Mt and/or by modulating the interaction of Proc with Mt. Futhermore, our data does not indicate whether the interactions between Prob and Mt are direct or indirect. For example, the interactions between these two domains could be mediated by signaling proteins involved in neurite outgrowth and neuronal plasticity.

2.5.4 The length of the projection domain of MAP2b is not the sole determinant of the spacing between microtubules

One known function of the projection domain is to set the spacing between microtubules. Previous studies suggested that the primary sequence of this domain is one primary determinant of the spacing between microtubules (Chen *et al.*, 1992; Leclerc *et al.*, 1996). Furthermore, the loss of MAP2 and MAP1B in MAP2/MAP1B knock-out

mice results in a decreased microtubule spacing in axons and dendrites (Teng *et al.*, 2001). In this study, we show that the deletion of equal portions of the projection domain of MAP2b gives different microtubule spacing. Moreover, MAP2b-1, which was deleted of a slightly shorter sequence than MAP2b-2 and MAP2b-3, induces a narrower spacing between microtubules than these proteins. This indicates that the primary sequence of the projection domain of MAP2, although important, is not the sole determinant of the spacing between microtubules. One possibility is that the deleted portions in the 1372 aa domain contain different phosphorylation sites. Previous studies suggested that the phosphorylation of the projection domain of MAP2 causes it to expand due to an increase in intramolecular repulsion. This in turn could cause the distance between adjacent microtubules to increase (Mukhopadhyay and Hoh, 2001). Thus, the phosphorylation state of MAP2b might also be a key determinant of the spacing between microtubules. This has previously been shown for neurofilament proteins whose phosphorylation state regulates the spacing between them by regulating their structural features (Glicksman *et al.*, 1987; Myers *et al.*, 1987). It is also well known that the phosphorylation of Tau protein increases its rigidity (Hagestedt *et al.*, 1989). Thus, the phosphorylation state of MAP2 might regulate its flexibility, determining the spacing between microtubules.

Another possibility is that those deleted portions are involved in different structural configuration regulating the length of the protein. Previous atomic force microscopy studies suggested that the projection domain of MAP2b could arbor different structural conformations due to the existence of repulsive intramolecular forces (Mukhopadhyay and Hoh, 2001). In this study, we demonstrate by co-

immunoprecipitation the interaction of the projection domain of MAP2b with its microtubule-binding domain. Thus, the deletion of different portions in the 1372 aa domain, although of equal length, might have affected differently the conformation of the projection domain.

2.5.5 Structural conformation of operative and inoperative MAP2b

Several studies, using different approaches, highlighted the possibility that Prob can exist in different structural configurations. Firstly, this domain was shown to be flexible (Woody *et al.*, 1983). Computer-generated secondary structure predictions suggest that the projection domain of MAP2b has a very important stretch of helices separated by short turns (Kindler *et al.*, 1990). This secondary structure could contribute to its flexiblity. Interestingly, tau's flexibility decreases considerably when it binds to microtubules but not that of MAP2b (Woody *et al.*, 1983). Phosphorylation also diminishes tau's flexibility (Hagestedt *et al.*, 1989). Such data do not exist for MAP2b. Given that the projection domain of MAP2b contains several sites of phosphorylation, it is possible that its phosphorylation has also some effects on MAP2's flexibility. Variation of phosphorylation of MAP2b could allow a higher or lower degree of extension which could result in masking or unmasking sites involved in process formation. Secondly, several studies point out that the length of the projection domain can vary. Voter and Erickson demonstrated by rotary shadowing that the length of MAP2b varies by folding back (Voter and Erickson, 1982). Moreover, it was shown that the length of the microtubule-binding domain is half of the length of the total protein despite the fact that it contains only one-sixth of the mass (Wille *et al.*, 1992a). Thirdly,

there is also evidence that MAP2b is able to form hairpin structures. This was demonstrated by electron microscopy (Wille *et al.*, 1992a). This indicates that Prob could fold back on the microtubule-binding domain in full-length MAP2b and thus interactions between these two domains could contribute to the low capacity of MAP2b to induce process formation in Sf9 cells. The detection of an interaction between Prob and Mt in cells that co-express these two domains indicates that such situation might exist in Sf9 cells. However, the fact co-expression of Prob and Mt does not completely reconstitute the low capacity of MAP2b to induce process formation might indicate that in these conditions the interactions between these two domains do not fully matched.

The folding back of the projection domain could mask binding sites to the cytoskeletal or signaling proteins located in the microtubule-binding domain and in the proline-rich region. This situation was reported for ezrin, a member of the ERM family protein that links the actin cytoskeleton to the membrane. It was shown that ezrin exists in a dormant form in which its actin binding site located in the COOH-terminus is masked by the NH_2-terminus that is folded back (Gary and Bretscher, 1995). Moreover, the folding back of the NH_2-terminus of ezrin also masks its binding site for EBP50, the ezrin-radixin-moesin-binding phosphoprotein 50 (Reezek and Bretscher, 1998). These conformational changes of ezrin are controlled by intramolecular interactions. Similarly, MAP2b function could be regulated by intramolecular interactions as suggested by our data.

The truncated form, MAP2b-3 that has a deletion from 1035 to 1519, had the highest capacity to induce process formation in Sf9 cells. This region is comprised in a

proline-rich region extending from 1370 to 1650 a.a. that includes the splicing site of MAP2c (1519 a.a.) (Kindler *et al.*, 1990). The computer programs predict that there are several secondary structures, 19 helices separated by very short turns, in the last two-thirds of the projection domain adjacent to MAP2c splicing site. Therefore, this region could serve as an hinge that would determine the position of projection domain. In the truncated form, MAP2b-3, one part of the hinge (1370 to 1519 a.a) was removed. This could compromise the folding back of the projection domain on the microtubule-binding domain. Consequently, it would have reduced the possibility of intramolecular interactions between the projection domain and the microtubule-binding domain and thereby increase process formation by this MAP2b truncated forms.

None of the deletions performed in the 1372 a.a. could induce the formation of multiple processes like MAP2c. In a previous study, we reported that the expression of a truncated form of MAP2b, that has deletion from 228 to 1621 induces two times less cells with multiple processes than MAP2c (Leclerc *et al.*, 1993). Therefore, the formation of multiple processes would not depend solely on the unfolding of the projection domain but it appears that the junctional sequence at the splicing site of MAP2c plays a role in this event.

Our data demonstrate that the projection domain of MAP2b regulates the capacity of the microtubule-binding domain to induce microtubule protrusion and process formation. As suggested by our present data, this regulation could happen through intramolecular interactions between the projection domain and the microtubule-binding domain most likely involving the 1372 a.a. domain present in MAP2b. Our data suggest that the projection domain would allow MAP2b to exist in an operative form

that is able to induce microtubule protrusion and process formation and in an inoperative form that would not induce microtubule protrusion and process formation. In the later form, the projection domain would be folded back on the microtubule-binding domain and this would result in the decrease of the capacity of the microtubule-binding domain to induce process formation. In the inoperative form, MAP2b would stabilize the cytoskeleton to maintain the dendritic shape whereas in the operative form, it would promote process formation and remodeling of dendrites.

Table 1. MAP2 protein level in Sf9 cells

Proteins	μg/10^6 cells 24h	72h
MAP2c	6	20
MAP2b	0.2	20
Mt	6	18
MAP2b-1	0.35	22
MAP2b-2	0.7	16
MAP2b-3	2	31

MAP2 protein level was measured as described in Materials and Methods.

Table 2. Spacing between microtubules in the processes induced by truncated and full length forms of MAP2

Construct	MAP2b	MAP2c	MAP2b-1	MAP2b-2	MAP2b-3
n	10	18	15	21	27
Average (nm)	53.00	16.40	33.40	39.70	41.00
SEM	1.90	0.51	1.11	1.10	1.00

Cells were fixed 72 hours post-infection and processed for electron microscopy as described in Materials and Methods. We performed 50 measurements per process, *n* being the number of processes. The statistical significance of the spacing between microtubules was determined by using a one-way ANOVA, followed by a Fisher's PLSD test. Statistical significance was accepted if $P<0.05$.

Figure 1. Baculoviral constructs of MAP2 expressed in Sf9 cells. A) The three open boxes represent the three repeat sequences involved in the microtubule binding activity of MAP2. The highlighted parts of the sequence correspond to the highly conserved regions. The percentage of cells with processes is indicated for each MAP2 construct. For details on the morphological analysis see MATERIALS AND METHODS. B) Sf9 cells were infected with the recombinant baculovirus containing the truncated forms of MAP2 at an m.o.i. of 5.0. At 72h post-infection, the cells were lysed and 30μg of cell lysates was separated on SDS-PAGE (7.5%). The proteins were transferred to a nitrocellulose membrane and the expression of the constructs was revealed using the anti-MAP2 antibodies HM2 except for the construct corresponding to the microtubule-binding domain (Mt) that was revealed with the antibody 46.1. The molecular weight of the standards is indicated on the left: myosin (209 kDa), β-galactosidase (134 kDa), bovine serum albumin (84 kDa), carbonic anhydrase (40 kDa), soybean trypsin inhibitor (32 kDa) and lysozyme (19 kDa). In lane MAP2b, MAP2b-1 and Prob, the multiple bands are imputable to protein degradation that occasionally occurs during preparation of cell lysates.

A

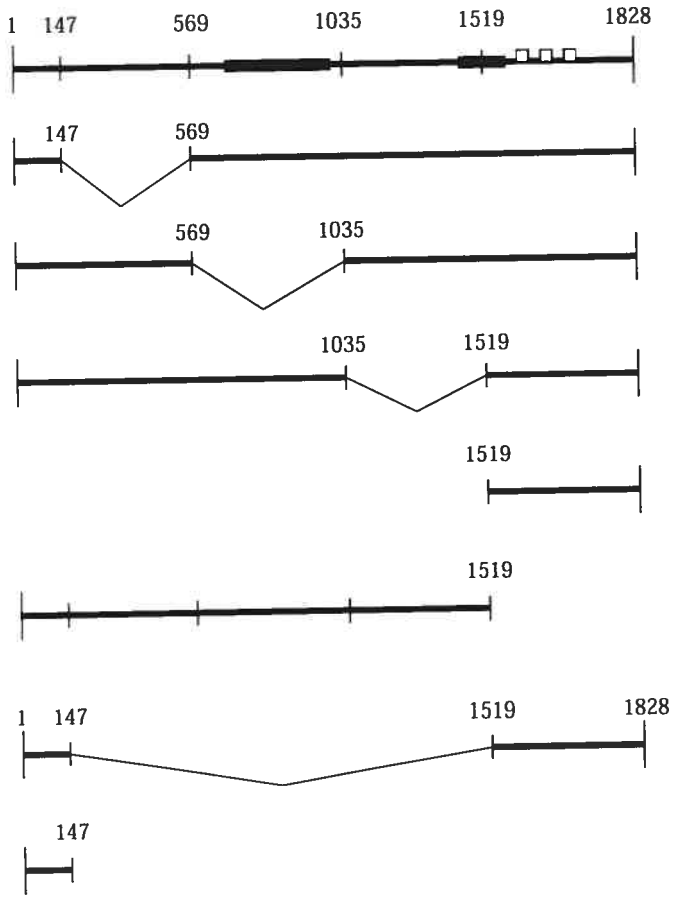

Construct	% process
MAP2b	7
MAP2b-1	12
MAP2b-2	11
MAP2b-3	21
Mt	44
Prob	0
MAP2c	80
Proc	0

B

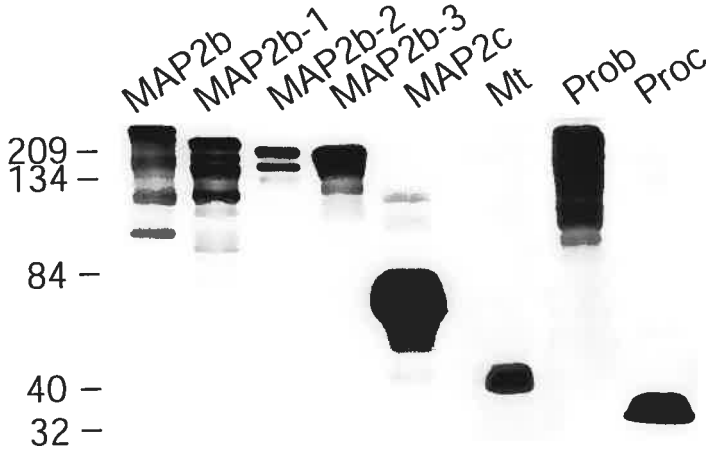

Figure 2. Micrographs illustrating the different patterns of process formation induced by the expression of the MAP2b and MAP2c truncated forms in Sf9 cells. All truncated forms and full-length MAP2b and MAP2c were revealed with the anti-MAP2 antibody, HM2 except for Mt that was revealed with the antibody 46.1. They were distributed uniformly in the cell body and along the processes. MAP2c and Mt induced the highest percentage of cells with multiple processes whereas MAP2b, MAP2b-1, MAP2b-2 and MAP2b-3 induced the formation of a unique process. Prob and Proc did not induce process outgrowth. Scale bar= 20μm.

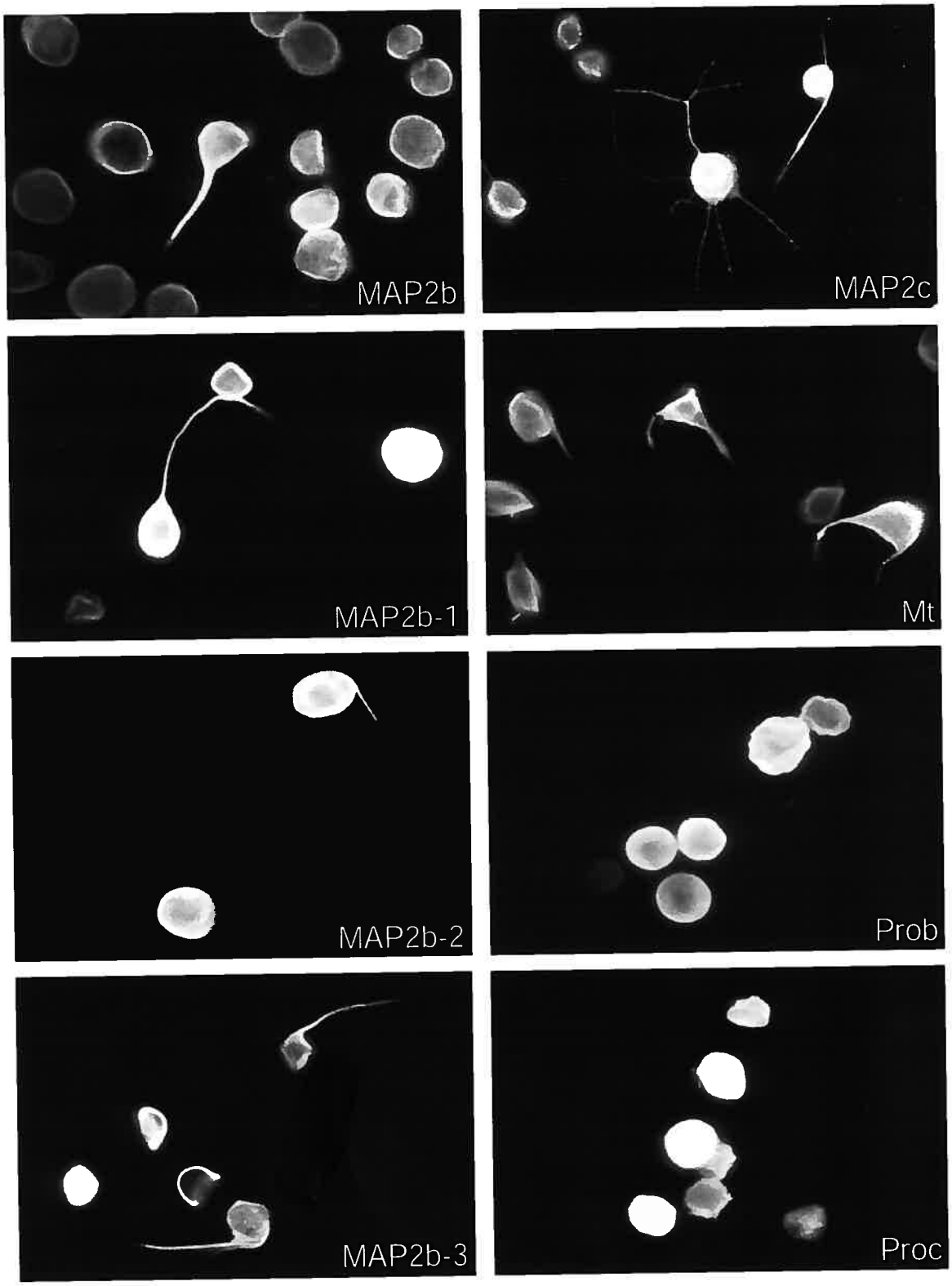
MAP2b
MAP2c
MAP2b-1
Mt
MAP2b-2
Prob
MAP2b-3
Proc

Figure 3. Histograms illustrating the quantitative analysis of process formation for each MAP2 construct. For cells expressing either a truncated or full-length MAP2c and MAP2b that had processes, the percentage of cells having one, two or more than two processes per cell was analyzed. Three sets of experiments were analyzed and 150 cells were measured for each protein in each set of experiment. The distribution of cells having one, two or more than two processes was analyzed by chi-square tests. Chi-square tests were performed to compare the pattern of process formation of the different MAP2 constructs. For all measurements, comparisons between the constructs were significant with a $p<0.0033$. The horizontal line indicates the constructs that are not statistically different.

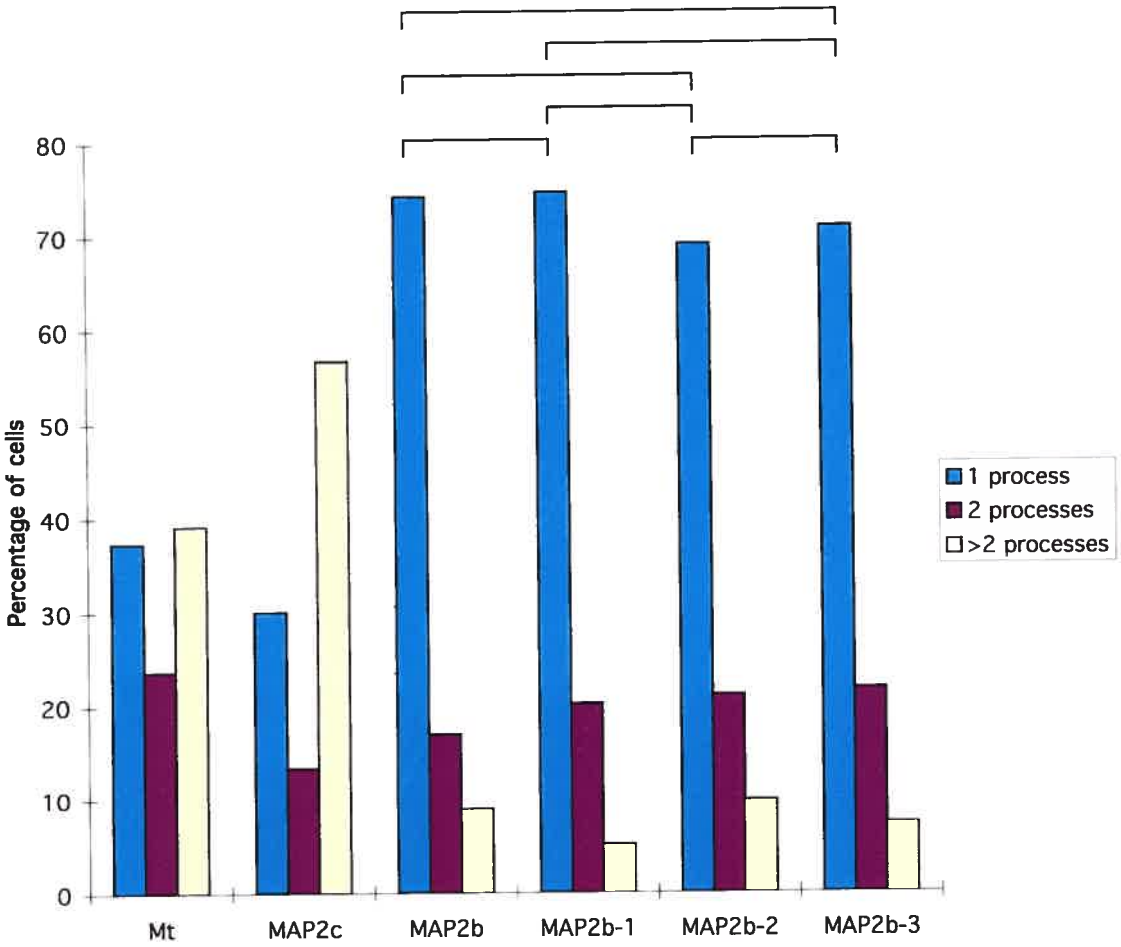
80
70
60
50
40
30
20
10
0
Percentage of cells
Mt
MAP2c
MAP2b
MAP2b-1
MAP2b-2
MAP2b-3
1 process
2 processes
>2 processes

Figure 4. Histogram illustrating the mean of process length induced by the expression of the MAP2 truncated forms in Sf9 cells. Three sets of 50 cells were analyzed for each construct. The data are shown as mean $\pm$ SEM. The length of process was analyzed by one-way ANOVA followed by the Sheffe test. The horizontal lines indicate the constructs that are not statistically different ($p > 0.05$).

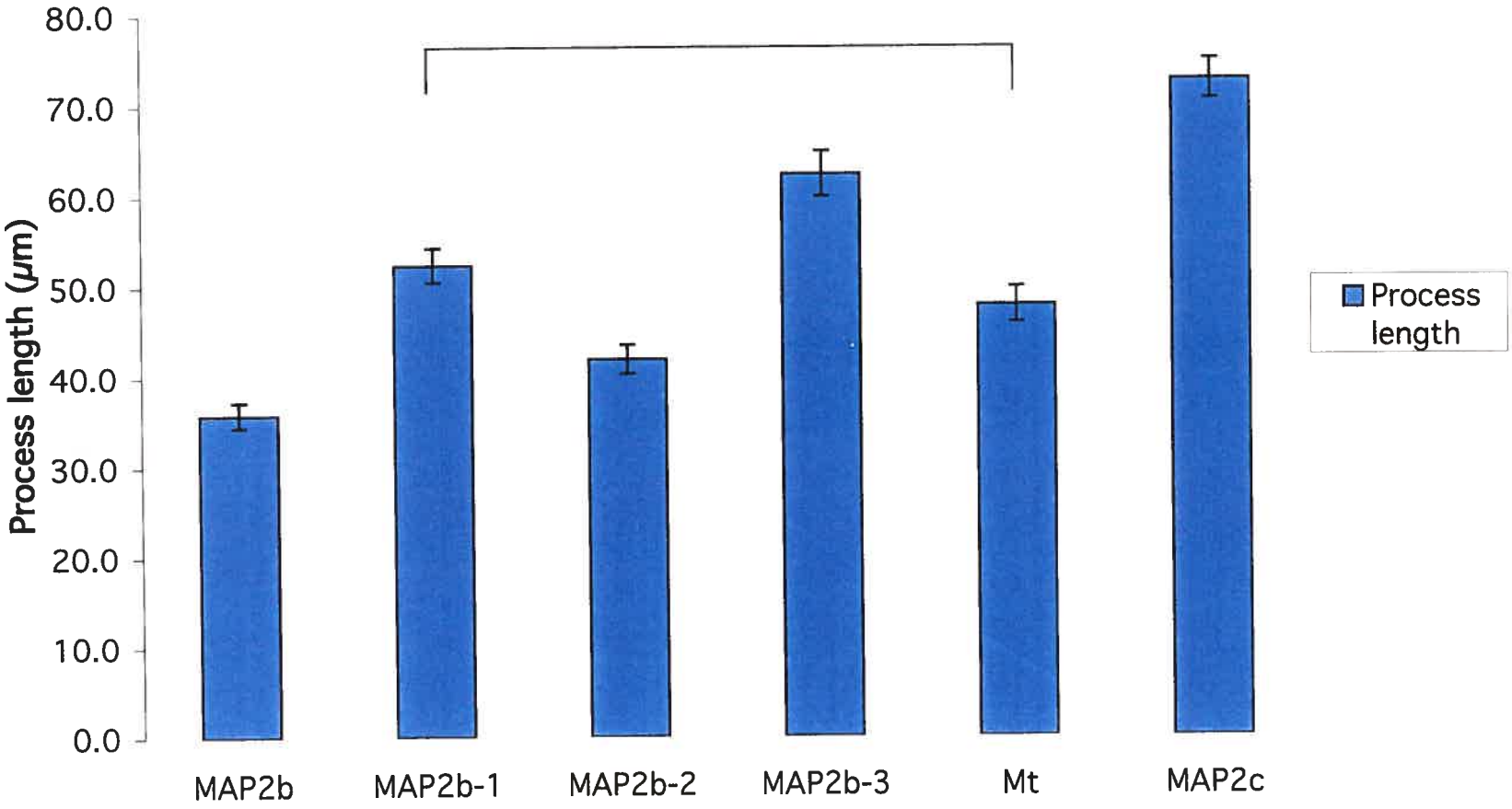
80.0
70.0
60.0
50.0
40.0
30.0
20.0
10.0
0.0
Process length (μm)
MAP2b
MAP2b-1
MAP2b-2
MAP2b-3
Mt
MAP2c
Process length

Figure 5. Micrographs showing the distribution of microtubules and F-actin in Sf9 cells expressing the truncated forms of MAP2. The analysis was done by confocal microscopy. Cells were fixed at 72 h post-infection and double-stained with an anti-α-tubulin antibody (DM1A, Sigma) and rhodamine-phalloidin (Molecular Probes) to reveal F-actin. Scale bar= 20μm.

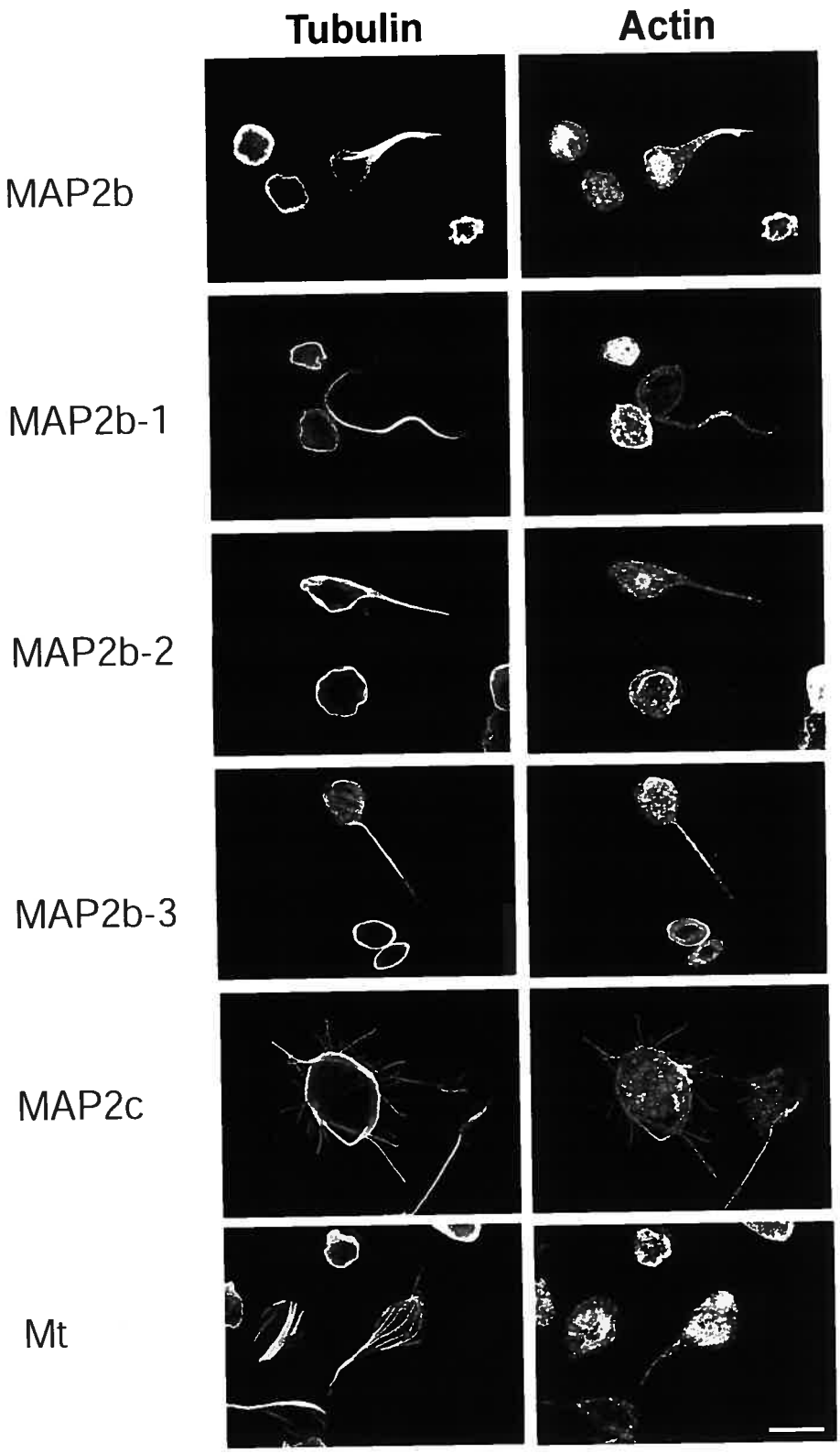
Tubulin
Actin
MAP2b
MAP2b-1
MAP2b-2
MAP2b-3
MAP2c
Mt

Figure 6. Micrographs showing the distribution of F-actin in cells expressing Prob and Proc. Cells were fixed at 72 h post-infection and double-stained with an anti-His antibody to reveal Prob and Proc and rhodamine-phalloidin to visualize F-actin. Scale bar=10μm.

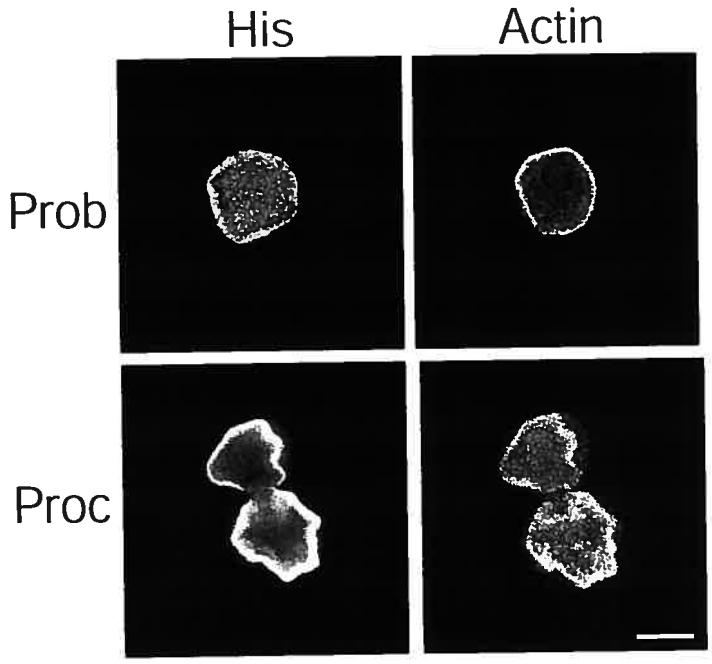
His
Actin
Prob
Proc

Figure 7. Electron micrographs illustrating longitudinal sections of a) MAP2b, cell body, b) MAP2c, cell body, c) MAP2c, process, d) MAP2b-1, process, e) MAP2b-2, cell body, f) MAP2b-2, process, g) MAP2b-3, cell body, h) MAP2b-3, process, i) Mt, process. Scale bar for c, f, h and i is 0.5 μm, for a, b, e and g, 0.25 μm and for d, 0.5 μm.

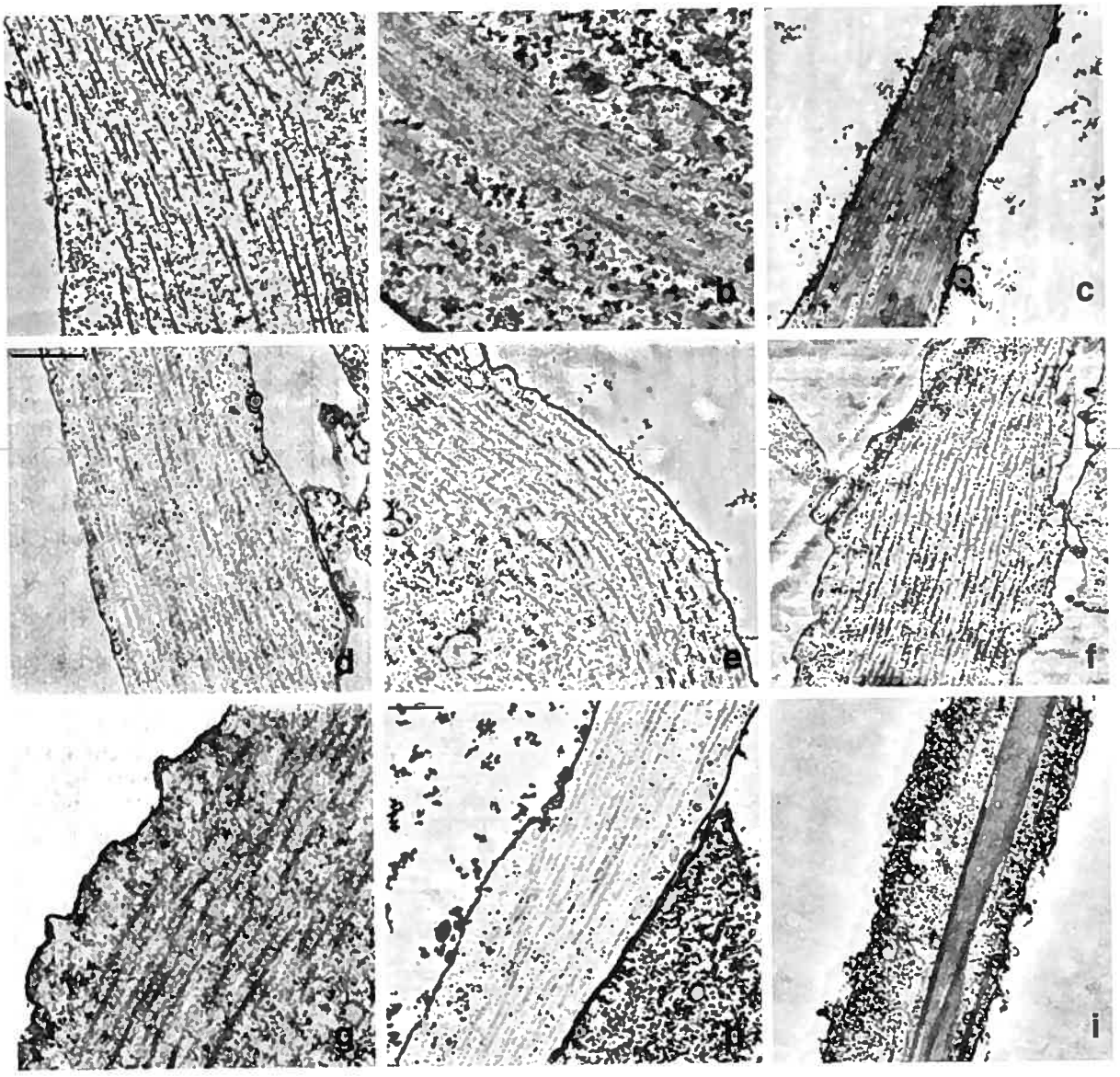
a
b
c
d
e
f
g
h
i

Figure 8. Purification of microtubules from Sf9 cells expressing the truncated forms of MAP2 and full length MAP2b and MAP2c. Microtubules were prepared 64 hrs following the infection as described in methods. A) The purity of microtubules was verified by Coomassie staining. 2 μg of microtubules were loaded per lane. Coomassie staining revealed microtubules as well as their associated protein. The numbers indicate respectively MAP2b, MAP2c, MAP2b-1, MAP2b-2, MAP2b-3 and Mt. The molecular weight standards are (top to bottom): Myosin (203 kDa), β-galactosidase (135 kDa), bovin serum albumin (86 kDa) and carbonic anhydrase (42 kDa). On a 7.5% acrylamide gel, Mt and tubulin migrate at the same level and thus it is not posssible to visualize Mt. However, Mt was revealed by dot blotting using the 46.1 antibody. B) To verify the level of tubulin, proteins were transferred on a nitrocellulose membrane. The membrane was revealed with an anti-tubulin monoclonal antibody.

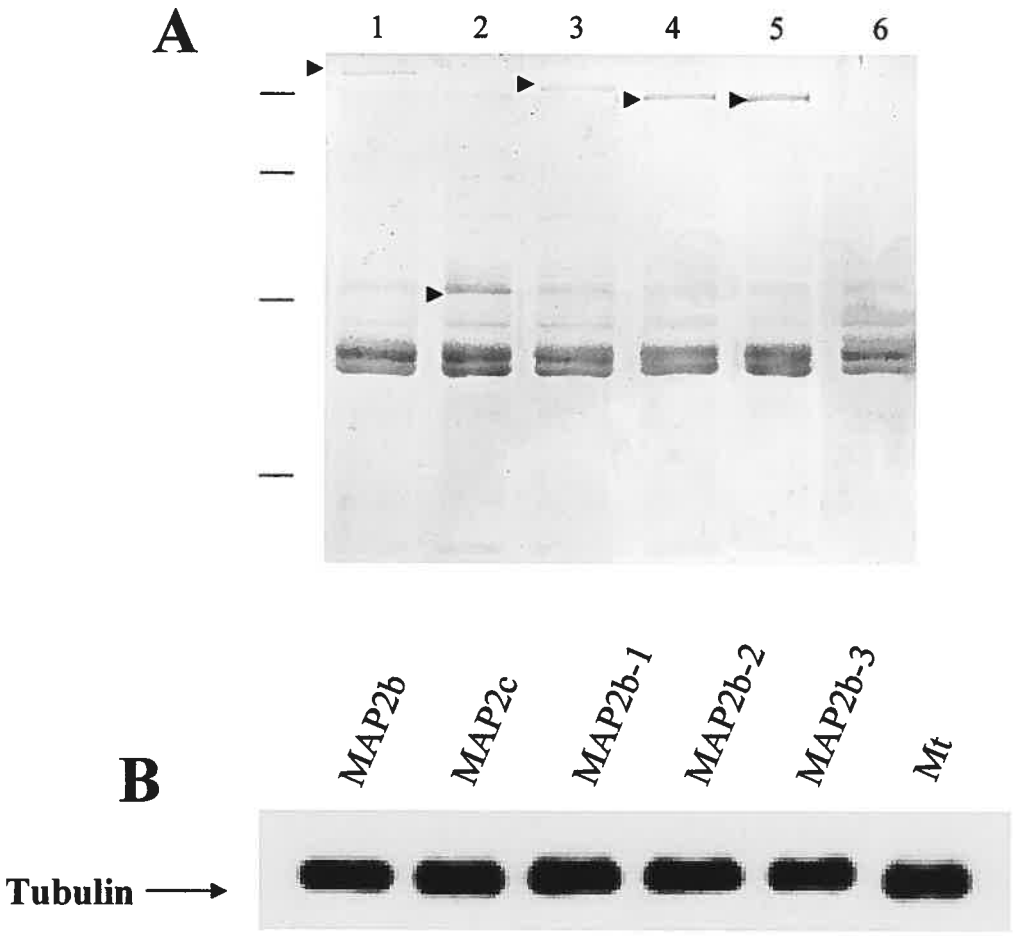
A
1
2
3
4
5
6
B
MAP2b
MAP2c
MAP2b-1
MAP2b-2
MAP2b-3
Mt
Tubulin

Figure 9. Sf9 cells co-infected with recombinant baculovirus containing Prob and Mt. Prob/Mt co-infectted cells were double-stained with a polyclonal antibody anti-MAP2 (A) to visualize the expression of Prob and the monoclonal antibody 46.1 to reveal the expression of Mt (D). Prob/Mt co-infected cells were also double-stained with the polyclonal antibody anti-MAP2 and a monoclonal antibody against α-tubulin to visualize the formation of microtubules by Mt. Cells expressing Prob were double-stained with the polyclonal antibody anti-MAP2 and a monoclonal antibody against α-tubulin to show that Prob does not induce the formation of microtubules in Sf9 cells. Scale bar=40μm.

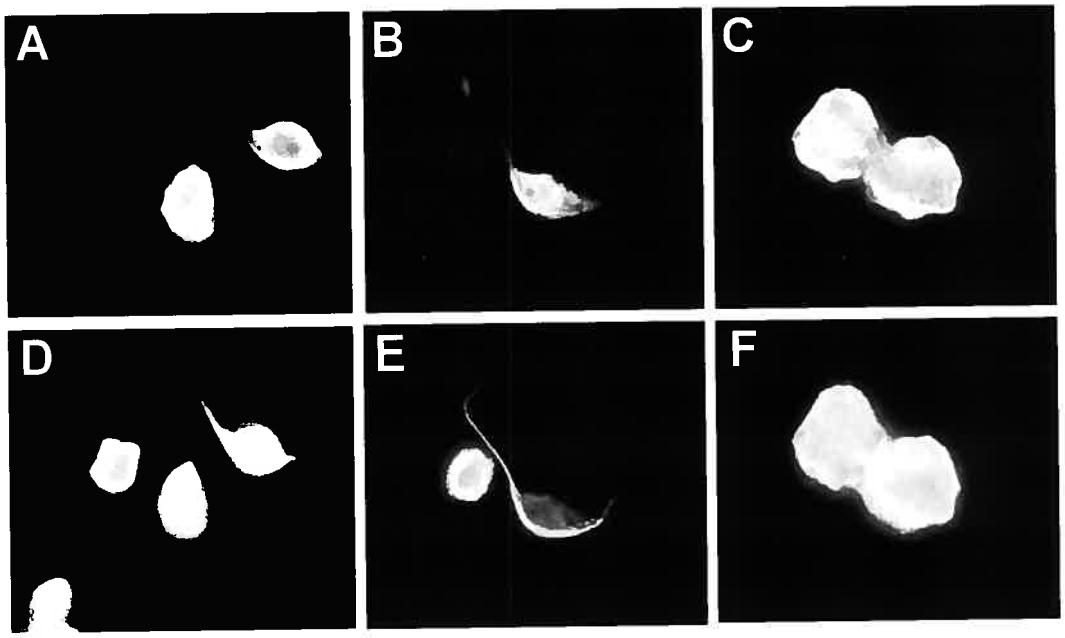
A
B
C
D
E
F

Figure 10. Quantitative morphological analysis of Sf9 cells co-expressing the constructs Prob and Mt. A viral m.o.i of 4 was used for each virus A) In Prob/Mt-expressing cells, the percentage of cells with processes was significantly lower than that of Mt-expressing cells. However, it was not the case in Proc/Mt-expressing cells. $p< 0.0166$ B)The percentage of cells presenting one, two or more than two processes was quantified in Sf9 cells co-expressing Prob and Mt and having processes. The number of processes per cell in Prob/Mt-expressing was statistically different from the one found in cells expressing Mt. $p<0.0166$. The horizontal lines indicate the constructs that are statistically different. The reproductibility of the data from one experiment to another was analyzed using a chi-square test. Chi-square tests were performed to compare the number of processes per cell induced by the different MAP2 constructs.

A

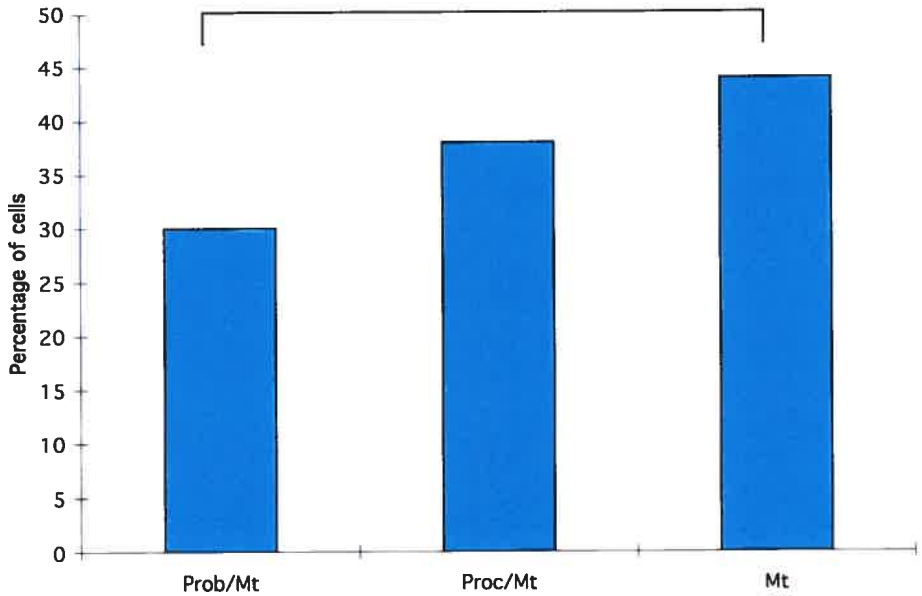
50
45
40
35
30
25
20
15
10
5
0
Percentage of cells
Prob/Mt
Proc/Mt
Mt

B

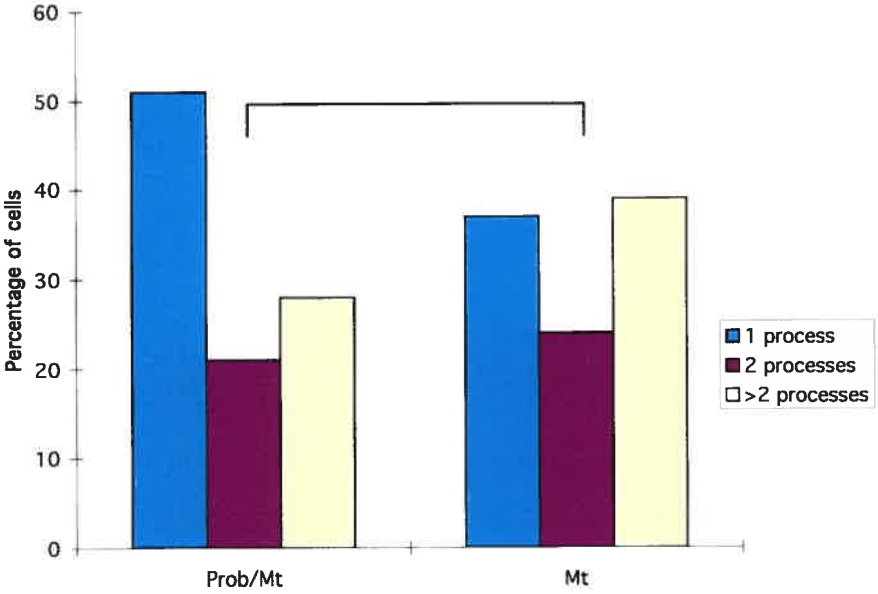
60
50
40
30
20
10
0
Percentage of cells
Prob/Mt
Mt
1 process
2 processes
>2 processes

Figure 11. Prob and Mt interact in Sf9 cells. Cells were co-infected with recombinant baculovirus containing Prob and Mt. At 72 h post-infection, cells were lysed. Total cell lysates were immunoprecipitated with either the anti-MAP2 antibody, AP20 or HM2 that recognize Prob. The presence of Mt in the immunoprecipitates was analyzed by immunoblotting using the antibody 46.1. In lane 1, no antibody was added to the cell lysates prepared from Prob/Mt expressing cells. In lane 2, the membrane was stained with AP20 to reveal the presence of Prob in the immunoprecipitates. In lane 3, the membrane probed with AP20 was stripped and stained with the antibody 46.1 to reveal the presence of Mt in the immunoprecipitates (arrowhead). In lane 4, Mt was immunoprecipitated using the antibody 46.1 from cells expressing only Mt. In lane 5, no antibody was added to the cell lysates prepared from Prob-expressing cells. In lane 6, the membrane was stained with AP20 to reveal the presence of Prob in the immunoprecipitates. In lane 7, the membrane probed with AP20 was stripped and stained with the antibody 46.1 to reveal the presence of Mt in the immunoprecipitates. No band corresponding to Mt was found in the immunoprecipitates. The arrow indicates the immunoglobulines.

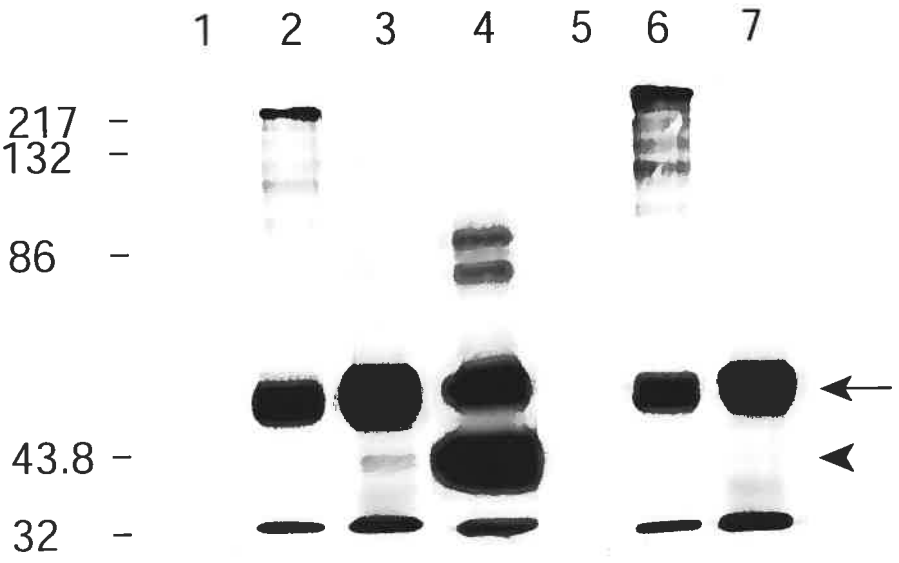
1
2
3
4
5
6
7
217
132
86
43.8
32

3 DEUXIÈME ARTICLE

"Abi Farah, C., Nguyen, M.D., Julien, J.P., et Leclerc, N. (2003) Altered levels and distribution of microtubule-associated proteins before disease onset in a mouse model of amyotrophic lateral sclerosis. *Journal of Neurochemistry* **84(1)**: 77-86."

Altered levels and distribution of microtubule-associated proteins before disease onset in a mouse model of amyotrophic lateral sclerosis

Carole Abi Farah, Minh Dang Nguyen*#, Jean-Pierre Julien* and Nicole Leclerc

*Département de pathologie et biologie cellulaire, Université de Montréal, Montréal, Québec, Canada, H3T 1J8; * Montreal General Hospital Research Institute in Neuroscience, McGill University, Montréal, Canada, H3G 1A4; # Present address: Harvard Medical School, Department of Pathology, Boston, MA 02115*

Running title: Microtubule-associated proteins in amyotrophic lateral sclerosis

Corresponding author:
Dr Nicole Leclerc
Département de pathologie et biologie cellulaire
Université de Montréal
C.P.6128, Succ. Centre-ville
Montréal, Québec
Canada H3C 3J7
Phone: (514)-343-5657
Fax: (514)-343-5755
[redacted]

ACKNOWLEDGEMENTS

We thank Dr. Virginia lee (University of Pennsylvania, USA) for providing the antibody 46.1, Dr. Doug Fambrough (The Johns Hopkins University, Baltimore, Maryland) for the anti-NAK-ATPase (2F), Dr. C. Bulinski (Columbia University, NY) for the anti-γ-actin and Dr. P. Davies (Albert Einstein College of Medicine, New York) for the PHF-1 antibody. This work was supported by Medical Research Council of Canada grant (MT-13245), by National Sciences and Engineering Research Council of Canada grant (NSERC) and by FCAR grant to N.L. NL is Scholar of the FRSQ. C. Abi Farah has a sudentship from CRSN and M.D. Nguyen has a K.M. Hunter/CIHR scholarship and holds a long-term fellowship from the Human Frontier Science Program Organization (HFSPO).

3.1 ABSTRACT

Alterations of the axonal transport and microtubule network are potential causes of motor neurodegeneration in mice expressing a mutant form of the superoxide dismutase 1 ($SOD1^{G37R}$) linked to amyotrophic lateral sclerosis (ALS). In the present study, we investigated the biology of microtubule-associated proteins (MAPs), responsible for the formation and stabilization of microtubules, in $SOD1^{G37R}$ mice. Our results show that the protein levels of MAP2, MAP1A, tau 100 kDa and tau 68 kDa species decrease significantly as early as 5 months before onset of symptoms in the spinal cord of $SOD1^{G37R}$ mice whereas decrease in levels of tau 52-55 kDa species is most often noted with the manifestation of the clinical symptoms. Interestingly, there was no change in the protein levels of MAPs in the brain of $SOD1^{G37R}$ mice, a CNS organ spared by the mutant SOD1 toxicity. Remarkably, as early as 5 months before disease onset, the binding affinities of MAP1A, MAP2 and tau isoforms to the cytoskeleton decreased in spinal cord of $SOD1^{G37R}$ mice. This change correlated with a hyperphosphorylation of the soluble tau 52-55 kDa species at epitopes recognized by the antibodies AT8 and PHF-1. Finally, a shift in the distribution of MAP2 from the cytosol to the membrane is detected in $SOD1^{G37R}$ mice at the same stage. Thus, alterations in the integrity of microtubules are early events of the neurodegenerative processes in $SOD1^{G37R}$ mice.

Keywords: Amyotrophic lateral sclerosis, microtubule-associated proteins, microtubules, dendrites, axon, phosphorylation.

3.2 INTRODUCTION

Amyotrophic lateral sclerosis (ALS) is an adult-onset neurodegenerative disease characterized by the progressive loss of motor neurons leading to paralysis and death within 3-5 years (for review see (Julien, 2001)). Five to ten percent of cases of ALS are familial and the others are believed to be sporadic. Mutations in the gene encoding superoxide dismutase 1 (SOD1) account for 20% of cases of familial ALS (Rosen, 1993; Cudkowicz *et al.*, 1997).

The SOD1 protein is a cytosolic copper- and zinc-dependent enzyme which converts superoxide anions into hydrogen peroxide. Transgenic mice expressing mutant SOD1 develop the ALS phenotype through the gain of novel, cytotoxic activity, of which nature remains unknown (Wong *et al.*, 1995; Bruijn *et al.*, 1997; Bruijn *et al.*, 1998). Several primary mechanisms have been proposed to explain this cytotoxicity such as oxidative stress (Wiedau-Pazos *et al.*, 1996); glutamate-mediated excitotoxicity (Trotti *et al.*, 1999); apoptosis mediated by caspase activation (Li *et al.*, 2000), deregulation of cyclin-dependent kinase 5 (Cdk5) (Nguyen *et al.*, 2001).

The most common pathological hallmark in both sporadic and SOD1-mediated ALS is the abnormal accumulation of cytoskeletal proteins such as neurofilaments, in the perikaryon or axon of spinal motor neurons (Hirano *et al.*, 1984; Rouleau *et al.*, 1996). Such accumulation has also been observed in SOD1 mutant mice (Wong *et al.*, 1995; Bruijn *et al.*, 1997). Furthermore, an accumulation of tubulin has been reported in the perikarya and/or proximal axonal segments of spinal motor neurons in SOD1 mutant mice (Williamson and Cleveland, 1999). These abnormalities are compatible with the

slowing of the axonal transport detected in these mice (Williamson and Cleveland, 1999).

Of particular interest, are the aberrant modifications of microtubule-associated proteins (MAPs) in ALS patients and in mice expressing SOD1 mutant. Indeed, the abnormal hyperphosphorylation of tau is detected in SOD1 mutant mice 10-11 months old (Nguyen *et al.*, 2001) and has been attributed to deregulation of Cdk5, a prominent kinase in the CNS (for a review see (Dhavan and Tsai, 2001)). Moreover, in dendrites, the expression levels of MAP2 decreased in patients with ALS (Kikuchi *et al.*, 1999). This decrease correlated with the degree of degeneration and with the clinical symptoms of limb weakness. Alternatively, the loss of the cytoskeleton within the dendrites of spinal motor neurons in ALS patients may constitute a mechanism of neuronal atrophy (Kiernan and Hudson, 1993).

It is however unclear whether alterations of the cytoskeleton occur at an early stage of the disease before initiation of neuronal death. In the present study, we examined the biology of axonal and dendritic MAPs in $SOD1^{G37R}$ mice before and after neurodegeneration. Our results provide compelling evidence that the molecular integrity of the dendritic and the axonal microtubules is compromised months before the onset of symptoms in $SOD1^{G37R}$ mice.

3.3 MATERIALS AND METHODS

3.3.1 Materials

The cocktail of protease inhibitors was purchased from Roche Diagnostics (Laval, Quebec, Canada). The Bio-Rad DC protein assay kit and the Bio-Rad protein

assay kit based on the method of Bradford were purchased from Bio-Rad Laboratories (Hercules, CA). The monoclonal anti-MAP2 (clone HM2), the anti-α-tubulin (clone DM1A), the anti-β-actin and Taxol were obtained from Sigma (Mississauga, Ontario, Canada); the monoclonal anti-MAP2 phosphodependent (clone AP18) from Neomarkers (Medicorp Inc., Montréal, Québec, Canada); the monoclonal antibodies anti-MAP1A, anti-NF-H (RT-97) and anti-NF-M (NN-18) from Chemicon (Temecula, California); the monoclonal anti-NF-L (NR4) and the monoclonal dephosphorylation dependent anti-Tau-1 from Boehringer Mannheim (Mannheim, Germany); the polyclonal anti-VDAC antibody from Oncogene (San Diego, California) and the monoclonal AT8 from Innogenetics (Zwijndrecht, Belgium). The monoclonal antibody 46.1 was kindly provided by Dr. V. Lee (University of Pennsylvania), the polyclonal anti-γ-actin by Dr. C. Bulinski (Columbia University, NY), the anti-NAK-ATPase (2F) by Dr. D. Fambrough (The Johns Hopkins University, Baltimore, Maryland) and the monoclonal PHF-1 by Dr. P. Davies (Albert Einstein College of Medicine, New York). The secondary antibodies were purchased from Jackson Immunoresearch Laboratories Inc. (Bio/Can, Mississauga, Ontario, Canada). The chemiluminescence kit was purchased from Amersham Biosciences (Baie d'Urfe, Quebec, Canada). The Image Quant program was purchased from Molecular Dynamics.

3.3.2 Generation of SOD1^{G37R} mice

Inbred C57BL6 SOD1^{G37R} mice (line 29) were used in this study. These mice have a life span of approximately 11-12 months (Nguyen *et al.*, 2000) (Nguyen *et al.*,

2001). The mouse genotypes were determined by Southern blotting of tail DNA. The use of animals and all surgical procedures described in this article were carried out according to The Guide to the Care and Use of Experimental Animals of the Canadian Council on Animal Care.

3.3.3 Preparation of total protein extracts

The mice were sacrificed by intraperitoneal injection of chloral hydrate. After dissection, the spinal cord samples were frozen immediately at -80°C. Total protein extracts were prepared by homogenization in SDS 0.5%, urea 8M buffer to which a cocktail of protease inhibitors has been added prior to use. The homogenate is then centrifuged at 12,000 g for 10 min at 4°C and the pellet is discarded. The protein concentration was estimated using the Bio-Rad DC protein assay.

3.3.4 Immunoblotting and dot blotting

Proteins were fractionated on a 7.5% polyacrylamide gel and transferred on a nitrocellulose membrane for Western blot analysis. For dot blotting, 30 μg of total protein were applied to a nitrocellulose membrane using a dot blot Manifold apparatus. The membrane was air dried for 20 min and was then incubated with the primary antibody for 60 min at room temperature. The membrane is then washed and incubated with the secondary antibody conjugated to HRP and revealed by chemiluminescence. To quantify the protein level, the autoradiographic bands or dots were scanned and the

digitized data were quantified using the program ImageQuant. Non-saturated blots were used for quatification and different exposure times insured consistency.

3.3.5 Taxol stabilized microtubule preparations

Spinal cord were dissected out and homogenized in a dounce homogenizer in 2ml of taxol 20 μM/Saponin 0.01% PHEM extraction medium (60 mM PIPES, 25mM HEPES, 10 mM EGTA, 2 mM $MgCl_2$) to which a cocktail of protease inhibitors was added prior to use (Zhu *et al.*, 1998) (Black *et al.*, 1986). The homogenates were incubated at room temperature for 8 min to solubilize unassembled tubulin and then centrifuged for 15 min at 30,000 rpm. The pellets were dissolved in 1% SDS-Tris buffer (50 mM Tris, pH 7.4) and the protein content was estimated using the Bio-Rad DC protein assay kit.

3.3.6 Preparation of membrane extracts

The spinal cord was homogenized in 10 volumes of 0.25 M sucrose dissolved in ice-cold 10 mM Tris-HCl buffer, pH 7.4 to which a cocktail of protease inhibitors was added prior to use. The homogenate was centrifuged at 1,500 g for 15 min at 4°C to remove cell debris. The supernatant was then centrifuged at 105,000 g for 1 hr at 4°C and the new supernatant was saved. This fraction was referred to as "soluble cytosol". The remaining pellet was resuspended in the above sucrose-Tris buffer and was referred to as "membrane fraction". The protein content of the different fractions was determined using the Bio-Rad protein assay kit based on the method of Bradford.

3.4 RESULTS

3.4.1 Decreased levels of MAPs before disease onset in the spinal cord of SOD1^{G37R} mice

To investigate the contribution of MAPs at an early stage of neurodegeneration in SOD1^{G37R} mice, we examined the protein levels of dendritic and axonal microtubule-associated proteins in SOD1^{G37R} mice 5 months before the onset of clinical symptoms. Using antibodies that recognize the dendritic MAP2 (HM2), the axonal tau (46.1) and MAP1A (MAB362), a MAP present in both compartments, we have determined by Western blotting or dot blotting the protein levels of these MAPs in total spinal cord extracts from normal mice (WT) and SOD1^{G37R} mice 5.5 months old. HM2, 46.1 and MAB362 are phospho-independent antibodies. Quantitative analysis was performed using the ImageQuant program. As shown in figures 1a and 1b, the protein levels of MAP2, tau isoforms and MAP1A do not change with aging in the spinal cord of normal mice but decrease dramatically in SOD1^{G37R} mice 5.5 months old following a distinct pattern: MAP1A levels are always altered, followed by MAP2 and finally by the tau isoforms. Levels of tau 52-55 kDa species are always the less affected. Figure 1a shows an example of a SOD1^{G37R} mouse 5.5 months old exhibiting a significant decrease in protein levels for all MAPs. The quantitative analyses revealed that the levels of MAP1A, MAP2, tau 100 kDa species and tau 68 kDa species decrease significantly in SOD1^{G37R} mice 5.5 months old as compared to normal mice with remaining levels of 60.35% ± 14.52, 41.99% ± 14.19, 55.1% ± 19.32 and 46.44% ± 15.53 respectively (figure 1b). Surprisingly, the level of tau 52-55 kDa species decreases importantly only

in three of the six SOD1^{G37R} mice 5.5 months old examined and thus the average percentage compared to normal mice is not significant (70.17% ± 19.31).

We also examined the change in the protein levels of MAP1A, MAP2 and tau isoforms in 10-11 months old SOD1^{G37R} mice. As shown in figures 1a and 1b, the protein levels of all MAPs have decreased significantly at this stage as compared to normal mice. The remaining levels for MAP1A, MAP2, tau 100 kDa species, tau 68 kDa species and tau 52-55 kDa species are 50.47% ± 13.72, 1.62% ± 0.46, 12.14% ± 3.03, 13.88% ± 4.80 and 50.11% ± 10.78 respectively. Taken together, the above results indicate that the protein levels of both axonal and dendritic MAPs decrease in the spinal cord of SOD1^{G37R} mice. This decrease occurs before disease onset for MAP1A, MAP2, tau 100 kDa and tau 68 kDa species whereas an important decrease of the protein level of tau 52-55 kDa species is noted mostly with the manifestation of clinical symptoms and paralysis. In contrast to other MAPs, the level of MAP1A decreases in SOD1^{G37R} mice 5.5 months old and then remains at the same level at later stages of the disease.

To confirm that the decrease of the protein levels of MAPs is specific to the neurodegenerative processes occurring in the spinal cord, we examined the levels of these proteins in the brain of SOD1^{G37R} mice, a CNS organ spared by the mutant SOD1 toxicity ((Wong *et al.*, 1995); Daigle, Nguyen, Julien and Rivest, personal communication). As shown in figures 2a and 2b, the protein levels of MAP2, MAP1A and of tau species do not change significantly with aging in normal brain even though the protein level of MAP1A appears to be decreased in two of the four SOD1^{G37R} mice 10 months old examined. No significant decrease of the protein levels of MAPs was detected either in the brain of SOD1^{G37R} mice 6.5 months old and SOD1^{G37R} mice 10

months old (figures 2a and 2b). However, a noticeable decrease in levels of MAP2 was detected in two of the four $SOD1^{G37R}$ mice 10 months old examined. Collectively, the above results demonstrate that the decrease of MAPs precedes neurodegeneration in the spinal cord of $SOD1^{G37R}$ mice.

3.4.2 No change of the protein levels of tubulin, actin or neurofilaments before disease onset in $SOD1^{G37R}$ mice

We next examined the change in the levels of tubulin, actin and neurofilaments in $SOD1^{G37R}$ mice 5.5 months before disease onset. Using antibodies that recognize tubulin (DM1A for the α isoform), actin (β and γ isoforms) and neurofilament subunits (RT-97 for NF-H, NN-18 for NF-M and NR4 for NF-L), we have determined by Western blotting the levels of these proteins in total spinal cord extracts from normal mice and $SOD1^{G37R}$ mice at 5.5 months and 10-11 months old. At the exception of RT-97, all of the antibodies used are phospho-independent. Quantitative analysis was performed as described in the previous section. There is no significant decrease in the levels of α-tubulin, β-actin, γ-actin, NF-H, NF-M or NF-L in $SOD1^{G37R}$ mice 5.5 months old (figures 3a and 3b). At 10-11 months, as illustrated in figures 3a and 3b, the levels of α-tubulin, γ-actin and NF-L are not significantly altered. However, the level of β-actin diminishes in these mice with a remaining of 31.28% ± 17.74. Furthermore, the levels of NF-H and NF-M also decrease at this stage with a remaining of 76.82% ± 1.44 and 70.42% ± 6.80 respectively. Collectively, our results reveal that the levels of tubulin, actin and neurofilaments do not decrease before disease onset in $SOD1^{G37R}$ mice.

However, the levels of β-actin, NF-H and NF-M decrease in SOD1^{G37R} mice 10-11 months old when the clinical symptoms begin to appear. Any decrease of the protein level in end-stage mutant mice could be due to the extensive neuronal loss observed at this age.

3.4.3 Decreased binding affinities of MAPs to the cytoskeleton before disease onset in SOD1^{G37R} mice

To further analyse the alterations of MAPS in ALS mice, we determined their binding affinities to the cytoskeleton. We prepared taxol-stabilized cytoskeletal fractions from the spinal cord of normal mice and SOD1^{G37R} mice 5.5 months old and compared their content in MAPs. As previously reported, this preparation contains microtubules, neurofilament subunits and actin (Black *et al.*, 1986; Zhu *et al.*, 1998). The "insoluble cytoskeletal fraction" and the "soluble cytoskeletal fraction" were prepared as described in methods and were analysed by Western blotting for their content in tubulin, MAP1A, MAP2 and tau isoforms. Quantitative analysis was performed as described above. The proportion of insoluble cytoskeletal fraction was determined for each microtubule-associated protein. Since taxol is used in the extraction buffer, tubulin is found almost exclusively in the insoluble cytoskeletal fractions in normal mice and SOD1^{G37R} mice 5.5 months old (figure 4a). In the control mouse, the amount of MAPs in the insoluble fraction was higher than in the soluble fraction whereas in mutant mice, the opposite was observed. The proportion of insoluble MAP1A in the normal mouse is 61.54%. This number decreases to become on average 32.32% in the three SOD1^{G37R} mice tested. Furthermore, the proportion of insoluble MAP2 is 56.71% in the normal mouse. This

number diminishes to become 20.84% in the three mutant mice examined. Moreover, we verified the proportion of insoluble tau isoforms in these mice with the phosphorylation-independent antibody 46.1. In the normal mouse, the proportion of insoluble tau 100 kDa, tau 68 kDa and tau 52-55 kDa species is 35.88%, 40.93% and 66.9% respectively. In the three mutant mice, this ratio decreases to 26.58%, 28.8% and 26.66% respectively. Figure 4b shows the relative proportion of insoluble MAPs in $SOD1^{G37R}$ mice 5.5 months old compared to normal mice. Our observations indicate that the binding affinities of MAP1A, MAP2 and tau isoforms to the cytoskeleton decrease in $SOD1^{G37R}$ mice as early as 5 months before disease onset.

Previous studies reported a change in the phosphorylation state of tau 52-55 kDa species in $SOD1^{G37R}$ mice 10-11 months old at the epitopes recognized by the AT-8 and the PHF-1 antibodies (Ser199/202, Thr205 for AT8 and Ser 396/404 for PHF-1) (Nguyen *et al.*, 2001). To determine whether a change in the phosphorylation state of tau is associated with decreasing its binding affinity to the cytoskeleton, the insoluble/soluble fractions were stained with the AT8 and the PHF-1 antibodies. As shown in figure 4a, there was an increase of the phosphorylation state of tau 52-55 kDa species in the three SOD1 mutants tested. Interestingly, this increase occurred in the soluble fraction suggesting that a change in the phosphorylation state of tau might be responsible for decreasing its binding affinity to the cytoskeleton. No change in the phosphorylation state of tau 100 kDa and tau 68 kDa species was observed at the epitopes recognized by the AT8 and the PHF-1 antibodies. Interestingly, the binding affinity of tau 52-55 kDa to the cytoskeleton is more severely affected than that of tau 100 and tau 68 kDa species. We also tested Tau-1 antibody that recognizes a

dephosphorylated epitope of tau at amino acids 191-224. No change in the staining of tau 100 kDa, tau 68 kDa or tau 52-55 kDa species was detected with this antibody (figure 4a).

Finally, to test whether the phosphorylation state of MAP2 was affected in $SOD1^{G37R}$ mice, we used the phospho-dependent antibody AP18 that recognizes residue Ser^{136} located in the projection domain of MAP2. This site is highly phosphorylated during dendritic outgrowth and plasticity (Riederer, 1992; Riederer *et al.*, 1995). In the mutant mice examined, the staining with the AP18 antibody was similar to that detected with the non-phosphorylation dependent antibody HM2 (figure 4a). Thus, we can conclude that the phosphorylation state of MAP2 at residue Ser^{136} does not change in $SOD1^{G37R}$ mice. However, this does not rule out the possibility of alteration in the phosphorylation of MAP2 in $SOD1^{G37R}$ mice.

3.4.4 Alteration of the membrane proportion of MAP2 in $SOD1^{G37R}$ mice

Previous studies reported that MAPs interact with membranous components. As such, tau is found at the plasma membrane in neuronal cell lines (Maas *et al.*, 2000). Furthermore, the interaction of MAP2 with plasma membrane associated proteins as well as integral plasma membrane proteins has also been observed (Davare *et al.*, 1999; Lim and Halpain, 2000). Moreover, an interaction of both MAP2 and tau with mitochondria has been reported (Jancsik *et al.*, 1989; Linden *et al.*, 1989a; Jung *et al.*, 1993). In the present study, a "total membrane fraction" and a 'soluble cytosol fraction' were prepared from the spinal cord of normal mice and $SOD1^{G37R}$ mice as described in methods (figure 5a). The fractions were analysed by Western blotting to determine their

content with the plasma membrane marker protein Na-K ATPase and with the mitochondrial marker protein VDAC (voltage-dependent anion channel). As shown in figure 5b, the total membrane fractions are enriched with plasma membranes and with mitochondria. These fractions were also analysed to determine their content with MAP1A, MAP2 and tau isoforms. Quantitative analysis was performed as described above. The membrane proportion was calculated for each protein. Four control mice; four $SOD1^{G37R}$ mice 5.5 months old and four $SOD1^{G37R}$ mice 10-11 months old were examined (figure 5c). The average membrane proportion of MAP2 in normal mice is 5.37% ± 3.3. This proportion increased in two of the four $SOD1^{G37R}$ mice 5.5 months old examined and then increased significantly to become on average 43.65% ± 2.41 in the four $SOD1^{G37R}$ mice 10-11 months old examined. From these observations, one can conclude that the alteration of the membrane proportion of MAP2 correlates with neurodegeneration in $SOD1^{G37R}$ mice. The average membrane proportions of tau 100 kDa and tau 68 kDa species in normal mice are 5.39% ± 3.57 and 20.84% ± 4.8 respectively. These proportions do not change significantly in 5.5 months old and in 10-11 months old SOD1 mutant mice. The average membrane proportion of tau 52-55 kDa species is 62.78% ± 2.67 in normal mice. This proportion decreases significantly in $SOD1^{G37R}$ mice 5.5 months old to become 52.44% ± 3.08. However, this decrease is observed in only two of the four $SOD1^{G37R}$ mice 10-11 months old examined. Thus, this lack of consistency does not allow us to correlate the alteration of the membrane proportion of tau 52-55 kDa species with neurodegeneration. The average membrane

proportion of MAP1A in normal mice is 29.03% ± 6.9. This number did not change significantly in SOD1^{G37R} mice 5.5 months old or 10-11 months old.

3.5 DISCUSSION

In the present study, we report decreased protein levels of MAPs before disease onset in SOD1^{G37R} mice. The fact that this decrease was only noted in the spinal cord where neuronal cell death mainly occurs indicates that it could contribute to cell dysfunction leading to neurodegeneration in SOD1 mutant mice. In different experimental contexts, a decrease of MAP protein levels was induced by excitotoxicity, traumatic brain injury, focal ischemia and oxidative stress (Irving *et al.*, 1996; Posmantur *et al.*, 1996; Arias *et al.*, 1997). In SOD1^{G37R} mutant, glutamate-induced excitotoxicity is one plausible mechanism contributing to neuronal cell death. This excitotoxicity would be mainly caused by a reduction of the astroglial glutamate transporter EAAT2 (Rothstein *et al.*, 1995). The involvement of other non-neuronal cells, possibly glial cells in ALS pathogenesis is supported by a recent study reporting that the expression of high levels of human SOD1^{G37R} mutant specifically in large motor neurons of the spinal cord of transgenic animals does not cause neurodegeneration (Pramatarova *et al.*, 2001). According to this hypothesis, the alterations of the protein levels of MAPs in SOD1^{G37R} mice might be secondary to a glutamate-induced neuronal excitotoxicity. In support of this idea, one study reported that glutamate receptor antagonists inhibit calpain-mediated proteolysis of cytoskeletal proteins such as MAP2 and tau (Minger *et al.*, 1998). Calpain activity was reported to be deregulated in

neurodegenerative diseases and could result from an altered calcium homeostasis due in part to an increase of extracellular glutamate, mitochondrial defects and oxidative stress (Saito *et al.*, 1993). Moreover, MAP2 and tau are substrates for calpains (Johnson *et al.*, 1989; Fischer *et al.*, 1991). Therefore, the early decrease of MAPs reported in the present study might indicate that calpain deregulation is one of the events leading to neuronal cell dysfunction and death in SOD1 ^{G37R} mice.

Interestingly, the protein level of MAP1A decreases as early as 5 months before disease onset in SOD1^{G37R} mice and does not diminish significantly afterwards even when neuronal loss is apparent. This might indicate an increase of the level of MAP1A during neurodegeneration in SOD1^{G37R} mice as a compensatory effect following the decrease of MAP2 and tau. Indeed, in tau knock out mice, an increase of MAP1A was reported (Harada *et al.*, 1994). In the case of tau proteins, the level of tau 52-55 kDa species is altered mostly when neurodegeneration is apparent in SOD1^{G37R} mice. This is the only tau isoform to present a change in its phosphorylation state at the epitopes recognized by the antibodies AT-8 and PHF-1. One explanation is that phosphorylated tau is more resistant to proteolysis as reported in previous studies (Litersky and Johnson, 1995). This selectivity towards tau 52-55 kDa species might also indicate that distinct signalling pathways regulate different tau isoforms. Distinct regulation of tau isoforms is observed in several "tauopathies" where a specific set of pathological tau proteins exhibit a typical biochemical pattern and different laminar and regional distribution (for review see (Buee *et al.*, 2000). Interestingly, the protein levels of other cytoskeletal proteins such as β-actin and the neurofilament subunits NF-H and NF-M decrease

significantly when the clinical symptoms begin to appear in $SOD1^{G37R}$ mice. β-actin is enriched in structures having high capacity of remodelling in mature neurons such as dendritic spines in contrary to γ-actin that is found in dendrites, axons and in the cell body (Micheva *et al.*, 1998). The decrease of β-actin might indicate that dendritic spines are affected severely with onset of symptoms in $SOD1^{G37R}$ mice. In the case of neurofilament subunits, a previous study reported that the level of NF-L mRNA decreases in ALS cases whereas that of NF-H and NF-M remains unchanged (Wong *et al.*, 2000). If subtle changes of the neurofilament protein levels occur before disease onset, preparation of a total spinal cord extract may not allow us to detect them.

The implication of the decrease of MAPs on microtubule structure and function remains elusive. However, recent studies demonstrated that a complete suppression of either tau or MAP2 expression does not lead to an important decrease of microtubule density in knock out mice (Harada *et al.*, 1994; Harada *et al.*, 2002). Therefore, a decrease of the protein levels of these MAPs before disease onset in $SOD1^{G37R}$ mice does not necessarily imply a decrease of the microtubule density in affected dendrites and axons. For instance, the apparent increase of the protein level of MAP1A observed in $SOD1^{G37R}$ mice might compensate for the described loss of MAP2 and tau species as previously reported.

Remarkably, a decrease in the binding affinities of MAP1A, MAP2 and tau isoforms to the cytoskeleton is observed as early as 5 months before disease onset in $SOD1^{G37R}$ mice. MAP1A, MAP2 and tau are phosphoproteins and their interaction with microtubules depends on their phosphorylation state (Buee *et al.*, 2000; Sanchez *et al.*,

2000a). Our present results reveal an increase in the phosphorylation state of the soluble tau 52-55 kDa at the epitopes recognized by the antibodies AT-8 and PHF-1 in $SOD1^{G37R}$ mice 5.5 months old. Thus, one explanation of the decrease of the binding affinities of MAPs to microtubules would be a deregulation of the activity of one or many kinases in $SOD1^{G37R}$ mice. Deregulation of kinases has been linked to ALS (Wagey *et al.*, 1998). For instance, cyclin-dependent kinase 5 (Cdk5), associated with oxidative stress in degenerating motor neurons in ALS patients, is abnormally hyperactivited in the spinal cord of $SOD1^{G37R}$ mice 10-11 months old (Nguyen *et al.*, 2001). This deregulation of Cdk5 in $SOD1^{G37R}$ mice 10-11 months was associated with the hyperphosphorylation of tau at sites recognized by the antibodies PHF-1 and AT-8. Moreover, activation of Cdk5 is known to abolish the binding of tau to microtubules (Wada *et al.*, 1998; Patrick *et al.*, 1999). The activity of other kinases such as the Ca(2+)-phospholipid-dependent-protein kinase C (PKC) has been also reported to be abnormally amplified in ALS patients (Lanius *et al.*, 1995) (Krieger *et al.*, 1996) and tau is a substrate for PKC via the mitogen-activated protein (MAP) kinase pathway (Ekinci and Shea, 1999). PKC also phosphorylates MAP2 (Ser-1703, Ser-1711 and Ser-1728) and abolishes its association with microtubules (Hoshi *et al.*, 1988). Furthermore, inhibition of Janus kinase-3 (JAK3) has been shown to increase survival in mice expressing mutant SOD1 (Trieu *et al.*, 2000) although it is still unknown whether JAK3 phosphorylates MAPs. Our observation of hyperphosphorylation of tau 5 months before disease onset indicates that deregulation of kinases and/or balance in phosphatases/kinases activity occurs early in the process of neurodegeneration in mutant SOD1mice.

Another alteration observed in $SOD1^{G37R}$ mice is a significant increase of the membrane proportion of MAP2 in two of the $SOD1^{G37R}$ mice 5.5 months old examined and in the four $SOD1^{G37R}$ mice 10-11 months old used in this study. MAP2 can interact with plasma membrane associated proteins such as Src and Grb2 as well as integral plasma membrane proteins such as the class C L-type calcium channel (Davare *et al.*, 1999; Lim and Halpain, 2000). The interaction of MAP2 with Src and Grb2 is phospho-dependent (Hoshi *et al.*, 1988; Lim and Halpain, 2000; Ozer and Halpain, 2000). Thus, one explanation of the altered distribution of MAP2 in $SOD1^{G37R}$ mice could be a change in the phosphorylation state of the protein affecting its interaction with membranous components. Another possibility is that MAP2 has an altered conformational state induced by unknown mechanisms in SOD1 mutant mice and thus behaves differently in the experimental conditions used to prepare membrane and cytosolic fractions.

In summary, our study shows that the molecular integrity of both dendritic and axonal microtubules is altered before onset of symptoms in $SOD1^{G37R}$ mice. Our results are compatible with a previous study which reported reduced transport of selective cargoes of the slow axonal transport before disease onset in SOD1 mutant mice indicating that microtubule function is affected (Williamson and Cleveland, 1999). Thus, our study indicates that microtubules are an early target in the neurodegeneration process in SOD1 mutant mice. The characterization of these early targets will help to elaborate preventive therapeutic strategies.

Figure 1. The protein levels of microtubule-associated proteins were examined in normal mice and in $SOD1^{G37R}$ mice. n indicates the number of animals. Quantitative analysis was performed using densitometry. The results are presented as average ± SEM. The statistical significance was determined using the t test. The asterisk indicates statistical difference (*$P<0.05$). a) Western blots of total spinal cord extracts from normal mice and from $SOD1^{G37R}$ mice were revealed using the HM2 antibody (anti-MAP2), the 46.1 (tau isoforms) and an anti-MAP1A (MAB362). 30 μg of protein were loaded per lane. The protein level is similar in the different lanes as indicated by actin staining (γ isoform). MAP1A was quantified using either western blot or dot blot technique. A western blot of MAP1A shows the specifity of the antibody MAB362. b) The protein levels of MAPs do not change with aging in the spinal cord of normal mice. In the $SOD1^{G37R}$ mice of 5.5 months of age, a significant decrease of the level of MAP1A, MAP2, tau 100 kDa and tau 68 kDa species is noted. An alteration of the protein level of tau 52-55 kDa species occurs in $SOD1^{G37R}$ mice of 10-11 months old.

Figure 2. a) Western blots of total brain extracts from normal mice and from $SOD1^{G37R}$ mice reveal the protein levels of MAPs. Quantification was performed as described above. b) The protein levels of MAPs do not change with aging in the normal brain or in the $SOD1^{G37R}$ mice brain.

Figure 3. The protein levels of tubulin, actin and neurofilaments were examined in $SOD1^{G37R}$ mice. n indicates the number of animals. Quantitative analysis was performed using densitometry. The results are presented as average ± SEM. The statistical significance was determined using the t test. The asterisk indicates statistical difference (*$P<0.05$). a) Western blots of total spinal cord extracts from $SOD1^{G37R}$ mice and from normal mice were revealed using the anti-α-tubulin, anti-β-actin, anti-γ-actin, anti-NF-H (RT-97), anti-NF-M (NN-18) and anti-NF-L (NR4). 30 μg of protein were loaded per lane. b) The protein levels of tubulin, actin and neurofilaments do not change in the spinal cord of $SOD1^{G37R}$ mice 5.5 months old compared to normal mice. However, the protein levels of actin (β-isoform), NF-H and NF-M decrease significantly in $SOD1^{G37R}$ mice 10-11 months old.

Figure 4. Taxol stabilized cytoskeletal fractions were prepared from spinal cord of normal mice and $SOD1^{G37R}$ mice 5.5 months old as described in material and methods. a) Western blots of insoluble and soluble cytoskeletal fractions were revealed using the anti-α-tubulin, the HM2 antibody (anti-MAP2), the 46.1 (tau isoforms) and an anti-MAP1A. The fractions were also stained with the phospho-dependent anti-tau antibodies AT8 and PHF-1 as well as the dephosphorylation dependent antibody Tau-1. 30 μg of protein were loaded per lane. Densitometric analysis was performed as described in material and methods. The proportion of insoluble MAP1A, MAP2 and tau isoforms decreases in $SOD1^{G37R}$ mice 5.5 months old indicating a decrease in the binding affinities of MAPs to the cytoskeleton. Furthermore, there is an increase of the phosphorylation state of the soluble tau 52-55 kDa species at the epitopes recognized by the AT8 and the PHF-1 antibodies. Membranes were also revealed with the phospho-dependent anti-MAP2 antibody AP18 that recognizes residue Ser136 located in the projection domain of MAP2. b) The relative decrease of the proportion of insoluble MAPs in $SOD1^{G37R}$ mice 5.5 months old is presented compared to normal mice.

Figure 5. a) Schematic of the protocol used for preparation of total membrane extract from spinal cord homogenate of normal mice and $SOD1^{G37R}$ mice. b) Western blots of the membrane fraction and the soluble cytosol from $SOD1^{G37R}$ mice and from normal mice were revealed using the anti-NA-K ATPase (2F), the anti-VDAC (mitochondria), the HM2 antibody (anti-MAP2), the 46.1 (tau isoforms) and an anti-MAP1A. 20 μg of protein were loaded per lane. c) The membrane proportions were determined for MAP1A, MAP2 and tau isoforms. The results are presented as average proportion ± SEM. n indicates the number of samples. The statistical significance was determined using the t test. The asterisk indicates statistical difference (*$P<0.05$).

4 TROISIÈME ARTICLE

"Abi Farah, C., Paiement, J., Liazoghli, D., Perreault, S., Desjardins, M., Guimont, A., Lauzon, M., Young, R., Kreibich, G., et Leclerc, N. Microtubule-associated protein-2: a new linker in the interaction between microtubules and rough endoplasmic reticulum membranes in neurons."

"article soumis"

Microtubule-associated protein-2: a new linker in the interaction between microtubules and rough endoplasmic reticulum membranes in neurons

Carole Abi Farah, Jacques Paiement, Dalinda Liazoghli, Sébastien Perreault, Mylène Desjardins, Alain Guimont, Michel Lauzon, Robin Young, Gert Kreibich¶, and Nicole Leclerc

Département de pathologie et biologie cellulaire, Université de Montréal, C.P.6128, Succ. Centre-ville, Montréal, Québec, Canada H3C 3J7 ¶Department of Cell Biology, New York University School of Medicine, New York, New York 10016

Running title: MAP2 links microtubules and ER membranes

Corresponding author:
Dr Nicole Leclerc
Département de pathologie et biologie cellulaire
Université de Montréal
C.P.6128, Succ. Centre-ville
Montréal, Québec
Canada H3C 3J7
Phone: (514)-343-5657
Fax: (514)-343-5755
[redacted]

ACKNOWLEDGEMENTS

The authors would like to thank Dr. M. G. Farquhar for providing the anti-mannosidase II antibody and Dr. D. Fambrough for the NaK-ATPase antibody. The monoclonal antibody E7 directed against β-tubulin developed by Michael Klymkowsky was obtained from the Developmental Studies Hybridoma Bank developed under the auspices of the NICHD and maintained by The University of Iowa, Department of Biological Sciences, Iowa City, IA 52242. We also thank Jean Léveillé and Annie Vallée for their excellent technical support and Diane Gingras for helpful discussion. This work was supported by the National Sciences and Engineering Research council of Canada grant (NSERC) and by the Canadian Institute of Health Research grants (CIHR), MOP-53218 (N.L.) and MOP-44022 (J.P.). N.L. is a scholar of Fonds de la recherche en santé du Québec (FRSQ) and C.A.F. and S.P. have a studentship from CRSN and M.D. a studentship from NSERC.

4.1 ABSTRACT

Neurons are polar cells presenting two distinct compartments: dendrites and an axon. Dendrites can be distinguished from the axon by the presence of rough endoplasmic reticulum (RER). The mechanisms by which the RER membranes maintain their structure and distribution are still unknown in neurons. In the present study we have examined the role of the dendritic microtubule-associated protein (MAP), MAP2 in the interaction between microtubules and RER. We have compared the distribution of MAP2 and RER in brain subfractions as well as in primary hippocampal cells in culture and have examined MAP2/microtubule interaction with RER membranes in vitro and in vivo. Subcellular fractionation of rat brain revealed a high MAP2 content in a fraction enriched with the ER markers calnexin and ribophorin. Electron microscope morphometry confirmed the enrichment of this fraction with RER membranes. Confocal microscope analysis of the distribution of MAP2 and ribophorin, a RER marker, in cultured hippocampal neurons, revealed that these two proteins are concomittantly compartmentalized to the dendritic processes during neuronal differentiation. Electron microscopy was employed to study microtubule interaction with RER membranes in vitro and in vivo. In an in vitro reconstitution assay, MAP2-containing microtubules were observed to bind to RER membranes in contrast to microtubules containing tau, the axonal MAP. In vivo, overexpression of MAP2c in a non-neuronal cell line, the Sf9 cells, was correlated to an increase of microtubule binding to RER membranes compared to overexpression of tau protein. The results suggest that MAP2 is involved in the interaction between microtubules and RER membranes and thereby could contribute to the differential distribution of RER membranes within neurons.

Keywords: MAP2, endoplasmic reticulum, microtubules, neuronal polarity

4.2 INTRODUCTION

Neurons are polar cells that present two distinct compartments, dendrites and an axon. These compartments can be distinguished by their morphology: dendrites are multiple and taper whereas the axon is unique and its diameter is uniform (Bartlett and Banker, 1984b, a; Dotti *et al.*, 1988; Hillman, 1988). Dendrites and axon also differ by their membranous organelle composition: RER is found in the somato-dendritic compartment but not in the axon and the number of free ribosomes is a lot higher in dendrites than in the axon (Bartlett and Banker, 1984b, a; Peters *et al.*, 1991). The cytoskeletal elements are also distinctly distributed in these neuronal compartments: the number of microtubules is higher in dendrites than in the axon whereas the opposite is noted for neurofilaments (Bartlett and Banker, 1984b, a; Hirokawa, 1991).

Microtubules are involved in the establishment of cell polarity. Notably, the microtubules of dendrites and axon contain different microtubule-associated proteins (MAPs): the microtubule-associated protein-2 (MAP2) is found in dendrites whereas tau is present only in the axon (Caceres *et al.*, 1984; Hirokawa, 1991; Ludin and Matus, 1993). The contribution of these MAPs to the establishment of neuronal polarity has been well documented. Tau contributes to the axonal differentiation in primary neuronal cultures whereas MAP2 is involved in the differentiation of minor neurites, the neuronal processes that become dendrites, and in the maintenance of dendrites in adult neurons (Caceres and Kosik, 1990; Caceres *et al.*, 1991; Dinsmore and Solomon, 1991; Caceres *et al.*, 1992; Sharma *et al.*, 1994; Sanchez *et al.*, 2000a). Despite the fact that MAP2 and tau are known to induce microtubule formation in neurons, their precise role in the elaboration of dendrites and axon remains elusive. Each of these proteins presents

different isoforms that are generated by alternative splicing. Splicing events occur in the microtubule-binding domain that is confined to three or four imperfect repeated domains of 18 amino acids located in the COOH-terminus and in the projection domain that extends at the surface of the microtubules (Buee *et al.*, 2000; Sanchez *et al.*, 2000a). The latter domain, the projection domain, regulates the spacing between microtubules (Chen *et al.*, 1992; Leclerc *et al.*, 1996; Belanger *et al.*, 2002). MAP2 and tau share sequence homology in the microtubule-binding domain and in the adjacent proline-rich region located between the projection domain and the microtubule-binding domain (Lewis *et al.*, 1989; Felgner *et al.*, 1997; Goode *et al.*, 1997). The presence of a distinct class of MAPs in dendrites and axon suggests that these proteins may have another function than the stabilization of microtubules. Consistent with this hypothesis, microtubule formation by MAP2 and tau is not sufficient to induce process outgrowth in Sf9 cells (Knops *et al.*, 1991; Leclerc *et al.*, 1996; Belanger *et al.*, 2002). Thus, the stabilization of microtubules does not seem to be the sole function of MAP2 and tau in dendritic and axonal outgrowth. In recent years, our work and that of others showed that MAP2 could also interact with actin microfilaments and neurofilaments (Leterrier *et al.*, 1982; Bloom and Vallee, 1983; Heimann *et al.*, 1985; Sattilaro, 1986; Hirokawa *et al.*, 1988; Correas *et al.*, 1990; Cunningham *et al.*, 1997). Thus, MAP2 could act as a cytoskeletal integrator in dendrites by linking together the three cytoskeletal elements. This role remains to be characterized.

Besides interacting with the three constituents of the neuronal cytoskeleton, MAP2 can also interact with signaling proteins. For example, MAP2 can interact with the regulatory subunit RII of the c-AMP dependent protein kinase (PKA) (Rubino *et al.*,

1989). In MAP2 knockout mice, there is a reduction of total PKA in dendrites and the rate of induction of phosphorylated CREB is reduced after forskolin stimulation (Harada *et al.*, 2002). These events were accompanied by a decrease of dendritic elongation. From these data, one can conclude that MAP2 plays an important role in the polarized distribution of signaling proteins that regulate dendritic differentiation and plasticity.

In a recent study, we reported that MAP2 was found in a crude membrane preparation from rat spinal cord homogenate suggesting that MAP2 could be associated to membranous organelles (Farah *et al.*, 2003). In neurons, membranous organelles present a polarized distribution as mentioned above. In recent years, families of proteins called CLIPs and Hooks were shown to mediate the interaction between microtubules and membranous organelles (Pierre *et al.*, 1992; De Zeeuw *et al.*, 1997; Hoogenraad *et al.*, 2000; Walenta *et al.*, 2001). Interestingly, CLIP-115 was shown to be responsible for the polarized distribution of a membranous organelle exclusively found in dendrites termed the dendritic lamellar bodies (DLB) (De Zeeuw *et al.*, 1997). Until now, no dendritic microtubule-associated protein has been identified that mediates the interaction between RER and microtubules. Our present data indicates that MAP2 could play such a role. Here, we report a novel association of MAP2 with RER membranes using subcellular fractionation and electron microscopy in an in vitro reconstitution assay and in Sf9 cells overexpressing MAP2c.

4.3 MATERIALS AND METHODS

4.3.1 Subcellular fractionation

4.3.1.1 Preparation of total membrane extract

Brain was dissected from adult Sprague-Dawley rats. Animals were purchased at Charles River (Charles River Laboratories Inc., Montreal, Quebec, Canada). The use of animals and all surgical procedures described in this article were carried out according to The guide to the Care and Use of Experimental Animals of the Canadian Council on Animal Care. Tissue was minced and homogenized in a Dounce homogenizer (15 strokes) in ice-cold 10 mM Tris-HCl, pH 7.4, 0.25M sucrose, 1mM PMSF, 1mM EDTA and a cocktail of protease inhibitors (Roche Molecular Biochemicals, Montréal, Québec, Canada). The homogenate was centrifuged twice at 1,500 x g for 15 min to remove cell debris. After centrifugation of the supernatant at 105,000 x g for 1 hr, the membrane pellet and the supernatant were preserved. The latter fraction was referred to as the cytosolic fraction. The pellet was resuspended in the same buffer and frozen at -80°C until use. See summary in Fig. 1A.

4.3.1.2 Preparation of plasma membrane enriched fraction using sucrose gradient

Rat brain tissue was homogenized in ice-cold lysis buffer (20 mM HEPES, pH 7.4, 2 mM EDTA, 2mM EGTA, 6mM $MgCl_2$, to which a cocktail of protease inhibitors is added prior to use), with 40 strokes of a tight fitting Dounce homogenizer. The total homogenate was centrifuged at 1,000 x g for 5 min to remove cellular debris. The resulting supernatant (10 ml) was applied to a discontinuous sucrose density gradient consisting of 43, 35, 31, 27, 23 and 19% w/w sucrose (from bottom to top, 5 ml each) and centrifuged for 60 min at 96,508 x g in a Beckman SW28 rotor. The fractions were collected at the sucrose interfaces, diluted 1:1 with the lysis buffer and the membrane

material sedimented by centrifugation for 60 min at 177,520 x g in a Beckman Ti60 rotor. See summary of the isolation procedure in Fig. 1B.

4.3.1.3 Preparation of a fraction enriched in rough microsomes (RM) using sucrose gradient

Brain was dissected from twenty adult Sprague-Dawley rats and the protocol previously described by Lavoie et al. was used to separate rough microsomes and Golgi elements from total microsomes (Lavoie *et al.*, 1996). A schematic of the protocol is shown in Fig. 1C. Briefly, total microsomes were isolated by differential centrifugation and ER and Golgi elements were subsequently purified by ultracentrifugation in a sucrose step-gradient.

4.3.2 Immunoblot analyses

Protein assay was performed (Bio-Rad kit, Bio-Rad Laboratories Ltd., Mississauga, Ontario, Canada). Equal amounts of proteins were loaded in each lane and electrophoresed in a 7.5% polyacrylamide gel. Following separation, proteins were electrophoretically transferred to a nitrocellulose membrane. The nitrocellulose strips were incubated with the primary antibodies during 90 min at room temperature. They were then washed with Phosphate Buffered Saline (PBS) and then incubated with the peroxidase-conjugated secondary antibodies. Membranes were again washed and then revealed by chemiluminescence (Amersham Pharmacia Biotech, Quebec, Quebec, Canada). The following primary antibodies were used: the monoclonal antibody anti-MAP2 (clone HM2, Sigma, Oakville, ON), the monoclonal antibody anti-tau (clone

Tau5, Oncogene Research Products, San Diego, California), the monoclonal antibody anti-α-tubulin (clone DM 1A, Sigma, Oakville, ON), a polyclonal antibody against ribophorin, a polyclonal antibody against calnexin (Stressgen Biotechnologies, Victoria, BC, Canada), a polyclonal antibody against Porin (Oncogene Research Products, San Diego, California), a polyclonal antibody against mannosidase II (kindly provided by Dr. M.G. Farquhar, University of California, San Diego) and a polyclonal against NaK-ATPase (kindly provided by Dr. D. Fambrough, The Johns Hopkins University, Maryland).

4.3.3 Electron microscopy

Microsomes isolated from brain were fixed using 2.5% glutaraldehyde, recovered onto Millipore membranes by the random filtration technique of Baudhuin et al. (Baudhuin *et al.*, 1967) and processed for electron microscopy as previously described (Lavoie *et al.*, 1996).

4.3.4 Morphometric Analysis of microtubule association with RER membranes in Sf9 cells

Rough endoplasmic reticulum cisternae were defined as ribosome-studded, membrane-limited structures that were often circular in profile, with a lumen that was mainly devoid of content. Microtubules were defined as cylinders of indefinite length with approximate diameter of 25 nm. Adjacent, non-overlapping micrographs were taken of the embedded and sectioned Sf9 cells at a magnification of 21,000x. Negatives were scanned at a resolution of 400dpi and converted to a positive image. All

microtubules that were within a 25 nm distance from RER cisternae were labeled with an arrow and the labeled images saved in separate file to keep count of the number of microtubules associated with RER cisternae. Rough endoplasmic reticulum cisternae were then highlighted in white using Photoshop 7.0 imaging software (Adobe Systems Inc., Mountain View, CA). The brightness and contrast of the regions excluding the RER cisternae was then lowered so that there were no other white objects on the image. The image was imported into the digital measurement system, Sigma Scan Pro (SPSS Science). The number of highlighted RER cisternae was automatically stored in computer memory and Sigma Scan Pro calculated the perimeter length of each cisternum.

4.3.5 Cell cultures

Primary embryonic hippocampal cultures were prepared as previously described (Banker and Goslin, 1998). Hippocampi from 18-day-old fetuses were treated with trypsin (0,25% at 37°C for 15 min) then washed in Hank's balanced solution and dissociated by several passages through a constricted Pasteur pipette. The cells were then plated on glass coverslips coated with polylysine. Then, after 4 h to allow the attachment of the cells to the substrate, the hippocampal cells were inverted to face a monolayer of glial cells in a serum-free medium. The Sf9 cells were purchased from the American Type Culture Collection (ATCC # CRL 1711; Rockville, MD). Sf9 cells were grown in Grace's medium (Gibco, BRL, Burlington, Ontario, Canada) supplemented with 10% fetal bovine serum (Hyclone, South Logan, UT) as a monolayer at 27°C. For

transmission electron microscopy, Sf9 cells were grown on glass coverslips at a density of 2.0 x 10^6 cells / 60 mm dish. Cells were infected for 48 or 72 hours with MAP2c or tau viral stocks (Knops *et al.*, 1991; Belanger *et al.*, 2002) at a multiplicity of infection (m.o.i.) of 5 and then harvested and processed for electron microscopy as described above.

4.3.6 Immunofluorescence

Neurons were fixed in 2% paraformaldehyde/PBS for 30 minutes. The cells were then permeabilized with 0.2% Triton X-100 in PBS for 5 minutes. The MAP2 protein was revealed using a monoclonal antibody directed against MAP2 (clone HM2, dilution 1:200) purchased from Sigma (Mississauga, Ontario, Canada). The endoplasmic reticulum was revealed using a polyclonal antibody directed against calnexin (Stressgen biotechnologies, Victoria, BC, Canada) or a polyclonal antibody directed against ribophorin. To visualize the microtubules, either a polyclonal antibody directed against tubulin (Abcam, Cambridge, UK) was used (1:100) or a monoclonal antibody directed against β-tubulin (DSHB, University of Iowa, Iowa City, IA). We used the following secondary antibodies: a donkey anti-rat conjugated to FITC (dilution 1:100), a donkey anti-rabbit conjugated to Rhodamine (1:500) (Jackson Immunoresearch Laboratories, Bio/Cam, Mississauga, Ontario, Canada), an Alexa Fluor 647 anti-mouse (1:400) and an Alexa Fluor 488 anti-rabbit (1:200) (Molecular Probes, Eugene, OR). All these antibodies were diluted in 5% BSA/PBS. Incubations were carried out at room temperature for 1 hour. After three washes in PBS, the coverslips were mounted in

polyvinyl alcohol (Calbiochem, CA, USA). Fluorescently labelled cells were visualized with a Leica TCS-SP1 confocal microscope using 63x or 100x objectives.

4.3.7 MAP2c and tau purification from Sf9 cells

For protein purification, Sf9 cells were grown as a suspension to obtain a final concentration of 1.5 x 10^6 cells/200ml total media volume and were then infected with MAP2c or tau viral stocks (Knops *et al.*, 1991; Belanger *et al.*, 2002). Infection was allowed to proceed for 48-72 hrs before the cells were centrifuged at 1000 x g. The cell pellet was kept at -80°C until protein purification. Protein purification was performed using the boiling preparation method as previously described (Hernandez *et al.*, 1986).

4.3.8 Preparation of nuclear fractions

Nuclear fractions were prepared from rat liver homogenates (1:2, w/v) in 0.25 M sucrose, 0.05 M Tris-HCl, pH 7.5, 0.025 M KCl and 0.005 M $MgCl_2$ (0.25 M sucrose-TKM) using the procedure of Blobel and Potter (1966). The isolated nuclei were resuspended in cold 0.25 M sucrose-TKM and centrifuged for 10 min at 1000 x g. Nuclei from 10 ml of homogenate were resuspended by gentle stirring with a glass rod in 1.2 ml G-PEM buffer (80mM PIPES, pH 6.9, 1mM $MgCl_2$ and 1mM EGTA to which 1mM GTP was added prior to use).

4.3.9 In vitro microtubule-membrane reconstitution

An in vitro microtubule-membrane reconstitution assay was modified from that previously described (Paiement, 1981). Bovine brain tubulin protein was purchased from

Cytoskeleton (Denver, CO). Tubulin (2mg/ml) was allowed to polymerize in the presence of MAP2c or tau protein (0.5 mg/ml) in the G-PEM buffer for 35 min at 37°C. Freshly prepared nuclear fraction was resuspended in the G-PEM buffer to which 5 mM $MgCl_2$, 1mM GTP, 2 mM ATP and a cocktail of protease inhibitors (Roche, Laval, Quebec, Canada) were added prior to use. 50µl of this fraction were added to the polymerized microtubules and incubation was allowed to proceed for another 30 min at 37°C. Nuclear membranes were then centrifuged at 1000 x g for 5 min at 37°C. The supernatant was discarded and the pellet was fixed using 2.5% glutaraldehyde and 1% sucrose in the G-PEM buffer. Fixation was performed at 37°C for 30 min and the samples were then processed for electron microscopy as described above.

4.3.10 Negative staining for electron microscopy

Tubulin (2mg/ml) was allowed to polymerize in the presence of MAP2c or tau protein (0.5 mg/ml) in the G-PEM buffer for 35 min at 37°C. Microtubules were then added to a freshly prepared nuclear fraction from rat liver and incubated for 30 min. To monitor the presence of microtubules in this preparation, 5 µl of the supernatant were placed on a carbon-coated formvar-supported EM grid. After an incubation of 30 seconds, the grid was rinsed with distilled water and stained with 1% (w/v) uranyl acetate for 30 seconds. Samples were visualized with a Zeiss CM 902 transmission electron microscope.

4.3.11 Statistical analysis

The statistical significance of the number of microtubules per micromiter of RER membrane in MAP2c- and tau-expressing SF9 cells was determined using paired T-Test. Statistical significance was accepted if $p<0.05$.

4.4 RESULTS

4.4.1 HMW MAP2 distribution in subcellular fractions of rat brain

In a previous study, we reported that high molecular weight MAP2 proteins (HMW MAP2) were present in a total membrane fraction isolated from mouse brain homogenates indicating that they could be associated to membrane organelles (Farah *et al.*, 2003). In the present study, this observation was confirmed in rat brain. Using a simple centrifugation protocol (Fig. 1A), the total membrane fraction (P) was separated from the cytosolic fraction (S) after rat brain homogonates were centrifuged at 105,000g. A significant amount of HMW MAP2 was found in both fractions as revealed by western blot analysis (Fig. 2A). To better define the membrane association of HMW MAP2, a brain homogenate was fractionated using a step-gradient of sucrose as described in Fig. 1B. MAP2 distribution was compared to that of various markers for different cellular organelles (Na-K-ATPase, a plasma membrane marker, calnexin, a marker of the endoplasmic reticulum and Voltage-Dependent Anion Channel or VDAC, a mitochondrial marker) (Fig. 2B). HMW MAP2 was found in a fraction enriched with the plasma membrane marker (I3) as expected since MAP2 interacts with plasma membrane associated proteins (Davare *et al.*, 1999; Lim and Halpain, 2000). However, HMW MAP2 was also found in a fraction enriched in endoplasmic reticulum (ER)

membranes (I1) and devoid of plasma membranes. To confirm HMW MAP2 association with the ER, HMW MAP2 distribution was examined in adult rat brain subfractions prepared using a fractionation protocol designed to purify rat liver ER (Lavoie *et al.*, 1996) and summarized in Fig. 1C. The organelle markers mentioned above as well as mannosidase II, a Golgi marker, ribophorin, a rough ER marker and the cytoskeletal marker tubulin were used to characterize the fractions. HMW MAP2 was found in the total microsomal fraction (P) as shown in Fig. 2C. When this fraction was separated on a step-gradient of sucrose, HMW MAP2 was found enriched in a subfraction containing mainly the two ER markers, calnexin and ribophorin. Based on the enrichment with these two markers, this subfraction was named RM for rough microsomes (Fig. 2C). This fraction also contained mitochondrial membranes as revealed by the anti-VDAC antibody. MAP2 is known to interact with mitochondria (Jancsik *et al.*, 1989; Linden *et al.*, 1989a; Jung *et al.*, 1993). However, it seemed unlikely that MAP2 in the RM fraction was associated only with mitochondria since: 1) the fraction I3 presented an amount of VDAC similar to that of the RM fraction but the amount of MAP2 in this fraction was much lower than that in the RM fraction and 2) electron microscope morphometry analysis confirmed that this fraction contained very few mitochondria. Since RER is mainly found in neuronal cell bodies and dendrites and MAP2 is a somato-dendritic microtubule-associated protein (Ludin and Matus, 1993), it seems reasonable to consider an association between this MAP and ER. In this case, the RM subfraction was expected to contain little or no tau, the microtubule-associated protein found in the axon (Ludin and Matus, 1993). Figure 2D confirms that RM was highly enriched in MAP2 but in contrast contained very little tau.

Electron microscopy of the RM subfraction confirmed the presence of rough microsomes (Figs. 3A and B). Furthermore, morphometric analysis indicated that 51% of the vesicles in this fraction presented ribosomes attached to the membrane. The microsomes in RM were heterogeneous in shape and size (Fig. 3B) and were often observed in association with membrane-free filaments with associated ribosomes (see ovals in Figs. 3A and B). Tubulin was detected by immunoblotting (Fig. 2C) but no microtubule was observed in the RM fraction (Fig. 3). Presumably, they were depolymerized at low temperature (4°C) during fractionation.

4.4.2 Somato-dendritic compartmentalization of MAP2 and ribophorin in primary hippocampal cultures

In primary hippocampal cultures, MAP2 is segregated to the somato-dendritic compartment during establishment of neuronal polarity (Caceres *et al.*, 1984; Hirokawa, 1991; Ludin and Matus, 1993). Similarly, in mature neurons, RER is also found in the cell body and dendrites (Bartlett and Banker, 1984b, a). We examined whether MAP2 and RER concomitantly segregate to the dendritic compartment in hippocampal neurons during their development. After one day in culture, the hippocampal neurons are polarized cells presenting 3 to 4 short minor neurites that will differentiate to become dendrites and a long thin neurite which develops into the axon (Bartlett and Banker, 1984b, a; Dotti *et al.*, 1988). All these neurites terminate in a growth cone, a motile structure presenting a rich actin network at the periphery and bundles of microtubules at the center (Goslin *et al.*, 1989). After ten days in culture, the dendrites and axon are differentiated and the synaptic contacts are established. MAP2 is found in both minor

neurites and axon in the first days in culture and becomes compartmentalized to the dendrites after 10 days in hippocampal cultures (Kempf *et al.*, 1996). To examine whether the compartmentalization of MAP2 and RER occurs concomitantly in hippocampal neurons, the distribution of ribophorin, an ER marker concentrated in RER, was examined before (three-day old cultures) and after (fifteen-day old cultures) MAP2 becomes concentrated in the somato-dendritic compartment. In three-day old primary hippocampal neurons, cells were labeled with the monoclonal antibody HM2 which recognizes both the high and low molecular weight isoforms of MAP2 expressed in these neurons and a polyclonal antibody directed against ribophorin to stain RER. Tubulin staining was used to visualize all neuronal compartments (Fig.4A" and B"). Confocal microscope analysis revealed that MAP2 was present in all neuronal compartments in three-day old primary hippocampal neurons including the growth cones (Fig. 4A) as previously reported (Kempf *et al.*, 1996). Similarly, ribophorin was also found in all neuronal compartments and in growth cones (Fig.4A'). The ribophorin staining was particularly strong in the growth cones and in some regions along the neurites. Interestingly, MAP2 staining was often enriched in the same regions along the neurites. In fifteen-day old hippocampal neurons, MAP2 and ribophorin became concentrated in the dendritic processes as indicated by the reduction of their protein level in the axon (arrows in Fig.4B"). In these neurons, ribophorin presented a punctate staining that appeared uniformly distributed along the dendrites as was MAP2 staining.

We next looked at the organization of the RER with respect to that of microtubules in hippocampal neurons. To this purpose, we overexpressed MAP2c in these neurons, a phenomenon which causes the reorganization of microtubules into thin

or thick bundles. Therefore, if RER is tightly associated to microtubules, it should undergo a reorganization similar to that of microtubules under MAP2c overexpression. Seven-day old neurons were transfected with a GFP vector containing cDNA of LMW MAP2, MAP2c. GFP-MAP2c was mostly found in dendrites in seven-day old control hippocampal neurons (Fig. 5A and A'). A similar distribution was noted for RER in these neurons. Seven-day old control neurons transfected with GFP vector revealed no discernable differences in RER distribution compared to control cells (Fig. 5B and B'). Overexpressing MAP2c produced no important changes in the structure of the dendrites and axon of seven-days old hippocampal neurons (data not shown) even though in some of the transfected cells, several thin extensions emerged from the cell body (Fig.5D). A similar phenotype has been previously described in Sf9 cells expressing MAP2c (Leclerc *et al.*, 1996; Belanger *et al.*, 2002). However, transfection with GFP-MAP2c led to a reorganization of the microtubule network in the neuronal cytoplasm (Fig.5C'' and D''). In most of the MAP2c-transfected neurons, large microtubule bundles were noted in the cell body (Fig.5C''). In these cells, RER staining was found along these bundles (arrows in Fig.5C, C' and C"). In the MAP2c-transfected neurons harboring multiple thin extensions, very thin microtubule bundles were randomly distributed in the cell body and an important reorganization of RER staining was noted in the perikaryon (arrowhead in the inset of Fig.5D, D' and D") along these bundles (Fig.5D, D' and D''). In both types of MAP2c-transfected neurons, GFP-MAP2c and RER distribution were closely associated with the MAP2c-containing microtubule bundles (Fig.5C, C' and C" and D, D' and D''). The concomitant reorganization of both microtubules and RER observed in MAP2c-overexpressing neurons showed that RER and microtubules are

intimately associated in hippocampal cells. However, the above results did not demonstrate whether MAP2c was directly involved in the association of RER with microtubules.

4.4.3 In vitro reconstitution of the microtubule-MAP2-ER complexes

To show that MAP2 can act as a linker between the ER and microtubules, an in vitro membrane–microtubule reconstitution assay was developed. To show the specificity of MAP2 to interact with ER membranes, tau, the axonal MAP, was used as a negative control in the present assay. MAP2c and tau proteins were purified from Sf9 cells using the method described by (Hernandez *et al.*, 1986). The microtubule binding affinity of these proteins was tested. To this purpose, MAP2c (0.5mg/ml) or tau (0.5mg/ml) was incubated with pure bovine brain tubulin (2mg/ml) in the presence of the microtubule-polymerizing agent taxol (20μM) in the G-PEM buffer. Following incubation for 30 minutes at 37°C and high speed centrifugation (100,000 x g), the pellet and the supernatant were analyzed by western blotting for their content in tubulin, MAP2c or tau. As expected, tubulin was found almost exclusively in the MAP2c and the tau-pellets (Fig. 6A). Furthermore, the majority of MAP2c and of tau (more than 80%) were found in the pellets indicating that these proteins have a similar microtubule binding affinity (Fig.6A). Next, we tested the microtubule polymerizing activity of MAP2c and tau. To this purpose, the same assay described above was performed except that no taxol was added. In this case, the amount of tubulin pelleted by MAP2c and tau was examined by western blotting. As shown in Fig. 6B, similar amounts of tubulin

were found in the MAP2c and the tau pellets indicating that these proteins have a similar tubulin polymerizing activity in the present conditions. Lastly, microtubule formation by MAP2c and tau was examined at the electron microscopic level by negative staining. Individual and bundles of microtubules were observed in both MAP2c- and tau-microtubule preparations (Fig. 6D and E).

To reconstitute the microtubules-MAP2-ER interaction, a nuclear fraction with nuclei and intact nuclear envelope membranes was prepared from rat liver homogenates using the Blobel and Potter procedure (Blobel and Potter, 1966). Since the outer nuclear envelope membrane has similar properties to RER (Gerace and Burke, 1988), the results generated with nuclei were of relevance to the mechanism of interaction between MAP2-microtubules and RER. Moreover, we chose to work with a nuclear preparation since nuclei sediment at low speed (1000 x g) in contrast to microtubules that co-sediment at high speed (100 000 x g). Therefore, the only way microtubules can co-sediment with nuclei in this assay is through an association with the outer nuclear membrane. A preparation of rat liver nuclei was used because it is devoid of MAP2 and tau. Moreover, no tubulin was detected in this fraction by western blotting (Fig.6C). Nuclei were incubated with exogenous microtubules that were pre-polymerized either in the presence of MAP2c or tau. Following the incubation, nuclei were pelleted at a centrifugation speed of 1000xg. Nuclei were then resuspended in fresh buffer and processed for electron microscopy. All incubations of nuclei with microtubules were performed at 37°C since microtubules depolymerize at lower temperature. No microtubule was observed associated with the nuclei when nuclei were incubated

without or with exogenous tubulin (Fig.7A and C). No microtubule was observed either in association with nuclei incubated in the presence of tau-prepolymerized microtubules (Fig. 7B and D). To verify that the tau-containing microtubules did not depolymerize during incubation, the presence of microtubules was confirmed by negative staining for electron microscopy as described above. After incubation of nuclei in the presence of tau-pre-polymerized microtubules nuclei were sedimented at low speed and the supernatant was applied to grids and negatively stained to reveal intact tau-polymerized microtubules (Fig6F). However, when nuclei were incubated with MAP2c-pre-polymerized microtubules, microtubules were observed as small cylinders with a constant diameter (~ 25 nm in diameter) sectioned in different orientations on the surface of the outer nuclear membrane (see arrows in Fig. 8). Thus the above experiments showed that MAP2- but not tau-pre-polymerized microtubules could associate with nuclei and this association was necessary for microtubules to co-sediment at 1000xg. These results were reproduced in five different series of experiments.

A quantitative analysis was carried out to evaluate the number of MAP2c-containing microtubules associated with the rat liver nuclei. Microtubules located within 25 nm of the outer nuclear membrane were included in the analysis since this is considered a physiologically relevant distance for microtubule interaction based on measurement of spacing between microtubules in bundles induced by MAP2c and tau in Sf9 cells (Leclerc *et al.*, 1993; Belanger *et al.*, 2002). Most of the microtubules (>80%) were organized in bundles of two or more microtubules. The number of microtubule bundles and of single microtubules was quantified on 19 nuclei from two different sets of experiments for a total of 38 nuclei. On average, 3.1$\pm$ 0.30 microtubule bundles and

1.1± 0.14 single microtubules were found associated with the outer nuclear envelope of one nucleus. These results indicate that MAP2c might be involved in the interaction of RER membranes with microtubules in vivo.

4.4.4 Higher number of microtubules per micrometer of RER membrane in MAP2c- than in tau-expressing Sf9 cells

To confirm in the intact cell that MAP2 can act as a linker between the RER and microtubules, Sf9 cells were infected either with MAP2c or tau baculoviral constructs. This system has been previously used successfully to study MAP2 and tau function (Knops *et al.*, 1991; Boucher *et al.*, 1999; Belanger *et al.*, 2002). Infection of Sf9 cells with baculovirus containing either MAP2c or tau cDNA was allowed to proceed for 48 or 72 hrs before the cells were processed for electron microscopy as described in Materials and Methods. At these times of infection, the protein level of MAP2c and tau is similar (Leclerc *et al.*, 1996). In uninfected or control Sf9 cells, sparse individual microtubules are found in the cytoplasm (Fig.9). However, the expression of MAP2c or tau in Sf9 cells induces the formation of microtubules that often assemble in bundles (Knops *et al.*, 1991; Belanger *et al.*, 2002). To test whether MAP2c is involved in the association of microtubules with RER in these cells, we quantified the number of microtubules directly associated with RER membranes in the cell body of control, MAP2c or tau-expressing Sf9 cells. Single microtubules and microtubule bundles located within ~25 nm of the RER cisternae were included in the analysis since similar distances were observed between microtubules in bundles induced by MAP2c and tau in Sf9 cells (Chen *et al.*, 1992; Belanger *et al.*, 2002). In the case of microtubule bundles,

only the microtubules in a bundle that were located within the 25 nm of the membranes were included in the analysis. Rough endoplasmic reticulum membranes were identified using ribosomes as a morphological marker. MAP2c and tau-expressing Sf9 cells that contained viral particles and which exhibited a high number of single microtubules and microtubule bundles were selected for the analysis. Three different sets of experiments were used, 10 cells being chosen per experiment. The results of the three sets of experiments are presented in Table 1. Figures 9, 10 and 11 show microtubules closely associated to RER membranes in the cytosol of control, MAP2c- and tau-expressing cells respectively. The size and shape of RER membranes varied in sf9 cells under different experimental conditions, however the significance of this is not yet clear. Since RER membranes are known to exhibit different sizes and shape (Paiement and Bergeron, 2001), microtubule-membrane density was expressed as microtubules per unit micrometer of RER membrane (units that are independent of shape or size of organelle membrane). In uninfected control cells, 1.0 ± 0.078 microtubule was found per □m of RER membrane. In MAP2c- and tau-expressing cells, 2.25 ± 0.368 microtubules and 1.07 ± 0.50 microtubules were counted per □m of RER membrane respectively. The number of microtubules per □m of RER membrane was statistically different between MAP2c- and tau-expressing cells ($p<0.030$) and MAP2c-expressing cells and uninfected cells ($p<0.035$). No statistical difference was noted between uninfected control cells and tau-expressing cells ($p<0.835$). In tau-expressing cells, microtubule bundles were sometimes found in the vicinity of RER membranes with no apparent association observed between these two elements (Fig. 11A). Therefore, RER membranes in

MAP2c-expressing Sf9 cells revealed a higher density of associated microtubules than did RER membranes in uninfected and tau-expressing Sf9 cells.

4.5 DISCUSSION

In the present study, we describe a novel type of ER-microtubule interaction that is mediated by the dendritic microtubule-associated protein, MAP2. A fraction enriched in rough ER microsomes (RM) was isolated from rat brain as indicated by its high content in calnexin and ribophorin as well as by an electron microscope morphometric analysis using the ribosome as a morphological marker for RER. An important amount of MAP2 was detected in the RM fraction by immunoblotting. In primary hippocampal neurons, MAP2 and ribophorin, a RER marker, were co-segregated to the dendritic compartment during neuronal differentiation. By in vitro reconstitution assay MAP2 was observed to mediate the interaction between microtubules and RER membranes. Finally, the number of microtubules per micrometer of RER membrane in MAP2c-expressing Sf9 cells was higher than in tau-expressing cells. Thus, our results point to a role of MAP2 in the distribution and maintenance of RER in neurons.

Our results in Sf9 cells showed that there are more microtubules associated with RER membranes in MAP2c-expressing cells than in uninfected cells. This can result from two possibilities: either MAP2c enhances the interaction between these two elements as a consequence of increased affinities or MAP2c increases the number of microtubules and this increases the probability of interaction between microtubules and RER membranes. The latter possibility does not seem to be the case since in tau-

expressing cells, the frequency of microtubules is increased but not the frequency of interaction between microtubules and RER membranes.

Previous studies have shown that the ER membranes are associated to microtubules (Terasaki *et al.*, 1986; Terasaki, 1990; Terasaki and Reese, 1994; Hirokawa, 1998; Aihara *et al.*, 2001). This association could be either dynamic for trafficking of ER membranes or stable for the positioning of these membranes within a cell (Terasaki, 1990; Cole and Lippincott-Schwartz, 1995; Hirokawa, 1998). Depolymerization of microtubules using the drug nocodazole affects both the trafficking and positioning of ER membranes (Terasaki *et al.*, 1986; Terasaki and Reese, 1994; Waterman-Storer and Salmon, 1998; Aihara *et al.*, 2001). The ER movement along microtubules has been well documented (Terasaki, 1990; Allan and Vale, 1994; Waterman-Storer and Salmon, 1998; Aihara *et al.*, 2001). The sliding of ER membranes along microtubules seems to be driven by motor proteins such as kinesin. Moreover, it was shown that ER could be moved within a cell by its attachement to the microtubule-plus end (Waterman-Storer and Salmon, 1998). However, when the expression of either dynein or kinesin is suppressed within a neuron, the association of membranous organelles including the ER to the microtubules is not completely eliminated indicating that other proteins are involved in this association (Feiguin *et al.*, 1994; Harada *et al.*, 1998). These proteins would be involved in the positioning of membranous organelles along microtubules and thereby would allow the maintenance of the structure of these organelles. The maintenance of membrane structure is particularly important in post-mitotic cells such as mature neurons where ER membranes are found along the length of dendrites and axon. Recently the relative proportion of dynamic and static ER was determined within

hippocampal neurons. It was found that only a small ER subcompartment is dynamic in mature hippocampal neurons (Bannai *et al.*, 2004). Proteins mediating the interaction between microtubules and membranous organelles could play a role in the maintenance of membrane structure and distribution. CLIPs (cytoplasmic linker proteins) for example, are known to establish a link between microtubules and membranous organelles. As such, CLIP-170 has been reported to mediate the interaction of endocytic carrier vesicles to microtubules (Pierre *et al.*, 1992). Furthermore, CLIP-115 was shown to be responsible for the polarized distribution of the dendritic lamellar bodies (DLB) in neurons (De Zeeuw *et al.*, 1997; Hoogenraad *et al.*, 2000). Recently, a new class of proteins termed CLASPs (CLIP-associated proteins) was identified (Akhmanova *et al.*, 2001). These proteins bind CLIPs and microtubules and have a microtubule-stabilizing effect. A family of proteins named Hooks also mediates the interaction between microtubules and membrane organelles. More specifically, Hook3 links the Golgi apparatus to microtubules (Walenta *et al.*, 2001). Futhermore, an integral membrane protein of the ER, p63, was shown to be involved in the interaction of ER with microtubules in a non-neuronal cell line (Klopfenstein *et al.*, 1998). Since p63 is an integral membrane protein, it was termed a CLIMP (cytoskeleton-linking membrane protein). To our knowledge, no dendritic cytosolic linker protein has been identified so far that mediates the interaction between the ER and microtubules in neurons. Our results show that MAP2 plays such a role. However, MAP2 is a dendritic cytosolic linker protein that has to be classified in a category of its own for three reasons: 1- the microtubule-binding domain of MAP2 has no sequence homology with that of CLIPs, CLASPs, Hooks and CLIMPs, 2- all the linker proteins identified so far bind to distal

end of microtubules whereas MAP2 binds to microtubules along their length (Al-Bassam *et al.*, 2002) and 3- in contrast to p63, MAP2 is not an integral membrane protein but a cytosolic one.

In hippocampal cultures, our data showed that MAP2 and ribophorin, a RER marker, were enriched in regions of the neurites during the first days in culture. However, ribophorin but not MAP2 was concentrated in growth cones. This corroborates previous studies that reported a high concentration of ER-like membranes in growth cones (Dailey and Bridgman, 1989, 1991; Deitch and Banker, 1993). However, in mature hippocampal neurons, the distribution of ribophorin was mostly uniform and concentrated in dendrites as noted for MAP2. The accumulation of ER membranes in the growth cones might indicate that the transport of these membranes is high during neurite formation indicating a predominant role of motor proteins such as kinesins in their cellular distribution. Later on, when the neurites are fully developped structural microtubule-associated proteins such as MAP2 would anchor the ER membranes to microtubules to maintain their morphology and position in the dendrites. Thus, the distribution of ER membranes within a neuron would result from the activity of both motor and structural microtubule proteins which would vary during neuronal differentiation.

Table 1	# of experiment	Total # of vesicles	Sum of length of RER membranes	Total # of microtubules	# of microtubules per μ of RER
Control	N1	319	45.77	45	0.98
	N2	335	57.16	61	1.07
	N3	335	56.89	62	1.09
Tau	N1	183	81.5	40	0.49
	N2	632	109.7	148	1.35
	N3	335	123	169	1.37
MAP2c	N1	231	59.39	116	1.95
	N2	543	58.6	156	2.66
	N3	337	73.51	157	2.14

Figure 1. Subcellular fractionation of rat brain homogenate. A) A total membrane extract (P) and a cytosolic fraction (S) were obtained by differential centrifugation of rat brain homogenate. B) A step-gradient of sucrose was used to generate a fraction enriched in plasma membranes (I3) and C) a different step-gradient of sucrose was used to separate both rough microsomes (RM) and golgi derivatives (I1 and I2) from total membrane extract (P). E: cytoplasmic extract, N: nuclear fraction, P: total membrane extract, S: cytosolic fraction, I: interface, ML: mitochondria and lysosomes, PS: microsomes and cytosol.

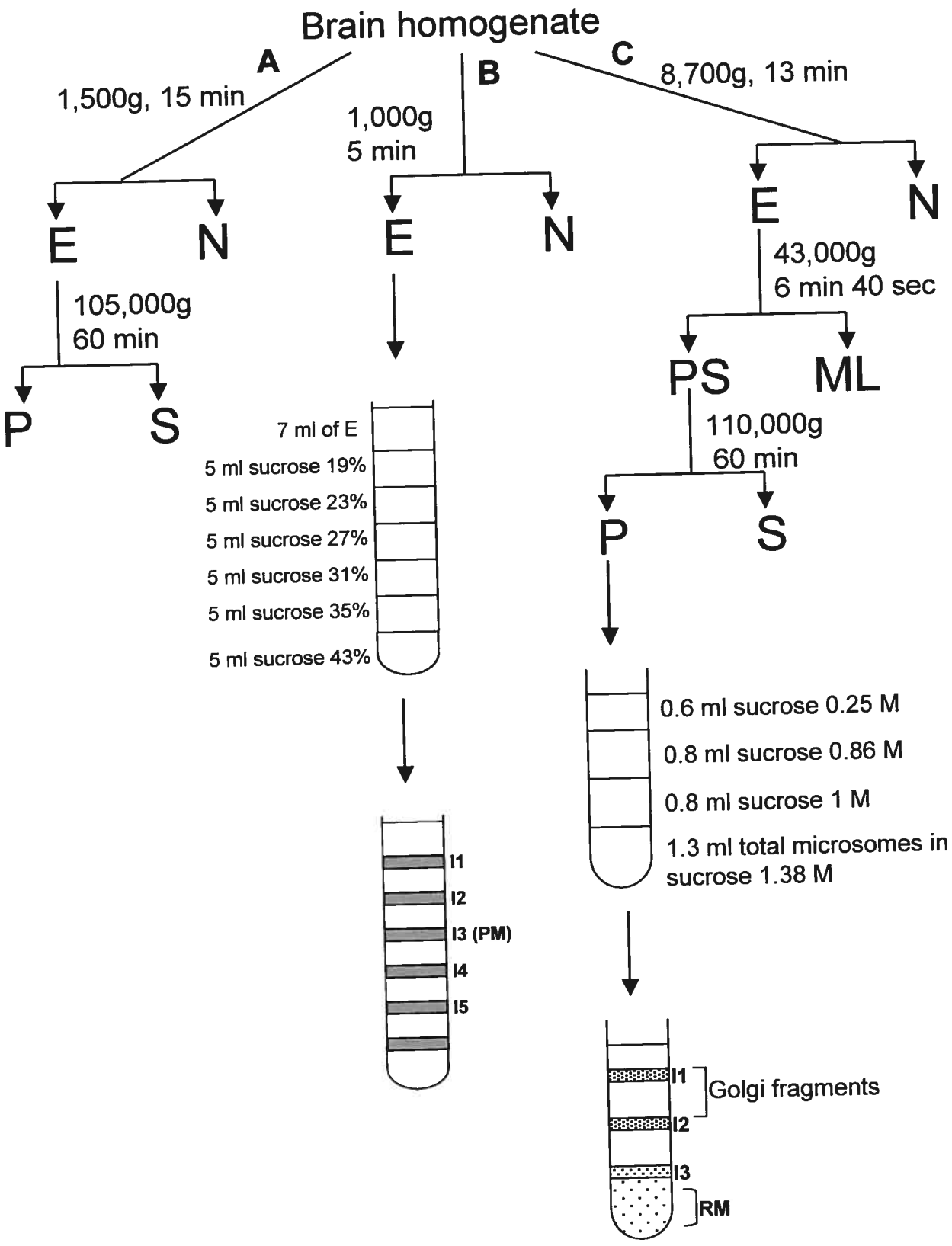
Brain homogenate
A
1,500g, 15 min
B
1,000g
5 min
C
8,700g, 13 min
E
N
E
N
E
N
105,000g
60 min
P
S
43,000g
6 min 40 sec
PS
ML
110,000g
60 min
P
S
7 ml of E
5 ml sucrose 19%
5 ml sucrose 23%
5 ml sucrose 27%
5 ml sucrose 31%
5 ml sucrose 35%
5 ml sucrose 43%
I1
I2
I3 (PM)
I4
I5
0.6 ml sucrose 0.25 M
0.8 ml sucrose 0.86 M
0.8 ml sucrose 1 M
1.3 ml total microsomes in sucrose 1.38 M
I1
Golgi fragments
I2
I3
RM

Figure 2. Immunoblot analysis of adult rat brain fractions. Fractions obtained following subcellular fractionation of adult rat brain were electrophoresed on a 7.5% polyacrylamide gel (30 μg/lane) and transferred to a nitrocelllulose membrane as described in methods. A) Western blot analysis of the total membrane extract (P) and the cytosolic fraction (S) obtained following the fractionation procedure described in figure 1A. The membrane was revealed with a monoclonal antibody directed against MAP2 (clone HM2). B) Western blot analysis of the fractions obtained following the step-gradient of sucrose described in Figure 1B. The anti-MAP2 (HM2) was used as well as the plasma membrane marker Na-K-ATPase, the endoplasmic reticulum marker calnexin and the mitochondrial marker porin (VDAC). C) Western blot analysis of the fractions obtained following the step-gradient of sucrose described in Figure 1C. The above markers were used as well as the RER marker, ribophorin, the Golgi marker mannosidase II and the cytoskeletal marker, tubulin. D) Fractions obtained following the step-gradient of sucrose described in Figure 1C were analyzed by western blotting for their content in MAP2 and tau, the axonal MAP. A monoclonal antibody directed against tau was used (clone tau5). E: cytoplasmic extract, P: total membrane extract, S: cytosolic fraction, I: interface, RM: rough microsomes.

A)

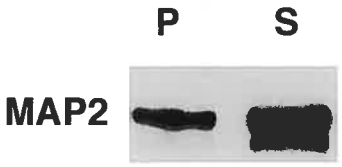

B)

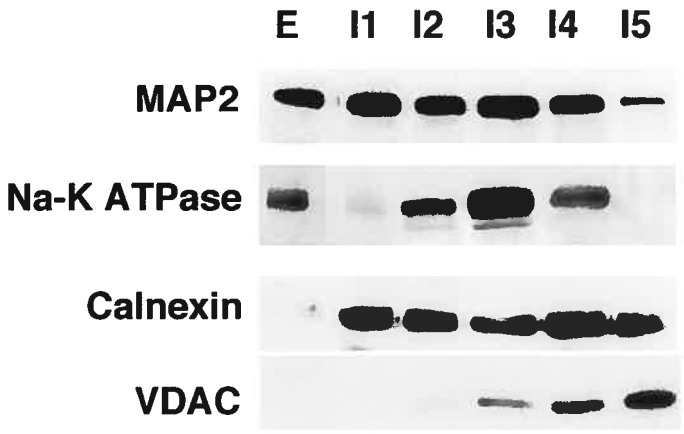

C)

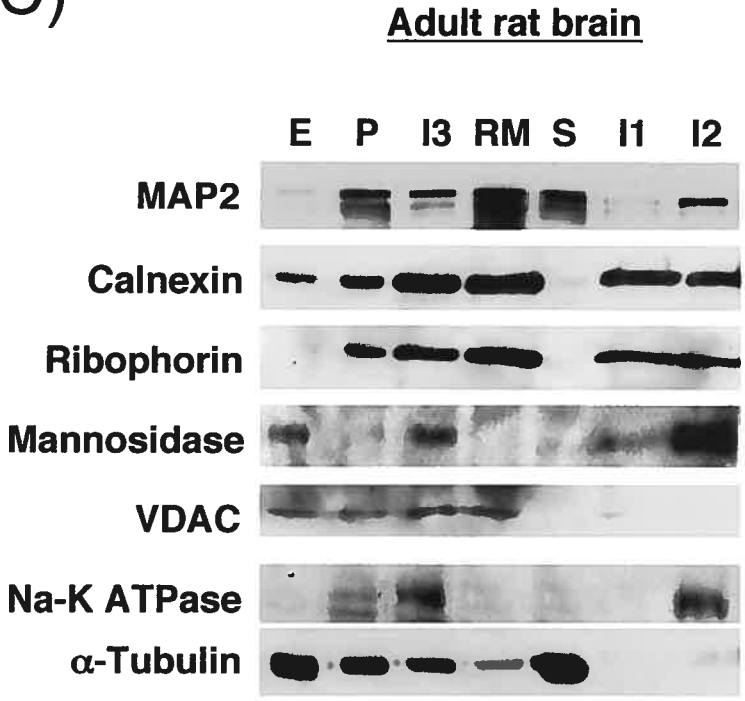
Adult rat brain
E
P
I3
RM
S
I1
I2
MAP2
Calnexin
Ribophorin
Mannosidase
VDAC
Na-K ATPase
α-Tubulin

D)

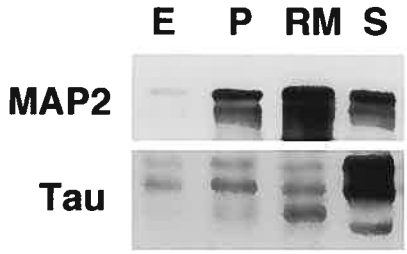
E
P
RM
S
MAP2
Tau

Figure 3. Electron microscopy of rat brain rough microsomes (RM). A) and B) Electron micrographs of the rough microsomal fraction. In A, arrowheads point to ribosomes on the membranes of rough microsomes. The arrows point to smooth microsomes. The ovals in Figures A and B surround ribosomes associated with membrane-free filamentous structures. In B, rough microsomes reveal different morphologies: tubular (1), oval (2), dilated (3), cup-shaped (4) and with a spiral alignment of ribosomes (5).

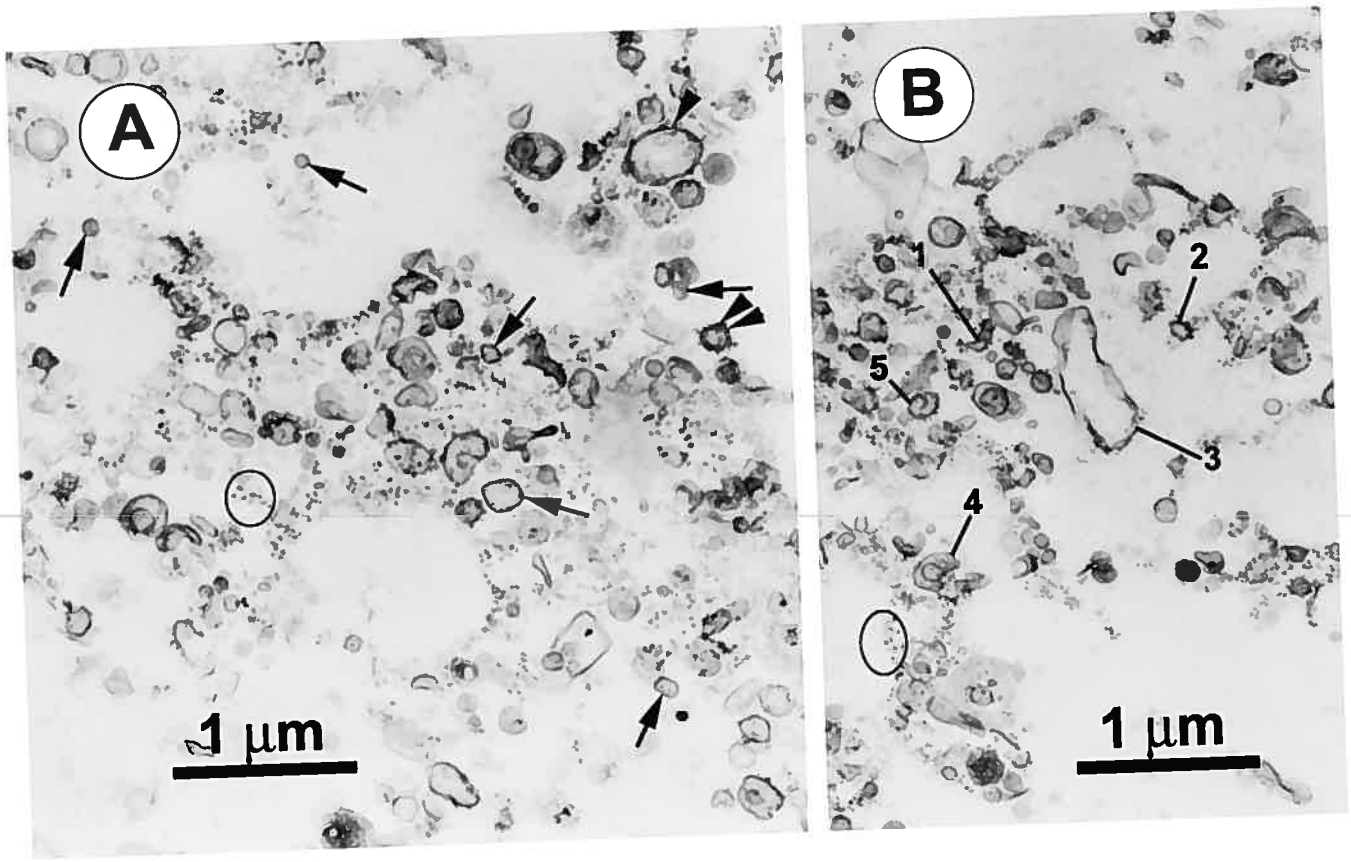
A
1 µm
B
1
2
3
4
5
1 µm

Figure 4. MAP2 and RER dendritic compartmentilization coincides in cultured hippocampal neurons. Distribution of MAP2, RER membranes and tubulin is shown in three- (A, A' and A'') and fifteen-day old (B, B' and B'') cultured hippocampal neurons. The monoclonal anti-MAP2 antibody (clone HM2) was revealed using a secondary anti-mouse conjugated to FITC. The polyclonal anti-ribophorin antibody used to stain RER membranes was revealed using a secondary anti-rabbit conjugated to rhodamine. The polyclonal anti-tubulin antibody was revealed using a secondary anti-rat conjugated to Alexa Fluor 647. Arrows point to axons. Scale bar: 20μm.

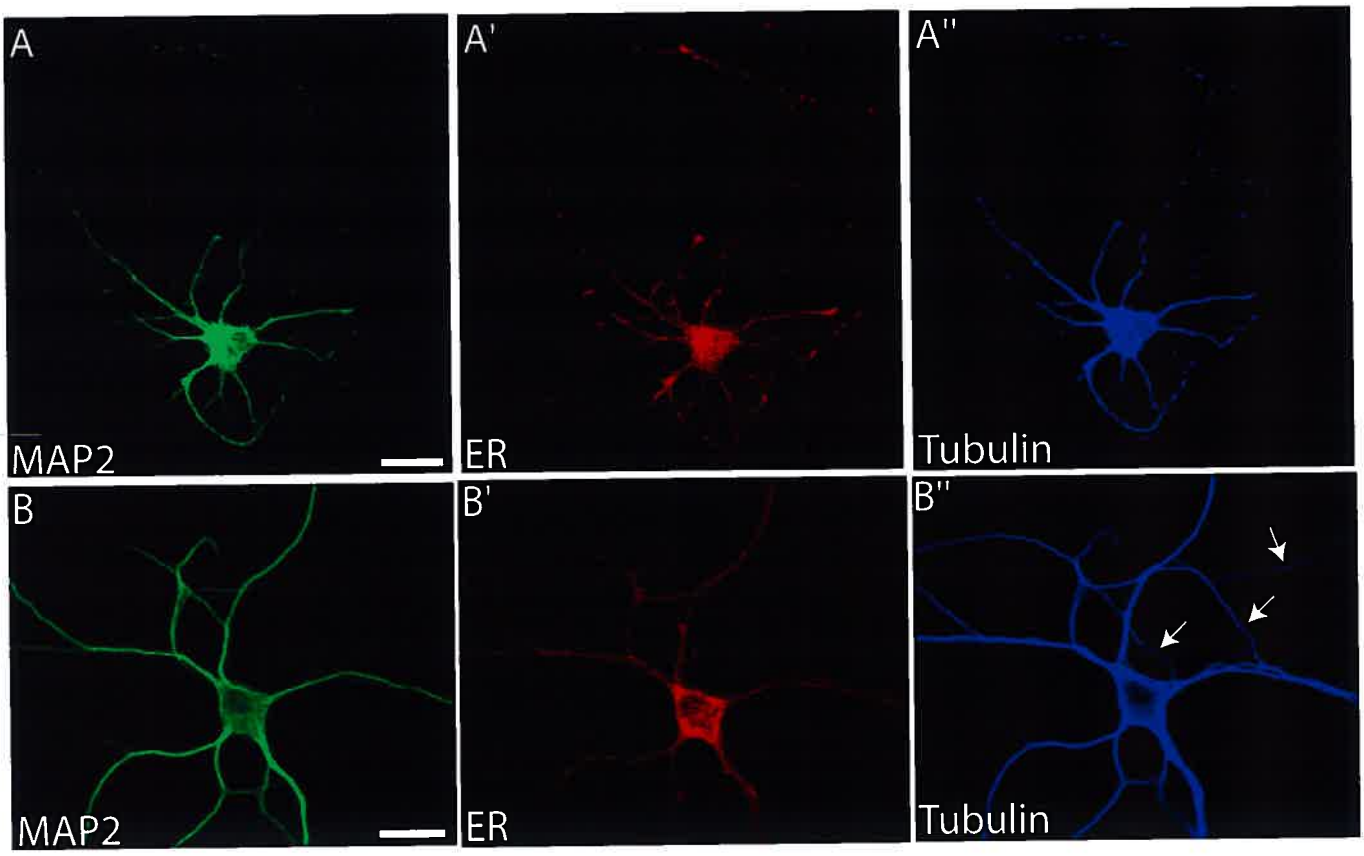
A
A'
A''
MAP2
ER
Tubulin
B
B'
B''
MAP2
ER
Tubulin

Figure 5. Overexpression of GFP-MAP2c fusion protein in hippocampal neurons. A and A' show the distribution of MAP2 (HM2 antibody) and the RER respectively in seven days old cultured hippocampal neurons. The polyclonal antibody against ribophorin was used to stain the RER. This antibody was revealed using a secondary anti-rabbit conjugated to Rhodamine. Insets show a higher magnification of the cell body. B) and B') Seven days old neurons were transfected with the GFP protein alone as a control. Protein expression was allowed to proceed for 24h before the cells were fixed and processed for immunofluorescence. Insets show that the GFP protein does not induce a reorganization of the ER membranes. C, C' and C" show the distribution of the GFP-MAP2c, ribophorin and tubulin staining in a transfected neuron arboring thick microtubule bundles. In these cells, ER staining is found on these bundles (arrows). D, D' and D'' show the distribution of the GFP-MAP2c, ribophorin and tubulin staining in a transfected neuron arboring multiple thin extensions. In these cells, a reorganization of the ER was noted in the perikaryon (arrowhead in the inset) and along the thin bundles. Scale bar for all figures except C, C' and C": 20μm. Scale bar for C, C' and C": 8μm. Scale bar for the insets: 4μm.

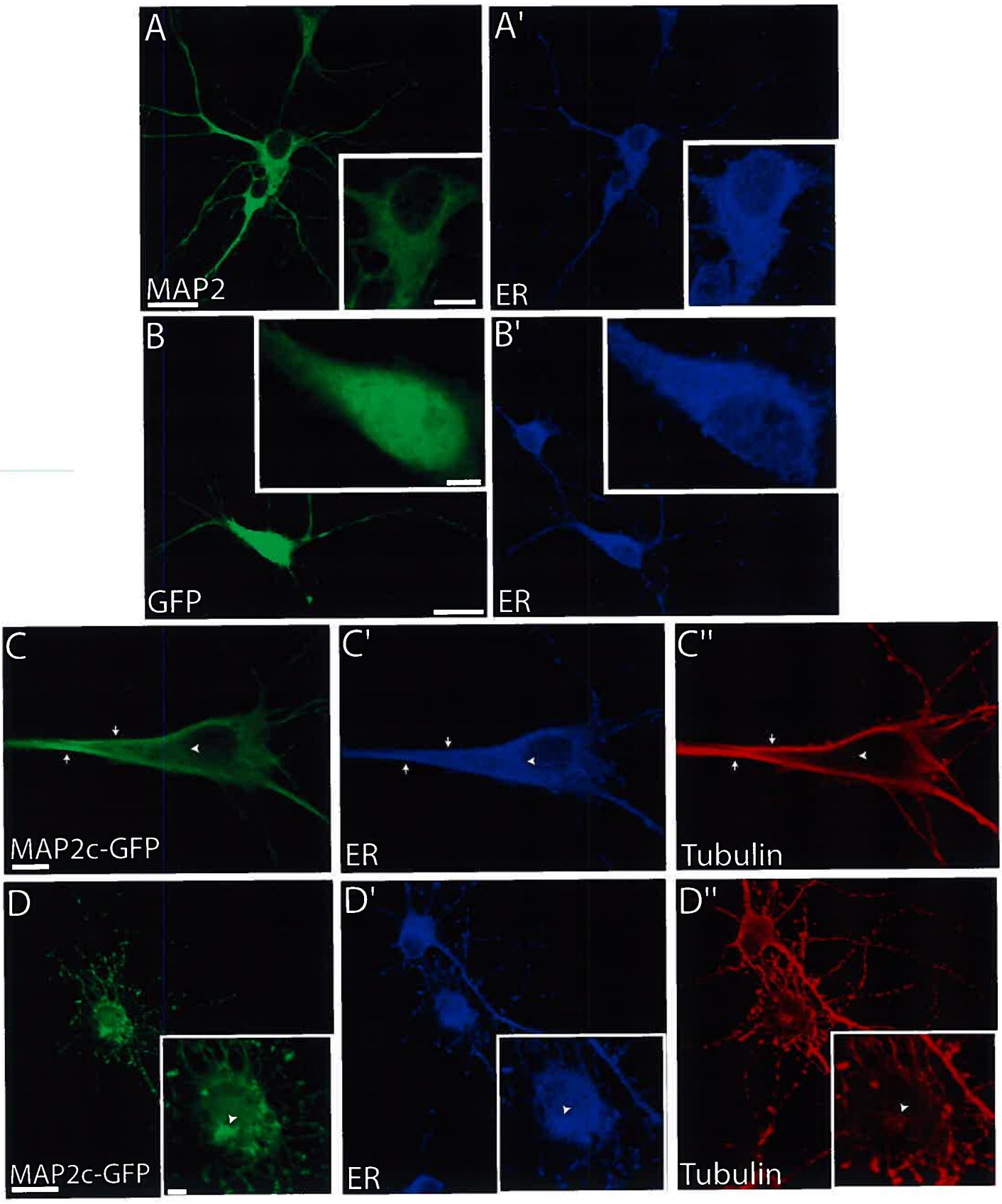
A
MAP2
A'
ER
B
GFP
B'
ER
C
MAP2c-GFP
C'
ER
C''
Tubulin
D
MAP2c-GFP
D'
ER
D''
Tubulin

Figure 6. Microtubule binding properties of MAP2c and tau. A) The microtubule binding affinity of MAP2c and tau was assessed as described in Materials and Methods. Western blotting revealed that similar amounts of MAP2c and tau (more than 80%) bound to the taxol-stabilized microtubules indicating that these proteins have similar microtubule binding affinities. B) The microtubule polymerizing activity of MAP2c and tau was determined as described in Materials and Methods. Western blotting shows similar amounts of tubulin in the MAP2c and in the tau pellets indicating that these proteins have similar capacities to polymerize microtubules. C) The nuclear fraction prepared was examined by western blotting for its content in tubulin. No endogenous tubulin was detected in this fraction. D) Electron micrograph of MAP2c-pre-polymerized microtubules visualized by negative staining. E) Electron micrograph of tau-pre-polymerized microtubules visualized by negative staining. F) Electron micrograph illustrating that tau-pre-polymerized microtubules were intact after incubation with nuclei. The microtubules were visualized by negative staining as in D and E. Bar D, E and F, .25μm

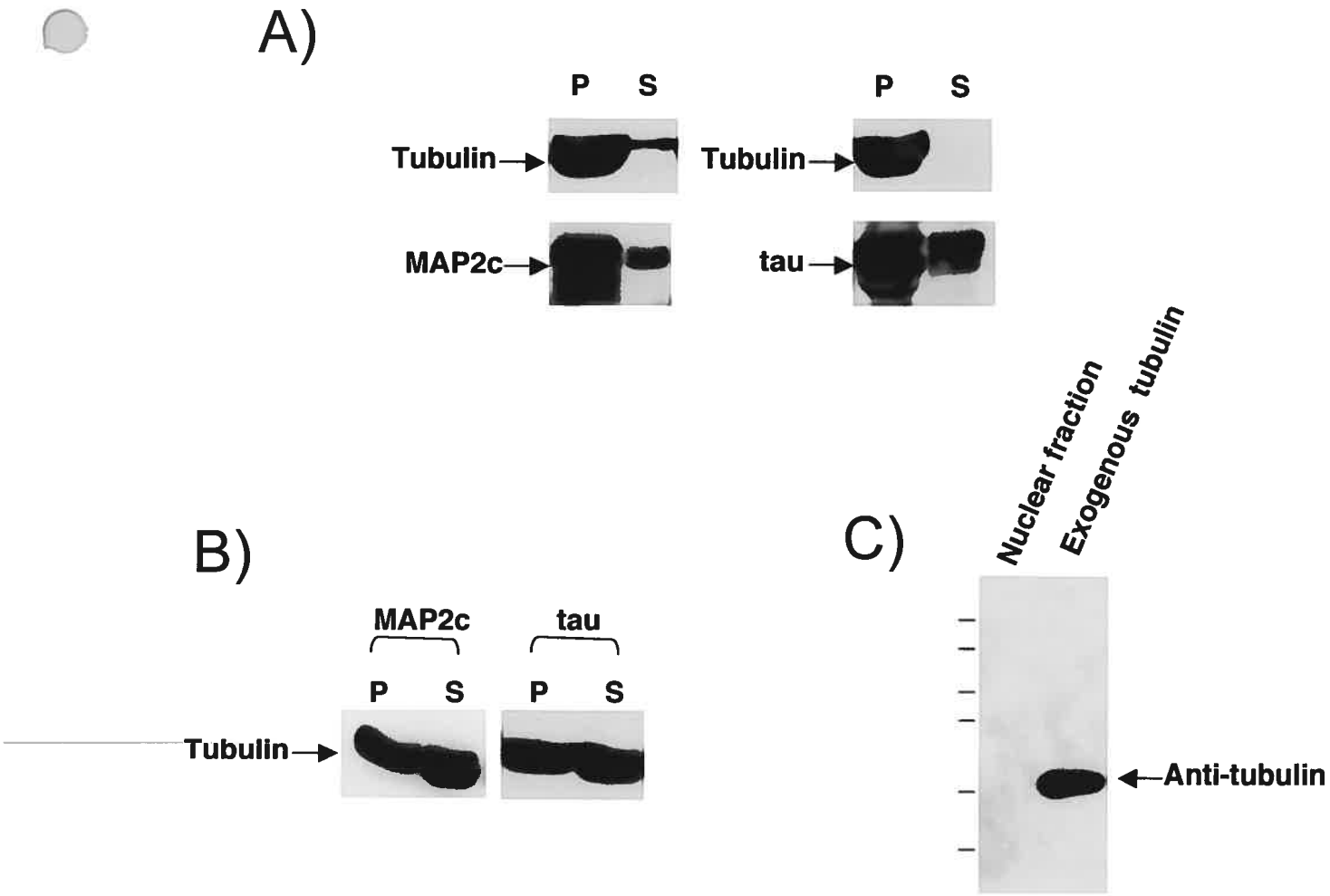
A)
P
S
Tubulin
MAP2c
P
S
Tubulin
tau
B)
MAP2c
tau
P
S
P
S
Tubulin
C)
Nuclear fraction
Exogenous tubulin
Anti-tubulin


F
E
D

Figure 7. Electron micrographs of control incubated nuclei. A) Nuclei are shown after incubation in the absence of exogenously added microtubules. A higher magnification of the region outlined by a rectangle in A is shown in C. No microtubules can be seen near the outer perimeter of the nuclei. B) Nuclei are shown after incubation in the presence of exogenously added tau-polymerized microtubules. Under these conditions no microtubules were observed in association with the nuclei. A higher magnification of the region outlined by a rectangle in B is shown in D. Arrowheads point to ribosomes on the outer nuclear membrane. N, nuclei; ONM, outer nuclear membrane. Bars A and C, 2 and 1μm respectively. Bars B and D, 500nm.

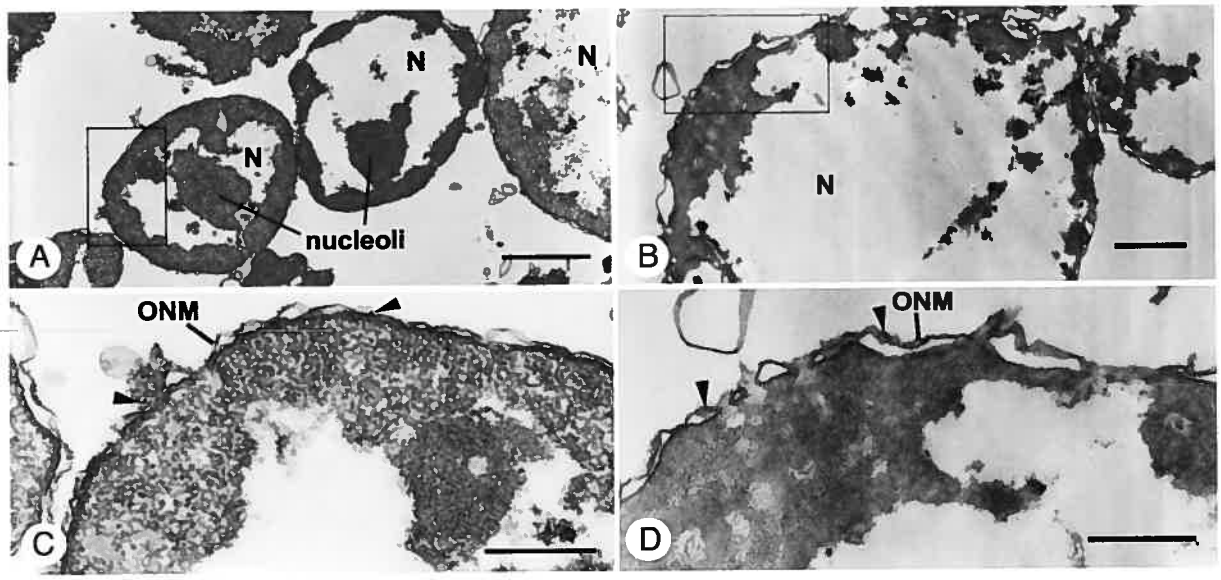
N
N
N
nucleoli
A
N
B
ONM
C
ONM
D

Figure 8. In vitro reconstitution of the ER-MAP2-microtubule complexes. Micrographs a-l show high power electron micrographs of the surface of nuclei after incubation in the presence of exogenously added MAP2c-polymerized microtubules. Arrows point to cross and oblique sections of microtubules located within 25nm of the outer nuclear membrane (ONM). Bar, 500 nm.

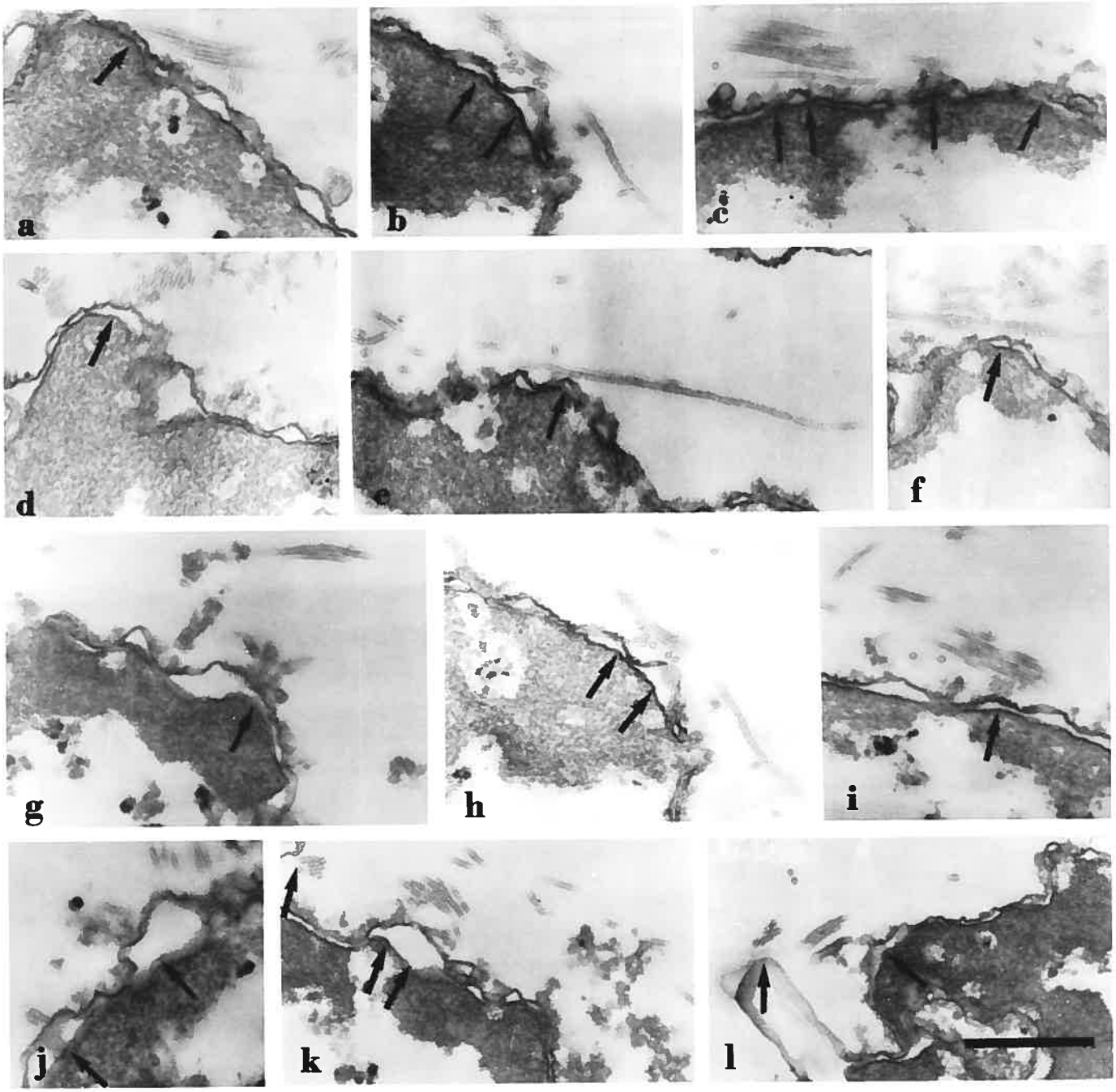
a
b
c
d
e
f
g
h
i
j
k
l

Figure 9. Electron micrograph of a control uninfected Sf9 cell. Uninfected Sf9 cells were processed for electron microscopy as described in Materials and Methods. Arrows point to regions of close associations between microtubules and RER membranes. M: mitochondria; N: nucleus; RER: rough endoplasmic reticulum. Scale bar, 500nm.

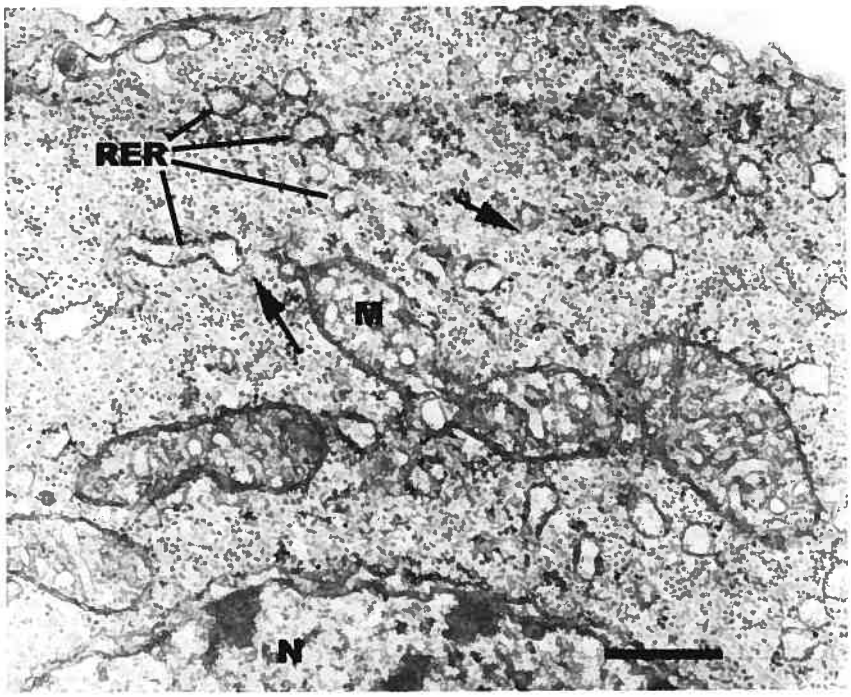
RER
M
N

Figure 10. Electron micrographs of MAP2c-expressing Sf9 cells. A-D) Arrows point to regions of close association between microtubules and RER membranes in the cytoplasm of MAP2c-expressing cells. M: mitochondria; N: nucleus. Scale bar, 500nm.

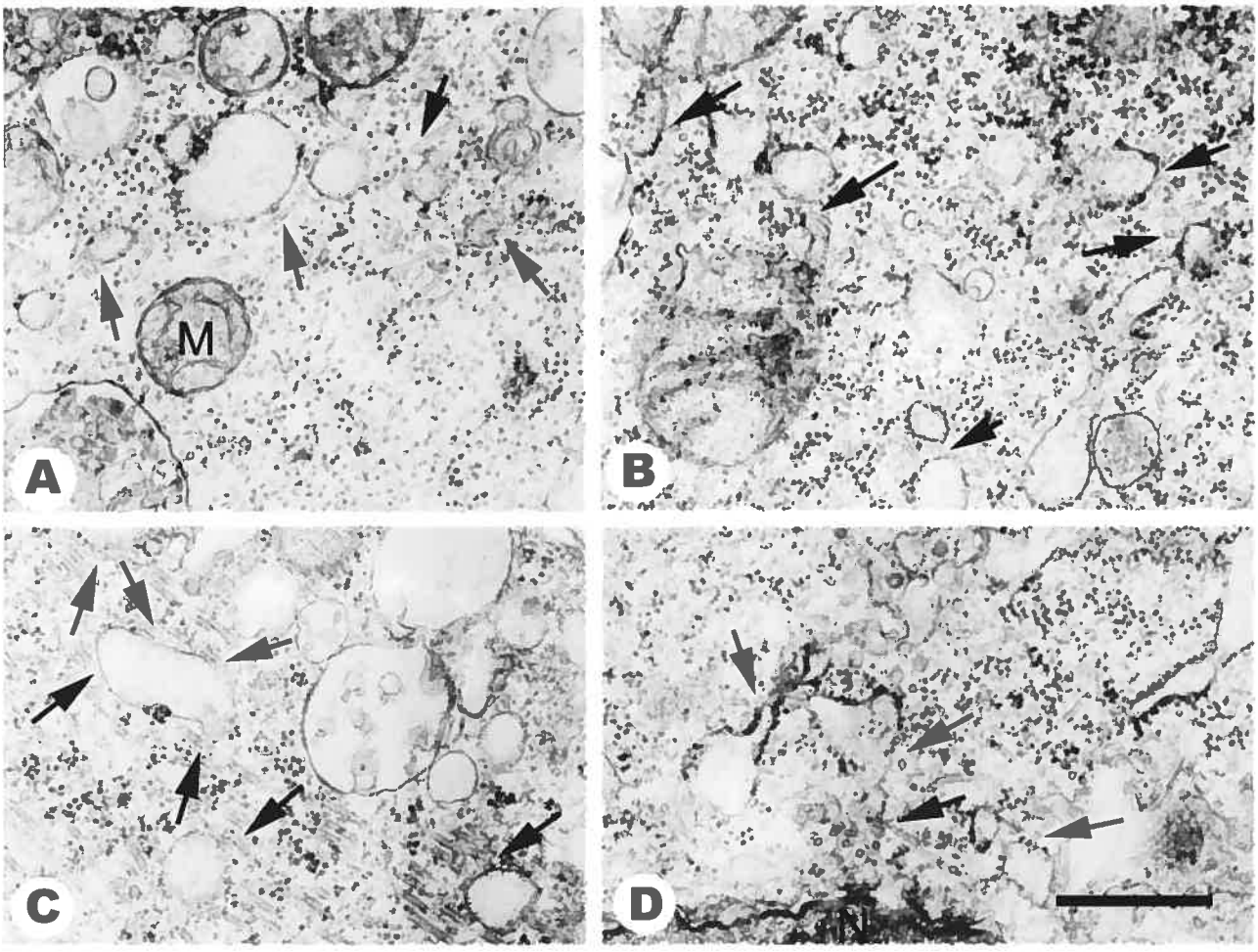
M
A
B
C
D

Figure 11. Electron micrographs of tau-expressing Sf9 cells. A-D) Arrows point to regions of close association between microtubules and RER membranes in the cytoplasm of tau-expressing cells. M: mitochondria; N: nucleus. Scale bar, 500nm.

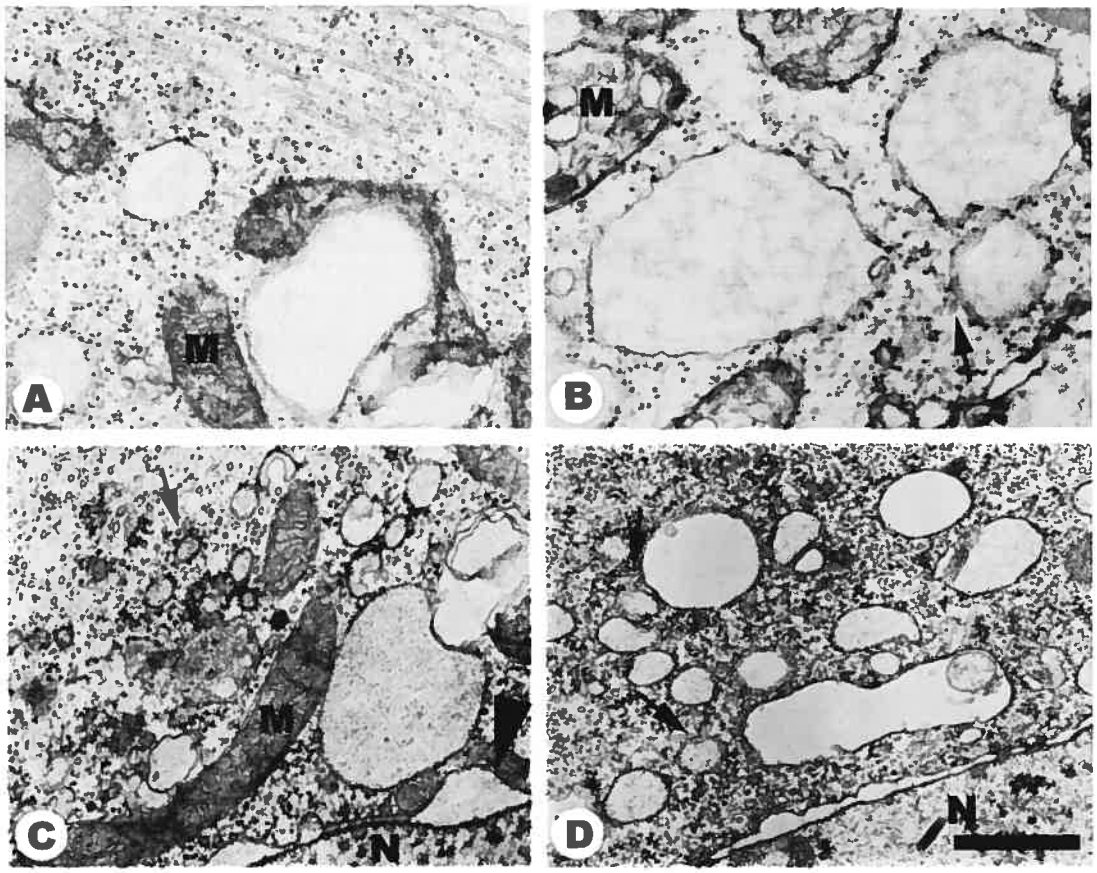
A
M
B
M
C
M
N
D
N

5 DISCUSSION GÉNÉRALE

5.1 Rôle de la MAP2 comme déterminant intrinsèque de la morphologie neuronale au cours du développement

La morphologie polaire complexe du neurone détermine sa fonction. Bien que les étapes de différenciation neuronale soient bien connues (Bartlett and Banker, 1984b, a; Dotti *et al.*, 1988), les mécanismes moléculaires exacts qui conduisent à l'élaboration de deux compartiments neuronaux distincts avec des fonctions distinctes le sont encore peu. Dans le cadre de la présente thèse, nous avons examiné le rôle de la protéine associée aux microtubules dendritiques, la MAP2, dans l'acquisition et le maintien du phénotype neuronal. Cette protéine est cruciale pour la différenciation neuronale puisque l'inhibition de son expression dans des cultures primaires de neurones à l'aide d'oligonucléotides antisens bloque la formation de neurites mineures (Dinsmore and Solomon, 1991; Caceres *et al.*, 1992; Sharma *et al.*, 1994). De plus, un changement dans le niveau d'expression et/ou l'état de phosphorylation de la MAP2 a été corrélé avec le remodelage dendritique dans le cerveau adulte (Diaz-Nido *et al.*, 1993; Sharma *et al.*, 1994; Quinlan and Halpain, 1996b; Faddis *et al.*, 1997). En outre, les souris mutantes nulles pour la MAP2 démontrent une diminution de la densité des microtubules dendritiques et de la longueur des dendrites (Harada *et al.*, 2002). On note également chez ces souris une altération du ciblage dendritique de la PKA et une diminution du taux d'induction du CREB phosphorylé suite à l'induction par la forskoline (Harada *et al.*, 2002).

En premier lieu, nous nous sommes penchés sur le rôle du domaine de projection de la MAP2 sur la capacité de cette protéine à induire la formation de prolongements cytoplasmiques dans les cellules Sf9 (Belanger *et al.*, 2002). Plusieurs études avaient

suggéré que ce domaine avait un rôle structurel à réguler l'espacement entre les microtubules mais aucune fonction particulière ne lui avait été attribuée. Afin de déterminer l'effet du domaine de projection de la MAP2 sur l'activité de cette protéine, nous avons construit des formes tronquées de la MAP2b et de la MAP2c et nous avons étudié l'effet de l'expression de ces protéines sur l'espacement entre les microtubules et sur la formation de prolongements cytoplasmiques dans les cellules Sf9. Ces cellules sont rondes et émettent des prolongements seulement lorsqu'elles surexpriment une protéine associée aux microtubules qui permet la formation de faisceaux de microtubules et la protrusion de ces faisceaux de la surface cellulaire (Baas *et al.*, 1991; Leclerc *et al.*, 1993; Kosik and McConlogue, 1994; Leclerc *et al.*, 1996; Boucher *et al.*, 1999; Belanger *et al.*, 2002). De plus, les propriétés des prolongements formés dépendent de la MAP exprimée (Leclerc *et al.*, 1996; Boucher *et al.*, 1999). Nos résultats démontrent que la formation de prolongements est induite par le domaine de liaison aux microtubules de la MAP2 et est régulée par son domaine de projection. Dans le cas de la MAP2c, le domaine de projection a un effet positif sur la capacité du domaine de liaison aux microtubules à induire la formation de prolongements. Par contre, le domaine de projection de la MAP2b, qui contient une séquence additionnelle de 1372 a.a., a un effet négatif sur la capacité du domaine de liaison aux microtubules à induire la formation de prolongements. Nos résultats suggèrent que l'effet négatif de la séquence peptidique de 1372 a.a. du domaine de projection de la MAP2b pourrait être du à des interactions intramoléculaires entre ce domaine et le domaine de liaison aux microtubules. Ces interactions pourraient permettre un changement de la configuration structurelle de la MAP2b affectant ainsi sa fonction.

Il est possible d'extrapoler à partir de cette étude sur le rôle de la MAP2b et la MAP2c dans l'élaboration et la stabilisation des dendrites. Au cours de l'établissement de la polarité neuronale, le cytosquelette est extrêmement dynamique pour permettre la formation des neurites et par la suite, leur différenciation en dendrites et axone (Tanaka and Sabry, 1995; Waterman-Storer and Salmon, 1999). Pendant les premières étapes de différenciation neuronale, le niveau d'expression de la MAP2c est élevé. Par la suite, ce niveau diminue et la MAP2c demeure exprimée à l'âge adulte seulement dans des régions où la neurogénèse persiste (Tucker and Matus, 1988; Viereck *et al.*, 1989; Tucker, 1990). On peut supposer que dans le cas de la MAP2c, le fait qu'elle ne possède pas le domaine de 1372 a.a. peut empêcher le repliement du domaine de projection sur le domaine de liaison aux microtubules. Ceci ferait en sorte que la MAP2c existe surtout dans un état opérationnel qui favorise la neurogénèse. Quant à la MAP2b, elle pourrait exister surtout dans un état non-opérationnel en étant repliée sur elle-même. Dans cet état, elle favoriserait la stabilisation du réseau cytosquelettique et le maintien des dendrites. En réponse à des signaux externes, il pourrait y avoir un changement dans l'état de phosphorylation de la MAP2b qui causerait un dépliement du domaine de projection rendant la protéine opérationnelle. Dans cet état, le remodelage dendritique serait favorisé chez l'adulte.

Dans un autre volet de cette thèse, nous avons étudié la contribution possible de la MAP2 à la ségrégation des composantes membranaires au cours du développement neuronal. En effet, le réticulum endoplasmique rugueux (RER), tout comme la MAP2 de haut poids moléculaire, est ségrégé dans le compartiment somato-dendritique dans les

neurones (Bartlett and Banker, 1984b, a; Peters *et al.*, 1991). Bien que les mécanismes qui sont responsables du déplacememt du RE le long des microtubules aillent été bien identifiés, ceux qui sont reponsables de l'association stable de celui-ci avec les microtubules ne le sont pas (Terasaki *et al.*, 1986; Terasaki, 1990; Terasaki and Reese, 1994; Cole and Lippincott-Schwartz, 1995; Hirokawa, 1998; Aihara *et al.*, 2001). Nous avons démontré par biochimie, immunocytochimie et microscopie électronique, que la MAP2 pouvait interagir avec le RER dans les neurones. De plus, notre essai de reconstitution *in vitro* démontre clairement que la MAP2 peut connecter les membranes du RER aux microtubules. MAP2 devient ainsi la première protéine dendritique à effectuer ce lien. Dans ce cas, MAP2 pourrait être classée dans la catégorie des CLIPs (cytosolic linker proteins). Ces protéines sont connues pour établir un lien entre les microtubules et les organelles membranaires. Par exemple, la CLIP-170 lie les vésicules de transport issus d'endosomes aux microtubules (Pierre *et al.*, 1992). De plus, la CLIP-115 est responsable de la distribution des DLB (dendritic lamellar bodies) dans les neurones (De Zeeuw *et al.*, 1997; Hoogenraad *et al.*, 2000). Récemment, les CLASPs (Clip-Associated Proteins) ont été identifiées. Ces protéines lient les CLIPs aux microtubules (Akhmanova *et al.*, 2001). En outre, il a été démontré qu'une protéine intégrale du RE, la p63, pouvait lier celui-ci aux microtubules (Klopfenstein *et al.*, 1998). Cependant, MAP2 est une CLIP unique en son genre puisque : 1) le domaine de liaison aux microtubules de la MAP2 n'a pas d'homologie de séquence avec celui des CLIPs connues, 2) toutes les protéines de liaison identifiées jusqu'à présent se lient à l'extrémité distale des microtubules alors que la MAP2 se lie le long des protofilaments

et 3) MAP2 n'est pas une protéine intégrale de la membrane mais une protéine cytosolique.

Nous avons récemment identifié la p63 comme un partenaire de la MAP2 au niveau du RE (article en préparation). Cependant, il est possible que MAP2 interagisse avec plusieurs protéines du réticulum endoplasmique. En accord avec ceci, nous avons démontré en utilisant la technique de recouvrement par immunobuvardage que la MAP2 se lie à au moins 7 protéines dans une fraction enrichie en membranes préparées à partir de cellules Sf9 (figure 1). Il est donc possible que MAP2 fasse partie d'un complexe protéique au niveau du RE.

Le réticulum est connu pour être la réserve de calcium intracellulaire dans la cellule (Rizzuto, 2001). En positionnant le réticulum au niveau d'endroits précis le long des microtubules dendritiques, MAP2 pourrait contrôler les endroits où la relâche locale de calcium est nécessaire. La concentration intracellulaire de calcium doit être hautement contrôlée au cours du développement neuronal. En effet, la relâche de calcium à partir des réserves intracellulaires est connue pour réguler l'activité de guidage de la nétrine-1 au cours de la différentiation neuronale (Hong *et al.*, 2000). De plus, le mouvement dirigé du cône de croissance au cours de la formation de neurites mineurs est médié par la réorganisation des microfilaments d'actine et des microtubules (Waterman-Storer and Salmon, 1999). L'activité de plusieurs protéines de liaison à l'actine et/ou aux microtubules tel que la MAP2 est contrôlée par le calcium (Yamamoto *et al.*, 1983; Yamamoto *et al.*, 1985; Quinlan and Halpain, 1996b, a). Le calcium contrôle donc la réorganisation du cytosquelette au cours du développement neuronal. D'ailleurs, la suppression de l'ATPase cationique de type P du RE (Cta4p), qui régule la

concentration intracellulaire de calcium, déstabilise les microtubules chez la moississure (Facanha *et al.*, 2002). D'un autre côté, le cytosquelette est aussi capable de contrôler la relâche de calcium par le RE. En effet, la dépolymérisation des microfilaments d'actine à l'aide de la cytochalasine D inhibe la relâche de calcium des réserves du RE dans des cultures primaires de neurones de l'hippocampe (Wang *et al.*, 2002).

5.2 Rôle de la MAP2 comme un joueur clé dans la plasticité neuronale normale chez l'adulte: apprentissage et mémoire

Plusieurs études supportent le rôle de la MAP2 comme un joueur clé induisant les changements morphologiques qui ont lieu dans les dendrites pendant la formation de la mémoire. En effet, Khuchua et collègues ont récemment démontré que la délétion des 158 premiers a.a. du domaine de projection de MAP2 par ciblage génique altère la morphologie des neurones de l'aire CA1 de l'hippocampe de souris (Khuchua *et al.*, 2003). De plus, des études de comportement sur ces souris ont révélé qu'elles avaient une déficience au niveau de la mémoire contextuelle reliée à la peur (Khuchua *et al.*, 2003). Les auteurs ont attribué ces résultats à la délétion des 31 a.a. dans la partie N-terminale responsables de l'interaction de MAP2 avec la sous-unité régulatrice RII de la protéine kinase AMP-cyclique dépendante (PKA). En outre, les auteurs ont démontré que la phosphorylation de la forme tronquée de MAP2 qui n'a plus les 158 premiers a.a. par la PKA diminue de manière significative. Le domaine de projection de MAP2 semble donc être important pour le développement de la mémoire contextuelle. En accord avec cette hypothèse, Woolf et collègues ont rapporté des altérations de MAP2 dans les dendrites apicales des cellules pyramidales de l'hippocampe suite à

l'entraînement (Woolf *et al.*, 1999). Ces altérations comprenaient la dégradation de MAP2a et MAP2b et la diminution de l'état de phosphorylation de MAP2c qui corrélaient avec l'acquisition de la mémoire contextuelle (Woolf *et al.*, 1999). De plus, Philpot et collègues ont rapporté des changements de l'état de phosphorylation de MAP2 qui étaient dépendants de l'expérience dans le bulbe olfactif de rats juvéniles et adultes (Philpot *et al.*, 1997). En effet, l'état de phosphorylation de MAP2 diminuait dans les cellules de la couche granulaire du bulbe olfactif suite à 30 jours de restriction olfactive (Philpot *et al.*, 1997). En outre, la phosphorylation de MAP2 par la PKA augmente lorsque l'animal est exposé à la lumière pour une courte période suite à l'élevage à la noirceur (Aoki and Siekevitz, 1985). Donc, la modification de l'état de phosphorylation de MAP2 semble être une étape importante conduisant à la l'emmagasinage de la mémoire à long terme. Il est possible que les changements d'efficacité synaptique activité-dépendants, qu'on soupçonne être sous-jacents à la formation de la mémoire, induisent un changement de l'état de phosphorylation de MAP2 ce qui permet la modification et/ou la consolidation de la cicuiterie neuronale. En accord avec ceci, l'activité synaptique évoquée par le glutamate cause une augmentation rapide de l'état de phosphorylation de MAP2 suivi par une déphosphorylation persistante (Quinlan and Halpain, 1996b). De plus, la dépolarisation induite par une concentration élevée de potassium extracellulaire dans des tranches d'hippocampe de rat conduit à une augmentation de l'état de phosphorylation de MAP2 (Diaz-Nido *et al.*, 1993). En outre, le méthyl-D-aspartate (NMDA), un joueur clé dans la plasticité neuronale, stimule la déphosphorylation de MAP2 (Halpain and Greengard, 1990).

D'un autre côté, la relâche de calcium intracellulaire, un autre déterminant de la plasticité neuronale, doit être hautement contrôlée dans les neurones matures. Par exemple, les phénomènes de potentiation et de dépression synaptique à long terme (LTP et LTD respectivement), qui sont sous-jacents à l'apprentissage et la mémoire chez l'adulte, sont contrôlés par la concentration de calcium intracellulaire (Malinow *et al.*, 2000). Bien que l'élévation de la concentration de calcium dans ces phénomènes soit surtout dûe à l'influx du calcium extracellulaire par les récepteurs NMDA, la relâche de calcium des réserves intracellulaires est également impliquée dans le processus. Plusieurs études supportent cette notion. Par exemple, la stimulation des fibres afférentes des cellules de Purkinje, qui est responsable de la LTD, augmente la concentration de calcium dans les épines dendritiques (Finch and Augustine, 1998). Cette augmentation comprend deux composantes : une rapide qui dépend de l'influx de calcium par les canaux opérés par le voltage et une deuxième lente qui dépend de la relâche de calcium par les récepteurs à l'inositol triphosphate (Finch and Augustine, 1998; Takechi *et al.*, 1998). Des observations similaires ont été rapportés dans les neurones de l'aire CA1 de l'hippocampe, la composente lente dépendant cette fois-ci des récepteurs à la ryanodine (Emptage *et al.*, 1999). Le fait que la MAP2 interagisse avec le RER laisse supposer qu'elle est impliquée dans le contrôle local du positionnement du réticulum endoplasmique au niveau des endroits où la relâche de calcium des réserves intracellulaires est nécessaire. Supportant cette hypothèse, la MAP2 est phosphorylée suite à l'induction de la LTP dans la région CA1 de l'hippocampe (Fukunaga *et al.*, 1995). Cette phosphorylation pourrait modifier son interaction avec les composantes du cytosquelette et/ou avec le réticulum endoplasmique et/ou avec des protéines de

signalisation, permettant ainsi les changements morphologiques qui ont lieu dans le phénomène de LTP (figure 2) (Collin *et al.*, 1997; Engert and Bonhoeffer, 1999; Kim and Lisman, 1999; Toni *et al.*, 1999; Krucker *et al.*, 2000).

5.3 Rôle de la MAP2 dans la plasticité neuronale pathologique chez l'adulte: maladies neurodégénératives

Dans le troisième volet de cette thèse, nous avons rapporté une altération du niveau protéique et de la distribution des MAPs dans un modèle animal qui récapitule le tableau neuropathologique de la sclérose latérale amyotrohpique (ALS) (Farah *et al.*, 2003). L'ALS est une maladie neurodégénérative de l'âge adulte qui est caractérisée par la mort progressive des motoneurones conduisant à la paralysie et la mort en dedans de trois à cinq ans (Julien, 2001). Nous avons démontré une diminution significative du niveau protéique de la MAP2, tau et la MAP1A cinq mois avant l'apparition des symptômes cliniques chez des souris mutantes $SOD1^{G37R}$. De plus, nous avons observé une augmentation de l'état de phosphorylation de tau au niveau des épitopes reconnus par les anticorps PHF-1 et AT8 au même stade. Il est possible qu'un changement de l'état de phosphorylation de la MAP2 aille également lieu chez les souris mutantes SOD1 avant l'apparition des symptômes cliniques surtout que les kinases qui phosphorylent tau sont également impliquées dans la phosphorylation de MAP2. Cependant, le manque d'anticorps phosphorylation-dépendants dirigés contre la MAP2 nous empêche de vérifier ceci. Le changement dans l'état de phosphorylation des MAPs est connu pour inhiber leur association avec les composantes du cytosquelette (Buee *et al.*, 2000; Sanchez *et al.*, 2000a). D'ailleurs, nous avons démontré que l'affinité de

liaison des MAPs au cytosquelette était sévèrement affectée chez les souris mutantes SOD1 cinq mois avant l'apparition des symptômes cliniques. Ces résultats impliquent une dérégulation de l'activité des protéines kinases très tôt dans la maladie. Une telle dérégulation a déjà été rapportée dans les maladies neurodégénératives (Coyle and Puttfarcken, 1993; Represa *et al.*, 1993; Perez *et al.*, 1996; Falke *et al.*, 2003).

D'un autre côté, nous avons démontré une altération de la distribution membranaire de la MAP2 qui corrélait avec la neurodégénérescence chez les souris mutantes SOD1. Nous n'avons pas identifié le sous-compartiment membranaire qui était impliqué dans cette altération. Cependant, un étude récente par Tobisawa et ses collègues a rapporté que la mutation de la SOD1 liée à la forme familiale de l'ALS induisait le stress du RE dans des cellules COS-7 et chez des souris transgéniques (Tobisawa *et al.*, 2003). Étant donné que la MAP2 interagit avec le RE, il est possible que l'altération de la distribution membranaire de la MAP2 que nous avons observée chez les souris mutantes SOD1 soit due entre autres à une modification de l'association de la MAP2 avec le RE dont la fonction serait affectée chez les souris mutantes SOD1. D'ailleurs, la présence d'une grande quantité de calcium dans le neurone 'au mauvais endroit et/ou au mauvais moment' peut conduire à la mort cellulaire. Il est bien établi que le phénomène d'excitotoxicité, qui est surtout relié à une augmentation incontrôlée de l'influx de calcium par les récepteurs NMDA, conduit à la neurodégénérescence (Sattler and Tymianski, 2000). Cependant, plusieurs études supportent la notion que la relâche incontrôlée de calcium des réserves intracellulaires est également reliée à la neurodégénérescence (Annaert and De Strooper, 1999; Leissring *et al.*, 2000; Yoo *et al.*, 2000). Par exemple, le traitement de cellules mutantes Préséniline-1 (PS1) 'knockin'

avec l'ionomycine (un ionophore calcique) et la thapsigargine (un inhibiteur de la Ca^{2+}-ATPase) a confirmé que le niveau de calcium dans le RE est augmenté de manière significative dans ces cellules par rapport aux contrôles (Leissring *et al.*, 2000). Il est donc possible qu'un changement de l'état de phosphorylation de MAP2 dans l'ALS la détache des microtubules tout en altérant son association avec le RER. Celui-ci serait positionné dans la cellule au mauvais endroit et/ou au mauvais moment causant ainsi une augmentation anormale de la concentration locale de calcium, ce messager second qui peut induire la mort neuronale.

Les maladies neurodégénératives peuvent être considérées comme une forme anormale de plasticité neuronale. En effet, on assiste parfois à une rétraction dendritique dasn ces maladies ou à une croissance axonale et dendritique (Coyle and Puttfarcken, 1993; Represa *et al.*, 1993; Perez *et al.*, 1996). Dans tous les cas, ceci conduit à la perte de la structure et de la polarité du neurone (Coyle and Puttfarcken, 1993; Represa *et al.*, 1993; Perez *et al.*, 1996; Falke *et al.*, 2003). Des altérations du niveau d'expression et/ou de l'état de phosphorylation de la MAP2 ont souvent été rapportées dans ces maladies. Par exemple, une augmentation de l'expression de la MAP2 a été rapportée dans l'hippocampe de patients schizophrènes (Cotter *et al.*, 1997; Cotter *et al.*, 2000). De plus, une altération du marquage immunocytochimique de la MAP2 a été rapporté dans les aires 9 et 32 du cortex préfrontal dans la schizophrénie (Jones *et al.*, 2002). Dans l'épilepsie, une augmentation de l'expression de la MAP2 a lieu dans un modèle expérimental de l'épilepsie du lobe temporal (Pollard *et al.*, 1994). De plus, une diminution de l'état de phosphorylation de la MAP2 a lieu dans le cortex du lobe

temporal chez les patients épileptiques (Sanchez *et al.*, 2001). Dans la maladie de Parkinson, un marquage immunocytochimique anormal de la MAP2 a été rapporté dans les noyaux des neurones et dans les corps de Lewy de la substance noire de tissu de cerveau (D'Andrea *et al.*, 2001). Que ces altérations de la MAP2 comptent parmi les premiers évènements qui conduisent à la perte de la structure et de la polarité neuronale ou bien qu'ils soient secondaires à la maladie reste encore à être déterminé. Cependant, le fait que dans les souris mutantes SOD1, les altérations du niveau des MAPs et de leurs affinités de liaison au cytosquelette aillent lieu très tôt dans la maladie laisse supposer un rôle primordial pour ces altérations dans le cours de la maladie.

5.4 Perspectives d'avenir

Il devient de plus en plus important de mieux connaître les mécanismes moléculaires exacts qui conduisent à l'acquisition de la polarité neuronale et à son maintien afin de mieux comprendre les altérations morphologiques qui conduisent à la perte de cette polarité dans les maladies neurodégénératives. Il est clair que la MAP2 joue un rôle clé dans l'élaboration de la structure neuronale. De plus, les altérations de son niveau d'expression et/ou de son état de phosphorylation dans le phénomène de plasticité normale (apprentissage) ou anormale (maladies neurodégénératives) indiquent qu'elle pourrait jouer un rôle déterminant dans le maintien de la polarité neuronale à l'âge adulte. Il reste bien sûr des questions auxquelles on devrait répondre afin de mieux définir son rôle dans ces phénomènes. Entre autres, il faudrait mieux définir son rôle dans le phénomène d'apprentissage par exemple en se servant de la LTP dans la région CA1 de l'hippocampe comme modèle. De plus, il faudrait mieux caractériser l'altération

de l'association de la MAP2 avec le réticulum endoplasmique et/ou avec des protéines de signalisation qui pourrait avoir lieu dans les maladies neurodégénératives à différents stades. La présente thèse aurait contribué à mieux définir le rôle de cette MAP dendritique à l'ère où les yeux sont tournés vers les dendrites.

Figure 1. La technique de recouvrement par immunobuvardage est utilisée pour identifier les partenaires de la MAP2. A) Un homogénat fut préparé à partir des cellules Sf9. Les protéines ont ensuite été séparées par SDS-PAGE et transférées à une membrane de nitrocellulose. La membrane fut incubée avec de la MAP2c pure (préparée à partir des cellules Sf9) et l'interaction de MAP2c avec des protéines de l'homogénat fut détectée à l'aide d'un anticorps monoclonal anti-MAP2 (HM2). Les flèches pointent vers les protéines qui constituent des partenaires potentiels de la MAP2. Ces bandes ne sont pas présentes lorsque la membrane est incubée avec le tampon tout seul comme contrôle négatif (résultat non-montré). B) Une fraction enrichie en membranes crues fut préparée à partir des cellules Sf9 et le même protocole décrit en A fut utilisé pour détecter les partenaires de la MAP2 sur les membranes. À noter que moins de bandes sont détectées par rapport à A. Cependant, des bandes de poids moléculaire similaire sont révélées dans les deux cas ce qui indique que ces interactions sont spécifiques. C) Une fraction cytosolique fut préparée cette fois-ci à partir des cellules Sf9 et le même protocole fut utilisé pour identifier les partenaires cytosoliques de la MAP2. MAP2c semble surtout interagir avec la tubuline dans le cytosol.

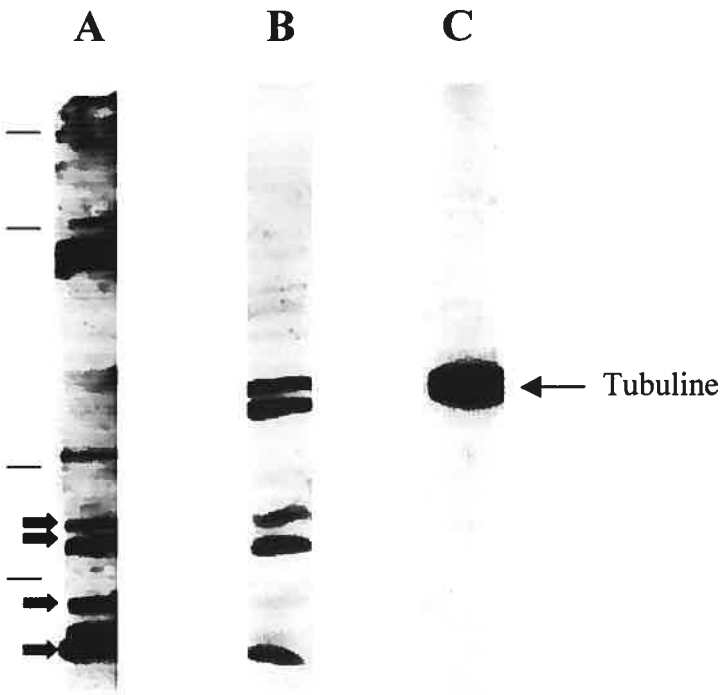
A
B
C
Tubuline

Figure 2. Lorsqu'un neurone mature reçoit des signaux externes, une modification de l'activité des kinases/phosphatases pourrait avoir lieu dans la cellule. Ceci conduirait à une modification de l'état de phosphorylation de la MAP2 affectant son interaction avec: 1) les microtubules, les microfilaments et les neurofilaments modulant ainsi leur dynamique, 2) le RE conduisant possiblement au repositionnement de celui-ci au niveau d'endroits spécifiques le long des microtubules dendritiques là où la relâche locale de calcium est nécessaire et 3) des protéines de signalisation tel que la PKA et les récepteurs NMDA qui jouent un rôle clé dans la formation de la mémoire. Un (ou plusieurs) de ces évènements conduirait au remodelage dendritique observé à l'âge adulte.

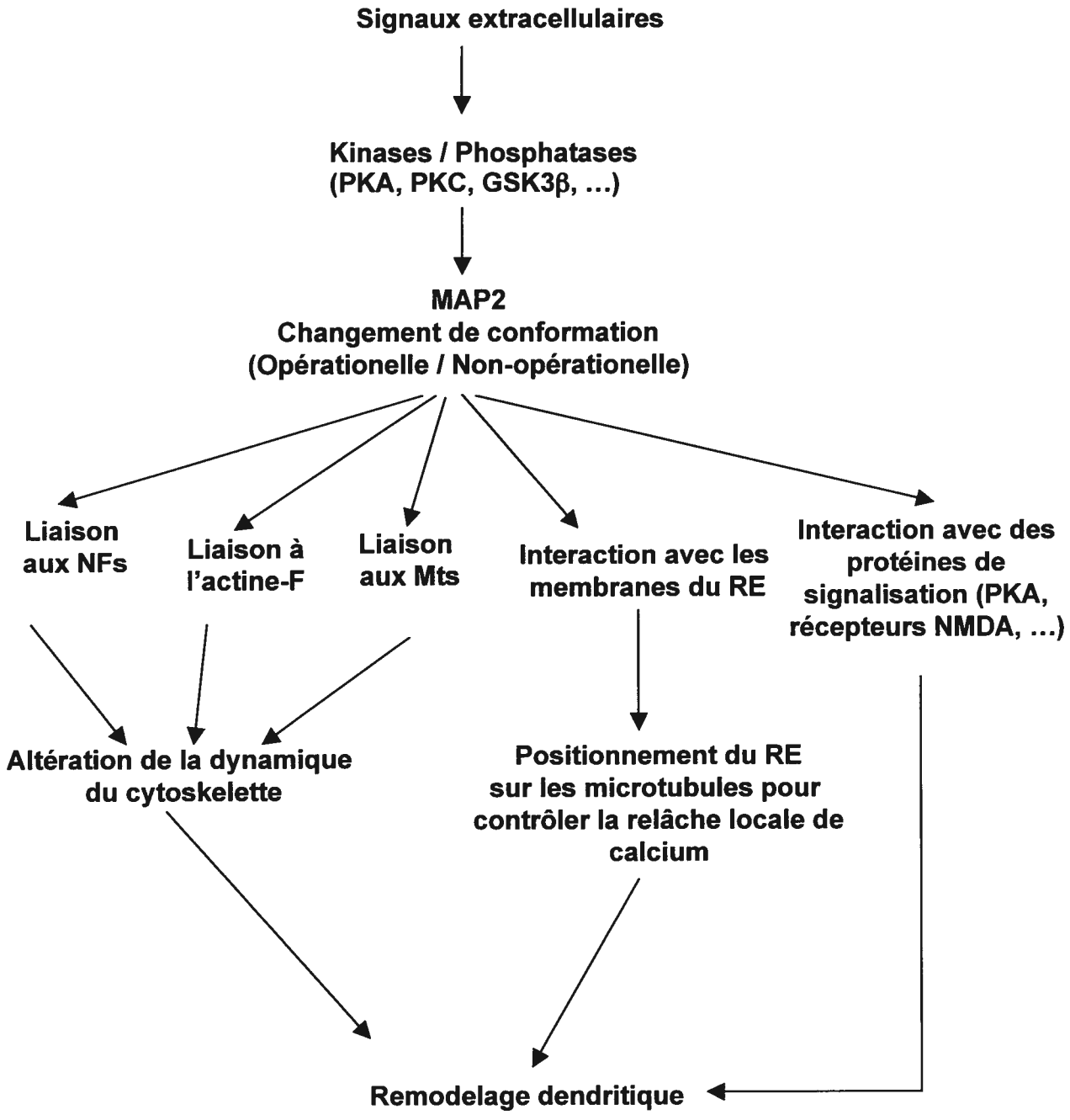
Signaux extracellulaires
Kinases / Phosphatases
(PKA, PKC, GSK3β, ...)
MAP2
Changement de conformation
(Opérationelle / Non-opérationelle)
Liaison aux NFs
Liaison à l'actine-F
Liaison aux Mts
Interaction avec les membranes du RE
Interaction avec des protéines de signalisation (PKA, récepteurs NMDA, ...)
Altération de la dynamique du cytoskelette
Positionnement du RE sur les microtubules pour contrôler la relâche locale de calcium
Remodelage dendritique

BIBLIOGRAPHIE

Abel, T., Nguyen, P.V., Barad, M., Deuel, T.A., Kandel, E.R., and Bourtchouladze, R. (1997). Genetic demonstration of a role for PKA in the late phase of LTP and in hippocampus-based long-term memory. Cell *88*, 615-626.

Aihara, Y., Inoue, T., Tashiro, T., Okamoto, K., Komiya, Y., and Mikoshiba, K. (2001). Movement of endoplasmic reticulum in the living axon is distinct from other membranous vesicles in its rate, form, and sensitivity to microtubule inhibitors. J Neurosci Res *65*, 236-246.

Ainsztein, A.M., and Purich, D.L. (1994). Stimulation of tubulin polymerization by MAP-2. Control by protein kinase C-mediated phosphorylation at specific sites in the microtubule- binding region. J Biol Chem *269*, 28465-28471.

Akhmanova, A., Hoogenraad, C.C., Drabek, K., Stepanova, T., Dortland, B., Verkerk, T., Vermeulen, W., Burgering, B.M., De Zeeuw, C.I., Grosveld, F., and Galjart, N. (2001). Clasps are CLIP-115 and -170 associating proteins involved in the regional regulation of microtubule dynamics in motile fibroblasts. Cell *104*, 923-935.

Akiyama, T., Nishida, E., Ishida, J., Saji, N., Ogawara, H., Hoshi, M., Miyata, Y., and Sakai, H. (1986). Purified protein kinase C phosphorylates microtubule-associated protein 2. J Biol Chem *261*, 15648-15651.

Albala, J.S., Kress, Y., Liu, W.K., Weidenheim, K., Yen, S.H., and Shafit-Zagardo, B. (1995). Human microtubule-associated protein-2c localizes to dendrites and axons in fetal spinal motor neurons. J Neurochem *64*, 2480-2490.

Al-Bassam, J., Ozer, R.S., Safer, D., Halpain, S., and Milligan, R.A. (2002). MAP2 and tau bind longitudinally along the outer ridges of microtubule protofilaments. J Cell Biol *157*, 1187-1196.

Al-Chalabi, A., and Miller, C.C. (2003). Neurofilaments and neurological disease. Bioessays *25*, 346-355.

Alexa, A., Tompa, P., Baki, A., Vereb, G., and Friedrich, P. (1996). Mutual protection of microtubule-associated protein 2 (MAP2) and cyclic AMP-dependent protein kinase II against mu-calpain. J Neurosci Res *44*, 438-445.

Allan, V., and Vale, R. (1994). Movement of membrane tubules along microtubules in vitro: evidence for specialised sites of motor attachment. J Cell Sci *107 (Pt 7)*, 1885-1897.

Allan, V.J., Vale, R.D., and Navone, F. (1991). Microtubule-based organelle transport in neurons. Wiley-Liss Inc.

Amano, M., Kaneko, T., Maeda, A., Nakayama, M., Ito, M., Yamauchi, T., Goto, H., Fukata, Y., Oshiro, N., Shinohara, A., Iwamatsu, A., and Kaibuchi, K. (2003). Identification of Tau and MAP2 as novel substrates of Rho-kinase and myosin phosphatase. J Neurochem *87*, 780-790.

Andra, K., Nikolic, B., Stocher, M., Drenckhahn, D., and Wiche, G. (1998). Not just scaffolding: plectin regulates actin dynamics in cultured cells. Genes Dev *12*, 3442-3451.

Annaert, W., and De Strooper, B. (1999). Presenilins: molecular switches between proteolysis and signal transduction. Trends Neurosci *22*, 439-443.

Aoki, C., and Siekevitz, P. (1985). Ontogenetic changes in the cyclic adenosine 3',5'-monophosphate-stimulatable phosphorylation of cat visual cortex proteins, particularly

of microtubule-associated protein 2 (MAP 2): effects of normal and dark rearing and of the exposure to light. J Neurosci *5*, 2465-2483.

Arias, C., Arrieta, I., Massieu, L., and Tapia, R. (1997). Neuronal damage and MAP2 changes induced by the glutamate transport inhibitor dihydrokainate and by kainate in rat hippocampus in vivo. Exp Brain Res *116*, 467-476.

Audesirk, G., Cabell, L., and Kern, M. (1997). Modulation of neurite branching by protein phosphorylation in cultured rat hippocampal neurons. Brain Res. Develop. Brain Res. *102*, 247-260.

Avruch, J. (1998). Insulin signal transduction through protein kinase cascades. Mol Cell Biochem *182*, 31-48.

Baas, P.W., Deitch, J.S., Black, M.M., and Banker, G.A. (1988). Polarity orientation of microtubules in hippocampal neurons: uniformity in the axon and nonuniformity in the dendrite. Proc Natl Acad Sci U S A *85*, 8335-8339.

Baas, P.W., Pienkowski, T.P., and Kosik, K.S. (1991). Processes induced by tau expression in Sf9 cells have an axon-like microtubule organization. J. Cell Biol. *115*, 1333-1344.

Banker, G., and Goslin, K. (1998). Culturing nerve cells. A Bradford Book, the MIT Press.

Bannai, H., Inoue, T., Nakayama, T., Hattori, M., and Mikoshiba, K. (2004). Kinesin dependent, rapid, bi-directional transport of ER sub-compartment in dendrites of hippocampal neurons. J Cell Sci *117*, 163-175.

Bartlett, W.P., and Banker, G.A. (1984a). An electron microscopic study of the development of axons and dendrites by hippocampal neurons in culture. I. Cells which develop without intercellular contacts. J Neurosci *4*, 1944-1953.

Bartlett, W.P., and Banker, G.A. (1984b). An electron microscopic study of the development of axons and dendrites by hippocampal neurons in culture. II. Synaptic relationships. J Neurosci *4*, 1954-1965.

Baudhuin, P., Evrard, P., and Berthet, J. (1967). Electron microscopic examination of subcellular fractions. I. The preparation of representative samples from suspensions of particles. J Cell Biol *32*, 181-191.

Belanger, D., Farah, C.A., Nguyen, M.D., Lauzon, M., Cornibert, S., and Leclerc, N. (2002). The projection domain of MAP2b regulates microtubule protrusion and process formation in Sf9 cells. J Cell Sci *115*, 1523-1539.

Belmont, L., Mitchison, T., and Deacon, H.W. (1996). Catastrophic revelations about Op18/stathmin. Trends Biochem Sci *21*, 197-198.

Belmont, L.D., and Mitchison, T.J. (1996). Identification of a protein that interacts with tubulin dimers and increases the catastrophe rate of microtubules. Cell *84*, 623-631.

Berling, B., Wille, H., Roll, B., Mandelkow, E.M., Garner, C., and Mandelkow, E. (1994). Phosphorylation of microtubule-associated proteins MAP2a,b and MAP2c at Ser136 by proline-directed kinases in vivo and in vitro. Eur J Cell Biol *64*, 120-130.

Black, M.M., Keyser, P., and Sobel, E. (1986). Interval between the synthesis and assembly of cytoskeletal proteins in cultured neurons. J Neurosci *6*, 1004-1012.

Blobel, G., and Potter, V.R. (1966). Nuclei from rat liver: isolation method that combines purity with high yield. Science *154*, 1662-1665.

Bloom, G.S., Luca, F.C., and Vallee, R.B. (1985). Identification of high molecular weight microtubule-associated proteins in anterior pituitary tissue and cells using taxol-dependent purification combined with microtubule-associated protein specific antibodies. Biochemistry *24*, 4185-4191.

Bloom, G.S., and Vallee, R.B. (1983). Association of microtubule-associated protein 2 (MAP 2) with microtubules and intermediate filaments in cultured brain cells. J Cell Biol *96*, 1523-1531.

Borradori, L., Trueb, R.M., Jaunin, F., Limat, A., Favre, B., and Saurat, J.H. (1998). Autoantibodies from a patient with paraneoplastic pemphigus bind periplakin, a novel member of the plakin family. J Invest Dermatol *111*, 338-340.

Boucher, M., Belanger, D., Beaulieu, C., and Leclerc, N. (1999). Tau-mediated process outgrowth is differentially altered by the expression of MAP2b and MAP2c in Sf9 cells. Cell Motil Cytoskeleton *42*, 257-273.

Brugg, B., and Matus, A. (1991). Phosphorylation determines the binding of microtubule-associated protein 2 (MAP2) to microtubules in living cells. J. Cell Biol. *114*, 735-743.

Bruijn, L., Houseweart, M., Kato, S., Anderson, K., Anderson, S., Ohama, E., Reaume, A., Scott, R., and Cleveland, D. (1998). Aggregation and motor neuron toxicity of an ALS-linked SOD1 mutant independent from wild-type SOD1. Science *281*, 1851-1854.

Bruijn, L.I., Becher, M.W., Lee, M.K., Anderson, K.L., Jenkins, N.A., Copeland, N.G., Sisodia, S.S., Rothstein, J.D., Borchelt, D.R., Price, D.L., and Cleveland, D.W. (1997). ALS-linked SOD1 mutant G85R mediates damage to astrocytes and promotes rapidly progressive disease with SOD1-containing inclusions. Neuron *18*, 327-338.

Buddle, M., Eberhardt, E., Ciminello, L.H., Levin, T., Wing, R., DiPasquale, K., and Raley-Susman, K.M. (2003). Microtubule-associated protein 2 (MAP2) associates with the NMDA receptor and is spatially redistributed within rat hippocampal neurons after oxygen-glucose deprivation. Brain Res *978*, 38-50.

Buee, L., Bussiere, T., Buee-Scherrer, V., Delacourte, A., and Hof, P.R. (2000). Tau protein isoforms, phosphorylation and role in neurodegenerative disorders. Brain Res Brain Res Rev *33*, 95-130.

Burgin, K., Ludin, B., Ferralli, J., and Matus, A. (1994). Bundling of microtubules in transfected cells does not involve an autonomous dimerization site on the MAP2 molecule. Mol. Biol. Cell *5*, 511-517.

Burns, R., and Surridge, C. (1995). The phosphatidylinositol-binding site of microtubule-associated protein MAP2. Biochem. Soc. Trans. *23*, 41-46.

Burns, R.G., Islam, K., and Chapman, R. (1984). The multiple phosphorylation of the microtubule-associated protein MAP2 controls the MAP2:tubulin interaction. Eur J Biochem *141*, 609-615.

Burton, P.R. (1988). Dendrites of mitral cell neurons contain microtubules of opposite polarity. Brain Res *473*, 107-115.

Caceres, A., Banker, G.A., and Binder, L. (1986). Immunocytochemical localization of tubulin and microtubule-associated protein 2 during the development of hippocampal neurons in culture. J Neurosci *6*, 714-722.

Caceres, A., Banker, G.A., Stewart, O., Binder, L., and Payne, M. (1984). MAP2 is localized to the dendrites of hippocampal neurons which develop in culture. Dev. Brain Res. *13*, 314-318.

Caceres, A., and Kosik, K.S. (1990). Inhibition of neurite polarity by tau antisense oligonucleotides in primary cerebellar neurons. Nature *343*, 461-463.

Caceres, A., Mautino, J., and Kosik, K.S. (1992). Suppression of MAP2 in cultured cerebellar macroneurons inhibits minor neurite formation. Neuron *9*, 607-618.

Caceres, A., Potrebic, S., and Kosik, K. (1991). The effect of tau antisense oligonucleotides on neurite formation of cultured cerebellar macroneurons. J. Neurosci. *11*, 1515-1523.

Cain, D.P. (1997). LTP, NMDA, genes and learning. Curr Opin Neurobiol *7*, 235-242.

Chan, W.K., Yabe, J.T., Pimenta, A.F., Ortiz, D., and Shea, T.B. (2003). Growth cones contain a dynamic population of neurofilament subunits. Cell Motil Cytoskeleton *54*, 195-207.

Chapin, S., and Bulinski, J. (1991). Non-neuronal 210 X 103 Mr microtubule-associated protein (MAP4) contains domain homologous to microtubule-binding domains of neuronal MAP2 and tau. J. Cell Sci. *98*, 27-36.

Charlton, C.A., and Volkman, L.E. (1991). Sequential rearrangement and nuclear polymerization of actin in baculovirus-infected Spodoptera frugiperda cells. J. Virol. *65*, 1219-1227.

Chen, J., Kanai, Y., Cowan, N.J., and Hirokawa, N. (1992). Projection domains of MAP2 and tau determine spacings between microtubules in dendrites and axons. Nature *360*, 674-676.

Chung, W.J., Kindler, S., Seidenbecher, C., and Garner, C.C. (1996). MAP2a, an alternatively spliced variant of microtubule-associated protein 2. J. Neurochem. *66*, 1273-1281.

Cobb, M.H., Robbins, D.J., and Boulton, T.G. (1991). ERKs, extracellular signal-regulated MAP-2 kinases. Current Opinion in Cell Biology *3*, 1025-1032.

Cohen, P. (1989). The structure and regulation of protein phosphatases. Annu Rev Biochem *58*, 453-508.

Cohen, P., and Cohen, P.T. (1989). Protein phosphatases come of age. J Biol Chem *264*, 21435-21438.

Cohen, P., Schelling, D.L., and Stark, M.J. (1989). Remarkable similarities between yeast and mammalian protein phosphatases. FEBS Lett *250*, 601-606.

Cole, N.B., and Lippincott-Schwartz, J. (1995). Organization of organelles and membrane traffic by microtubules. Curr Opin Cell Biol *7*, 55-64.

Colella, R., Lu, C., Hodges, B., Wilkey, D.W., and Roisen, F.J. (2000). GM1 enhances the association of neuron-specific MAP2 with actin in MAP2-transfected 3T3 cells. Brain Res Dev Brain Res *121*, 1-9.

Collin, C., Miyaguchi, K., and Segal, M. (1997). Dendritic spine density and LTP induction in cultured hippocampal slices. J Neurophysiol *77*, 1614-1623.

Correas, I., Padilla, R., and Avila, J. (1990). The tubulin-binding sequence of brain microtubule-associated proteins, tau and MAP-2, is also involved in actin binding. Biochem J *269*, 61-64.

Cotter, D., Kerwin, R., Doshi, B., Martin, C.S., and Everall, I.P. (1997). Alterations in hippocampal non-phosphorylated MAP2 protein expression in Schizophrenia. Brain Res. *765*, 238-246.

Cotter, D., Wilson, S., Roberts, E., Kerwin, R., and Everall, I.P. (2000). Increased dendritic MAP2 expression in the hippocampus in schizophrenia. Schizophr Res *41*, 313-323.

Couchie, D., Chabas, S., Mavilia, C., and Nunez, J. (1996). New forms of HMW MAP2 are preferentially expressed in the spinal cord. FEBS Letters *388*, 76-79.

Coyle, J.T., and Puttfarcken, P. (1993). Oxidative stress, glutamate, and neurodegenerative disorders. Science *262*, 689-695.

Cudkowicz, M.E., McKenna-Yasek, D., Sapp, P.E., Chin, W., Geller, B., Hayden, D.L., Schoenfeld, D.A., Hosler, B.A., Horvitz, H.R., and Brown, R.H. (1997). Epidemiology of mutations in superoxide dismutase in amyotrophic lateral sclerosis. Ann Neurol *41*, 210-221.

Cunningham, C., Leclerc, N., Flanagan, L., Lu, M., Janmey, P., and Kosik, K. (1997). Microtubule-associated protein 2c reorganizes both microtubules and microfilaments into distinct cytological structures in an actin-binding protein-280-deficient melanoma cell line. J. Cell Biol. *136*, 845-857.

Dailey, M.E., and Bridgman, P.C. (1989). Dynamics of the endoplasmic reticulum and other membranous organelles in growth cones of cultured neurons. J Neurosci *9*, 1897-1909.

Dailey, M.E., and Bridgman, P.C. (1991). Structure and organization of membrane organelles along distal microtubule segments in growth cones. J Neurosci Res *30*, 242-258.

Dalpe, G., Leclerc, N., Vallee, A., Messer, A., Mathieu, M., De Repentigny, Y., and Kothary, R. (1998). Dystonin Is Essential for Maintaining Neuronal Cytoskeleton Organization. Mol Cell Neurosci *10*, 243-257.

Dalpe, G., Mathieu, M., Comtois, A., Zhu, E., Wasiak, S., De Repentigny, Y., Leclerc, N., and Kothary, R. (1999). Dystonin-deficient mice exhibit an intrinsic muscle weakness and an instability of skeletal muscle cytoarchitecture. Dev Biol *210*, 367-380.

D'Andrea, M.R., Ilyin, S., and Plata-Salaman, C.R. (2001). Abnormal patterns of microtubule-associated protein-2 (MAP-2) immunolabeling in neuronal nuclei and Lewy bodies in Parkinson's disease substantia nigra brain tissues. Neurosci Lett *306*, 137-140.

Davare, M.A., Dong, F., Rubin, C.S., and Hell, J.W. (1999). The A-kinase anchor protein MAP2B and cAMP-dependent protein kinase are associated with class C L-type calcium channels in neurons. J Biol Chem *274*, 30280-30287.

De Zeeuw, C.I., Hoogenraad, C.C., Goedknegt, E., Hertzberg, E., Neubauer, A., Grosveld, F., and Galjart, N. (1997). CLIP-115, a novel brain-specific cytoplasmic linker protein, mediates the localization of dendritic lamellar bodies. Neuron *19*, 1187-1199.

Deitch, J.S., and Banker, G.A. (1993). An electron microscopic analysis of hippocampal neurons developing in culture: early stages in the emergence of polarity. J Neurosci *13*, 4301-4315.

Dhavan, R., and Tsai, L.H. (2001). A decade of CDK5. Nat Rev Mol Cell Biol *2*, 749-759.

Diaz-Nido, J., Montoro, R.J., Lopez-Barneo, J., and Avila, J. (1993). High external potassium induces an increase in the phosphorylation of the cytoskeletal protein MAP2 in rat hippocampal slices. Eur J Neurosci *5*, 818-824.

Diez-Guerra, F.J., and Avila, J. (1995). An increase in phosphorylation of microtubule-associated protein 2 accompanies dendrite extension during the differentiation of cultured hippocampal neurones. Eur J Biochem *227*, 68-77.

Dinsmore, J.H., and Solomon, F. (1991). Inhibition of MAP2 expression affects both morphological and cell division phenotypes of neuronal differentiation. Cell *64*, 817-826.

Doll, T., Meichsner, M., Riederer, B.M., Honegger, P., and Matus, A. (1993a). An isoform of microtubule-associated protein 2 (MAP2) containing four repeats of the tubulin binding motif. J. Cell Sci. *106*, 633-640.

Doll, T., Meichsner, M., Riederer, B.M., Honegger, P., and Matus, A. (1993b). An isoform of microtubule-associated protein 2 (MAP2) containing four repeats of the tubulin-binding motif. J Cell Sci *106 (Pt 2)*, 633-639.

dos Remedios, C.G., Chhabra, D., Kekic, M., Dedova, I.V., Tsubakihara, M., Berry, D.A., and Nosworthy, N.J. (2003). Actin binding proteins: regulation of cytoskeletal microfilaments. Physiol Rev *83*, 433-473.

Dotti, C.G., Sullivan, C.A., and Banker, G.A. (1988). The establishment of polarity by hippocampal neurons in culture. J Neurosci *8*, 1454-1468.

Drechsel, D.N., Hyman, A.A., Cobb, M.H., and Kirschner, M.W. (1992). Modulation of the dynamic instability of tubulin assembly by the microtubule-associated protein tau. Mol Biol Cell *3*, 1141-1154.

Drewes, G., Ebneth, A., and Mandelkow, E.M. (1998). MAPs, MARKs and microtubule dynamics. Trends Biochem Sci *23*, 307-311.

Drewes, G., Ebneth, A., Preuss, U., Mandelkow, E.M., and Mandelkow, E. (1997). MARK, a novel family of protein kinases that phosphorylate microtubule-associated proteins and trigger microtubule disruption. Cell *89*, 297-308.

Edson, K., Weisshaar, B., and Matus, A. (1993). Actin depolymerisation induces process formation on MAP2-transfected non-neuronal cells. Development *117*, 689-700.

Ekinci, F.J., and Shea, T.B. (1999). Free PKC catalytic subunits (PKM) phosphorylate tau via a pathway distinct from that utilized by intact PKC. Brain Res *850*, 207-216.

Emptage, N., Bliss, T.V., and Fine, A. (1999). Single synaptic events evoke NMDA receptor-mediated release of calcium from internal stores in hippocampal dendritic spines. Neuron *22*, 115-124.

Engert, F., and Bonhoeffer, T. (1999). Dendritic spine changes associated with hippocampal long-term synaptic plasticity. Nature *399*, 66-70.

Facanha, A.L., Appelgren, H., Tabish, M., Okorokov, L., and Ekwall, K. (2002). The endoplasmic reticulum cation P-type ATPase Cta4p is required for control of cell shape and microtubule dynamics. J Cell Biol *157*, 1029-1039.

Faddis, B.T., Hasbani, M.J., and Goldberg, M.P. (1997). Calpain activation contributes to dendritic remodeling after brief excitotoxic injury in vitro. J Neurosci *17*, 951-959.

Falke, E., Nissanov, J., Mitchell, T.W., Bennett, D.A., Trojanowski, J.Q., and Arnold, S.E. (2003). Subicular dendritic arborization in Alzheimer's disease correlates with neurofibrillary tangle density. Am J Pathol *163*, 1615-1621.

Fanara, P., Oback, B., Ashman, K., Podtelejnikov, A., and Brandt, R. (1999). Identification of MINUS, a small polypeptide that functions as a microtubule nucleation suppressor. Embo J *18*, 565-577.

Farah, C.A., Nguyen, M.D., Julien, J.P., and Leclerc, N. (2003). Altered levels and distribution of microtubule-associated proteins before disease onset in a mouse model of amyotrophic lateral sclerosis. J Neurochem *84*, 77-86.

Feiguin, F., Ferreira, A., Kosik, K.S., and Caceres, A. (1994). Kinesin-mediated organelle translocation revealed by specific cellular manipulations. J Cell Biol *127*, 1021-1039.

Felgner, H., Frank, R., Biernat, J., Mandelkow, E.M., Mandelkow, E., Ludin, B., Matus, A., and Schliwa, M. (1997). Domains of neuronal microtubule-associated proteins and flexural rigidity of microtubules. J Cell Biol *138*, 1067-1075.

Fellous, A., Kubelka, M., Thibier, C., Taieb, F., Haccard, O., and Jessus, C. (1994). Association of p34cdc2 kinase and MAP kinase with microtubules during the meiotic maturation of Xenopus oocytes. Int J Dev Biol *38*, 651-659.

Ferhat, L., Ben-Ari, Y., and Khrestchatisky, M. (1994b). Complete sequence of rat MAP2d, a novel MAP2d isoform. C.R. Acad.Sci. Paris *317*, 304-309.

Ferhat, L., Bernard, A., Ribas de Pouplana, L., Ben-Ari, Y., and Khrestchatisky, M. (1994). Structure, regional and developmental expression of rat MAP2d, a MAP2 splice variant encoding four microtubule-binding domains. Neurochemistry International *25*, 327-338.

Ferhat, L., Represa, A., Bernard, A., Ben-Ari, Y., and Khrestchatisky, M. (1996). MAP2d promotes bundling and stabilization of both microtubules and microfilaments. J. Cell Science *109*, 1095-1103.

Ferralli, J., Doll, T., and Matus, A. (1994). Sequence analysis of MAP2 function in living cells. J. Cell Sci. *107*, 3115-3125.

Finch, E.A., and Augustine, G.J. (1998). Local calcium signalling by inositol-1,4,5-trisphosphate in Purkinje cell dendrites. Nature *396*, 753-756.

Fischer, I., Romano-Clarke, G., and Grynspan, F. (1991). Calpain-mediated proteolysis of microtubule associated proteins MAP1B and MAP2 in developing brain. Neurochem Res *16*, 891-898.

Forleo, P., Couchie, D., Chabas, S., and Nunez, J. (1996). Four Repeat High-Mol-Wt MAP2 Forms in Rat Dorsal Root Ganglia. Journal of Molecular Neuroscience *7*, 193-201.

Fujiwara, S., Takeo, N., Otani, Y., Parry, D.A., Kunimatsu, M., Lu, R., Sasaki, M., Matsuo, N., Khaleduzzaman, M., and Yoshioka, H. (2001). Epiplakin, a novel member of the Plakin family originally identified as a 450-kDa human epidermal autoantigen. Structure and tissue localization. J Biol Chem *276*, 13340-13347.

Fukazawa, Y., Saitoh, Y., Ozawa, F., Ohta, Y., Mizuno, K., and Inokuchi, K. (2003). Hippocampal LTP is accompanied by enhanced F-actin content within the dendritic spine that is essential for late LTP maintenance in vivo. Neuron *38*, 447-460.

Fukunaga, K., Muller, D., and Miyamoto, E. (1995). Increased phosphorylation of Ca2+/calmodulin-dependent protein kinase II and its endogenous substrates in the induction of long-term potentiation. J Biol Chem *270*, 6119-6124.

Gary, R., and Bretscher, A. (1995). Ezrin self-association involves binding of an N-terminal domain to a normally masked C-terminal domain that includes the F-actin binding site. Mol. Biol. Cell *6*, 1061-1075.

Gautreau, A., Louvard, D., and Arpin, M. (2000). Morphogenic effects of ezrin require a phosphorylation-induced transition from oligomers to monomers at the plasma membrane. J. Cell Biol. *150*, 193-203.

Gerace, L., and Burke, B. (1988). Functional organization of the nuclear envelope. Annu Rev Cell Biol *4*, 335-374.

Gleeson, J.G. (2000). Classical lissencephaly and double cortex (subcortical band heterotopia): LIS1 and doublecortin. Curr Opin Neurol *13*, 121-125.

Glicksman, M.A., Soppet, D., and Willard, M.B. (1987). Posttranslational modification of neurofilament polypeptides in rabbit retina. J Neurobiol *18*, 167-196.

Goldenring, J.R., and DeLorenzo, R.J. (1986). Phosphorylation of MAP-2 at distinct sites by calmodulin- and cyclic AMP-dependent kinases. Ann N Y Acad Sci *466*, 457-459.

Goldenring, J.R., Vallano, M.L., and DeLorenzo, R.J. (1985). Phosphorylation of microtubule-associated protein 2 at distinct sites by calmodulin-dependent and cyclic-AMP-dependent kinases. J Neurochem *45*, 900-905.

Gong, C.X., Lidsky, T., Wegiel, J., Zuck, L., Grundke-Iqbal, I., and Iqbal, K. (2000a). Phosphorylation of microtubule-associated protein tau is regulated by protein phosphatase 2A in mammalian brain. Implications for neurofibrillary degeneration in Alzheimer's disease. J Biol Chem *275*, 5535-5544.

Gong, C.X., Wegiel, J., Lidsky, T., Zuck, L., Avila, J., Wisniewski, H.M., Grundke-Iqbal, I., and Iqbal, K. (2000b). Regulation of phosphorylation of neuronal microtubule-associated proteins MAP1b and MAP2 by protein phosphatase-2A and -2B in rat brain. Brain Res *853*, 299-309.

Goode, B., Denis, P., Panda, D., Radeke, M., Miller, H., Wilson, L., and Feinstein, S. (1997). Functional interactions between the proline-rich and repeat regions of tau enhance microtubule binding and assembly. Mol. Biol. Cell *8*, 353-365.

Goslin, K., Birgbauer, E., Banker, G., and Solomon, F. (1989). The role of cytoskeleton in organizing growth cones: a microfilament-associated growth cone component depends upon microtubules for its localization. J. Cell Biol. *109*, 1621-1631.

Goto, S., Yamamoto, H., Fukunaga, K., Iwasa, T., Matsukado, Y., and Miyamoto, E. (1985). Dephosphorylation of microtubule-associated protein 2, tau factor, and tubulin by calcineurin. J Neurochem *45*, 276-283.

Green, K.J., Guy, S.G., Cserhalmi-Friedman, P.B., McLean, W.H., Christiano, A.M., and Wagner, R.M. (1999). Analysis of the desmoplakin gene reveals striking conservation with other members of the plakin family of cytolinkers. Exp Dermatol *8*, 462-470.

Hagestedt, T., Lichtenberg, B., Wille, H., Mandelkow, E.-M., and Mandelkow, E. (1989). Tau protein becomes long and stiff upon phosphorylation: correlation between paracrystalline structure and degree of phosphorylation. J. Cell Biol. *109*, 1643-1651.

Halpain, S., and Greengard, P. (1990). Activation of NMDA receptors induces rapid dephosphorylation of the cytoskeletal protein MAP2. Neuron *5*, 237-246.

Harada, A., Oguchi, K., Okabe, S., Kuno, J., Terada, S., Ohshima, T., Sato-Yoshitake, R., Takei, Y., Noda, T., and Hirokawa, N. (1994). Altered microtubule organization in small-calibre axons of mice lacking tau protein. Nature *369*, 488-491.

Harada, A., Takei, Y., Kanai, Y., Tanaka, Y., Nonaka, S., and Hirokawa, N. (1998). Golgi vesiculation and lysosome dispersion in cells lacking cytoplasmic dynein. J Cell Biol *141*, 51-59.

Harada, A., Teng, J., Takei, Y., Oguchi, K., and Hirokawa, N. (2002). MAP2 is required for dendrite elongation, PKA anchoring in dendrites, and proper PKA signal transduction. J Cell Biol *158*, 541-549.

Heimann, R., Shelanski, M.L., and Liem, R.K. (1985). Microtubule-associated proteins bind specifically to the 70-kDa neurofilament protein. J Biol Chem *260*, 12160-12166.

Hernandez, M.A., Avila, J., and Andreu, J.M. (1986). Physicochemical characterization of the heat-stable microtubule-associated protein MAP2. Eur J Biochem *154*, 41-48.

Hernandez, M.A., Wandosell, F., and Avila, J. (1987a). Localization of the phosphate sites for different kinases in the microtubule-associated protein MAP2. J. Neurochem. *48*, 84-93.

Hernandez, M.A., Wandosell, F., and Avila, J. (1987b). Localization of the Phosphorylation Sites for Different Kinases in the Microtubule-Associated Protein MAP2. Journal of Neurochemistry *48*, 84-93.

Hillman, D.E. (1988). Parameters of dendritic shape and substructure: Intrinsic and extrinsic determinants? In: Intrinsic determinants of neuronal form and function, ed. R.J.L.a.M.M. Black, New York: Alan R., Inc., 83-113.

Hirano, A., Nakano, I., Kurland, L.T., Mulder, D.W., Holley, P.W., and Saccomanno, G. (1984). Fine structural study of neurofibrillary changes in a family with amyotrophic lateral sclerosis. J Neuropathol Exp Neurol *43*, 471-480.

Hirokawa, N. (1991). Molecular architecture and dynamics of the neuronal cytoskeleton. In: The Neuronal Cytoskeleton, ed. R.D. Burgoyne, New York: Wiley-Liss, 5-74.

Hirokawa, N. (1994). Microtubule organization and dynamics dependent on microtubule-associated proteins. Curr. Opin. Cell Biol. *6*, 74-81.

Hirokawa, N. (1998). Kinesin and dynein superfamily proteins and the mechanism of organelle transport. Science *279*, 519-526.

Hirokawa, N., Hisanaga, S., and Shiomura, Y. (1988). MAP2 is a component of crossbridges between microtubules and neurofilaments in the neuronal cytoskeleton: quick-freeze, deep-etch immunoelectron microscopy and reconstitution studies. J Neurosci *8*, 2769-2779.

Hong, K., Nishiyama, M., Henley, J., Tessier-Lavigne, M., and Poo, M. (2000). Calcium signalling in the guidance of nerve growth by netrin-1. Nature *403*, 93-98.

Hoogenraad, C.C., Akhmanova, A., Grosveld, F., De Zeeuw, C.I., and Galjart, N. (2000). Functional analysis of CLIP-115 and its binding to microtubules. J Cell Sci *113 (Pt 12)*, 2285-2297.

Horio, T., and Hotani, H. (1986). Visualization of the dynamic instability of individual microtubules by dark-field microscopy. Nature *321*, 605-607.

Hoshi, M., Akiyama, T., Shinohara, Y., Miyata, Y., Ogawara, H., Nishida, E., and Sakai, H. (1988). Protein-kinase-C-catalyzed phosphorylation of the microtubule-binding domain of microtubule-associated protein 2 inhibits its ability to induce tubulin polymerization. Eur J Biochem *174*, 225-230.

Hoshi, M., Ohta, K., Gotoh, Y., Mori, A., Murofushi, H., Sakai, H., and Nishida, E. (1992). Mitogen-activated-protein-kinase-catalyzed phosphorylation of microtubule-

associated proteins, microtubule-associated protein 2 and microtubule-associated protein 4, induces an alteration in their function. Eur J Biochem *203*, 43-52.

Huang, X., and Hampson, D. (2000). Inhibition of microtubule formation by metabotropic glutamate receptors. J. Neurochem. *74*, 104-113.

Irving, E.A., McCulloch, J., and Dewar, D. (1996). Intracortical perfusion of glutamate in vivo induces alterations of tau and microtubule-associated protein 2 immunoreactivity in the rat. Acta Neuropathol (Berl) *92*, 186-196.

Isokawa, M. (2000). Remodeling dendritic spines of dentate granule cells in temporal lobe epilepsy patients and the rat pilocarpine model. Epilepsia *41 Suppl 6*, S14-17.

Itoh, T.J., Hisanaga, S., Hosoi, T., Kishimoto, T., and Hotani, H. (1997). Phosphorylation states of microtubule-associated protein 2 (MAP2) determine the regulatory role of MAP2 in microtubule dynamics. Biochemistry *36*, 12574-12582.

Jancsik, V., Filliol, D., Felter, S., and Rendon, A. (1989). Binding of microtubule-associated proteins (MAPs) to rat brain mitochondria: a comparative study of the binding of MAP2, its microtubule-binding and projection domains, and tau proteins. Cell Motil Cytoskeleton *14*, 372-381.

Janson, M.E., de Dood, M.E., and Dogterom, M. (2003). Dynamic instability of microtubules is regulated by force. J Cell Biol *161*, 1029-1034.

Johnson, G.V., and Foley, V.G. (1993). Calpain-mediated proteolysis of microtubule-associated protein 2 (MAP- 2) is inhibited by phosphorylation by cAMP-dependent protein kinase, but not by Ca2+/calmodulin-dependent protein kinase II. J Neurosci Res *34*, 642-647.

Johnson, G.V., Jope, R.S., and Binder, L.I. (1989). Proteolysis of tau by calpain. Biochem Biophys Res Commun *163*, 1505-1511.

Jones, L.B., Johnson, N., and Byne, W. (2002). Alterations in MAP2 immunocytochemistry in areas 9 and 32 of schizophrenic prefrontal cortex. Psychiatry Res *114*, 137-148.

Julien, J.P. (2001). Amyotrophic lateral sclerosis. unfolding the toxicity of the misfolded. Cell *104*, 581-591.

Jung, D., Filliol, D., Miehe, M., and Rendon, A. (1993). Interaction of brain mitochondria with microtubules reconstituted from brain tubulin and MAP2 or TAU. Cell Motil Cytoskeleton *24*, 245-255.

Kaech, S., Ludin, B., and Matus, A. (1996). Cytoskeletal plasticity in cells expressing neuronal microtubule-associated proteins. Neuron *17*, 1189-1199.

Kalcheva, M., Weidenheim, K.M., Krees, Y., and Shafit-Zagardo, B. (1997). Expression of microtubule-associated protein-2a and other novel microtubule-associated protein-2 transcripts in human fetal spinal cord. J. Neurochem. *68*, 383-391.

Kalcheva, N., Rockwood, J.M., Kress, Y., Steiner, A., and Shafit-Zagardo, B. (1998). Molecular and functional characteristics of MAP-2a: ability of MAP-2a versus MAP-2b to induce stable microtubules in COS cells. Cell Motil Cytoskeleton *40*, 272-285.

Karakesisoglou, I., Yang, Y., and Fuchs, E. (2000). An epidermal plakin that integrates actin and microtubule networks at cellular junctions. J Cell Biol *149*, 195-208.

Kaytor, M.D., and Orr, H.T. (2002). The GSK3 beta signaling cascade and neurodegenerative disease. Curr Opin Neurobiol *12*, 275-278.

Kempf, M., Clement, A., Faissner, A., Lee, G., and Brandt, R. (1996). Tau binds to the distal axon early in development of polarity in a microtubule- and microfilament-dependent manner. J. Neurosci. *16*, 5583-5592.

Khuchua, Z., Wozniak, D.F., Bardgett, M.E., Yue, Z., McDonald, M., Boero, J., Hartman, R.E., Sims, H., and Strauss, A.W. (2003). Deletion of the N-terminus of murine map2 by gene targeting disrupts hippocampal ca1 neuron architecture and alters contextual memory. Neuroscience *119*, 101-111.

Kiernan, J.A., and Hudson, A.J. (1993). Changes in shapes of surviving motor neurons in amyotrophic lateral sclerosis. Brain *116 (Pt 1)*, 203-215.

Kikuchi, H., Doh-ura, K., Kawashima, T., Kira, J.-I., and Iwaki, T. (1999). Immunohistochemical analysis of spinal cord lesions in amyotrophic lateral sclerosis using microtubule-associated protein 2 (MAP2) antibodies. Acta Neuropathol. *97*, 13-21.

Kim, C.H., and Lisman, J.E. (1999). A role of actin filament in synaptic transmission and long-term potentiation. J Neurosci *19*, 4314-4324.

Kim, H., Binder, L.I., and Rosenbaum, J.L. (1979). The periodic association of MAP2 with brain microtubules in vitro. J Cell Biol *80*, 266-276.

Kindler, S., Schulz, B., Goedert, M., and Garner, C.C. (1990). Molecular structure of Microtubule-associated Protein 2b and 2c from Rat Brain. J Biol Chem *265*, 19679-19684.

Klopfenstein, D.R., Kappeler, F., and Hauri, H.P. (1998). A novel direct interaction of endoplasmic reticulum with microtubules. Embo J *17*, 6168-6177.

Knops, J., Kosik, K.S., Lee, G., Pardee, J.D., Cohen-Gould, L., and McConlogue, L. (1991). Overexpression of Tau in a Nonneuronal Cell Induces Long Cellular Processes. J Cell Biol *114*, 725-733.

Knowles, R., Leclerc, N., and Kosik, K.S. (1994). Organization of actin and microtubules during process formation in tau-expressing Sf9 cells. Cell Motil. Cyto. *28*, 256-264.

Kosik, K., Orecchio, L., Binder, L., Trojanowski, J., Lee, V.-Y., and Lee, G. (1988). Epitopes that span the tau molecule are shared with paired helical filaments. Neuron *1*, 817-825.

Kosik, K.S., and McConlogue, L. (1994). Microtuble-Associated Protein Function: Lessons From Expression in *Spodoptera frugiperda* Cells. Cell Motility and the Cytoskeleton *28*, 195-198.

Kotani, S., Nishida, E., Kumagai, H., and Sakai, H. (1985). Calmodulin inhibits interaction of actin with MAP2 and tau, two major microtubule-associated proteins. J. Biol. Chem. *260*, 1.

Kozireski-Chuback, D., Wu, G., and Ledeen, R.W. (1999). Upregulation of nuclear GM1 accompanies axon-like, but not dendrite-like, outgrowth in NG108-15 cells. J Neurosci Res *55*, 107-118.

Krieger, C., Lanius, R.A., Pelech, S.L., and Shaw, C.A. (1996). Amyotrophic lateral sclerosis: the involvement of intracellular Ca2+ and protein kinase C. Trends Pharmacol Sci *17*, 114-120.

Krucker, T., Siggins, G.R., and Halpain, S. (2000). Dynamic actin filaments are required for stable long-term potentiation (LTP) in area CA1 of the hippocampus. Proc Natl Acad Sci U S A *97*, 6856-6861.

Kwei, S.L., Clement, A., Faissner, A., and Brandt, R. (1998). Differential interactions of MAP2, tau and MAP5 during axogenesis in culture. Neuroreport *9*, 1035-1040.

Langkopf, A., Guilleminot, J., and Nunez, J. (1995). Tau and microtubule-associated protein 2c transfection and neurite outgrowth in ND 7/23 cells. J Neurochem *64*, 1045-1053.

Lanius, R.A., Paddon, H.B., Mezei, M., Wagey, R., Krieger, C., Pelech, S.L., and Shaw, C.A. (1995). A role for amplified protein kinase C activity in the pathogenesis of amyotrophic lateral sclerosis. J Neurochem *65*, 927-930.

Lavoie, C., Lanoix, J., Kan, F.W., and Paiement, J. (1996). Cell-free assembly of rough and smooth endoplasmic reticulum. J Cell Sci *109 (Pt 6)*, 1415-1425.

Leclerc, N., Baas, P.W., Garner, C.C., and Kosik, K.S. (1996). Juvenile and mature MAP2 isoforms induce distinct patterns of process outgrowth. Mol Biol Cell *7*, 443-455.

Leclerc, N., Kosik, K.S., Cowan, N., Pienkowski, T.P., and Baas, P.W. (1993). Process formation in Sf9 cells induced by the expression of a microtubule-associated protein 2C-like construct. Proc. Natl. Acad. Sci. USA *90*, 6223-6227.

Lee, G., Newman, S., Gard, D., Band, H., and Panchamoorthy, G. (1998). Tau interacts with src-family non-receptor tyrosine kinases. J.Cell Sci. *111*, 3167-3177.

Lee, S., and Kolodziej, P.A. (2002). The plakin Short Stop and the RhoA GTPase are required for E-cadherin-dependent apical surface remodeling during tracheal tube fusion. Development *129*, 1509-1520.

Leissring, M.A., Akbari, Y., Fanger, C.M., Cahalan, M.D., Mattson, M.P., and LaFerla, F.M. (2000). Capacitative calcium entry deficits and elevated luminal calcium content in mutant presenilin-1 knockin mice. J Cell Biol *149*, 793-798.

Leterrier, J.F., Liem, R.K., and Shelanski, M.L. (1982). Interactions between neurofilaments and microtubule-associated proteins: a possible mechanism for intraorganellar bridging. J Cell Biol *95*, 982-986.

Letourneau, P.C. (1982). Analysis of microtubule number and length in cytoskeletons of cultured chick sensory neurons. J Neurosci *2*, 806-814.

Leung, C.L., Liem, R.K., Parry, D.A., and Green, K.J. (2001). The plakin family. J Cell Sci *114*, 3409-3410.

Leung, C.L., Sun, D., and Liem, R.K. (1999a). The intermediate filament protein peripherin is the specific interaction partner of mouse BPAG1-n (dystonin) in neurons. J Cell Biol *144*, 435-446.

Leung, C.L., Sun, D., Zheng, M., Knowles, D.R., and Liem, R.K. (1999b). Microtubule actin cross-linking factor (MACF): a hybrid of dystonin and dystrophin that can interact with the actin and microtubule cytoskeletons. J Cell Biol *147*, 1275-1286.

Lewis, S.A., Ivanov, I.E., Lee, G.-H., and Cowan, N.J. (1989). Organization of microtubules in dendrites and axons is determined by a short hydrophobic zipper in microtubule-associated proteins MAP2 and tau. Nature *342*, 498-505.

Lewis, S.A., Wang, D.H., and Cowan, N.J. (1988). Microtubule-associated protein MAP2 shares a microtubule binding motif with tau protein. Science *242*, 936-939.

Li, M., Ona, V.O., Guegan, C., Chen, M., Jackson-Lewis, V., Andrews, L.J., Olszewski, A.J., Stieg, P.E., Lee, J.P., Przedborski, S., and Friedlander, R.M. (2000). Functional role of caspase-1 and caspase-3 in an ALS transgenic mouse model. Science *288*, 335-339.

Lim, R.W., and Halpain, S. (2000). Regulated association of microtubule-associated protein 2 (MAP2) with Src and Grb2: evidence for MAP2 as a scaffolding protein. J Biol Chem *275*, 20578-20587.

Lin, P.T., Gleeson, J.G., Corbo, J.C., Flanagan, L., and Walsh, C.A. (2000). DCAMKL1 encodes a protein kinase with homology to doublecortin that regulates microtubule polymerization. J Neurosci *20*, 9152-9161.

Linden, M., Nelson, B.D., and Leterrier, J.F. (1989a). The specific binding of the microtubule-associated protein 2 (MAP2) to the outer membrane of rat brain mitochondria. Biochem J *261*, 167-173.

Linden, M., Nelson, B.D., Loncar, D., and Leterrier, J.F. (1989b). Studies on the interaction between mitochondria and the cytoskeleton. J Bioenerg Biomembr *21*, 507-518.

Litersky, J.M., and Johnson, G.V. (1995). Phosphorylation of tau in situ: inhibition of calcium-dependent proteolysis. J Neurochem *65*, 903-911.

Ludin, B., Ashbridge, K., Funfschilling, U., and Matus, A. (1996). Functional analysis of the MAP2 repeat domain. J. Cell Sci. *109*, 91-99.

Ludin, B., and Matus, A. (1993). The neuronal cytoskeleton and its role in axonal and dendritic plasticity. Hippocampus *3*, 61-72.

Maas, T., Eidenmuller, J., and Brandt, R. (2000). Interaction of tau with the neural membrane cortex is regulated by phosphorylation at sites that are modified in paired helical filaments. J Biol Chem *275*, 15733-15740.

Mahoney, M.G., Aho, S., Uitto, J., and Stanley, J.R. (1998). The members of the plakin family of proteins recognized by paraneoplastic pemphigus antibodies include periplakin. J Invest Dermatol *111*, 308-313.

Maletic-Savatic, M., Malinow, R., and Svoboda, K. (1999). Rapid dendritic morphogenesis in CA1 hippocampal dendrites induced by synaptic activity. Science *283*, 1923-1927.

Malinow, R., Mainen, Z.F., and Hayashi, Y. (2000). LTP mechanisms: from silence to four-lane traffic. Curr Opin Neurobiol *10*, 352-357.

Mandelkow, E., and Mandelkow, E.M. (1995). Microtubules and microtubule-associated proteins. Curr Opin Cell Biol *7*, 72-81.

Mandell, J., and Banker, G. (1996). Microtubule-associated proteins, phosphorylation gradients, and establishment of neuronal polarity. Perspec. Dev. neurobiol. *4*, 125-135.

Matus, A. (1994). Stiff microtubules and neuronal morphology. Trends Neurosci. *17*, 19-22.

McNally, F.J., and Vale, R.D. (1993). Identification of katanin, an ATPase that severs and disassembles stable microtubules. Cell *75*, 419-429.

Meichsner, M., Doll, T., Reddy, D., Weisshaar, B., and Matus, A. (1993). The low molecular weight form of microtubule-associated protein 2 is transported into both axons and dendrites. Neuroscience *54*, 873-880.

Micheva, K.D., Vallee, A., Beaulieu, C., Herman, I.M., and Leclerc, N. (1998). beta-Actin is confined to structures having high capacity of remodelling in developing and adult rat cerebellum. Eur J Neurosci *10*, 3785-3798.

Minger, S.L., Geddes, J.W., Holtz, M.L., Craddock, S.D., Whiteheart, S.W., Siman, R.G., and Pettigrew, L.C. (1998). Glutamate receptor antagonists inhibit calpain-mediated cytoskeletal proteolysis in focal cerebral ischemia. Brain Res *810*, 181-199.

Mitchison, T., and Kirschner, M. (1984). Dynamic instability of microtubule growth. Nature *312*, 237-242.

Mitchison, T., and Kirschner, M. (1988). Cytoskeletal dynamics and nerve growth. Neuron *1*, 761-777.

Mukhopadhyay, R., and Hoh, J.H. (2001). AFM force measurements on microtubule-associated proteins: the projection domain exerts a long-range repulsive force. FEBS Lett *505*, 374-378.

Murphy, D.B., and Borisy, G.G. (1975). Association of high-molecular-weight proteins with microtubules and their role in microtubule assembly in vitro. Proc Natl Acad Sci U S A *72*, 2696-2700.

Myers, M.W., Lazzarini, R.A., Lee, V.M., Schlaepfer, W.W., and Nelson, D.L. (1987). The human mid-size neurofilament subunit: a repeated protein sequence and the relationship of its gene to the intermediate filament gene family. Embo J *6*, 1617-1626.

Neve, R.L., Harris, P., Kosik, K.S., Kurnit, D.M., and Donlon, T.A. (1986). Identification of cDNA clones for the human microtubule-associated protein tau and chromosomal localization of the genes for tau and microtubule-associated protein 2. Mol. Brain Res. *1*, 271-280.

Nguyen, M.D., Lariviere, R.C., and Julien, J.P. (2000). Reduction of axonal caliber does not alleviate motor neuron disease caused by mutant superoxide dismutase 1. Proc Natl Acad Sci U S A *97*, 12306-12311.

Nguyen, M.D., Lariviere, R.C., and Julien, J.P. (2001). Deregulation of Cdk5 in a mouse model of ALS: toxicity alleviated by perikaryal neurofilament inclusions. Neuron *30*, 135-147.

Olivry, T., Alhaidari, Z., and Ghohestani, R.F. (2000). Anti-plakin and desmoglein autoantibodies in a dog with pemphigus vulgaris. Vet Pathol *37*, 496-499.

Olmsted, J.B., Stemple, D.L., Saxton, W.M., Neighbors, B.W., and McIntosh, J.R. (1989). Cell cycle-dependent changes in the dynamics of MAP 2 and MAP 4 in cultured cells. J Cell Biol *109*, 211-223.

Ozer, R.S., and Halpain, S. (2000). Phosphorylation-dependent localization of microtubule-associated protein MAP2c to the actin cytoskeleton [In Process Citation]. Mol Biol Cell *11*, 3573-3587.

Paiement, J. (1981). Interactions of microtubule proteins with outer nuclear membranes in vitro. Journal of Cell Biology *91*, 329a.

Paiement, J., and Bergeron, J. (2001). The shape of things to come: regulation of shape changes in endoplasmic reticulum. Biochem Cell Biol *79*, 587-592.

Papandrikopoulou, A., Doll, T., Tucker, R.P., Garner, C.C., and Matus, A. (1989). Embryonic MAP2 lacks the cross-linking sidearm sequences and dendritic targeting signal of adult MAP2. Nature *340*, 650-652.

Patrick, G.N., Zukerberg, L., Nikolic, M., de la Monte, S., Dikkes, P., and Tsai, L.H. (1999). Conversion of p35 to p25 deregulates Cdk5 activity and promotes neurodegeneration. Nature *402*, 615-622.

Patterson, C.L., Jr., and Flavin, M. (1986). A brain phosphatase with specificity for microtubule-associated protein-2. J Biol Chem *261*, 7791-7796.

Patzke, H., and Tsai, L.H. (2002). Cdk5 sinks into ALS. Trends Neurosci *25*, 8-10.

Pei, J.J., Sersen, E., Iqbal, K., and Grundke-Iqbal, I. (1994). Expression of protein phosphatases (PP-1, PP-2A, PP-2B and PTP-1B) and protein kinases (MAP kinase and P34cdc2) in the hippocampus of patients with Alzheimer disease and normal aged individuals. Brain Res *655*, 70-76.

Perez, Y., Morin, F., Beaulieu, C., and Lacaille, J.C. (1996). Axonal sprouting of CA1 pyramidal cells in hyperexcitable hippocampal slices of kainate-treated rats. Eur J Neurosci *8*, 736-748.

Peters, A., Palay, S.L., and Webster, H.D. (1991). The fine structure of the nervous system. Oxford University Press, Inc.

Philpot, B.D., Lim, J.H., Halpain, S., and Brunjes, P.C. (1997). Experience-dependent modifications in MAP2 phosphorylation in rat olfactory bulb. J Neurosci *17*, 9596-9604.

Pickering, D., Thomsen, C., Suzdak, P., Fletcher, E., Robitaille, R., Salter, M., MacDonald, J., Huang, X.-P., and Hampson, D. (1993). A comparison of two alternatively spliced forms of a metabotropic glutamate receptor coupled to phosphoinositide turnover. J. Neurochem. *61*, 85-92.

Pierre, P., Scheel, J., Rickard, J.E., and Kreis, T.E. (1992). CLIP-170 links endocytic vesicles to microtubules. Cell *70*, 887-900.

Pollard, H., Khrestchatisky, M., Moreau, J., Ben-Ari, Y., and Represa, A. (1994). Correlation between reactive sprouting and microtubule protein expression in epileptic hippocampus. Neuroscience *61*, 773-787.

Posmantur, R.M., Kampfl, A., Taft, W.C., Bhattacharjee, M., Dixon, C.E., Bao, J., and Hayes, R.L. (1996). Diminished microtubule-associated protein 2 (MAP2) immunoreactivity following cortical impact brain injury. J Neurotrauma *13*, 125-137.

Pramatarova, A., Laganiere, J., Roussel, J., Brisebois, K., and Rouleau, G.A. (2001). Neuron-specific expression of mutant superoxide dismutase 1 in transgenic mice does not lead to motor impairment. J Neurosci *21*, 3369-3374.

Puius, Y.A., Mahoney, N.M., and Almo, S.C. (1998). The modular structure of actin-regulatory proteins. Curr Opin Cell Biol *10*, 23-34.

Quinlan, E.M., and Halpain, S. (1996a). Emergence of activity-dependent, bidirectional control of microtubule- associated protein MAP2 phosphorylation during postnatal development. J Neurosci *16*, 7627-7637.

Quinlan, E.M., and Halpain, S. (1996b). Postsynaptic mechanisms for bidirectional control of MAP2 phosphorylation by glutamate receptors. Neuron *16*, 357-368.

Ray, P., Strott, C.A., and Nath, J. (1979). Purification of bovine adrenocortical and brain tubulin. A comparative study. Biochim Biophys Acta *581*, 79-86.

Reezek, D., and Bretscher, A. (1998). The carboxyl-terminal region of EBP50 binds to a site in the amino-terminal domain of ezrin that is masked in the dormant molecule. J. Biol. Chem. *273*, 18452-18458.

Represa, A., Jorquera, I., Le Gal La Salle, G., and Ben-Ari, Y. (1993). Epilepsy induced collateral sprouting of hippocampal mossy fibers: does it induce the development of ectopic synapses with granule cell dendrites? Hippocampus *3*, 257-268.

Riederer, B., and Matus, A. (1985). Differential expression of distinct microtubule-associated proteins during brain development. Proc Natl Acad Sci U S A *82*, 6006-6009.

Riederer, B.M. (1992). Differential phosphorylation of some proteins of the neuronal cytoskeleton during brain development. Histochem J *24*, 783-790.

Riederer, B.M., Draberova, E., Viklicky, V., and Draber, P. (1995). Changes of MAP2 phosphorylation during brain development. J Histochem Cytochem *43*, 1269-1284.

Rizzuto, R. (2001). Intracellular Ca(2+) pools in neuronal signalling. Curr Opin Neurobiol *11*, 306-311.

Rosen, D.R. (1993). Mutations in Cu/Zn superoxide dismutase gene are associated with familial amyotrophic lateral sclerosis. Nature *364*, 362.

Rothstein, J.D., Van Kammen, M., Levey, A.I., Martin, L.J., and Kuncl, R.W. (1995). Selective loss of glial glutamate transporter GLT-1 in amyotrophic lateral sclerosis. Ann Neurol *38*, 73-84.

Rouleau, G.A., Clark, A.W., Rooke, K., Pramatarova, A., Krizus, A., Suchowersky, O., Julien, J.P., and Figlewicz, D. (1996). SOD1 mutation is associated with accumulation of neurofilaments in amyotrophic lateral sclerosis. Ann Neurol *39*, 128-131.

Rubino, H.M., Dammerman, M., Shafit-Zagardo, B., and Erlichman, J. (1989). Localization and characterization of the binding site for the regulatory subunit of type II cAMP-dependent protein kinase on MAP2. Neuron *3*, 631-638.

Ruhrberg, C., Hajibagheri, M.A., Parry, D.A., and Watt, F.M. (1997). Periplakin, a novel component of cornified envelopes and desmosomes that belongs to the plakin family and forms complexes with envoplakin. J Cell Biol *139*, 1835-1849.

Saito, K., Elce, J.S., Hamos, J.E., and Nixon, R.A. (1993). Widespread activation of calcium-activated neutral proteinase (calpain) in the brain in Alzheimer disease: a potential molecular basis for neuronal degeneration. Proc Natl Acad Sci U S A *90*, 2628-2632.

Sanchez, C., Arellano, J.I., Rodriguez-Sanchez, P., Avila, J., DeFelipe, J., and Diez-Guerra, F.J. (2001). Microtubule-associated protein 2 phosphorylation is decreased in the human epileptic temporal lobe cortex. Neuroscience *107*, 25-33.

Sanchez, C., Diaz-Nido, J., and Avila, J. (2000a). Phosphorylation of microtubule-associated protein 2 (MAP2) and its relevance for the regulation of the neuronal cytoskeleton function. Prog Neurobiol *61*, 133-168.

Sanchez, C., Perez, M., and Avila, J. (2000b). GSK3beta-mediated phosphorylation of the microtubule-associated protein 2c (MAP2c) prevents microtubule bundling. Eur. J. Cell Biol. *79*, 252-260.

Sanchez, C., Tompa, P., Szücs, K., Friedrich, P., and Avila, J. (1996). Phosphorylation and dephosphorylation in the proline-rich C-terminal domain of microtubule-associated protein-2. Euro. J. Biochem. *241*, 765-771.

Sattilaro, R.F. (1986). Interaction of microtubule-associated protein 2 with actin filaments. Biochemistry *25*, 2003-2009.

Sattilaro, R.F., Dentler, W.L., and LeCluyse, E.L. (1981). Microtubule-associated proteins (MAPs) and the organization of actin filaments in vitro. J Cell Biol *90*, 467-473.

Sattler, R., and Tymianski, M. (2000). Molecular mechanisms of calcium-dependent excitotoxicity. J Mol Med *78*, 3-13.

Selden, S.C., and Pollard, T.D. (1983). Phosphorylation of microtubule-associated proteins regulates their interaction with actin filaments. J. Biol. Chem. *258*, 7064-7071.

Selden, S.C., and Pollard, T.D. (1986). Interaction of actin filaments with microtubules is mediated by microtubule-associated proteins and regulated by phosphorylation. Ann N Y Acad Sci *466*, 803-812.

Shafit-Zagardo, B., and Kalcheva, N. (1998). Making sense of the multiple MAP-2 transcripts and their role in the neuron. Mol Neurobiol *16*, 149-162.

Sharma, N., Kress, Y., and Shafit-Zagardo, B. (1994). Antisense MAP-2 oligonucleotides induce changes in microtubule assembly and neuritic elongation in pre-existing neurites of rat cortical neurons. Cell Motil Cytoskeleton *27*, 234-247.

Shaw, G. (1991). Neurofilament proteins. Wiley-Liss Inc.

Sloboda, R.D., Rudolph, S.A., Rosenbaum, J.L., and Greengard, P. (1975). Cyclic AMP-dependent endogenous phosphorylation of a microtubule-associated protein. Proc Natl Acad Sci U S A *72*, 177-181.

Surridge, C., and Burns, R. (1994). The difference in the binding of phosphatidylinositol distinguishes MAP2 from MAP2C and Tau. Biochemistry *33*, 8051-8057.

Takechi, H., Eilers, J., and Konnerth, A. (1998). A new class of synaptic response involving calcium release in dendritic spines. Nature *396*, 757-760.

Takemura, R., Okabe, S., Umeyama, T., and Hirokawa, N. (1995). Polarity orientation and assembly process of microtubule bundles in nocodazole-treated, MAP2c-transfected COS cells. Mol Biol Cell *6*, 981-996.

Takemura, R., Okabe, S., Umeyama, T., Kanai, Y., Cowan, N., and Hirokawa, N. (1992). Increased microtubule stability and alpha tubulin acetylation in cells transfected with microtubule-associated proteins MAP1B, MAP2 or tau. J. Cell Sci. *103*, 953-964.

Tanaka, E., Ho, T., and Kirschner, M.W. (1995). The role of microtubule dynamics in growth cone motility and axonal growth. Journal of Cell Biology *128*, 139-155.

Tanaka, E., and Sabry, J. (1995). Making the connection: Cytoskeletal rearrangements during growth cone guidance. Cell *83*, 171-176.

Taylor, K.R., Holzer, A.K., Bazan, J.F., Walsh, C.A., and Gleeson, J.G. (2000). Patient mutations in doublecortin define a repeated tubulin-binding domain. J Biol Chem *275*, 34442-34450.

Teng, J., Takei, Y., Harada, A., Nakata, T., Chen, J., and Hirokawa, N. (2001). Synergistic effects of MAP2 and MAP1B knockout in neuronal migration, dendritic outgrowth, and microtubule organization. J Cell Biol *155*, 65-76.

Terasaki, M. (1990). Recent progress on structural interactions of the endoplasmic reticulum. Cell Motil Cytoskeleton *15*, 71-75.

Terasaki, M., Chen, L.B., and Fujiwara, K. (1986). Microtubules and the endoplasmic reticulum are highly interdependent structures. J Cell Biol *103*, 1557-1568.

Terasaki, M., and Reese, T.S. (1994). Interactions among endoplasmic reticulum, microtubules, and retrograde movements of the cell surface. Cell Motil Cytoskeleton *29*, 291-300.

Tobisawa, S., Hozumi, Y., Arawaka, S., Koyama, S., Wada, M., Nagai, M., Aoki, M., Itoyama, Y., Goto, K., and Kato, T. (2003). Mutant SOD1 linked to familial amyotrophic lateral sclerosis, but not wild-type SOD1, induces ER stress in COS7 cells and transgenic mice. Biochem Biophys Res Commun *303*, 496-503.

Toni, N., Buchs, P.A., Nikonenko, I., Bron, C.R., and Muller, D. (1999). LTP promotes formation of multiple spine synapses between a single axon terminal and a dendrite. Nature *402*, 421-425.

Travis, J.L., Allen, R.D., and Sloboda, R.D. (1980). Preparation and characterization of native, fluorescently labelled brain tubulin and microtubule-associated proteins (MAPs). Exp Cell Res *125*, 421-429.

Trieu, V.N., Liu, R., Liu, X.P., and Uckun, F.M. (2000). A specific inhibitor of janus kinase-3 increases survival in a transgenic mouse model of amyotrophic lateral sclerosis. Biochem Biophys Res Commun *267*, 22-25.

Trotti, D., Rolfs, A., Danbolt, N.C., Brown, R.H., Jr., and Hediger, M.A. (1999). SOD1 mutants linked to amyotrophic lateral sclerosis selectively inactivate a glial glutamate transporter. Nat Neurosci *2*, 427-433.

Tsuyama, S., Terayama, Y., and Matsuyama, S. (1987). Numerous phosphates of microtubule-associated protein 2 in living rat brain. J. Biol. Chem. *262*, 10886-10892.

Tucker, R. (1990). The role of microtubule-associated proteins in brain morphogenesis: a review. Brain Res. Rev. *15*, 101-120.

Tucker, R., and Matus, A. (1988). Microtubule-associated proteins characteristic of embryonic brain are found in the adult mammalian retina. Dev. Biol. *130*, 423-434.

Tucker, R.P., Binder, L.I., Viereck, C., Hemmings, B.A., and Matus, A. (1988). The Sequential Appearance of Low- and High-Molecular-Weight Forms of MAP2 in the Developing Cerebellum. The Journal of Neuroscience *8*, 4503-4512.

Umeyama, T., Okabe, S., Kanai, Y., and Hirokawa, N. (1993). Dynamics of microtubules bundled by microtubule-associaed protein 2C (MAP2C). J. Cell Biol. *120*, 451-465.

Vallee, R.B., and Collins, C.A. (1986). Purification of microtubules and microtubule-associated proteins from sea urchin eggs and cultured mammalian cells using taxol, and use of exogenous taxol-stabilized brain microtubules for purifying microtubule-associated proteins. Methods Enzymol *134*, 116-127.

van den Heuvel, A.P., de Vries-Smits, A.M., van Weeren, P.C., Dijkers, P.F., de Bruyn, K.M., Riedl, J.A., and Burgering, B.M. (2002). Binding of protein kinase B to the plakin family member periplakin. J Cell Sci *115*, 3957-3966.

Viereck, C., Tucker, R.P., and Matus, A. (1989). The adult rat olfactory system expresses microtubule-associated proteins found in the developing brain. J Neurosci *9*, 3547-3557.

Voter, W.A., and Erickson, H.P. (1982). Electron microscopy of MAP 2 (microtubule-associated protein 2). J Ultrastruct Res *80*, 374-382.

Wada, Y., Ishiguro, K., Itoh, T.J., Uchida, T., Hotani, H., Saito, T., Kishimoto, T., and Hisanaga, S. (1998). Microtubule-stimulated phosphorylation of tau at Ser202 and Thr205 by cdk5 decreases its microtubule nucleation activity. J Biochem (Tokyo) *124*, 738-746.

Wagey, R., Pelech, S.L., Duronio, V., and Krieger, C. (1998). Phosphatidylinositol 3-kinase: increased activity and protein level in amyotrophic lateral sclerosis. J Neurochem *71*, 716-722.

Walaas, S.I., and Nairn, A.C. (1989). Multisite phosphorylation of microtubule-associated protein 2 (MAP-2) in rat brain: peptide mapping distinguishes between cyclic AMP-, calcium/calmodulin-, and calcium/phospholipid-regulated phosphorylation mechanisms. J Mol Neurosci *1*, 117-127.

Walenta, J.H., Didier, A.J., Liu, X., and Kramer, H. (2001). The Golgi-associated hook3 protein is a member of a novel family of microtubule-binding proteins. J Cell Biol *152*, 923-934.

Wang, J.Z., Grundke-Iqbal, I., and Iqbal, K. (1996a). Glycolysation of microtubule-associated protein tau: an abnormal posttranslational modification in Alzheimer's disease. Nature Med. *2*, 871-875.

Wang, L.J., Colella, R., and Roisen, F.J. (1998). Ganglioside GM1 alters neuronal morphology by modulating the association of MAP2 with microtubules and actin filaments. Brain Res Dev Brain Res *105*, 227-239.

Wang, L.J., Colella, R., Yorke, G., and Roisen, F.J. (1996b). The ganglioside GM1 enhances microtubule networks and changes the morphology of Neuro-2a cells in vitro by altering the distribution of MAP2. Exp Neurol *139*, 1-11.

Wang, Y., Mattson, M.P., and Furukawa, K. (2002). Endoplasmic reticulum calcium release is modulated by actin polymerization. J Neurochem *82*, 945-952.

Waterman-Storer, C.M., and Salmon, E. (1999). Positive feedback interactions between microtubule and actin dynamics during cell motility. Curr Opin Cell Biol *11*, 61-67.

Waterman-Storer, C.M., and Salmon, E.D. (1998). Endoplasmic reticulum membrane tubules are distributed by microtubules in living cells using three distinct mechanisms. Curr Biol *8*, 798-806.

Weisshaar, B., Doll, T., and Matus, A. (1992). Reorganisation of the microtubular cytoskeleton by embryonic microtubule-associated protein 2 (MAP2c). Development *116*, 1151-1161.

West, R., Tenbarge, K., and Olmstead, J. (1991). A model for microtubule-associated protein 4 structure. Domains defined by comparisons of human, mouse and bovine sequences. J. Biol. Chem. *266*, 21886-21896.

Wiche, G. (1989). High-Mr microtubule-associated proteins: properties and functions. Biochem J *259*, 1-12.

Wiedau-Pazos, M., Goto, J.J., Rabizadeh, S., Gralla, E.B., Roe, J.A., Lee, M.K., Valentine, J.S., and Bredesen, D.E. (1996). Altered reactivity of superoxide dismutase in familial amyotrophic lateral sclerosis. Science *271*, 515-518.

Wille, H., Drewes, G., Biernat, J., Mandelkow, E.-M., and Mandelkow, E. (1992a). Alzheimer-like paired helical filaments ad anti-parallel dimers formed from microtubule-associated protein tau in vitro. J. Cell Biol. *118*, 573-584.

Wille, H., Mandelkow, E.-M., Dingus, J., Vallee, R.B., Binder, L.I., and Mandelkow, E. (1992b). Domain Structure and Antiparallel Dimers of Microtubule-Associated Protein 2 (MAP2). Journal of Structural Biology *108*, 49-61.

Wille, H., Mandelkow, E.M., and Mandelkow, E. (1992c). The juvenile microtubule-associated protein MAP2c is a rod-like molecule that forms antiparallel dimers. J Biol Chem *267*, 10737-10742.

Williamson, T.L., and Cleveland, D.W. (1999). Slowing of axonal transport is a very early event in the toxicity of ALS-linked SOD1 mutants to motor neurons. Nat Neurosci *2*, 50-56.

Wong, N.K., He, B.P., and Strong, M.J. (2000). Characterization of neuronal intermediate filament protein expression in cervical spinal motor neurons in sporadic amyotrophic lateral sclerosis (ALS). J Neuropathol Exp Neurol *59*, 972-982.

Wong, P., Pardo, C., Borchelt, D., Lee, M., Copeland, N., Jenkins, N., Sisodia, S., Cleveland, D., and Price, D. (1995). An adverse property of a familial ALS-linked SOD1 mutation causes motor neuron disease characterized by vacuolar degeneration of mitochondria. Neuron *14*, 1105-1116.

Woody, R.W., Clark, D.C., Roberts, G.C., Martin, S.R., and Bayley, P.M. (1983). Molecular flexibility in microtubule proteins: proton nuclear magnetic resonance characterization. Biochemistry *22*, 2186-2192.

Woolf, N.J., Zinnerman, M.D., and Johnson, G.V. (1999). Hippocampal microtubule-associated protein-2 alterations with contextual memory. Brain Res *821*, 241-249.

Yamamoto, H., Fukunaga, K., Goto, S., Tanaka, E., and Miyamoto, E. (1985). Ca2+, calmodulin-dependent regulation of microtubule formation via phosphorylation of microtubule-associated protein 2, tau factor, and tubulin, and comparison with the cyclic AMP-dependent phosphorylation. J Neurochem *44*, 759-768.

Yamamoto, H., Fukunaga, K., Tanaka, E., and Miyamoto, E. (1983). Ca2+- and calmodulin-dependent phosphorylation of microtubule- associated protein 2 and tau factor, and inhibition of microtubule assembly. J Neurochem *41*, 1119-1125.

Yamauchi, P., and Purich, D. (1987). Modulation of microtubule assembly and stability by phosphatidylinostol action on microtubule-associated protein-2. J. Biol. Chem. *262*, 3369-3375.

Yamauchi, P.S., and Purich, D.L. (1993). Microtubule-associated protein interactions with actin filaments: evidence for differential behavior of neuronal MAP-2 and tau in the presence of phosphatidyl-inositol. Biochem Biophys Res Commun *190*, 710-715.

Yamauchi, T., and Fujisawa, H. (1982). Phosphorylation of microtubule-associated protein 2 by calmodulin-dependent protein kinase (Kinase II) which occurs only in the brain tissues. Biochem Biophys Res Commun *109*, 975-981.

Yamauchi, T., and Fujisawa, H. (1988). Regulation of the interaction of actin filaments with microtubule-associated protein 2 by calmodulin-dependent protein kinase II. Biochim. Biophys. Acta *968*, 77-85.

Yang, Y., Bauer, C., Strasser, G., Wollman, R., Julien, J.-P., and Fuchs, E. (1999). Integrators of the cytoskeleton that stabilize microtubules. Cell *98*, 229-238.

Yoo, A.S., Cheng, I., Chung, S., Grenfell, T.Z., Lee, H., Pack-Chung, E., Handler, M., Shen, J., Xia, W., Tesco, G., Saunders, A.J., Ding, K., Frosch, M.P., Tanzi, R.E., and Kim, T.W. (2000). Presenilin-mediated modulation of capacitative calcium entry. Neuron *27*, 561-572.

Zhu, Q., Lindenbaum, M., Levavasseur, F., Jacomy, H., and Julien, J.P. (1998). Disruption of the NF-H gene increases axonal microtubule content and velocity of neurofilament transport: relief of axonopathy resulting from the toxin beta,beta'-iminodipropionitrile. J Cell Biol *143*, 183-193.

Zorumski, C.F., and Izumi, Y. (1998). Modulation of LTP induction by NMDA receptor activation and nitric oxide release. Prog Brain Res *118*, 173-182.

ANNEXE I

QUATRIÈME ARTICLE

"article de revue en préparation"

The microtubule-associated protein MAP2: New functions to an old protein?

Carole Abi Farah and Nicole Leclerc

Département de pathologie et biologie cellulaire, Université de Montréal, C.P.6128, Succ. Centre-ville, Montréal, Québec, Canada, H3C 3J7

Corresponding author:
Dr. Nicole Leclerc
Département de pathologie et biologie cellulaire
Université de Montréal
C.P.6128, Succ. Centre-ville
Montréal, Québec
Canada H3C 3J7
Phone: (514)-343-5657
Fax: (514)-343-5755
[redacted]

INTRODUCTION

Neurons are the functional signalling units of the nervous system. The morphology of these highly complex polarized cells defines their function. Morphological remodelling occurs during neuronal differentiation and during adaptative events in adult brain. Neuronal differentiation follows specific steps in vitro (Dotti *et al.*, 1988). At the first step, the neuron develops a lamellipodia that consolidates to form cytoplasmic processes called minor neurites. Then, one of these neurites elongates faster than the others and becomes the axon. The remaining minor neurites differentiate into dendrites. Finally, the formation of synaptic contacts takes place (Dotti *et al.*, 1988). Neuronal circuitry is rather stable in adult brain. However, dendritic remodelling has been observed during learning and memory formation in adult hippocampus (Engert and Bonhoeffer, 1999; Maletic-Savatic *et al.*, 1999; Toni *et al.*, 1999). Furthermore, plastic changes were observed in adult brain under certain pathological conditions (Represa *et al.*, 1993; Isokawa, 2000).

The cytoskeleton is the major intrinsic structure defining the shape of neurons (Letourneau, 1982). The neuronal cytoskeleton is composed of three fibrous structures: microtubules, neurofilaments and actin microfilaments (Hirokawa, 1991). Microtubules are tubular polymers of 24nm diameter composed of 13 protofilaments, each of which is formed by heterodimers of α- and β-tubulin (Hirokawa, 1991). They have a fast growing end, called the plus end and a slow growing end called the minus end. Microtubules are highly dynamic structures that can undergo rapid transitions between growth and shrinkage states during cell division. Microtubules play an important role in a variety of

cellular functions such as cell division and intracellular transport. Most importantly, microtubules and their associated proteins play a crucial role in the formation of neuronal processes and thus, in the establishment of neuronal polarity during differentiation. They are also important for the maintenance of neuronal structure and function in adult brain (Mitchison and Kirschner, 1988; Allan *et al.*, 1991; Tanaka and Sabry, 1995; Waterman-Storer and Salmon, 1999).

The neuronal intermediate filaments or neurofilaments (NF) are composed of three protein subunits, NF-L (60 kDa), NF-M (100 kDa) and NF-H (115 kDa) that co-polymerize to form filaments of 10nm diameter (Shaw, 1991). Two other intermediate filament proteins may be present in neurons: α-internexin and peripherin. Neurofilaments seem to be important for the maintenance of axonal caliber (for a recent review, see Al-Chalabi and Miller (2003)). Furthermore, highly dynamic neurofilaments in the axonal growth cone may participate in regional cytoskeletal remodelling during axonal elongation (Chan *et al.*, 2003).

Actin microfilaments (F-actin) are polarized polymers of about 8nm diameter composed of monomers of globular actin (G-actin) together with a large number of different actin-binding proteins (ABPs). ABPs are thought to mediate microfilament structure and function (dos Remedios *et al.*, 2003). Actin is involved in a variety of cellular functions, ranging from cell division to growth cone motility during the establishment of neuronal polarity (Tanaka *et al.*, 1995; Waterman-Storer and Salmon, 1999).

The basis of neuronal polarity lies in the two distinct neuronal compartments: the dendrites and the axon. First, these compartments have different functions: dendrites receive electrical information and relay it to the cell body whereas the axon propagates the signal away from the cell body. Second, these two compartments can be distinguished by their morphology: the dendrites are multiple, relatively short (extending less than 500μm from the cell body) and have a tapering diameter whereas the axon is unique, uniform in diameter along most of its length and can extend many centimetres from the cell body (Bartlett and Banker, 1984b, a; Dotti *et al.*, 1988; Hillman, 1988). Third, dendrites and axon differ in their content with membranous organelles: the rough endoplasmic reticulum (RER) is found in the somato-dendritic compartment but not in the axon and the number of free ribosomes is a lot higher in dendrites than in the axon (Bartlett and Banker, 1984b, a; Peters *et al.*, 1991). Fourth, at the cytoskeletal level, the number of microtubules is higher in dendrites than in the axon whereas the opposite is noted for neurofilaments (Bartlett and Banker, 1984b, a; Hirokawa, 1991). Furthermore, the dendritic microtubules are of mixed polarity with the plus end pointing away and toward the cell body whereas the axonal microtubules are of uniform polarity with the plus end pointing away from the cell body (Baas *et al.*, 1988; Burton, 1988). Most importantly, the dendritic and the axonal microtubules differ in their content with structural microtubule-associated proteins (MAPs), MAP2 being found in the dendritic compartment and tau in the axonal one (Caceres *et al.*, 1984; Hirokawa, 1991; Ludin and Matus, 1993). These structural MAPs are known for their ability to promote the assembly of microtubules and to stabilize them in the cytoplasm (Tucker, 1990;

Hirokawa, 1994; Mandelkow and Mandelkow, 1995; Sanchez *et al.*, 2000a). However, the presence of distinct classes of MAPs in dendrites and axon suggests that the stabilization of microtubules is not the sole function of these proteins.

In the present review, we will focus on the family of heat-stable dendritic MAPs: MAP2. This protein is one of the most abundant cytoskeletal proteins in the dendrites of the adult mammalian central nervous system (Wiche, 1989). MAP2 has been shown to be crucial for neuronal differentiation since no neurite outgrowth is observed when the expression of MAP2 is inhibited in primary neuronal cultures using antisense oligonucleotide treatment (Dinsmore and Solomon, 1991; Caceres *et al.*, 1992; Sharma *et al.*, 1994). Furthermore, our work and that of others have shown that the overexpression of MAP2 in non-neuronal cells induces the formation of cytoplasmic processes similar to neurites (Edson *et al.*, 1993; Leclerc *et al.*, 1993; Langkopf *et al.*, 1995; Leclerc *et al.*, 1996; Kalcheva *et al.*, 1998; Boucher *et al.*, 1999; Belanger *et al.*, 2002). Moreover, MAP2 was suggested to be important for the maintenance of neuronal morphology in adult brain since its suppression or degradation was correlated with dendritic loss or remodelling (Sharma *et al.*, 1994; Faddis *et al.*, 1997; Sanchez *et al.*, 2000a).

The precise means by which MAP2 contributes to the establishment of neuronal polarity during development and to the maintenance of neuronal structure in adult brain are still unknown. One way by which MAP2 could modify neuronal function is by modulating microtubule stability. Indeed, a change in the phosphorylation state of MAP2 in response to extracellular signals could alter its association with microtubules thus, affecting microtubule dynamics and neuronal morphology (Sanchez *et al.*, 2000a).

However, several studies reported that MAP2 could interact with membranous organelles, with several signalling proteins and with cytoskeletal components other than microtubules. This forces us to consider new means by which MAP2 could affect neuronal function. In the present review, we will elaborate on possible new functions of MAP2 in the light of recent discoveries.

The Microtubule-Associated Protein MAP2: An Old Protein

Primary structure

The microtubule-associated protein MAP2 was first discovered co-purifying with cytoplasmic microtubules from brain tissue (Ray *et al.*, 1979; Travis *et al.*, 1980; Bloom *et al.*, 1985). The primary structure of MAP2 contains two major functional domains: the microtubule-binding domain and the projection domain. The microtubule-binding domain is located at the carboxy-terminus of the protein and is highly basic (Lewis *et al.*, 1988; Lewis *et al.*, 1989). This domain contains 3 to 4 imperfect repeats of 18 amino acids (a.a.) separated by 13-14 a.a. These repeats bind to tubulin and reduce the critical concentration of tubulin required to polymerize into microtubules, thus promoting microtubule assembly (Murphy and Borisy, 1975; Sloboda *et al.*, 1975; Lewis *et al.*, 1988; Lewis *et al.*, 1989). The projection domain of MAP2, which is highly acidic, is located at the amino-terminus of the protein and is known to project at the surface of microtubules. This domain was mostly attributed a structural role in determining the spacing between microtubules (Kim *et al.*, 1979; Chen *et al.*, 1992). Between the microtubule-binding domain and the projection domain lays a proline-rich region. This region is thought to regulate microtubule binding and assembly activities through

intramolecular interactions with the repeat regions of the microtubule-binding domain (Sanchez *et al.*, 1996; Felgner *et al.*, 1997; Goode *et al.*, 1997).

Alternative splicing

During development, several MAP2 isoforms are generated by alternative splicing from a single gene located on chromosome 2 (Neve *et al.*, 1986; Shafit-Zagardo and Kalcheva, 1998). There exists at least four MAP2 isoforms that can be divided in two groups: 1) HMW MAP2: MAP2a (280kDa) and MAP2b (270kDa) and 2) LMW MAP2: MAP2c (70kDa) and MAP2d (75kDa). The main difference between HMW and LMW MAP2 isoforms is the insertion of a 1372 a.a. sequence in the projection domain of HMW MAP2 (Lewis *et al.*, 1988; Kindler *et al.*, 1990). MAP2a differs from MAP2b by the insertion of an additional sequence of 82 a.a. in its projection domain (Chung *et al.*, 1996). MAP2d contains 4 repeats in the microtubule-binding domain whereas MAP2c contains 3 (Ferhat *et al.*, 1994). MAP2a, MAP2b and MAP2c are neuron-specific whereas MAP2d can also be found in glial cells (Doll *et al.*, 1993a; Ferhat *et al.*, 1994).

The expression of MAP2 isoforms is developmentally regulated. MAP2b expression precedes that of MAP2a during neuronal development. MAP2a appears around postnatal day 10 and is more prominent in the brain of older rats (Tucker, 1990; Chung *et al.*, 1996). MAP2c is highly expressed during early neuronal development and remains expressed only in the retina and the olfactory bulb of the mature brain where neurogenesis persists throughout adulthood (Tucker *et al.*, 1988; Viereck *et al.*, 1989; Tucker, 1990). MAP2d protein is detected around postnatal day 5 (Doll *et al.*, 1993a;

Ferhat *et al.*, 1994). HMW MAP2 isoforms are specifically found in the cell body and the dendrites of the mammalian central nervous system whereas LMW isoforms are present in all neuronal compartments (Caceres *et al.*, 1984; Caceres *et al.*, 1986; Tucker and Matus, 1988; Meichsner *et al.*, 1993; Albala *et al.*, 1995; Chung *et al.*, 1996).

MAP2 as a regulator of microtubule dynamics

The term 'dynamic instability' refers to the phases of elongation and rapid shortening exhibited by microtubules and the abrupt transitions between these phases (Mitchison and Kirschner, 1984; Horio and Hotani, 1986; Janson *et al.*, 2003). MAP2 has been shown to modulate the dynamic behaviour of microtubules in vitro and in vivo. MAP2 is thought to bind to microtubules along individual protofilaments, possibly bridging the tubulin interfaces (Al-Bassam *et al.*, 2002). When bound to microtubules in vitro, MAP2 reduces the rate of rapid shortening of microtubules and increases the elongation rate (Hirokawa, 1991). In vivo, our work and that of others have shown that the expression of MAP2 in non-neuronal cells causes the formation of bundles of stiff microtubules (Weisshaar *et al.*, 1992; Leclerc *et al.*, 1993; Matus, 1994). The 18 a.a. repeats of the microtubule-binding domain, especially the third repeat, as well as the flanking regions seem to be important for microtubule bundling (Takemura *et al.*, 1995; Ludin *et al.*, 1996). Whether microtubule bundling is the consequence of the cross-linking of microtubules by MAP2 dimerization or a non-specific consequence of the increased microtubule stiffness and rigidity due to presence of MAP2 is still unknown (for a review, see Sanchez et al. (2000a)).

MAP2 as an actin- and neurofilament-binding protein

Actin was shown to bind to a large number of proteins collectively called actin-binding proteins (ABPs). ABPs modulate actin structure and function. According to a recent review by Dos Remedios and colleagues (dos Remedios *et al.*, 2003), ABPs can be classified in seven groups: 1) Monomer-binding proteins sequester globular actin (G-actin) and prevent its polymerization, 2) Filament-depolymerizing proteins induce the conversion of filamentous actin (F-actin) to G-actin, 3) Filament end-binding proteins cap the ends of the actin filament preventing the exchange of monomers at the pointed end and at the barbed end, 4) Filament severing proteins shorten the average length of filaments by binding to the side of F-actin and cutting it into two pieces, 5) Cross-linking proteins contain at least two binding sites for F-actin, or can dimerize, thus facilitating the formation of filament bundles, branching filaments, and three-dimensional networks, 6) Stabilizing proteins bind to the sides of actin filaments and prevent depolymerization and 7) Motor proteins that use F-actin as a track upon which to move. Several studies have shown that MAP2 is an ABP that can bind and cross-link individual actin filaments *in vitro* and that actin-binding and cross-linking activities of MAP2 are both phosphorylation dependent (Sattilaro *et al.*, 1981; Selden and Pollard, 1983; Sattilaro, 1986; Selden and Pollard, 1986; Yamauchi and Fujisawa, 1988; Cunningham *et al.*, 1997). To cause the formation of actin filament bundles, a protein needs to have two binding sites for F-actin or needs to be able to dimerize (Puius *et al.*, 1998). In the case of MAP2, one actin-binding site has been identified so far that corresponds to the second 18 a.a. repeat in the microtubule-binding domain of MAP2 (Sattilaro, 1986; Correas *et al.*, 1990). However, one cannot rule out the possibility of

the existence of another actin-binding site in the projection domain of MAP2. In support of this hypothesis, the projection domain of MAP2 can cause the bundling of actin filaments *in vitro* (Leclerc, N. and Jamney, P., personal communication). Furthermore, the projection domains of both MAP2b and MAP2c co-localize with peripheral actin in Sf9 cells (Belanger *et al.*, 2002). Thus, MAP2 may contain two actin-binding sites, one located in the microtubule-binding domain and another in the projection domain, allowing for microfilament bundling. MAP2 was also shown to have a pronounced tendency to form dimers whose components are nearly in register but of opposite polarity (Wille *et al.*, 1992c; Wille *et al.*, 1992b). This is another possible means by which MAP2 may cause the formation of actin filament bundles. *In vivo*, MAP2 was shown to reorganize F-actin in Sf9 cells (Boucher *et al.*, 1999; Belanger *et al.*, 2002). Furthermore, MAP2c was shown to induce the formation of actin-rich lamellae in an actin-binding protein-280-deficient melanoma cell line (Cunningham *et al.*, 1997). Moreover, an increase of the localization of MAP2c to the peripheral actin network was observed when MAP2c was phosphorylated at three specific serine residues, one within each tubulin-binding repeat (Ozer and Halpain, 2000).

Besides interacting with microtubules and microfilaments, MAP2 was also shown to interact with the 70kDa neurofilament subunit and to cross-bridge microtubules with neurofilaments *in vitro* (Leterrier *et al.*, 1982; Heimann *et al.*, 1985; Hirokawa *et al.*, 1988). *In vivo*, MAP2 was shown to be a component of the cross-bridges between microtubules and neurofilaments in the dendrites of rat spinal cord motoneurons (Hirokawa *et al.*, 1988).

By connecting together microtubules, microfilaments and neurofilaments, MAP2 might act as an integrator of the neuronal cytoskeleton. Recently, a family of proteins called plakins (also referred to as cytolinkers) was reported to link cytoskeletal networks to each other and to membrane-associated adhesive junctions (Ruhrberg *et al.*, 1997; Green *et al.*, 1999; Karakesisoglou *et al.*, 2000; Leung *et al.*, 2001; van den Heuvel *et al.*, 2002). Mutations in plakin family genes lead to defects in tissue integrity and function in skin, muscle and the nervous system in human and in mouse, whereas in *Drosophila*, mutations lead to loss of adhesion between muscle and epidermal cells, as well as defects in neuronal outgrowth (Borradori *et al.*, 1998; Mahoney *et al.*, 1998; Green *et al.*, 1999; Leung *et al.*, 1999b; Karakesisoglou *et al.*, 2000; Olivry *et al.*, 2000; Fujiwara *et al.*, 2001; Leung *et al.*, 2001; Lee and Kolodziej, 2002). Furthermore, several reports on 'plakin'-type cytoskeletal linkers confirmed the importance of these proteins on cytoskeletal organization and function (Andra *et al.*, 1998; Dalpe *et al.*, 1998; Dalpe *et al.*, 1999; Yang *et al.*, 1999). MAP2 being a crosslinking protein that connects cytoskeletal networks suggests not only a structural role for this protein in maintaining cytoskeletal architecture but also a functional role in stabilizing and destabilizing the networks to which it binds. Consistent with this hypothesis, MAP2 was observed to switch from microfilaments to microtubules during axonal growth of cultured rat hippocampal neurons (Kwei *et al.*, 1998). Furthermore, the morphological changes induced by the ganglioside GM1 in Neuro-2a neuroblastoma cells are accompanied by rearrangements in the association of MAP2 with both microtubules and microfilaments (Wang *et al.*, 1996b; Wang *et al.*, 1998; Kozireski-Chuback *et al.*, 1999; Colella *et al.*, 2000).

Known associations of MAP2 with signalling proteins

Besides interacting with the three constituents of the neuronal cytoskeleton, MAP2 can also interact with signalling proteins. For example, MAP2 can interact with the regulatory subunit RII of the c-AMP dependent protein kinase (PKA) and plays an important role in anchoring PKA protein to specific cellular compartments (Rubino *et al.*, 1989; Davare *et al.*, 1999). In MAP2 knockout mice, there is a reduction of total PKA in dendrites and the rate of induction of phosphorylated CREB is reduced after forskolin stimulation (Harada *et al.*, 2002). Furthermore, MAP2b was shown to bind directly to the α-1 subunit of the class C - L type calcium channels in neurons (Davare *et al.*, 1999). By interacting simultaneously with the regulatory subunit of the PKA and with the class C- L type calcium channel, MAP2b could allow the phosphorylation of the calcium channels clustered at postsynaptic sites and thus, regulate neuronal function (Davare *et al.*, 1999). MAP2 isoforms were also reported to interact with the SH3 domains of c-Src and Grb2 in vitro (Lim and Halpain, 2000). Src and Grb2 interact preferentially with the non-microtubule-associated MAP2c (Lim and Halpain, 2000). The 1372 a.a. sequence of MAP2b contains a binding site for calmodulin, which is known to decrease the actin-binding activity of MAP2b (Kotani *et al.*, 1985; Kindler *et al.*, 1990). MAP2b also contains two binding sites for phosphatidylinositol (PI): one low affinity binding site located at the carboxy-terminal and one high affinity binding site located in the 1372 a.a. insert in the projection domain of MAP2b (Surridge and Burns, 1994; Burns and Surridge, 1995). Binding of PI to MAP2c was shown to reduce its binding to tubulin thus, modulating microtubule dynamics (Yamauchi and Purich, 1987).

PI was also shown to decrease the binding of MAP2 to actin (Yamauchi and Purich, 1993).

Phosphorylation regulates MAP2 function

Phosphorylation is the most important post-translational modification that MAP2 undergoes. In vivo, MAP2 could contain up to 46 moles of phosphate per mole of protein (Tsuyama *et al.*, 1987). MAP2 was shown to be the substrate for several kinases and phophatases (for a detailed review, see Sanchez et al., (2000a)). Here, we will provide a short summary of the main kinases and phosphatases and their major effect on MAP2 function since a detailed analysis of these proteins is beyond the scope of this review.

MAP2 is rich in Serine/Threonine residues and thus, is a good substrate for Ser/Thr kinases. As such, PKA phosphorylates MAP2 *in vitro* at least on 11 different serines that are located in the microtubule-binding domain and in the projection domain of MAP2 (Goldenring *et al.*, 1985; Yamamoto *et al.*, 1985; Goldenring and DeLorenzo, 1986). Phophorylation of MAP2 by the PKA was shown to: 1) reduce the microtubule-binding and microtubule-nucleating activities of MAP2 *in vivo* and *in vitro*, 2) inhibit the actin microfilaments cross-linking activity of MAP2 *in vitro* and increase the localization of MAP2c to the peripheral actin microfilaments *in vivo* when MAP2c is phosphorylated at three specific serine residues, one within each tubulin-binding repeat and 3) protect MAP2 against calpain-mediated proteolysis (Burns *et al.*, 1984; Yamamoto *et al.*, 1985; Yamauchi and Fujisawa, 1988; Johnson and Foley, 1993; Alexa *et al.*, 1996; Itoh *et al.*, 1997; Ozer and Halpain, 2000). Ca^{2+}/calmodulin-dependent

protein kinase II (CAMKII) is another Ser/Thr kinase that was shown to phosphorylate MAP2 *in vitro* on at least 18 sites located both in the microtubule-binding domain and the projection domain of MAP2 (Yamauchi and Fujisawa, 1982; Hernandez *et al.*, 1987b; Walaas and Nairn, 1989). Phosphorylation of MAP2 by CAMKII was shown to: 1) inhibit the microtubule assembly-promoting activity of MAP2 *in vitro* and 2) inhibit the actin microfilaments cross-linking activity of MAP2 *in vitro* (Yamamoto *et al.*, 1983; Yamamoto *et al.*, 1985; Yamauchi and Fujisawa, 1988). Protein kinase C (PKC) was also shown to phosphorylate MAP2 on at least 15 different sites in vitro, most of which are located in the projection domain of the protein (Akiyama *et al.*, 1986; Hernandez *et al.*, 1987b; Tsuyama *et al.*, 1987; Walaas and Nairn, 1989; Ainsztein and Purich, 1994). Phosphorylation of MAP2 by PKC: 1) reduces tubulin-polymerizing activity of MAP2, 2) when 3 specific serine residues are phosphorylated in the microtubule-binding domain, MAP2 association with microtubules is completely abolished, 3) inhibits binding of MAP2 to microfilaments and 4) protects MAP2 against calpain-mediated proteolysis (Akiyama *et al.*, 1986; Hoshi *et al.*, 1988; Ainsztein and Purich, 1994; Alexa *et al.*, 1996).

Proline-directed kinases are another group of kinases that can phophorylate MAP2 in proline-rich regions of the protein. Proline groups can exist in two conformations, cis or trans, and thus, can modulate protein structure. Phosphorylation of a protein at proline residues can cause important changes in its conformation leading to important modifications of the protein's function. Extracellular signal regulated kinases (ERKs) are one group of proline-directed kinases that was shown to phosphorylate MAP2 *in vitro* (Cobb *et al.*, 1991; Avruch, 1998). Most of the phosphorylation sites

seem to be located in the projection domain of MAP2 (Fellous *et al.*, 1994). Phosphorylation of MAP2 by ERKs was shown to inhibit its tubulin-polymerizing activity (Hoshi *et al.*, 1992). GSK3β is another proline-directed kinase that was shown to phosphorylate MAP2 on Ser^{136} and on two threonines, Thr^{1620} and Thr^{1623}, both of which are located in the proline-rich region of MAP2 (Berling *et al.*, 1994; Sanchez *et al.*, 1996). Phosphorylation of MAP2 by GSK3β was shown to inhibit its microtubule binding and bundling capacities *in vivo* (Sanchez *et al.*, 2000b).

Several other kinases were shown to phosphorylate MAP2. As such, Rho-associated kinase phosphorylates MAP2 on Ser^{1796} in vitro and the microtubule-affinity regulating kinases (MARKs) phosphorylate the microtubule-binding domain of MAP2 (Drewes *et al.*, 1997; Drewes *et al.*, 1998; Amano *et al.*, 2003). Phosphorylation of MAP2 by MARKs was proposed to detach it from microtubules (Drewes *et al.*, 1997; Drewes *et al.*, 1998).

MAP2 was also shown to be the substrate for numerous phosphatases. The main protein phosphatases (PP) expressed in the brain are: PP1, PP2A, PP2B and PP2C (Cohen, 1989; Cohen and Cohen, 1989; Cohen *et al.*, 1989; Pei *et al.*, 1994). MAP2 has been reported to be dephosphorylated *in vitro* by PP1, PP2A and PP2B (Goto *et al.*, 1985; Patterson and Flavin, 1986; Sanchez *et al.*, 1996). *In vivo*, inhibition of PP2A using okadaic acid was shown to reduce the microtubule-binding capacity of MAP2 (Gong *et al.*, 2000b). Recently, MAP2 was found to be a substrate for myosin phosphatase (Amano *et al.*, 2003).

As previously suggested by Sanchez and colleagues (2000a), a modification in the phosphorylation state of MAP2 in response to extracellular signals could underlie the cytoskeletal and morphological changes that take place during neuronal differentiation and remodeling. As such, an increase in the phosphorylation state of HMW MAP2 was correlated with dendritic arborization in primary hippocampal cultures (Diez-Guerra and Avila, 1995). Furthermore, an increase of the phosphorylation state of MAP2 was shown to stimulate neurite branching and a decrease of its phosphorylation state to reduce branching in primary hippocampal cultures (Audesirk *et al.*, 1997). At the adult stage, a change in the phosphorylation state of HMW MAP2 accompanies activity-dependent changes in synaptic efficacy, which are thought to underlie morphological remodeling (Diaz-Nido *et al.*, 1993; Quinlan and Halpain, 1996b). A change in the phosphorylation state of MAP2 was also shown to alter its association with cytoskeletal components (Sattilaro *et al.*, 1981; Yamamoto *et al.*, 1983; Burns *et al.*, 1984; Yamamoto *et al.*, 1985; Hoshi *et al.*, 1988; Brugg and Matus, 1991; Ainsztein and Purich, 1994; Itoh *et al.*, 1997; Ozer and Halpain, 2000).

Interaction of MAP2 with mitochondria

Besides interacting with the three components of the cytoskeleton and with signalling proteins, MAP2 can also interact with mitochondria (Jancsik *et al.*, 1989; Linden *et al.*, 1989a; Jung *et al.*, 1993). Mitochondrial movement and structure are regulated through interactions with the cytoskeleton especially microtubules (Linden *et al.*, 1989b). The interaction between MAP2 and the outer surface of rat brain mitochondria has been demonstrated *in vitro* and *in situ* (Jancsik *et al.*, 1989; Linden *et*

al., 1989a; Jung *et al.*, 1993). Upon binding, MAP2 is released from microtubules and induces a physical change in the outer membrane properties which leads to a tighter association of the pore-forming protein (porin) with mitochondria (Linden *et al.*, 1989a; Linden *et al.*, 1989b). Although both the microtubule-binding and the projection domains of MAP2 were shown to be involved in the interaction, it was suggested that MAP2 binds to mitochondria preferentially through its microtubule-binding domain (Jancsik *et al.*, 1989).

The Microtubule-Associated Protein MAP2: New functions?

MAP2: a dendritic cytosolic linker protein (CLIP) between the rough endoplasmic reticulum membranes and microtubules

As mentioned above, membranous organelles composition is different in dendrites and in the axon. As such, the rough endoplasmic reticulum (RER), is found in the somato-dendritic compartment but not in the axon (Bartlett and Banker, 1984b, a; Peters *et al.*, 1991). Several studies have shown that the ER membranes are associated to microtubules (Terasaki *et al.*, 1986; Terasaki, 1990; Terasaki and Reese, 1994; Hirokawa, 1998; Aihara *et al.*, 2001). This association could be either dynamic for trafficking of ER membranes or stable for the positioning of these membranes within a cell (Terasaki, 1990; Cole and Lippincott-Schwartz, 1995; Hirokawa, 1998). Depolymerization of microtubules using the drug nocodazole affects both the trafficking and positioning of ER membranes (Terasaki *et al.*, 1986; Terasaki and Reese, 1994; Waterman-Storer and Salmon, 1998; Aihara *et al.*, 2001). The ER movement along microtubules has been well documented (Terasaki, 1990; Allan and Vale, 1994;

Waterman-Storer and Salmon, 1998; Aihara *et al.*, 2001). The sliding of ER membranes along microtubules seems to be driven by motor proteins such as kinesin. Moreover, it was shown that ER could be moved within a cell by its attachment to the microtubule-plus end (Waterman-Storer and Salmon, 1998). Stable positioning of the ER membranes along microtubules has been much less documented in neurons. CLIPs (cytosolic linker proteins) were shown to establish a link between microtubules and membranous organelles. As such, CLIP-170 was reported to mediate the interaction of endocytic carrier vesicles to microtubules (Pierre *et al.*, 1992). Furthermore, CLIP-115 was shown to be responsible for the polarized distribution of the dendritic lamellar bodies (DLB) in neurons (De Zeeuw *et al.*, 1997; Hoogenraad *et al.*, 2000). Recently, a new class of proteins termed CLASPs (CLIP-associated proteins) was identified (Akhmanova *et al.*, 2001). These proteins bind CLIPs and microtubules and have a microtubule-stabilizing effect. A family of proteins named Hooks also mediates the interaction between microtubules and membrane organelles. More specifically, Hook3 links the Golgi apparatus to microtubules (Walenta *et al.*, 2001). Furthermore, an integral membrane protein of the ER, p63, was shown to be involved in the interaction of ER with microtubules in a non-neuronal cell line (Klopfenstein *et al.*, 1998). Since p63 is an integral membrane protein, it was termed a CLIMP (cytoskeleton-linking membrane protein).

Recently, we identified MAP2 as the first dendritic CLIP that mediates the interaction between the ER and microtubules in neurons (Farah et al., manuscript under review). Indeed, we have shown that MAP2 interacts with the ER membranes and can connect RER to microtubules. However, we decided to classify MAP2 in a category of

its own since: 1- the microtubule-binding domain of MAP2 has no sequence homology with that of known CLIPs, CLASPs, Hooks and CLIMPs, 2- all the linker proteins identified so far bind to distal end of microtubules whereas MAP2 binds to microtubules along their length and 3- in contrary to p63, MAP2 is not an integral membrane protein but a cytosolic one.

The fact that MAP2 can connect the ER to microtubules lead us to propose a model where MAP2 could be important for the proper positioning of RER membranes along microtubules in the neurites and in the growth cone during neuronal differentiation. In response to extracellular signals in a mature neuron, MAP2 could reposition the ER membranes at specific locations along the dendritic microtubules to allow for plastic changes in the adult brain. Stable positioning of the ER along microtubules might be important for the modulation of local calcium pools (Rizzuto, 2001). The binding activity of several proteins that control F-actin and microtubule organization such as MAP2 is regulated by calcium (Yamamoto *et al.*, 1983; Yamamoto *et al.*, 1985; Quinlan and Halpain, 1996b, a). Furthermore, the cytoskeleton seems to be able to influence the capacity of ER to release Ca2+ since depolymerization of actin microfilaments using cytochalasin D was shown to reduce Ca2+ release from ER stores in cultured hippocampal neurons (Wang *et al.*, 2002).

The projection domain of MAP2: a key regulator of protein activity

The projection domain of MAP2 has long been attributed a structural role as a regulator of the spacing between microtubules (Chen *et al.*, 1992; Leclerc *et al.*, 1996). However, we have recently shown that the projection domain of MAP2 regulates the

capacity of the microtubule-binding domain to induce process formation in Sf9 cells (Belanger *et al.*, 2002). In these cells, microtubule protrusion from cell surface and subsequent formation of processes was induced by the expression of the microtubule-binding domain of MAP2 that is common to MAP2b and MAP2c. Interestingly, the projection domain of MAP2c positively regulated process formation activity of the microtubule-binding domain and enhanced the formation of thin bundles of microtubules. In contrast, the projection domain of MAP2b, which contains an additional insert of 1372 a.a., inhibited process formation activity of the microtubule-binding domain and enhanced the formation of one thick bundle of microtubules. This showed that the 1372 a.a. domain had a negative effect on the capacity of MAP2b to induce process formation in Sf9 cells. Our results further showed that the last 466 a.a. sequence of this domain had the most important inhibitory effect.

The negative effect of the additional domain of 1372 a.a. did not seem to be due solely to the action of this domain on the microtubule binding or bundling properties of MAP2b. Our results rather showed that the 1372 a.a. domain allowed for intramolecular interactions between the projection domain of MAP2b and its microtubule-binding domain. In the light of these results, we proposed a model where these intramolecular interactions allow for MAP2b to exist at least in two conformations: 1) the projection domain of MAP2b might be folded back on the microtubule-binding domain resulting in an inoperative MAP2b that would stabilize the cytoskeleton and maintain dendritic shape and 2) the projection domain is not folded back resulting in an operative MAP2b that would promote process formation and remodeling of dendrites. The proline-rich region located between the projection domain and the microtubule-binding domain

might act as a hinge domain allowing for MAP2b to exist in several conformations. A similar model had previously been reported for ezrin, a member of the ERM family of proteins that links the actin cytoskeleton to the membrane (Gary and Bretscher, 1995). Ezrin was reported to exist in two forms: 1) a dormant form in which the carboxy-terminus is masked by the amino-terminus that is folded back and 2) an operative form in which the amino-terminus is not folded back. It was suggested that the folding back of the amino-terminus of ezrin masks its binding site to ezrin-radixin-moesin binding phosphoprotein, EBP50 (Reezek and Bretscher, 1998). This could be the case for MAP2b. The folding back of the amino-terminus could mask domains that are involved in the interaction of MAP2b with signaling proteins. It could also affect the association of MAP2 with cytoskeletal components thus altering their dynamics.

For the projection domain of MAP2b to adopt different structural conformations is not surprising. Indeed, previous studies had shown that this domain was flexible (Woody *et al.*, 1983). Furthermore, secondary structure predictions suggested that this domain had a very important stretch of helices separated by short turns that could contribute to its flexibility (Kindler *et al.*, 1990). Moreover, several studies had pointed out that the length of this domain could vary (Voter and Erickson, 1982; Wille *et al.*, 1992b).

Thus, our study pointed to an important new function for the projection domain of MAP2 as a regulator of protein activity. Consistent with this view, Khuchua and colleagues reported recently that the deletion of the first 158 a.a. from the projection domain of MAP2 by gene targeting disrupts neuronal morphology of the CA1 area of mice hippocampus (Khuchua *et al.*, 2003). Furthermore, behavioral studies suggested

that these mice had an altered fear-related contextual memory (Khuchua *et al.*, 2003). The authors attribute these results to the deletion of the 31 a.a. sequence in the N-terminus responsible for the binding of MAP2 to the regulatory subunit RII of the c-AMP dependent protein kinase (PKA). Indeed, the authors showed that phosphorylation of truncated MAP2 lacking the first 158 a.a. by PKA was markedly reduced. Thus, one can conclude that phosphorylation of MAP2 is important for the selective development of contextual memory. Consistent with this hypothesis, Woolf and colleagues had reported MAP2 alterations in the apical dendrites of hippocampal pyramidal cells as a function of training (Woolf *et al.*, 1999). These alterations included degradation of MAP2a and MAP2b and a decrease of the phosphorylation state of MAP2c concomitant with contextual memory formation (Woolf *et al.*, 1999). Furthermore, Philpot and colleagues had reported experience-dependent changes of MAP2 phosphorylation in the developing and adult rat olfactory bulb (Philpot *et al.*, 1997). The phosphorylation state of MAP2 was shown to decrease in the granule cell layer of the olfactory bulb following 30 days of olfactory restriction (Philpot *et al.*, 1997). Moreover, PKA-mediated phosphorylation of MAP2 is induced if the animal is exposed to light for a short period after dark-rearing (Aoki and Siekevitz, 1985). Thus, alteration of the phosphorylation state of MAP2 seems to be an important step leading to long-term memory storage. It is possible that activity-dependent changes in synaptic efficacy, that are thought to underlie learning and memory formation, cause an alteration of the phosphorylation state of MAP2 to allow for modification and/or consolidation of neuronal circuitry. Consistent with this hypothesis, synaptic activity evoked by glutamate was reported to cause a biphasic change in MAP2: a rapide increase in phosphorylation followed by a persistent

dephosphorylation (Quinlan and Halpain, 1996b). Furthermore, depolarization induced by a high concentration of extracellular potassium in rat hippocampal slices leads to an increase in the phosphorylation state of MAP2 (Diaz-Nido *et al.*, 1993). Moreover, N-Methyl-D-Aspartate (NMDA), a key player in synaptic plasticity, was shown to stimulate the dephosphorylation of MAP2 (Halpain and Greengard, 1990).

An alteration of the phosphorylation state of MAP2 in response to activity-dependent changes of synaptic efficacy, may: 1) alter its association with microtubules and actin microfilaments thus modulating cytoskeletal dynamics and 2) modulate its association with signalling proteins which are key for learning and memory formation. For instance, MAP2 was shown to interact strongly with the NMDA receptor subunits 2A/B (Buddle *et al.*, 2003). Activation of NMDA receptors was shown to be crucial for the induction of long-term potentiation (LTP), which is thought to underlie memory formation in the CA1 hippocampal area (Cain, 1997; Zorumski and Izumi, 1998). Furthermore, MAP2 was shown to interact simultaneously with the regulatory subunit of the PKA and with the class C- L type calcium channel thus allowing for phosphorylation of the calcium channels clustered at postsynaptic sites (Davare *et al.*, 1999). PKA was shown to be crucial for the maintenance of LTP and hippocampus-based long-term memory (Abel *et al.*, 1997).

MAP2: an expanded view of its functions

MAP2 could be key in regulating neuronal function in response to extracellular signals during neuronal differentiation and plasticity events in adult brain. The whole cascade may start when the cell receives a signal that leads to an alteration of the activity

of protein kinases and phosphatases within the cell (Figure 1). This would cause a modification of the phosphorylation state of MAP2 and of its conformation leading to: 1) an altered binding of MAP2 to microtubules, actin microfilaments and neurofilaments thus affecting cytoskeletal dynamics to allow for morphological changes, 2) an altered interaction of MAP2 with the ER membranes, thus affecting positioning of the ER along the dendritic microtubules to allow for modulation of local calcium release and plastic changes and 3) an altered association of MAP2 with signalling proteins such as PKA and NMDA receptors which are key to learning and memory formation.

A deregulation of the activity of protein kinases was reported to take place in neurodegenerative diseases (Lanius *et al.*, 1995; Patrick *et al.*, 1999; Kaytor and Orr, 2002; Patzke and Tsai, 2002). These pathological conditions are characterized by a loss of neuronal structure and polarity (Coyle and Puttfarcken, 1993; Represa *et al.*, 1993; Perez *et al.*, 1996; Falke *et al.*, 2003). Alterations of the protein level and/or phosphorylation state of MAP2 were reported in neurodegenerative diseases. As such, we have recently reported a decreased protein level and an altered membranous distribution of MAP2 in a mouse model of amyotrophic lateral sclerosis (Farah *et al.*, 2003). In schizophrenia, an increased expression of MAP2 was reported in the hippocampus and an altered immunocytochemistry of MAP2 was reported in areas 9 and 32 of schizophrenic prefrontal cortex (Cotter *et al.*, 1997; Cotter *et al.*, 2000; Jones *et al.*, 2002). In epilepsy, an increase in the expression of MAP2 was reported in an experimental model of temporal lobe epilepsy (Pollard *et al.*, 1994). However, MAP2 phosphorylation was shown to decrease in the human epileptic temporal lobe cortex (Sanchez *et al.*, 2001). In Parkinson's disease, abnormal MAP2 immunolabeling was

observed in the neuronal nuclei and in the Lewy bodies of the substantia nigra brain tissue (D'Andrea *et al.*, 2001). Whether these alterations of MAP2 are one of the leading events in neurodegeneration or a consequence of the disease remains to be characterized. Understanding the molecular mechanisms by which MAP2 regulates neuronal function will help to unravel abnormal cytoskeletal modifications that occur in neurodegenerative diseases.

Figure 1. MAP2 could be key in regulating neuronal function in response to extracellular signals. A modification of the phosphorylation state of MAP2 and of its conformation might lead to: 1) an altered binding of MAP2 to microtubules, actin microfilaments and neurofilaments thus affecting cytoskeletal dynamics, 2) an altered interaction of MAP2 with the ER membranes, thus affecting positioning of the ER along the dendritic microtubules and 3) an altered association of MAP2 with signalling proteins such as PKA and NMDA receptors.

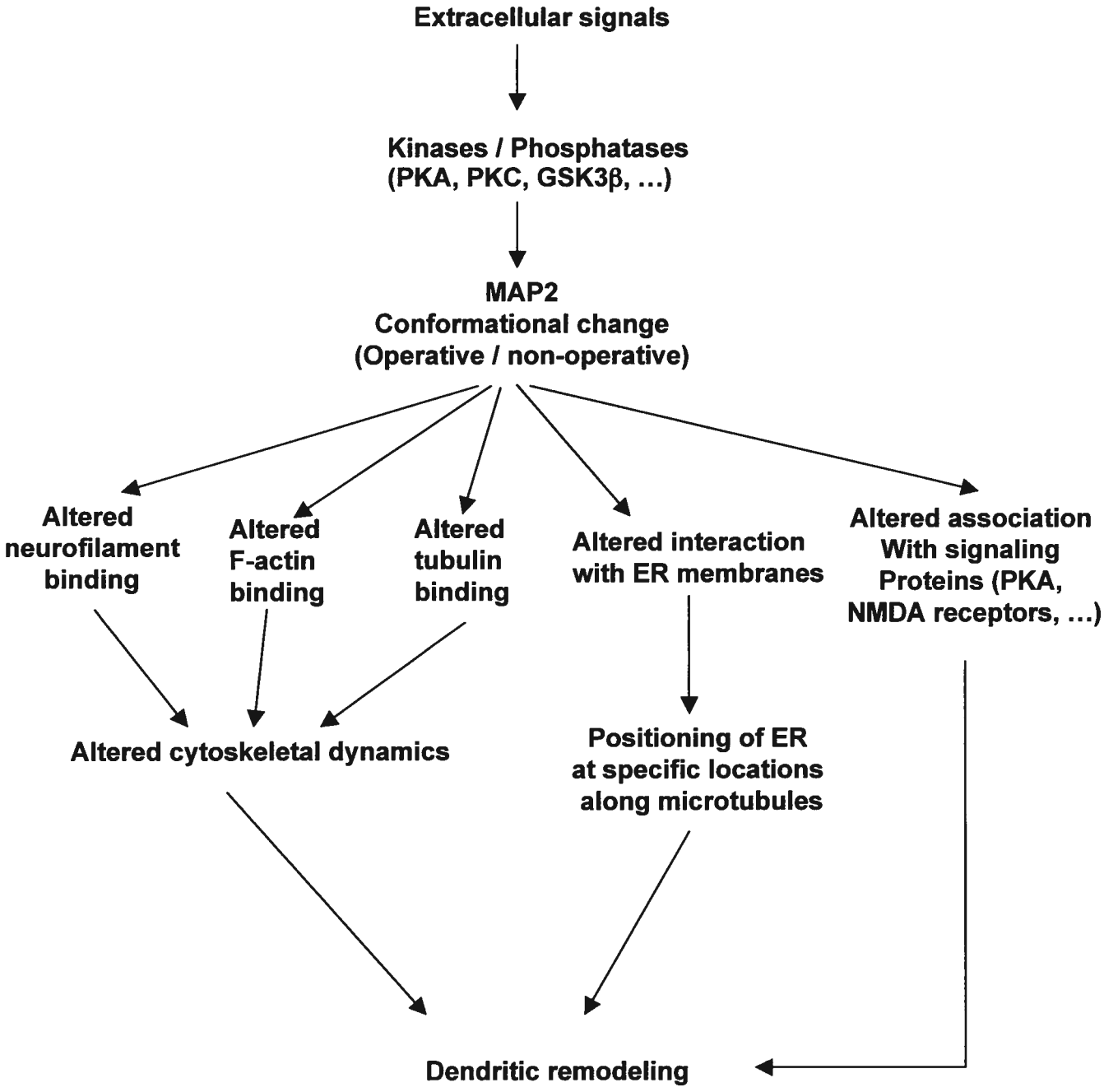
Extracellular signals
Kinases / Phosphatases
(PKA, PKC, GSK3β, ...)
MAP2
Conformational change
(Operative / non-operative)
Altered
neurofilament
binding
Altered
F-actin
binding
Altered
tubulin
binding
Altered interaction
with ER membranes
Altered association
With signaling
Proteins (PKA,
NMDA receptors, ...)
Altered cytoskeletal dynamics
Positioning of ER
at specific locations
along microtubules
Dendritic remodeling

ANNEXE II – CONTRIBUTION AUX ARTICLES

Article 1

Je suis intervenue dans ce projet pour compléter et publier les travaux initiés par D. Bélanger (étudiant en maîtrise), après son départ du laboratoire. J'ai effectué les expériences de microscopie électronique sur l'espacement entre les microtubules ainsi que les mesures et l'analyse de ces données. J'ai également fait les préparations des microtubules et les extractions du cytosquelette en condition contrôle, après traitement au froid et à la colchicine, pour les formes tronquées et complètes de la MAP2c et la MAP2b. J'ai aussi mise au point en collaboration avec N. Leclerc la stratégie de purification des formes tronquées et complètes de la MAP2c et la MAP2b. De plus, j'ai participé à l'analyse statistique des données obtenues par D. Bélanger. Finalement, j'ai fait les figures 4 et 8 et j'ai participé activement à la rédaction avec N. Leclerc. D. Bélanger a produit les constructions baculovirales des formes tronquées de la MAP2c et la MAP2b. Il a exprimé ces constructions dans les cellules Sf9 et a fait une analyse morphométrique détaillée du phénotype produit par chaque construction. M.D. Nguyen et S. Cornibert ont participé à la production des constructions baculovirales. M.D. Nguyen a aussi participé à la révision du manuscrit. Michel Lauzon a fait les coupes de microscopie électronique et a participé à l'analyse des données. Il a également fait la figure 7.

Article 2

Je suis responsable de toutes les expériences effectuées sauf une partie des dissections de moelle épinière qui a été faite par M.D. Nguyen. J'ai fait toutes les figures et rédigé le manuscrit avec N. Leclerc. M.D. Nguyen et J.P. Julien ont participé à la rédaction et étaient nos collaborateurs sur cette étude.

Article 3

Je suis responsable de toutes les expériences effectuées dans ce papier sauf la culture des neurones qui a été faite par M. Desjardins et la transfection des neurones ainsi que la culture des cellules gliales qui ont été faites par D. Liazoghli. J'ai fait les figures 1 à 6 et le Dr. Paiement a fait les figures 7 à 11. J'ai rédigé le manuscrit avec J. Paiement et N. Leclerc. J. Paiement a aussi effectué les quantifications en microscopie électronique pour l'étude dans les cellules Sf9. S. Perreault a participé à la prise des photos au microscope confocal. A.Guimont a produit la protéine de fusion GFP-MAP2c. R. Young a mis au point la technique de quantification du périmètre des vésicules du RER en microscopie électronique. M. Lauzon a fait les coupes de microscopie électronique. G. Kreibich et J. Paiement étaient nos collaborateurs sur cette étude.

Article 4

J'ai rédigé le texte de cet article de revue en collaboration avec N. Leclerc.